THE ORGANISATION OF THE ENTERIC NERVOUS SYSTEM IN THE PIG AND GOAT, AND CHANGES INDUCED BY GRANULOMATOUS INFLAMMATION IN PIGS INFECTED WITH *SCHISTOSOMA JAPONICUM*

PhD THESIS
ONESMO BALEMBA BEGIRA

Department of Anatomy and Physiology
The Royal Veterinary and Agricultural University
Copenhagen, Denmark

September, 2001

PREFACE

This thesis is composed of **four chapters, six papers** and a summary in English as well as in Danish. In chapters one to three the literature in the fields of study has been reviewed and the objectives set forth in the current investigation and what was achieved are highlighted. Chapter four gives a brief overview discussion of the results and perspectives. The remaining part of the thesis is composed of publications/manuscripts describing findings from the current work as well as respective discussions and conclusions and will be referred to as **papers I-VI** in the text.

Paper I deals with the organisation of the enteric nervous system in the small intestine of the pig with emphasis on the submucous and mucous plexuses. **Paper II** gives an insight of the organisation of the ganglia, isolated neurons and subplexuses in the mucous plexus in the intestine of the pig. **Paper III** presents the organisation of the enteric nervous system in the goat with emphasis on the subdivisions in the outer and inner submucous plexuses and salient features to differentiate them as well as the extent of ganglia and isolated neurones in the mucous plexus. Intra-plexus variations along segments, inter-plexus variation with respect to the size of ganglia nerve stands and neurons are elaborated. **Paper IV** focuses on problems associated with methods used to quantify neurons, enterochromaffin cells as well as estimation of the surface area of Peyer's patches in the gut in the previous studies. A simple, cheap, unbiased sampling method is demonstrated using the pig jejunum as an example. **Papers V and VI** present findings on the plasticity of neurochemical contents in the enteric nervous tissue in the caecum and colon of pigs infected with *Schistosoma japonicum*.

Paper I: O.B. Balemba, M.-L. Grøndahl, G.K. Mbassa, W.D. Semuguruka, A. Hay-Schmidt, E. Skadhauge, V. Dantzer. The organisation of the enteric nervous system in the submucous and mucous layers of the small intestine of the pig studied by VIP and neurofilament protein immunohistochemistry. *Journal of Anatomy* 1998; 192: 257-267.

Paper II: O.B. Balemba, A. Hay-Schmidt, R.J. Assey, C.K.B. Kahwa, W.D. Semuguruka, V. Dantzer. An immunohistochemical study of the organisation of ganglia and nerve fibres in the mucosa of the porcine intestine. *Autonomic Neuroscience: Basic and Clinical.* (Submitted).

Paper III: O.B. Balemba, W.D. Semuguruka, A. Hay-Schmidt, V. Dantzer. The organisation and variations of ganglionated plexuses of the enteric nervous system in the goat. *Journal of Anatomy.* (Submitted).

Paper IV: O.B. Balemba, A. Hay-Schmidt, V. Dantzer, H.J.G. Gundersen. A very simple and efficient stereological sampling scheme for large mammalian gut, with estimation of the total number of specific neurons in distinct plexuses using unbiased principles. (Draft).

Paper V: O. B. Balemba, W. D. Semuguruka, A. Hay-Schmidt, M. V. Johansen, V. Dantzer. Vasoactive intestinal peptide and substance P-like immunoreactivities in the enteric nervous system of the pig correlate with the severity of pathological changes induced by *Schistosoma japonicum*. *International Journal for Parasitology*. (In press).

Paper VI: O.B. Balemba, K. Mortensen, W.D. Semuguruka, A. Hay-Schmidt, M.V. Johansen, V. Dantzer. Neuronal nitric oxide synthase activity is increased during granulomatous inflammation in the colon and caecum of pigs infected with *Schistosoma japonicum*. *Autonomic Neuroscience: Basic and Clinical*. (Submitted).

Onesmo Balemba Begira (OBB), *PhD thesis*

Department of Anatomy and Physiology,
The Royal Veterinary and Agricultural University,
Grønnegärdsvej 7, 1870 Frederiksberg C,
Copenhagen, Denmark.
e-mail: balemba@suanet.ac.tz,
September, 2001

TABLE OF CONTENTS

Paper I: O.B. Balemba, M.-L. Grøndahl, G.K. Mbassa, W.D. Semuguruka, A. Hay-Schmidt, E. Skadhauge, V. Dantzer. The organisation of the enteric nervous system in the submucous and mucous layers of the small intestine of the pig studied by VIP and neurofilament protein immunohistochemistry. *Journal of Anatomy* 1998; 192: 257-267.

Paper II: O.B. Balemba, A. Hay-Schmidt, R.J. Assey, C.K.B. Kahwa, W.D. Semuguruka, V. Dantzer. An immunohistochemical study of the organisation of ganglia and nerve fibres in the mucosa of the porcine intestine. *Autonomic Neuroscience: Basic and Clinical.* (Submitted).

Paper III: O.B. Balemba, W.D. Semuguruka, A. Hay-Schmidt, V. Dantzer. The organisation and variations of ganglionated plexuses of the enteric nervous system in the goat. *Journal of Anatomy.* (Submitted).

Paper IV: O.B. Balemba, A. Hay-Schmidt, V. Dantzer, H.J.G. Gundersen. A very simple and efficient stereological sampling scheme for large mammalian gut, with estimation of the total number of specific neurons in distinct plexuses using unbiased principles. (Draft).

Paper V: O. B. Balemba, W. D. Semuguruka, A. Hay-Schmidt, M. V. Johansen, V. Dantzer. Vasoactive intestinal peptide and substance P-like immunoreactivities in the enteric nervous system of the pig correlate with the severity of pathological changes induced by *Schistosoma japonicum. International Journal for Parasitology.* (In press).

Paper VI: O.B. Balemba, K. Mortensen, W.D. Semuguruka, A. Hay-Schmidt, M.V. Johansen, V. Dantzer. Neuronal nitric oxide synthase activity is increased during granulomatous inflammation in the colon and caecum of pigs infected with *Schistosoma japonicum*. *Autonomic Neuroscience: Basic and Clinical*. (Submitted).

ACKNOWLEDGEMENTS

I am deeply indebted to my supervisor Dr. Vet. Sci. Associate Prof. V. Dantzer for introducing me to the world of science, for her friendship, never failing enthusiasm, guidance and a close constant supervision and encouragement. I am indebted to my supervisors Associate Prof. W.D. Semuguruka and Dr. Sci. A. Hay-Schmidt for their tireless guidance, scientific support and excellent co-operation throughout my study period. I am grateful to Professor H.J.G. Gundersen for excellent scientific support and collaboration. I am also grateful to my co-scientists Prof. G.K. Mbassa, Drs. M.V. Johansen, K. Mortensen, and T. Iburg for the fruitful collaboration and thrilling discussions. I am thankful to the late, Prof. P. Nansen for valuable support and willingness to share his experience in the early stages of this work. I am highly indebted to Professors J. Jacobsen, P. Hyttel, A. Kassuku, D.M. Kambarage and Associate Prof. R.J. Assey for excellent working conditions.

I wish to highly acknowledge the financial assistance received from the Danish International Development Agency (DANIDA), the Danish National Research Foundation and Centre for Experimental Parasitology. Liaison between the Royal Danish Embassy in Dar-es Salaam, Tanzania, DANIDA Fellowship Centre, and my supervisors as well as excellent co-operation from staff at DANIDA Fellowship Centre has made this study successful and is deeply acknowledged.

Sincere thanks are due to Prof. A. Kassuku for allowing me to keep research animals at Magadu Research Animal Unit. Many thanks are due to Mr. Hussein Fadhili for taking very good care of the goats and maximum co-operation. Co-operation received from Mr. A.K. Mwigune and the rest of the staff at Magadu research animal unit in the upkeep of the animals is highly appreciated. It is my pleasure to thank Drs. M.V. Johansen, H. Bøgh and E. Sørensen and Ms C. Bergholdt for breeding the *S. japonicum* cercariae and infections and collaboration at sampling. Similarly, I thank Mr E. Nielsen for very good co-operation during sampling. The excellent technical assistance from Mrs G. Holden and A.M. Thomsen, Mr. J. Mwangalimi, Mrs M. Blenda, J. Mbessa, Mr. E. Sibala, M. Mukama, and Ms. M. Mwasampeta is greatly appreciated. I highly acknowledge Mrs H. Holm and G. Hahn for helping to prepare beautiful illustrations. I wish to thank Mr. D. Mkuki, Mrs B. Beyerholm and Dr. T. C. Santos for the excellent drawings, and Dr. C.D. Pfarrer for assistance with taking photographs. I salute associate Prof. Jose Braciani for excellent assistance with scanning electron microscopy, close friendship and hospitality. Assistance from Prof. B. Pakkenberg, Dr. T. Bock to use DMLB microscope is highly appreciated. The kind donation of the polyclonal rabbit anti-cow S-100 protein antibody by Dako, Glostrup, Denmark, monoclonal rabbit anti-swine substance P antibody by Dr. P.J. Larsen of Panum institute, Copenhagen University and monoclonal rabbit

anti swine-vasoactive intestinal peptide antibody by and Dr. J. Fahrenkrug, of Bispebjerg Hospital, Copenhagen, Denmark is highly appreciated. I warmly acknowledged Dr. C. Jones and Prof. D. Murell for their help with language corrections and scientific suggestions. Assistance received from A.A. Robert, Dr. H. Winther, Dr. A. Harrison and Dr. P.D. Thompsen with computer softwares is highly appreciated. I am very thankful to Mrs M Balisidya, N.P. Janet and L. Kolbøl for secretarial help. I am grateful to staff at the both the RVAU and Copenhagen University Libraries for excellent assistance to acquire literature material. I wish also to thank those not mentioned but did contribute substantially toward success of this work. To Mr. A.H. Mbarak, Ms D. Kilyeyi, J. Kahwa, and E. Begira, Dr. L.S.B. Mellau and all my royal friends, this work would have not been successful without you being close. I salute you all. To my daughter B. Kulwa, my father P. Begira, my mother V. Nyamwiza, I thank you very much for being very patient with my academic endeavours. Finally, I dedicate this thesis for the memory of my daughter the late Dotto Balemba and my closest friend and colleague Dr. C.B.K. Kahwa.

ABBREVIATIONS AND SYMBOLS

The following abbreviations were used in the thesis and the accompanying papers.

a	Area
a(fra)	Area fraction of the small frames used for counting (corrected for magnification)
a(sample)	Total area of sampling covered by using the X and Y step lengths in one field of vision.
ABComplex	Avidin biotin complex
AP(pp/js)	Area profile of the Peyer's patches in a tissue sample
APP(jej)	absolute area of the Peyer's patches in the jejunum
bNOS	Brain/neuronal/type I nitric oxide synthase
CC	Caecum
CE	Coefficient of error
CL	Colon
D	Dimensional
DD	Duodenum
DJ	Distal jejunum
DPX	Distren xylen plasticizer (mounting medium)
EC	Enterochromaffin
ENS	Enteric nervous system
EPP	External proprial subplexus
ESP	External submucous plexus
f	Fraction
F	Fields
G	Ganglion/ganglia
GSEP	Glandular subepithelial subplexus
H & E	Haematoxylin and Eosin
HRP	Horse radish peroxidase
5-HT	5-Hydroxytryptamine
ICM	Inner circular muscle layer
IFN-gamma	Interferon gamma
IGPP*	Interglandular proprial subplexus
IL	Ileum
IL-	Interleukin(s)
ILMM	Inner lamina muscularis mucosae

IPP	Inner proprial subplexus/internal proprial subplexus
IR	Immunoreactive/immunoreactivity
ISP	Inner (internal) submucous plexus
Jej	Jejunum
L/l	Length
LG	Length of ganglia/ganglion
Ljej	Length of jejunum
LMM	Lamina muscularis mucosae
LMMP*	Lamina muscularis mucosae subplexus
LP	Lamina propria
Lps	Length of primary sample
lss	Length of secondary sample
lts	Length of tertiary sample
MJ	Middle jejunum
MP	Myenteric plexus
mRNA	Messenger ribonucleic acid
MUC	Mucous plexus
n	Number of primary samples
N	Total number (neurons, or EC cells)
NADH	Dihydronicotinamide adenine dinucleotide
NADPH-d	Nicotinamide adenine dinucleotide phosphate-diaphorase
NANC	Non adrenergic non cholinergic
N_d	Numerical density
NF	Neurofilament protein(s)
NO	Nitric oxide
NOS	Nitric oxide synthase
OL	Outer longitudinal muscle layer
OLM	Outer longitudinal muscle layer
OPP*	Outer proprial subplexus
OSP	Outer submucous plexus
PBS	Phosphate buffered saline
PCP	Pericryptal subplexus
Pcor	The total number of corners of the sampling frame hitting the tissue
PJ	Proximal jejunum

Pjs	Point hitting on the grid which hit the sample during the estimation of the surface area of Peyer's patches
pp	Point hitting on the grid which hit the Peyer's patches during estimation of their surface area
PS	Primary nerve strand(s)
ps	Primary sample
PSE	*Plexus submucosus externus*
PSI	*Plexus submucosus internus*
PVP	Perivascular subplexus
Q	Total number of 3D count
qs	Quarternary sample
rand	Random
RC	Rectum
SEM	Scanning electron microscopy
SEP	Subepithelial subplexus
shr	Shrinkage
SP	Substance P
SS	Secondary nerve strand(s)
ss	Secondary sample
SVA	Submucous vascular arcade(s)
TI	Type one tertiary nerve strands
TII	Type two tertiary nerve strands
TS	Tertiary nerve strand(s)
ts	Tertiary sample
VIP	Vasoactive intestinal peptide
VP	Villous subplexus
W/w	Width
WG	Width of ganglia/ganglion
Who	Wholemount
WPS	Width of primary strand(s)
WSS	Width of secondary strand(s)

SUMMARY

The enteric nervous system (ENS) also called the little brain of the gut or the brain-in-the gut, is a complex system of intrinsic neurons, nerves and supporting cells, and the extrinsic afferent and efferent nerves of the sympathetic and parasympathetic divisions of the nervous system. The organisation of the ENS in the submucous and the mucous layers and the extent of ganglia in the mucous layer are not well established. Additionally, the effect of granulomatous inflammation induced by schistosoma infection is not adequately studied. In the present work, immunohistochemical, histochemical and histological methods were used to study the organisation of the ENS and changes caused by *Schistosoma japonicum* induced granulomatous inflammation in the intestine of the pig as well as the organisation of the ENS in the goat. A stereological study of vasoactive intestinal peptide (VIP) and nitric oxide synthase (NOS) immunoreactive (IR) neurons was also undertaken using the jejunum of the pig to establish a simple sampling method for estimating the number of neurons and other structures in the gut based on unbiased principles.

The first three chapters consist of literature reviews and highlight areas that are not well studied, and the objectives and findings of the present thesis. (1) In the first chapter, the current knowledge on the organisation of the enteric plexuses in the pig, man and other large mammals has been reviewed. (2) In the second chapter, a short review of morphometric studies on the ENS, enterochromaffin cells is presented. Pitfalls of previous studies that include biased sampling, use of distended organs, and problems associated with simple numerical densities and the objectives of the current work are also presented. (3) The third chapter consists of a review on some aspects of the ENS during inflammation and the life cycle of *S. japonicum* in the pig model. The mechanisms of neuroplasticity, interactions of the neuro-immune systems and alterations in nervous tissue caused by granulomatous inflammation during schistosoma infections are briefly reviewed. (4) Chapter 4 provides an overall discussion of the results obtained in the present study that are described briefly below and detailed in the accompanying **papers I-VI.**

Papers I-III the organisation of ENS was studied by VIP, neurofilament proteins (NF), substance P (SP), and NOS immunohistochemistry in wholemounts from the intestine of the pig and goat. The studies aimed to clarifying organisation mainly in the submucous and mucous layers and around Peyer's patches. In addition, S-100 protein immunostaining was used to study the ENS and clarify segmental and inter-plexus variations of the size of the ganglia, nerve strands and neurons among the ganglionated plexuses in the intestine of the goat. Chopped and paraffin sections were used to study the ENS in the small intestine of the pig whereas, paraffin sections from immuno-stained wholemounts were used to clarify the organisation in the mucous plexus (MUC) in the

intestine of both the pig and goat. The organisation of the submucous plexuses in the intestine of the pig and goat was very much similar with the OSP and ISP being situated at different topographical levels and clearly demarcated by the vascular arcades. The two plexuses differed also in the amount, size and shape of ganglia, and size of neurons as well as the staining pattern, intensity and density of VIP, SP, NF, NOS and S100 protein immunoreactivity (IR) in the nerves and neurons, and the respective proportions of IR neurons/ganglion. In the goat, large ganglia and nerve strands, S-100 protein and NF IR neurons in the OSP were polarised with respect to inner circular muscle and the primary nerve strands appeared mainly beneath the larger ganglia. These features showed further morphologic differences between the OSP and ISP compared to previous studies. Within each submucous plexus, two subplexuses, the outer and inner subplexuses were distinguished based on the topography and density of nerve meshworks, size and outline of ganglia and size of neurons. In the OSP, the outer OSP subplexus (*Plexus submucous extremus)* was composed of a network of small ganglia and nerves strands located immediately on the inner side of ICM. The inner OSP subplexus (Schabadasch's plexus) was composed of large ganglia and nerve strands located close to the submucous vascular arcades. In the ISP, the outer ISP subplexus (intermediate plexus) and inner ISP subplexus (Meissner's plexus) differed in the proportion of NOS IR/ganglion as well. The ISP was the only contributor to the plexus surrounding the follicles of the Peyer's patches as a continuous mesh of 3 ganglionated subplexuses. Sparse VIP IR nerve fibres and a dense network of SP IR nerves from the ISP were observed in the dome of the follicles in the small intestine of the pig and goat respectively. It was concluded that the organisation the ENS in submucous layer of large mammals is complex and is still not well elucidated. Therefore, morphological and corollary function studies were suggested to re-examine the need to distinguish existence of four plexuses in the submucous layer of large mammals.

In the mucous layer, a clearly oriented, inner proprial subplexus (IPP) was identified close to the crypt opening and the MUC was subdivided into the lamina muscularis mucosae subplexus (LMMP), outer proprial (OPP), interglandular proprial (IGPP), IPP, perivascular (PVP), villous (VP) and subepithelial (SEP) subplexuses. It was established that the MUC of both large and small intestine contained ganglia and isolated neurons being located at different topographic levels in the LMMP, OPP and IGPP. The perivascular, inner proprial, villous and subepithelial subplexuses were aganglionic. In the intestine of the pig, intramucosal ganglia and isolated neurons were abundant in the caecum, many in colon and ileum and few in the jejunum. Morphometric study in the goat showed the highest numerical density of intramucosal ganglia in the caecum followed by ileum, colon, duodenum, proximal jejunum, distal jejunum, rectum and the lowest density was seen in the middle jejunum. It was concluded that there are many small ganglia and isolated neurons in the MUC.

Therefore, it was suggested that the MUC in the intestine of the pig and goat to be considered as one of the major ganglionated plexuses, others being the ISP, OSP and the myenteric plexuses. The need to elucidate the functional significance of MUC was emphasised.

A study in the goat showed that in all plexuses, largest ganglia, nerve strands as well as S-100 protein IR neurons were found in the caecum and colon. They were medium sized in the duodenum, rectum, ileum and distal jejunum and relatively smaller in the middle and proximal jejunum. The size of ganglia, nerve strands and neurons were largest in the myenteric plexus and decreased gradually towards the mucosa. It was concluded that the observed segmental variations might explain differences in the total number and numerical densities (distributions) of neurons as well as functional differences between intestinal compartments and their ability to react and adapt differently during pathophysiological conditions. Due to the controversy of the names accorded to the submucous plexuses and the need for appropriate descriptive terminologies to name the plexuses in the submucosa and lamina propria, a number of new terminologies were suggested to name the submucous and mucous subplexuses.

Paper VI presents a novel, simple and cheap method for quantification of neurons, enterochromaffin cells and estimation of the surface area of Peyer's patches in the mammalian gut using unbiased principles. The results show an enormous amount of neurons in the pig jejunum. The total number neurons in the pig jejunum was ~68.4 x 10^6 and ~19.83 x 10^6 VIP and NOS IR neurons respectively. The number of intramucosal VIP IR neurons was larger than that observed in the myenteric plexus which shows that intramucosal neurons although a neglected entity could have great influence in the regulation of the mucosa. These data support the contention that the ENS is really the brain-in-the-gut. The total number of enterochromaffin cells was estimated to be 3.038 x 10^9 and the surface area of the Peyer's patches was 403.725 cm^2. Finally, the importance of the absolute total number of neurons in a defined segment when referring to the number of neurons in any morphometric investigations instead of numerical density was emphasised.

In **papers V and VI**, the effects of *S. japonicum* induced granulomatous inflammation on the enteric nervous tissue in the caecum and colon were studied in the pig model. Ganglia situated within or near granulomas showed ganglionitis, and necrosis of neurons as well as infiltration by eosinophils, mast cells, lymphocytes, plasma cells, neutrophils and macrophages. The inner submucous and mucous plexuses were the most damaged. The content of VIP in inflamed tissues was reduced. That of SP, NOS and nicotinamide adenine dinucleotide phosphatase-diaphorase (NADPH-d) was increased at lower levels of inflammation and decreased in severe lesions. The alterations of the levels of VIP, SP, NOS and NADPH-d correlated with severity of inflammation. More intensely stained neurons and varicosities were observed in tissue from prenatally and prenatally infected subsequent

postnatally challenge infected pigs compared with only postnatally infected pigs. Morphometry of the number of NOS IR neurons showed significant increase of the numerical density of NOS IR neurons in the ISP followed by the myenteric plexus and then the OSP. In both compartments, the highest number densities were recorded in the postnatally infected pigs. These findings support the concept that during inflammation, there is up and down regulation of neurotransmitters with alterations that is dependent of /on the level of inflammation occurring in selective pathways in the ENS. The observations show alterations of VIP, SP and nitric oxide contents in the local microenvironment in the SP-, VIP- and nitric oxide- mediated reflex pathways that regulate intestinal motility, epithelial transport and modulate immunity. These changes may cause alterations in bowel motility, electrolyte and fluid secretion, vascular and neuro-immune functions, influence the pathobiology of migration and egress of schistosome eggs, trapping of eggs in granulomas as well as tissue repair. Therefore, there is a need to study further neuroplasticity during schistosoma infections so as to elucidate the mechanisms of adaptation by the ENS as well as modulation of inflammation and influence to schistosome biology by the neuro-immune interactions.

Dansk titel: Organisationen af det enteriske nervesystem fra svin og ged og ændringer induceret af granulomatøse inflammationer i svin inficeret med *Schistosoma japonicum*.

Dansk sammendrag

Nervesystemet i fordøjelseskanalen, det enteriske nervesystem (ENS), også kaldet "tarmens lillehjerne" er et komplekst system af intrinsic neuroner, nerver og støtteceller, og extrinsic tilførende/afferente og fraførende/ efferente nerver fra det sympatiske og parasympatiske nervesystem. Organisationen af ENS i tela submucosae og tunica mucosae samt udbredningen af ganglier i tunica mucosae og tela submucosae er ikke godt klarlagt. Desuden er effekten af granulomatøs inflammation, der skyldes schistosome infektion, ikke tilstrækkeligt undersøgt. I dette arbejde er der brugt forskellige immunohistokemiske, histokemiske og histologiske metoder for at klarlægge den histologiske opbygning af ENS i tarmvæggen hos svin og ged, samt de ændringer, der induceres ved infektion med *Schistosoma japonicum* hos svin. Et stereologisk studium af vasoactive intestinalt peptid (VIP) og nitric oxid syntase (NOS) immunoreaktive (IR) neuroner i svinets jejunum er brugt som model for udviklingen af en enkel og hurtig metode til at skønne det totale antal af disse immunoreaktive neuroner baseret på unbiased/objektive principper. Denne systematiske metoden, der er beskrevet i detaljer, vil kunne anvendes på hvilke som helst andre genkendelige strukturer i tarmvæggen, når der anvendes "wholemounts" og dermed bidrage til at opnå gode histologiske data, der kan korreleres til funktionelle og patofysiologiske data.

De første 3 kapitler består af litteraturoversigter og fremhæver de områder der bør studeres nærmere, hvilket leder frem til formålet med dette arbejde og de resultater, der er opnået. (1) I det første kapitel gives en opdatering af den viden der findes om organiseringen af ENS hos svin, menneske og andre større pattedyr. (2) I det andet kapitel gives en kort gennemgang af de stereologiske studier af ENS og de enterochromaffine celler i tarmvæggen, der sammenholdes med de fejlkilder der kan henhøres til udtagningmønster, brug af udspilede organer og problemer med simple numeriske densitets målinger, hvilket fører frem til formålet, at udarbejde en metode der ved enkle og billige midler kan give et særdeles godt skøn over antallet af en given genkendelig struktur i tarmkanalen. (3) Det tredje kapitel giver et overblik over nogle af de aspekter der skyldes infektioner og som kan relateres til livscyklus og infektion med *Schistosoma japonicum*. Mekanismen bag "neuroplasticity", interaktion med nervesystemet og immunapparatet i tarmkanalen forårsaget af granulomatøs infiltration under schistosom infektion er ganske kort belyst.

(4) Kapitel 4 giver en generel diskussion af de opnåede resultater som her beskrives kortfattet, men mere detaljeret i de medfølgende 6 artikler **I-VI.**

I artiklerne **I-III** er studier af det ENS´s organisation og arkitektur belyst ved VIP, neurofilament (NF), substance P (SP) og NOS IR i wholemounts fra gris og ged. Studierne har hovedsageligt haft til formål at belyse opbygningen i tela submucosae og tunica mucosae samt deres relation til de lymfatiske områder, Peyer's pletter. Desuden er der blevet anvendt, immunohistokemisk farvning for S-100 protein for, blandt de ganglionære plexus'er i gedens tyndtarm, at belyse størrelsesvariationer af ganglier, nerve fibre og neuroner, både mellem tarmafsnit og imellem plexus'er i tarmvæggen. Der blev brugt "chopped", (50-100 µm tykke snit) og paraffinsnit for at studere ENS i svinets tyndtarm. Mens paraffinsnit fra wholemounts blev brugt til at opklare organisationen i slimhinde plexus fra både svin og ged.

Organisationen af det submukøse plexus i tarmvæggen fra svin og ged havde store ligheder, idet beliggenheden af det ydre og indre submukøse plexus'er på to forskellige niveauer var tydeligt adskilt ved karbuerne. De to plexus'er adskilte sig dog ved mængde, størrelse og form af ganglier, størrelse af neuroner samt farvningsmønster og intensitet samt tætheden af VIP, SP, NF, NOS og S-100 protein immunoreaktivitet i nervefibre og nerveceller samt ved proportionen af IR neuroner per ganglion. I geden var store ganglier og nervefibe i det ydre plexus, S-100 protein og NF IR, polariserede med hensyn til det indre cirkulære lag i tunica muscularis og med de primære nervefibre beliggende hovedsageligt under de store ganglier. Disse fund viser yderligere morfologiske forskelle mellem det ydre og indre submukøse plexus i forhold til tidligere studier. Indenfor hvert af de to plexus'er ses to underplexus'er. De ydre og indre underplexus'er kunne differentieres på grund af topografi og netværkstæthed, størrelse og afgrænsning af ganglier og på størrelsen af neuronerne. I det ydre submukøse plexus er det ydre underplexus sammensat af et net af små ganglier og nerver fibre placeret tæt op ad tunica muscularis, medens det indre underplexus (Schabadasch's plexus) består af store ganglier tæt ved karbuerne i tela submucosae. I det indre submukøse plexus kan det ydre underplexus (intermediære plexus) og det indre underplexus (Meissner's plexus) adskilles ved proportionen af NOS IR ganglier. Det er kun det indre underplexus der bidrager til det plexus, med 3 undergrupper, der ses omkring Peyer's pletter. Få VIP IR nervefibre og et tæt netværk af SP IR nerver fra det indre submukøse underplexus kunne ses i folliklernes "dome" i tarmen fra såvel gris som ged.

Det kunne konkluderes, at organisationen af ENS i tela submucosae fra større pattedyr er kompleks og ikke fuldt klarlagt. Derfor bør yderligere morfologiske og sammensatte funktionsstudier udføres for at vurdere om der er basis for at inddele ENS plexus i tela submucosa i disse 4 underplekser.

Slimhinden's ENS kunne underinddeles i følgende underplexus'er: et tæt ved lamina muscularis mucosae (LMMP), ydre propia plexus (OPP), interglandulært plexus (IGPP), et velorienteret indre propria plexus (IPP) tæt ved kryptåbningerne, et perivaskulært plexus (PVP), et villus plexus (VP) og et subepithelialt plexus (SEP). Det blev konstateret at slimhinden i både tynd og tyktarm indeholder ganglier og isolerede neuroner i forskellige topografiske niveauer i LMMP, OPP og IGPP, mens det PVP, IPP, VP og SEP var uden ganglier. Ganglier og isolerede neuroner i slimhinden i svinets tarm forekom i rigelig mængde i cecum, der var mange i colon og ileum, men kun få i jejunum. Morphometriske studier fra ged viste den højeste numeriske densitet af ganglier i slimhinden i cecum fulgt af ileum, colon, duodenum, proksimale jejunum, distale jejunum og rectum med den laveste densitet i den midterste del af jejunum.

Det kunne konkluderes, at der var mange små ganglier og isolerede neuroner i slimhinden. Derfor foreslås det, at plexus'et i slimhinden skal betragtes som et af de store plexus'er i tarmvæggen, hvor det indre og ydre submukøse plexus og myenteric plexus er de tre andre velkendte plexus'er. Der er et stort behov for at få belyst den funktionelle betydning af dette store plexus i tarmkanalens slimhinden.

Studiet i ged viste at de største ganglier og nervefibre samt S-100 IR neuroner fandtes i cecum og colon, mens de var mellemstore i duodenum, rectum , ileum og distal jejunum og relativt mindre i den midterste og proksimale del af jejunum. Ganglier, nerve fibre og neuroner var størst i plexus myentericus og aftog i størrelse mod lumen. Det kunne konkluderes, at de observerede segmentelle variationer vil kunne bidrage til at forklare forskelle mellem tarmafsnit og deres evne til at reagere og tilpasse sig på forskellig vis under patofysiologiske tilstande. Grundet de diskussioner, der er vedrørende terminologien for plexus'erne i ENS i tela submucosae og tunica mucosae er der et behov for en beskrivende terminologi som er fremført i disse artikler og baseret på de ovennævnte undersøgelser.

Artikel **IV** beskriver en ny enkel og billig metode baseret på unbiased/objektive kriterier, der kan bruges til kvantificering, her vist ved eksempler på kvantificering af neuroner, enterochromaffine celler og Peyer's pletter i pattedyrs tarmvæg. Resultaterne viste en enorm forekomst af neuroner i svinets tyndtarm, jejunum. Det totale antal af VIP-positive neuroner var 68.4×10^6 og for NOS 19.828×10^6. Antallet af VIP IR neuroner i slimhinden var større end i plexus myentericus, hvilket viser at neuroner i slimhinden kan have stor indflydelse på regulering af slimhindens funktioner. Dette understøtter teorien om at ENS virkelig er tarmens "lillehjerne". Det totale antal enterochromaffine celler er vurderet til at være 3.038×10^9 og Peyer's pletternes overfladen 403.725 cm^2. Betydningen af at kunne bestemme det absolutte, totale antal neuroner i et givet tarmafsnit i forhold til data der angiver numerisk densitet fremhæves.

I artiklerne **V og VI** studeres effekten af *S. japonicum* induceret granulomatøse forandringer på ENS i svinets caecum og colon. Ganglier i eller nær granuloma viste ganglionitis og nekrose af neuroner såvel som infiltrationer med eosinofile celler, mastceller, lymfocytter, plasmaceller, neutrofile celler og makrofager. Det indre submukøse og det mukøse plexus var det mest beskadigede. Indholdet af VIP IR i inflameret væv var reduceret, hvorimod SP, NOS og nicotinamide adenine dinucleotid phosphatase-diaphorase (NADPH-d) blev forøget ved lavere grader af inflammation og nedsat ved alvorlige lesioner. Ændringerne i niveauet af VIP, SP, NOS og NADPH-d er korreleret til graden af inflammation. Kraftigere immunofarvning i neuroner og Avaricosities" sås i væv fra prenatalt inficerede og fra prenatalt og reinficerede grise sammenlignet med kun postnatalt inficerede svin. Morphometri til bestemmelse af antallet af NOS IR neuroner viste en signifikant stigning i den numeriske densitet af NOS IR neuroner i det indre submucøse plexus efterfulgt af plexus myentericus og så det ydre submucøse plexus. I begge afsnit var den højeste numeriske densitet målt i de postnatalt inficered svin. Disse observationer understøtter teorien om, at der under betændelsestilstand er en op- og ned- regulering af neurotransmittorer. Ændringerne er afhængige af niveauet af inflammation og de optræder i selektive forbindelser i ENS. Observationen viser at der sker ændringer af VIP, SP og NOS indholdet i mikromiljøet omkring SP, VIP og NOS-medierede refleksforbindelser, der regulerer tarm motilitet, epithelial transport og immunitet. Disse ændringer kan fremkalde forandringer i tarmens motilitet, elektrolyt og vædske sekretion, vaskulære og neuro-immun funktioner, påvirkning af patobiologien under vandring og udstødelse af schistosom æg, afgrænsning af æg i granuloma såvel som vævs rekonstitution. Der er således et behov for at belyse neuroplasticiten under schistosom infektion for at opnå viden om hvorledes ENS tilpasser sig, samt hvorledes inflammationen moduleres og påvirkes af schistosome biologien via neuro-immun-interaktioner.

CHAPTER 1: ORGANIZATION OF THE ENTERIC NERVOUS SYSTEM

1.1 Introduction

The enteric nervous system (ENS) is the third component of the autonomic division of the nervous system (others being the parasympathetic and sympathetic) (Langley, 1921). It is a complex system of the intrinsic enteric neurons, nerves and supporting cells, and the extrinsic nerve processes of the sympathetic and parasympathetic nervous system embedded in the wall of the gut (Fig. 1). The ENS extends from the pharynx to the anal sphincter and into the pancreas and gall bladder (Costa et al., 1987). The ganglia in the ENS are interconnected to form a nervous system with mechanisms for reflexes, integration and processing of information like those in the brain and spinal cord. The ENS organises and co-ordinates the activity of the effector system namely musculature, mucosal epithelium and vasculature to produce meaningful patterns of behaviour in the specific organ (Wood, 2000). The ENS also has many similarities with the brain including structural features (Brehmer et al., 1994) and functional capacity of programming different behaviour patterns, neurotransmitters chemistry, and the organisation of microcircuitry with sensory neurons, interneurons and motor neurons (Wood, 2000). Hence, it is to day regarded as the little brain or the brain-in-the-gut (Wood, 2000; Grundy et al., 2000).

The ENS was discovered about 150 years ago by Meissner (1857) and Auerbach (1862, 1864) when they first observed ganglionated plexuses that for a long time has been bearing their names (Furness et al., 1988). However, the functional significance of the ENS being capable of instituting reflex activities independent of the central nervous system was established about 32 years later by Bayliss and Starling (1899, 1900 a, b). Since then the ENS has been the goal of many studies aiming at: (a) unravelling its intricate organisation (topography, structure, architecture), neuronal cell types and variability of neuronal phenotypes and their projections, and dynamics of its development (microscopic Anatomy), (b) understanding it physiological functions and phamarcological actions, and (c) understanding how these aspects are affected by factors such as age and pathophysiological conditions.

In any mammalian species the ENS contains vast neuronal populations (10^7-10^8) approximating to the number of neurons in the spinal cord (Furness and Costa, 1980). Considering the large numbers of neurons in the stomach and large intestine, the number of neurons is probably larger than that in the spinal cord (Gabella, 1990). There are enormous differences in the extent of the enteric plexuses when equivalent compartments of the gut in different mammals are compared and thereby the organisation and neuronal phenotype compositions (Gabella, 1990; Timmermans et al., 1997, 2001; Brehmer et al., 1999).

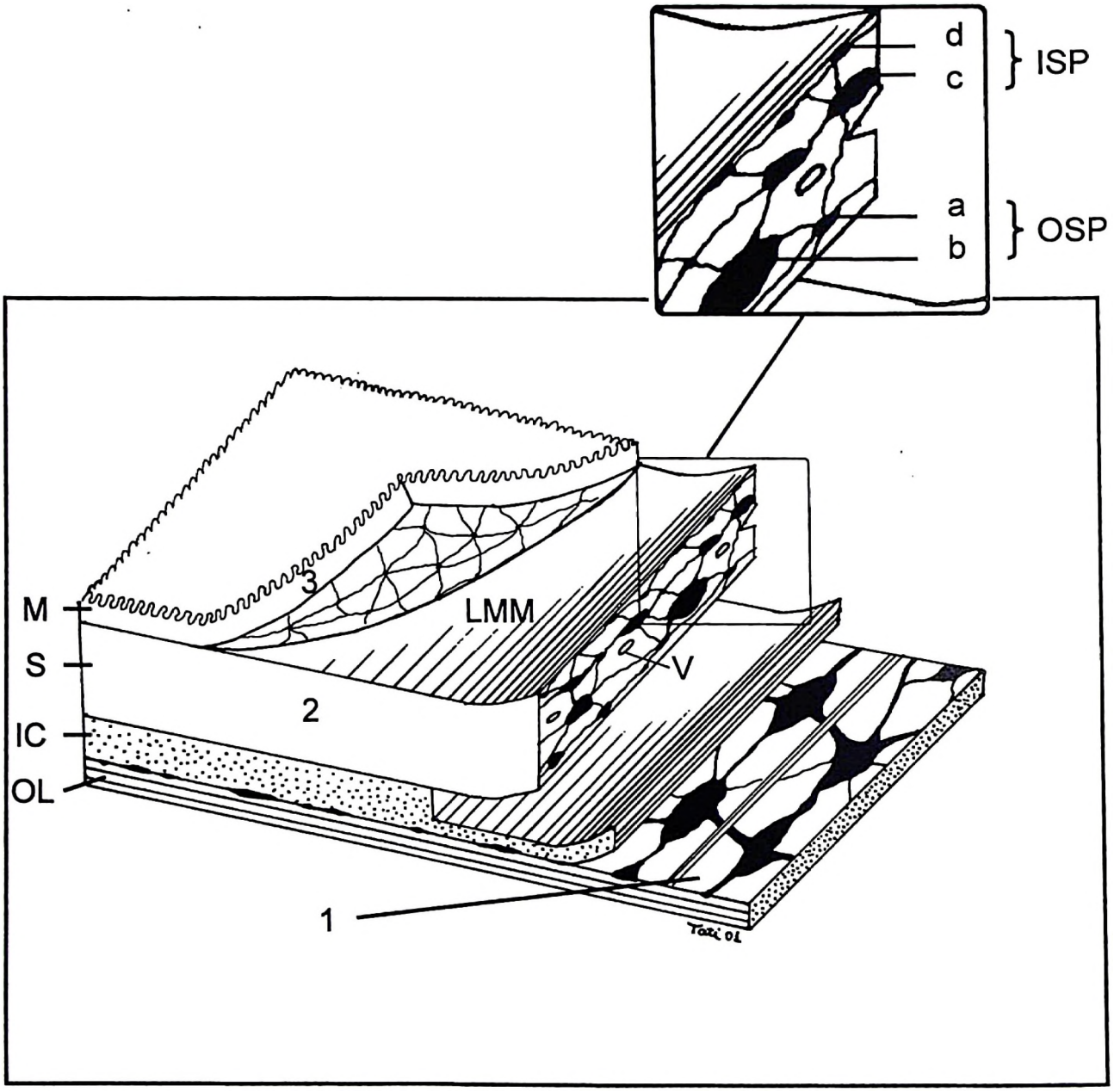

Fig. 1. Schematic drawing (not to scale) illustrating microdissection of the three main layers (wholemounts) namely the myenteric plexus (1), the submucous plexus (2) and the mucous plexus (3) usually done under a stereoscopic microscope as well as the network of ganglia and nerve fibres seen in each layer (wholemount) after staining. In the submucous layer, ganglia vary in size and topography. Using the submucous vascular arcades as the landmark (arrow) one can split the submucous layer into the outer and inner layers which contain the outer (OSP) and inner (ISP) submucous plexuses respectively. In the pig and goat, by using appropriately stained wholemounts it is possible to differentiate two subplexuses in each of the submucous plexuses namely the outer OSP subplexus (a) and inner OSP subplexus (b) in the OSP, and the outer ISP subplexus (c) and inner ISP subplexus (d) in the ISP. Notice small ganglia often seen in the outer proprial plexus (OPP) in the subgalandular region in the mucous plexus. Lamina muscularis mucosae (arrow head) is usually dissected along with the submucous layer. The inner circular (IC) and outer longitudinal muscle (OL) layers are also shown.

The structure of the ENS ganglia is very dynamic, their dimensions change during contraction and relaxation of muscles, causing reorganisation and changes in the shapes of neurons. They undergo vast changes in form and composition during growth, senescence and pathological conditions (Gabella, 1990).

Two types of nerve meshworks can be differentiated in the ENS. One is that comprised of ganglia which are linked by the internodal stands to form the major ganglionated plexuses. Two, is the nerve meshworks comprised of aganglionic nerves strands (fascicles) and fibres with extremely sparse isolated neurons or networks of exclusively nerve strands and fibres without any neurons.

1.2 Staining methods

The understanding of morphological complexities of ENS has been fostered by various staining methods to visualise neuronal perikarya, their cytoplasmic extensions, glia and Schwann cells, and nerve strands (Gabella, 1979; Furness and Costa, 1980; Furness et al., 1988; Stach, 1989; Timmermans et al., 1992, 1997, 2001). These methods include the conventional stains such as methylene blue and toluidine blue, silver stains, Giemsa stain, cuprolinic blue, histochemical methods and immunohistochemical methods for neurochemical coding and retrograde tracing chemicals for elucidating projections of neurons (Gabella, 1976; Karaosmanoglu et al., 1996; Timmermans et al., 1997, 2001). Special techniques such as scanning electron microscopy (SEM) (Scheuermann et al., 1986; 1987a, b) and transmission electron microscopy (Gabella, 1979; Scheuermann et al., 1991; Mestres et al., 1992b; Brehmer et al., 1994) have also been used. The success in the vast majority of these studies is credited to the character of the gut wall to be separable into several laminae, the wholemounts (Fig. 1).

1.3 The ENS plexuses

1.3.1 Subserous plexus

It is comprised of fine branches of nerves located between the serosa and outer longitudinal muscle layer (OLM) connecting extrinsic nerves with intrinsic nerves. It is prominent close to the mesenteric attachment and has few small ganglia that are usually seen occasionally in the stomach and large intestine (Furness and Costa, 1980; Furness et al., 1988). The subserous plexus is associated with the intestinal pacemaker cells, the interstitial cells of Cajal on the inner side (Thuneberg, 1989).

1.3.2 Muscular plexuses

The muscular plexus is mainly comprised of aganglionic nerve strands embedded in the interstitial connective tissue between smooth muscles cells coursing parallel to smooth muscles (Furness and

Costa, 19980, 1987; Furness et al., 1988). The muscular plexus can be subdivided into the longitudinal muscle plexus, circular muscle plexus and a specialised plexus called the deep muscular plexus which is found in the small intestine. The latter, consist a dense network of anastomosing nerve strands with few or no ganglia lying between the outer and inner laminae of the circular smooth muscle layer (ICM) (Furness and Costa, 19980, 1987; Furness et al., 1988) and is intimately associated with the interstitial cells of Cajal on the outer side (Thuneberg, 1989).

1.3.3 Myenteric plexus

The ENS has been for a long time recognised as having two ganglionated plexuses the myenteric (Auerbach's) plexus and the submucous (Meissner's) plexus (Furness and Costa, 1980; Scheuermann et al., 1987a-c; Timmermans et al., 1992). However, to date, it is well founded that in large mammals the ENS comprises at least three ganglionated plexuses namely the myenteric, outer submucous (OSP) and inner submucous (ISP) plexuses (Scheuermann et al., 1987a; Timmermans et al., 1992; 1997, 2001; Pearson, 1994; Balemba et al., 1999; **Papers I, III**). The myenteric plexus is a system ganglia and interconnecting nerve strands that extends, uninterrupted, from the most oral part of the oesophagus to the margin of the internal anal sphincter, around the full circumference of the digestive tract between the outer and inner muscle layers of tunica muscularis. The myenteric plexus is sandwiched in a network of interstitial cells of Cajal to which it is intimately linked (Thuneberg, 1989). Isolated neurons are also found in nerve strands. It is well developed in the terminal rectum and oesophagus between striated muscle fibres and their motor end plates (Furness and Costa, 1987; Furness et al., 1988; Gabella, 1990).

Based on the size of ganglia and nerve strands, location, orientation and architectural cross linkages, the myenteric plexus can be subdivided into the primary, secondary and tertiary components. The primary plexus is formed by ganglia and internodal nerve strands. The secondary component is composed of fine nerve strands branching from primary (internodal) strands and ganglia. Usually they do not link adjacent ganglia. They run parallel to ICM and often cross primary strands. The secondary plexus is located between the ICM and the primary plexus and can be traced into the ICM. Tertiary plexus is made up of the most fine nerves in the spaces between the meshwork formed by the primary plexus at the interface between the longitudinal and circular muscle layers (Furness and Costa, 1987). The size, shape and orientation of ganglia vary between species and intestinal compartments. However, in the jejunum-ileum in the guinea pig, mouse and sheep the pattern of the myenteric plexus is uniform both around the circumference and length showing no obvious gradient in any structural parameter and has a constant neuronal density. In the colon of the guinea pig, ganglia are very large and extensively fused with one another and show variations along the mesenteric-antimesenteric axis,

and it is thicker with narrow mesh beneath taenia (Gabella, 1990). The patterns of segmental variations of the myenteric plexus along the whole intestinal tract are not well established. In the present study (**Paper III**) all plexuses showed a similar pattern of segmental variations with significantly larger ganglia, nerve strands and neurons being observed in the caecum and colon compared to other compartments which however, showed some variations between themselves.

1.3.4 Submucous plexuses (overview)

The organisation of the enteric ganglia and nerve strands in the submucous layer is complex compared to that of the myenteric plexus. Ganglia are distributed at different topographical levels showing differences in structure, orientation, compactness and branching patterns of nerve strands. They also differ in the size of neurons, compositions of neuronal phenotypes and neuronal projections (Gunn, 1968; Stach, 1977; Scheuermann et al., 1987b; Timmermans et al., 1992, 1997, 2001; Brehmer et al., 1999; **Papers I, III, IV, V, VI**). As a result, the description of the total number of distinct plexuses in the submucous layers has not been consistent even in the same animal species. The present literature shows three distinct plexuses, the OSP, ISP and an intermediate plexus in the submucous layer in the intestine of humans and two plexuses namely the OSP and ISP in the intestine of other large mammals (Timmermans et al, 1997, 2001, for review). However, the OSP and the ISP (Scheuermann et al., 1987b; Timmermans et al., 1992, 1997, 2001) are the most studies. Bearing in mind their historical precedence and the amount of knowledge for these two plexuses, they are considered first mainly by focusing on the characteristics to identify them and their differences. In the intestine of pig and other larger mammals, the OSP and ISP are situated at two different topographical levels and are generally demarcated by the submucous vascular arcades. The OSP is situated in a dense connective tissue on serosal side close to the ICM. The ISP is located on mucosal side close to lamina muscularis mucosae (LMM) (Scheuermann et al., 1987a, b; Thompsen et al., 1997; Timmermans et al., 1992, 1997, 2001; Balemba et al., 1999; **Papers I, III, IV**). They differ in amount, shape, outline and size of ganglia, amount, aggregation and size of neurons, and width and tortuousness of nerve fibres (Mannl, et al., 1986; Stach, 1977; Scheuermann et al., 1987a, b; Krammer and Kühnel, 1992; **Papers I, III, IV**), as well as in electrophysiological properties (Pearson et al., 1997; Thompsen et al., 1997). The glial cell mass (glia index) is more abundant in OSP than ISP, and the OSP meshwork is wider than that of ISP (Brehmer et al., 1994; Thompsen et al., 1997). Direct membrane to membrane appositions between neuronal perikarya and compartmentalisation of neurons by the neuropil are found in the ISP (Brehmer, 1994). The two submucosal plexuses also vary in the distributions of distinct neuronal phenotypes and the proportions of distinct neuronal populations that project into the mucosa or into the myenteric and muscular layers

(Timmermans et al., 1990, 1997, 2001 for review; **Papers I, III-VI**) with viscerofugally projecting neurons being exclusively located in the OSP. Clearly, the two interconnected submucous plexuses in the intestine of large mammals are morphologically distinct and perform different functions (Timmermans et al., 1990, 2001). However, there are reports documenting two submucous plexuses in the colon of the guinea pig and four plexuses in the intestine of large mammals indicating even a more complex organisation as highlighted hereafter.

1.3.4.1 *Plexus submucous extremus*

The *Plexus submucous extremus* also called *Plexus entericus submucosus extremus* is a delicate ganglionated plexus closely associated with the ICM on the inner side. It was observed first by Stach (1972) in the colon of rat and guinea pigs and later on was confirmed in the human colon (Hoyle and Burnstock, 1989a; Wedel et al., 1999. Its larger nerve fascicles contain isolated neurons, small and medium sized ganglia and are oriented parallel or oblique to the ICM. In the small intestine of the pig (**Paper I**), goat (**Paper III**) and cattle (Balemba et al., 1999), OSP ganglia were observed at different topographical level. In a way, these observations reflect the possibility for the existence of the *Plexus submucous extremus* also in the small intestine of these species.

1.3.4.2 Outer submucous plexus (OSP)

The OSP is also called Henle's, or Schabadasch's plexus or external submucosus plexus (ESP) or *Plexus submucosus externus* (PSE). It is situated in the outer region of the submucosa against the ICM (Gunn, 1968; Scheuermann et al., 1987b; Timmermans et al., 1990, 1992, 1997, 2001; Balemba et al., 1999, **Papers I, III, IV**). The OSP is also defined as a plexus closely associated with plexus submucous extremus being composed of larger ganglia and thicker nerve strands compared to the former (Wedel et al., 1999). The composition of the ganglia resembles that of the myenteric plexus with neurons being loosely arranged (Gunn, 1968, **Paper III**). The degree of development varies widely in different regions. In most regions of the small intestine it is thin and poorly developed while in the colon of herbivores it is very thin and is not found in all preparations. In sheep it is well developed in distal ileum with large ganglia and large neurons. The contrast between OSP and ISP is not so great since the OSP is composed of smaller ganglia (Gunn, 1968). However, a study in the goat (Paper III) revealed the OSP to be well developed in the whole intestinal tract of the goat and new features showing clear morphological differences between the OSP and ISP. The OSP regulates motor activity of both the ICM and outer longitudinal smooth muscle layer and is suggested to be a relay station between the ISP and myenteric plexuses (Timmermans et al., 1992, 1997, 2001; Hens et al., 2000). Retrograde tracing techniques by using a lipophylic dye

1,1′-didodecyl-3,3,3′, 3′-tetramethyl indocarbocyanine perchlorate (DIL) show that the OSP could plays a role in the regulation of absorption and secretion as well as the activity of LMM (Timmermans et al., 2001). Apparently, morphological and functional differences between the OSP and *Plexus submucous extremus* are not well established. In addition, there is no clear-cut line of demarcation between the two thus, in most reports these plexuses are described as the OSP.

1.3.4.3 Intermediate plexus

The third, intermediate plexus was observed first by Gunn (1968) and thereafter by Stach (1977) in the small intestine of pig, and has now been confirmed in the intestine of humans (Timmermans et al. 1997, 2001, for review). In the human colon, the intermediate plexus is located closer to the LMM than to the ICM and assuming a similar distribution of ganglia between ISP and OSP, it constitutes about 52% of the ganglia in the ISP (Hoyle and Burnstock, 1989b). The intermediate plexus was also reported in the colon of opossum (Christensen and Rick, 1987). In the pig, the intermediate plexus has compact and convoluted fibre tracts of smaller calibre than those of OSP and is usually closely associated with ISP. The ganglia are compact and enclosed by a very prominent capsule. Small ganglia are globular, larger ones are oval or irregular. It seems to be present in certain regions of the gut being more prominent at the ileo-colic sphincter (Gunn, 1968). In humans, the OSP, intermediate plexus and ISP differ in the structure, and chemistry and projection of neurons. In the small intestine, the intermediate plexus resembles phenotypically the ISP (Dhatt and Buchan, 1994) whereas in the large intestine, it shows similarities to the OSP (Crowe et al., 1992; Porter et al., 1999).

1.3.4.4 Inner submucous plexus

The ISP also called Meissner's plexus or internal submucous plexus (ISP) or *Plexus submucosus internus* (PSI) is located close to the outer surface of LMM (Gunn, 1968; Scheuermann et al., 1987a, Timmermans et al., 1990, 1992, 1997, 2001; Wedel. et al., 1999; Balemba et al., 1999; **Papers I, III-VI**). It is composed of compact and numerous ganglia with much smaller and more regular patterned meshworks than the OSP (Gunn, 1968; Scheuermann et al., 1987a). Its neurons are small unipolar or bipolar, globular or pear-shaped with eccentrically placed nuclei (Gunn, 1968). In the small intestine of the pig, the ISP ganglionic clusters and nerve fibre strands were observed at two topographic levels. The smallest ganglia were situated close to and associated with LMM (Scheuermann et al., 1987a). A similar observation was reported in the small intestine of pig (**paper I**), calves (Balemba et al., 1999) and goat (**paper III**) leading to a suggestion for further subdivisions of the ISP into the inner and outer ISP subplexuses. These observations indicate the possibility for distinguishing two distinct ganglionated networks within the ISP, namely, the intermediate plexus and

ISP, although functional differences between the two subplexuses have not yet been described in these species.

In the pig, submucosal vascular arcades (which demarcate the OSP from ISP, see above) underlie the lymphoid follicles in the Peyer's patches (Lowden and Heath, 1994). However, the OSP ganglia were observed close to the base of the lymphoid follicles and those of ISP were seen in the interfollicular regions (Krammer et al., 1993) indicating that the organisation of the ENS plexuses in the in the Peyer's patches need to be further elucidated (**Paper I**). There is no agreement on the exact number of distinct plexuses in the submucous layer of man and large mammals and it is not yet clear which system of nomenclature should be adopted (Hoyle and Burnstock, 1989b; Scheuermann et al., 1987a, b; Crowe et al., 1992; Timmermans et al., 1992, 1997, 2001; Balemba et al., 1999; Wedel et al., 1999, **Paper I, III, IV**). These issues need to be properly addressed to avoid confusion (Scheuermann et al., 1987a; Hoyle and Burnstock, 1989b) and to ensure consistency both in descriptive and morphometric reports thus facilitating the availability and use of comparable results between different laboratories.

1.3.5 Mucous plexus

The mucous plexus in the enteric nervous system (ENS) is a dense network of fine interconnecting nerve bundles found through out the lamina propria and is divided into 3-4 different subplexuses namely a subglandular plexus, a periglandular plexus, vascular plexus and a villous subepithelial subplexus (Furness and Costa, 1980; Furness et al., 1988). Costa and Brookes, (1994) described 5 subplexuses by subdividing the vascular plexus into the perivascular plexus as fine anastomosing nerve strands which supplies the arterial innervation and the paravascular nerves which followed the arterioles. Keast et al. (1984) proposed subdivision of nerve fibre meshwork in the lamina propria into a subepithelial plexus being adjacent to mucosal epithelium and close to the crypts, and a loose network in the lamina propria.

About 120 years ago, it was reported for the first time that there are neurons in the in the mucous layer in cattle (Drasch, 1881; Vau, 1932). Similar observations were subsequently reported in the stomach and intestine of man (Stöhr (1934, 1944), in the colon and rectum of cows (Lassmann, 1975) and in rat ileum (Newson et al., 1979). Thereafter, many observations of ganglia and isolated neurons in the mucosa have appeared in different animal species and different intestinal segments (**Papers I-VI**). It has been reported that in the colon of rat, mucosal neurons play a role in regulating electrolyte transport (Bridges et al., 1986). Recent studies in the colon of rat (Mestres et al., 1992a, b), in the small intestine (Fang et al., 1993) and colon of humans (Wedel et al., 1999) and the present study (**Papers II-VI**), refute the previous suggestion that intramucosal neurons are ectopic from the

submucosa (Stöhr 1934, Lassmann 1975). However, in the previous studies, extent of ganglia and neurons in the mucous plexus was not well established. There appears to be less studies of the organisation of the mucous plexus that are based on the use of wholemounts.

Immunohistochemical methods, a tool for neurochemical coding have played a significant role to elucidate the organisation of the enteric plexuses (Gabella, 1976; Furness and Costa, 1980; Furness et al., 1988; Timmermans et al., 1997, 2001, **Papers I-IV**). VIP and SP outlined the organisation of the ENS in the small intestines of pig and showed differences in the proportion of IR neurons among the ISP and OSP (Timmermans et al., 1990). Pooled antisera against neurofilament proteins (NF 200, 70 and 60Kda) revealed clearly the organisation in the pig small intestine (Krammer and Kühnel, 1992) and the sheep omasum (Yamamoto et al., 1994). S-100 protein allowed delineation of superimposed OSP and ISP and was commended for defining structural and topographical relationship of different subplexuses in the small intestine of the pig (Scheuermann et al., 1989). The organisation of the ENS in the small intestine of pig has been studied mainly by immunohistochemistry (Timmermans *et al.*, 1990, 1992; Krammer et al., 1992) and SEM (Scheuermann et al., 1986, 1987a, b). The most recent study by conventional light microscopy is that of Mannl et al. (1986) using toluidine blue and safranin staining to reveal topographical and neuronal differences between the two submucosal plexuses. There are marked species differences in the organisation of ENS of mammals (Timmermans et al., 1992, 1997; Brehmer et al., 1999) however, there is apparently only one study on silver impregnation and cholinesterase staining of the ENS in the goat (Gunn, 1968). Therefore, immunohistochemical and histological methods were used to study the ENS in the intestine of pig and goat. Emphasis was put on the organisation of the ENS in the submucous the mucous layers.

In contrast to conventional cross-sections by which the characteristic network interconnections are not depicted clearly, wholemounts almost completely preserve the integrity of the plexuses providing a clear demonstration of the organisation of ENS. Therefore, wholemounts have been extensively used to unravel the complexities of the organisation of the ENS. However, stretching which is mandatory in order to obtain optimal separation of different plexuses decreases the distance between the topographical levels of the plexuses, causes flattening of ganglia and enlargement of interganglionic area so that the *in situ* topography and structure of ganglia are altered (Wedel et al., 1999). Therefore, the combination of both wholemounts and sections might reveal better the 3D topographical and architectural organisation of plexuses in the ENS.

1.4 Objectives of the study

-To study the topography, architecture and structure of the ENS in the intestine of large mammals, the pig and goat.

-Clarify the organisation of the submucous plexuses by establishing clear-cut landmarks and structural features to differentiate them.

-Elucidate the organisation and determine the numerical density of ganglia to study the extent of ganglia and isolated neurons in the mucous plexus in order to provide data which might be of importance for further morphological and functional investigations.

-To give suggestions on the nomenclature of plexuses in the ENS.

What was accomplished with respect to these objectives is shown in **papers I-III** and also shown partly in **papers IV-VI.**

CHAPTER 2: MORPHOMETRIC STUDIES OF THE ENS, EC CELLS AND PEYER'S PATCHES

2.1 Introduction

It may be comparatively easy to show clear-cut abnormalities qualitatively in a few, fully developed disease conditions however, the evaluation of minor changes during physiological and pathophysiological circumstances might be difficult to asses qualitatively. When, comparing two or more levels of treatments, the semiquantitative evaluation may not reflect the actual trend of events in terms of alteration in the numbers of cells or other structures concerned. Therefore, complementation of qualitative microscopic observations with the quantitative approaches is very valuable when minor or initial differences are to be considered since, for purpose of analysis of tissue organisation, hardly any other technique can match the degree of resolution and discrimination which are characteristic of microscopic morphometry (Ferri, 1988). Therefore, the present study was designed to establish a cheap stereological method for elucidation of the normality and alterations in the number of enteric neurons and others structures in the gut using unbiased principles to obtain the best possible estimates by using appropriate efforts in the sampling and counting procedures.

Paper IV describes some of the many studies in which ganglia, neurons, neuronal and nuclear profiles, nerve length density in the enteric plexuses of various compartments, in different animals were quantified (See, Tables 1, 2, 3 **in Paper IV**; Liberti et al., 1998; Yunker et al., 1999; Xiang et al., 2000). However, the majority of these studies aimed at determining either the numerical density also called packing or spatial density (neurons per unit area of serosal surface of the gut) or area profiles of specific neurochemically defined neurons in specified plexuses during normal, ageing and pathological conditions (Tables 2, 3). In many other studies neurons were counted in the ganglia and presented as number/cm^2 using the established ganglia density/cm^2 (Young, et al., 1993; Furness and et al., 1994) or as percentages relative to total counts (Furness et al, 1984; Burns and Cummings, 1993; Brehmer and Stach, 1998). Numerical densities have also been referred to as neurons/cm^2 of ganglion area because, ganglion per unit length of gut was observed to be independent of stretch and did not vary between gut compartments (Timmermans et al., 1990; Karaosmanoglu et al., 1996). However, (a) numerical densities referred to serosal surface area or ganglion area and percentages per total number of neurons in ganglia can only be referred to specific tissue preparations, (b) ganglia are highly heterogeneous in size and their dimensions could be influenced by stretch (Gabella, 1990; Wedel et al., 1999) as well as shrinkage during fixation and subsequent procedures.

The majority of the sampling methods (both for estimation of the total number of neurons and numerical densities were done using fully distended compartments or stretched wholemounts.

Procedures for distension are variable, depending on subsequent staining procedures and size of the gut (Gabella, 1971, 1987, 1989, Van Ginnekenn et al., 1998; Maifrino et al., 1999; de Miranda-Neto, et al., 2001). For instance, to estimate the number of neurons in adult (6 months old) and newborn (1-16 h old) rats, Gabella, (1971) gently injected saline into the lumen of the stomach, small intestine, colon and rectum, distending the muscle coat. After applying ligatures to maintain the distension, the gut was cut into lengths (segments), the mesentery being sectioned as far as possible from the gut wall. The gut segments were then frozen on dry ice in a moist chamber, and after slow thawing were immersed in the incubation medium (Dihydronicotinamide adenine dinucleotide-diaphorase, NADH-diaphorase) at room temperature. After fixation for at least 24 h the gut was washed in saline and the external surface measured, it was then trimmed into small (5-10 mm) segments which were used to prepare wholemounts that were subsequently used to estimate number and sizes of neurons.

Neuronal packing density expressed in terms of number of neurons per cm^2 of stretched serosal surface is greatly influenced by how much the wall is stretched during the preparation (Gabella, 1987; Karaosmanoglu et al., 1996) which makes it difficult to compare different investigations (Table 2). In the human colon, stretching increased the length of tissues by up to 200% of the original length (Wedel et al., 1999). In the colon and small intestine of guinea pig, stretching increased serosal surface area by 32% and reduced the number density by 19% to 31% (Karaosmanoglu et al., 1996). To avoid the influence of distension on numerical density, Young et al. (1993) washed and placed the middle ileum from guinea pigs into bicarbonate-buffered, Kreb's solution, containing the muscle relaxant nicardipine®. The segment was opened along the mesenteric border and pinned tight on balsa wood serosal surface up followed by processing for staining with different antibodies. In another approach, Karaosmanoglu et al. (1996) removed the full length of small and large intestine from the guinea pigs, washed in Kreb's solution and measured length ("resting length"). They cut 10cm long pieces of samples (not random) from duodenum (5cm oral to ligament of Treitz (ileo-colic ligament), jejunum-ileum (5cm oral to ileo-caecal valve), and colon (20cm aboral to caeco-colical junction). Each sample was subdivided through the mid-point to yield two 5cm long pieces and cut open along the mesenteric boarder. One piece was pinned mucosa up as 2x5cm flat rectangle (not stretched) (in a dish lined with Silicone elastoma (Sylgaard). Another one was pinned stretched to give a 2.2x6 cm^2 rectangle. Mucosa, submucosa and circular muscle layer were dissected to produce wholemounts containing the myenteric plexus. The wholemounts were fixed and stained with cuprolinic blue or stained for Fos related antigen, neuron specific enolase and S-100 protein IR. Indeed, very few studies done using non-distended compartments or unstretched wholemounts ("resting lengths") (Leaming and Cauna, 1961;Young et al., 1993; Karaosmanoglu et al., 1996) showed significant variations from those which were done by using distended organs or

stretched wholemounts (table 2, 3).

Different methods have been employed to count the number of enteric neurons in various tissue preparations. The widely used technique was that of photographic montages (cf. Leaming and Cauna, 1961;Gabella, 1971, 1987, 1989). Gabella, (1987) prepared photographic montages of selected areas of tissue lamina by taking micrographs on 35 mm film at a magnification of x25, printing them at a final magnification of x125. Thereafter, photographs were collated into a montage. Each montage was covered with a sheet of thin tracing paper, or, alternatively, a light Xerox copy was made. The lamina was then re-examined in the microscope at a magnification of x 56 and each neuron was identified and marked with a red pencil on the tracing paper lying over the montage or on the Xerox copy. The counts were carried out on these photographic montages, checking cell by cell on the original preparation under the microscope.

Young et al. (1993) stained neurons in the myenteric plexus in the ileum of the guinea pig with NADH-d, nerve cell body antibody, calbindin, toluidine blue and methylene blue. They drew every stained neuron (all focal planes) in relation to the outline of each of the selected ganglia using a drawing tube attached to a microscope at 50x and counted all neurons by superimposing drawings. Tissues were embedded in araldite, cut into serial sections (1µm), counterstained with a mixture of toluidine blue and methylene blue. In each section, every nerve cell body profile was drawn in relation to the outline of the ganglion and followed serially by superimposing drawings from successive sections on a light box. Therefore, all neurons were counted and ganglia could be reconstructed. Numerical densities were calculated based on known density of ganglia/cm^2.

To estimate the number of neurons/cm^2 in the myenteric plexus in the small intestine of man, and rats, de Souza et al. (1993) and Fregonesi et al. (2001) respectively counted neurons in 20 microscope fields per fragment (with a known area for each field of vision), located by means of two orthogonal co-ordinates taken from a table of random number and measured on the movable stage of the microscope. The neurons intersected by the field's superior and inferior hemi-circumferences were, respectively, disregarded and considered. Meciano-Filho et al. (1995) counted all the perikarya at a x 100 magnification in each of the 1cm^2 wholemount to determine the number of neurons/cm^2 in the myenteric plexus in the oesophagus of humans. Similarly, Timmermans et al. (1990) counted all neurons and ganglia within the 1cm^2 piece of wholemount stained for specific neuropeptide IR to establish their numerical densities in the submucous plexuses in the small intestine of the pig.

Karaosmanoglu et al. (1996) used computer-assisted morphometry (Joyce-Loebl, Grnias 25, Gateshead, England) to estimate the total number and numerical densities of neurons in the small intestine and colon of guinea pig, to measure serosal area of each segment and areas occupied by ganglia. A video camera attached to a microscope was used to project images at x 40 onto a 512 by

480 pixel array. Measurements were obtained from 30 non-overlapping rectangular windows (0.052 mm^2) projected onto each specimen. The outline of each ganglion was traced with a cursor and the areas of these ganglia were computed. All neurons in each of the measuring windows were traced and care was taken to ensure that all neurons in all focal planes were counted. Computerised image analysis (computerised stereological softwares) have been used for similar purposes in other studies (Brehmer and Beleites, 1996; Van Ginneken, et al., 1998; Maifrino et al., 1999; de Miranda-Neto et al., 2001).

Apparently, the vast majority of the previous studies suffer from several limitations. (a) The majority of morphometric studies were done on the myenteric plexus of smaller mammals. (b) They were limited to short segments (Tables 2, 3). (c) Sampling was not randomised either while sampling tissues from animals or during microscopical counting or both (cf. Gabella, 1971, 1987, 1989; Karaosmanoglu et al., 1996). Therefore, differences of densities along segments such as those reported between the oesophagus, stomach, duodenum, ileum and distal colon (Furness et al., 1994), duodenum and ileum (Karaosmanoglu et al., 1996) in the guinea pig and the small intestine in the pig (Brehmer and Stach, 1998) were not considered. Variations along antimesenteric- mesenteric axis (Table 3) were not taken into consideration. (d) Estimation of sizes of organs and tissues to obtain serosal surface areas was done mainly after distension and fixation of tissues or they were stretched and often the extent of distension or stretch was not corrected for. (e) Counting in tissues was time consuming and in some studies not randomised. (f) Neurons/cm^2 referred to serosal surface area or ganglion area or percentages per total number of neurons in ganglia and can only be referred to specific tissue preparations. (g) Data from different laboratories can hardly be compared.

A more meaningful measure of local specific innervation for drawing biological conclusions regarding the functional capacity might therefore be the absolute (total) number of specific neurons per unit length of intact gut.

Attempts to count the total number of neurons in the enteric nerve plexuses have been limited by lack of stain(s) that could virtually specifically stain all the neurons and are well discussed by Karaosmanoglu et al. (1996). Hence, in the present study, specific immunohistochemical staining was used to stain and count the total number of a subpopulation of neurons in different plexuses in the jejunum of the pig but, not the total neuronal population.

There are reports on morphometry of enterochomaffin (EC) cells and Peyer's patches in health and pathological states. The counting of EC cells (Krause et al., 1984; Rantala et al., 1996; Oshima et al., 1999) and morphometry in the Peyer's patches (Chu and Liu, 1984; Rothkötter et al., 1990; Barman et al., 1997) are usually done by using paraffin sections and have had limitations which are almost similar to those highlighted for quantification of neurons in sampling and counting procedures.

Estimatation of the total number of EC cells by using wholemounts and the surface area of Peyer's patches by using spread tissues segments based unbiased systematic random sampling might provide some advantages in the easiness of the methodology and precision of the estimates.

A sound morphometric analysis must be founded on unbiased sampling design (Howard and Reed, 1998). The fractionator is the simplest, but the most powerful sterological sampling scheme which is based upon uniform random sampling with a known and predetermined probability and then deriving the total number in the reference space from the number in the sample and the sampling probability (Gundersen, 1986). A three dimensional (3-D) probe the optical disector is beneficial and efficient to count differentially stained cells in semi-transparent volumes (Gundersen, 1986; Gundersen et al., 1988). Surfaces areas are best estimated by using the unbiased quadratic (2D) point-sampling grid (Gundersen et al., 1988; Howard and Reed, 1998).

2.2 Objectives of the study

-The present study aimed at establishing a simple, cheap and efficient stereological sampling scheme for estimation of the total number of specific neurons in a distinct plexus in the intestine of a large mammal using unbiased principles.

-To apply the same method to estimate the total number of EC cells by using wholemounts and to estimate the surface area of Peyer's patches.

- What was accomplished with respect to these objectives is shown in paper IV.

CHAPTER 3: THE ENTERIC NERVOUS SYSTEM IN DISEASES

3.1 Introduction

During inflammation of the gut, nerves contribute to the pathophysiology of diseases in three interrelated mechanisms. (a) Inflammation may disturb the functional interactions of the ENS with their target cells within the inflamed microenvironment. This may cause alterations in the motor and secretory function of the gut, accounting for alterations in contractility and responsiveness to luminal stimuli, and may contribute to symptoms such as cramps and diarrhoeas. (b) The ENS may release neurotransmitters that may prime, perpetuate or otherwise modify the inflammatory and healing processes. (c) ENS relay systemic regulatory influence of the psyche and central nervous system on immune responses in the gut. Modulation of immune system in the gut by neuroendocrine system may be altered during inflammation (Read, 1991; Shanahan, 1998). The role of the ENS in various disorders of the gut is increasingly being realised such that several new and successful hybrid disciplines within the field of gastroenterology such as neuroimmunophysiology and psychoneuroimmunology have emerged (Shanahan, 1998). The combination of classical and neurochemical coding techniques to explore structural and neurochemical changes (plasticity) in the ENS is growing. However, compared to investigations of normal morphology, physiology and pharmacological actions of the ENS, studies of neuropathology in the gut are still limited.

3.2 Schistosomosis japonica

3.2.1 Life cycle

Schistosomosis japonica is a zoonotic, parasitic disease of economic importance in human beings and livestock industry in the main land China, Philippines and Indonesia. It is caused by a helminth, *Schistosoma japonicum* transmitted naturally between man and a variable number of vertebrate species. In endemic areas, livestock act as important reservoirs the pig, cattle, water buffaloes and dogs being probably the most important in the epidemiology (He et al., 1991; He, 1993; Wu et al., 1992; Hunter et al., 1993). The adult worms (Fig. 3) live and lay eggs (usually within 23-28 days post infection) in the mesenteric +/- submucosal vasculature in the definitive host (He and Yang, 1980; Willingham III, 1996) Immature worms can also be found in the liver and lung (Ozaki et al., 1997; Imbert-Establet et al., 1998). Each egg contains an ovum that matures fast into a miracidium which secrete lytic enzymes through the micropores in the egg shell. Most of laid eggs, penetrate through the wall of blood vessels (by using enzymes) into the intestinal wall eliciting host immune response (granulomatous inflammation) that in turn facilitate egg movement towards the intestinal lumen and where they become shed in faeces. A percentage of eggs that detach from vessels are transported by

blood to the liver, lung, brain and other sites where they cause hepatic and extrahepatic lesions. Eggs passed out from hosts species into the environment, hatch to produce the miracidia, which swim chemotactically to locate and penetrate into the Oncomelania snails (intermediate hosts), reproduce asexually to produce many cercariae which are released into fresh water (Haas et al., 1991; Faust and Russell, 1964). The cercariae by using enzymes and mechanical movement penetrate through the skin of mammalian (definitive) hosts and in so doing, they lose their tails and are transformed into schistosomula. In a few hours, schistosomula migrate via the circulatory system of the host to the lungs from where they migrate either directly through the pleura and diaphragm (Wilks, 1967) or indirectly via circulation (Miyagawa & Takemoto, 1821) to the liver where they develop into adult worms. The life cycle is completed when adult male and female worms pairs up and migrate to intestinal veins where oviposition takes place. In pregnant animals, during late gestation, a few schistosomula migrating from the lung of the "mother" cross the placenta barrier and infect the foetuse(s) (Willingham III, 1999). Probably, migratory schistosomula cross the maternal-foetal vascular barrier in the placenta and via the umbilical vein enter into the foetal circulation. The routes for migration of schistosomula in the foetuses are not known, however, the migration and establishment of worms to lay eggs seem to take place in foetuses and "mothers" simultaneously (Iburg et al., 2001). The consequences of prenatal schistosome infections on the resistance to postnatal challenge infections and subsequent inflammatory effects are not known precisely.

In schistosome infections, the key pathological event in the definitive host is the egg stage of the life cycle due to the formation of inflammatory granulomas around migratory schistosome eggs. Granulomatous inflammation is T cell dependent, dynamic, tissue destructive process caused by host defence reaction against migrating larvae stages (eggs) and is characterised by aggregation of eosinophils, lymphocytes, macrophages and mast cells in variable proportions around eggs (Weinstock, 1991; Hurst et al., 2000). The presence of multiple areas of granulomas in the intestinal tract has been associated with several mild and very severe changes (see below) and these seem to contribute substantially to morbidity and mortality seen in schistosomosis. Both natural and experimental *S. japonicum* infections have shown that granulomas affect mainly the large intestine. They cause severe intestinal disorders, namely proliferation and disruption of the epithelium, bleeding, diarrhoea, fibrosis and thickening of the submucosa, alteration of bowel motility, intestinal distortion and stricture (Chen et al., 1978). They may cause intestinal obstruction (Ming-Chai and Shan-Chi, 1957; Warren, 1969) and fistula (Nai-Kuang and Pen-Chung, 1957; Wu, et al., 1999). Granulomas are also speculated to be a predisposing factor to malignant adenocarcinoma (Ching-Fan, 1957; Cheever, 1981). Schistosomosis exacerbates malnutrition in the host (Johansen et al., 1997) and repeated exposures in early age are suggested to cause dwarfism (Ming-Hsin et al., 1957).

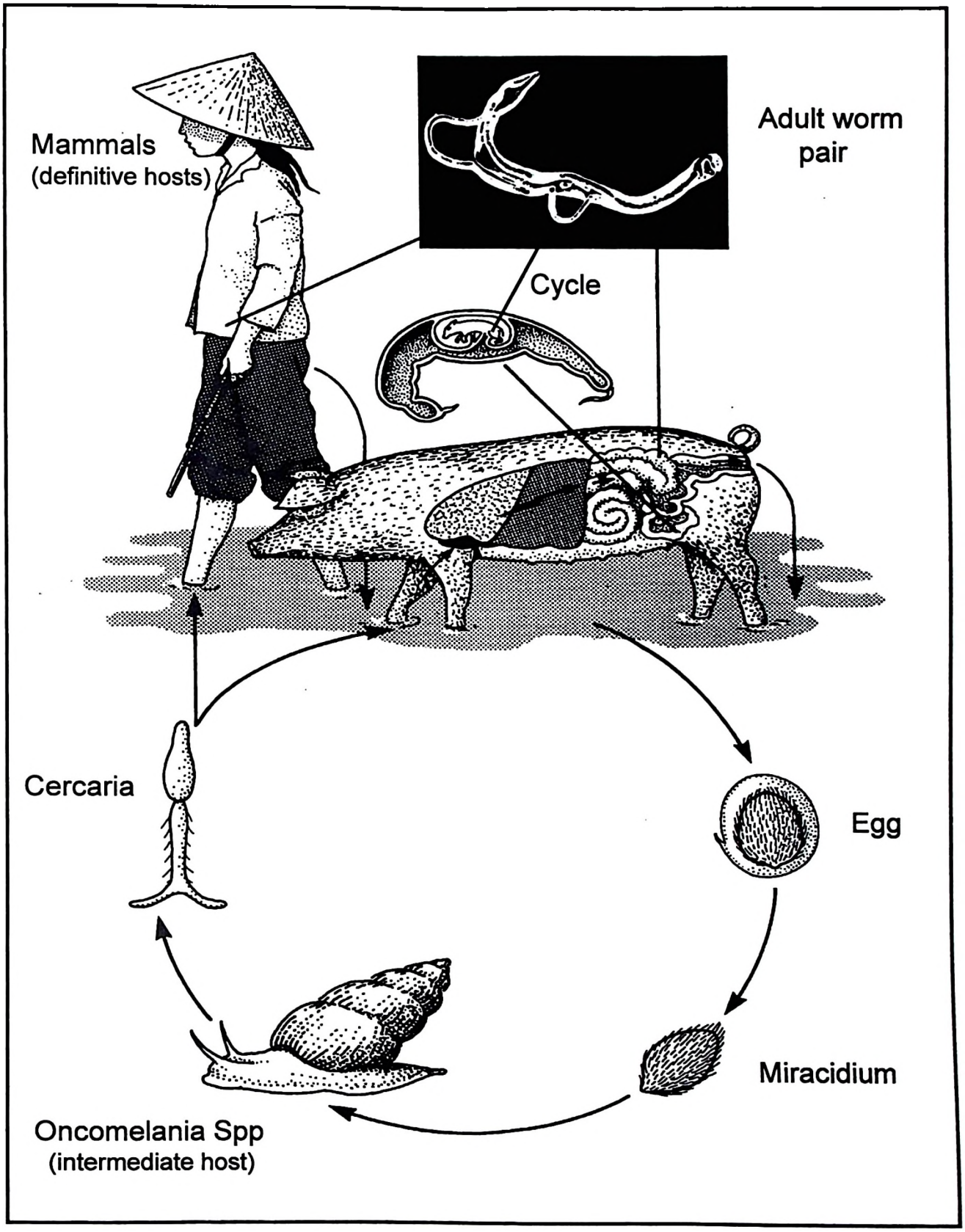

Fig. 2. A schematic drawing (not to scale) showing the life cycle of *S. japonicum*. The scanning electron micrograph on top shows a pair of male and female adult worms found in the liver and intestinal vasculature in mature intermediate hosts. They can also be found in the foetal liver and intestinal vasculature when "mothers" become infected during late gestation. (Modified after Willingham III, 1996).

The pathology of postnatal infection (Yason and Novilla, 1984; Hurst et al., 2000) and postnatal challenge infection of congenitally infected (Johansen et al., 2001) pigs have been thoroughly described. However, the mechanisms by which granulomatous inflammation causes all the changes stated above are not entirely clear.

3.2.2 The pathogenesis of diarrhoea and migration of eggs in schistosomosis

In schistosomosis, diarrhoea is considered to be due to physical damage done to the intestinal venules and mucosa by eggs exiting through the intestinal wall which cause haemorrhages and subsequent inflammatory reactions (Lawrence, 1978; Saad et al., 1980; Semuguruka, 1992). The mechanisms of egg exition from intravascular areas and thereafter emigration into the intestinal lumen are not very well understood. It has been reported that endothelial cells, leukocytes and fibroblasts, periovular inflammatory cells particularly eosinophils (Lenzi et al., 1987) neutrophils and mononuclear cells (Semuguruka, 1992; Doenhoff, 1997) particularly monocytes facilitates extravasation of schistosome eggs. On the other hand, peristalsis and lytic excretions from eggs (Kuba, 1963) and immune complexes around the egg (Doenhoff et al., 1986; Doenhoff, 1997) contribute greatly to the emigration of eggs into the intestinal lumen. The precise nature of how these as well as other factors operate in the pathogenesis of diarrhoea and egress of schistosome eggs are not entirely clear.

It now well established that the ENS, inflammatory cells and neuroendocrine cells communicate via chemical messengers in highly integrated and complicated mechanisms to regulate intestinal functions such as motility, mucosal transport, blood flow, immune responses and in the mechanisms of diarrhoeas (Sjöqvist et al., 1992; Wood, 1994; Powel, 1994). Inflammatory cells such as neutrophils, lymphocytes (Wallis et al., 1990) and mast cells (Pothoulakis et al., 1998) play a role in inducing fluid secretion. Diarrhoea due to nematode infestation is speculated to be due to intestinal anaphylaxis induced by mast cell activation (Powel, 1994). The inflammatory mediators from mast cells and phagocytes are suggested to cause intestinal chloride and water secretion as well as inhibition of sodium and chloride absorption. These events occur by direct effects of the mediators on the epithelium, release of prostaglandins from lamina proprial fibroblasts and activation of the enteric nervous system (Powel, 1994). It is hypothesized that diarrhoea due to infectious agents results from colonization, adherence and or epithelial invasion which is followed by release of cytokines from enterocytes which activates resident phagocytes and recruitment of new phagocytes in the lamina propria and activation of the ENS (Powel, 1994). In secretory diarrhoea, 5-hydroxytryptamine, substance P (SP) and neurokinins and other chemical messengers from mucosa cells activate the ENS plexuses to stimulate secretory diarrhoea. Activation of the ENS causes release of neurotransmitter and other endogenous effectors which induce chloride secretion. Acetylcholine,

VIP, prostaglandins, nitric oxide, and others chemical messengers are speculated to play a major role in the effector pathways to stimulate secretion (Sjöqvist et al., 1992; Hansen and Skadhauge 1995; Argenzio, 1997). It has been suggested that neuro-immune interactions may result into increased propulsive motility, secretion of electrolytes, water and mucus, mucosal blood flow and epithelial restitution turnover. These interactions may influence the trapping of migrating eggs and enhancement of egg exition as well as diarrhoea and other clinical signs seen in schistosomosis (Varilek et al,. 1991; Balemba et al., 2000, Bogers et al., 2000; Van Nassau et al., 2001). However, the entire mechanisms are not known.

3.2.3 Neuropeptides and interleukins in schistosome induced granulomas

It is well founded that in murine schistosomosis mansoni, granuloma eosinophils produce authentic VIP and SP. Macrophages produce somatostatin 1-14 in response to, interferon gamma (IFN-gamma), interleukin 10 (IL-10) or several other inflammatory mediators and express somatostatin receptor subtype number 2 (SSTR2) (Weinstock, 1990; 1991; Matthew et al., 1992; Metwali et al., 1993;Weinstock, 1996; Blum et al., 2001). In the granulomas, the VIP via authentic VIP receptors (VIPr1 and VIPr2 subclasses) can enhance production of interleukin-5 (IL-5) by T cells but, suppress T cell proliferation and T lymphocyte IL-2 production. It has been suggested that expression of VIP receptors on T cells is subject to immunoregulation and each may have unique immunoregulatory functions in inflammation (Matthew et al., 1992; Weinstock, 1996). A substance P (SP)/somatostatin neurokine immunoregulatory circuit controls interferon gamma (IFN- gamma) production via authentic SP (SPr) and somatostatin (SSTR2) receptors on T cells. IFN is an inflammatory cytokine important in macrophage activation and B-cell differentiation in schistosome granulomas. SP stimulates, while somatostatin inhibits IFN-gamma release. Substance P and somatostatin can modulate the amount of immunoglobulin G2a secretion (Blum et al, 1993; Weinstock et al., 1998; Weinstock and Elliott, 2000; Blum et al., 2001).

Granulomas also produce other cytokines such as IL-2, IL-5 (Matthew et al., 1992; Metwali, et al., 1993) and tumour necrosis factor α (Amiri et al., 1992). Both Th1 (IFN-gamma) and Th2 (IL-4, IL-5 and IL-13) cytokines are important in modulating granuloma immune and anti-fibrotic responses in *S. japonicum* (Hirata, et al. 2001) and *S. mansoni* (Hesse et al., 2000) egg-induced granuloma formation in mice. These responses are accompanied by inducible nitric oxide synthase regulated down-streaming influence of the effector cells, which result into the shift from the type-2 cytokine profile to the one dominated by type-1 cytokines (Hirata, et al. 2001). Pigs infected with *S. japonicum* developed a Th2 response as characterised by the increased level of mRNA encoding for IL-4 and IL-10 in their large intestine (caecum and colon). The orally infected pigs produced higher

IL-4 and IL-10 levels (Oswald et al., 2001). Clearly, the granuloma inflammatory cells and the ENS show one fascinating feature in common, the "intersection between the neuro-immune systems" composed of putative transmitter substances VIP, SP and somatostatin which play a role in regulating the complex immune processes and dynamicity of the granulomatous lesions. The above findings show neurotransmitters, receptors, and interleukins (see, below) to be key members of the "intersection" between the neuro-immune systems in the gut and play a role in interacting the neuro-immune systems during normal, inflammatory and allergic conditions.

3.3 Neuroplasticity in the ENS

The term neuroplasticity embraces a great variety of changes in the structure and functions of neurons in response to alterations of input. Understanding neuroplasticity has great functional (physiological, pathological and clinical) implications which includes: (a) Defining the basic mechanisms of the ability of the ENS to adapt to a changes in both the macro and microenvironments. (b) Elucidation of the mechanisms underlying neuronal alterations, regeneration of neuronal circuits and restoration of normal intestinal functions (neuropathophysiology of diseases) and development of new therapeutic strategies to collect them (Giaroni, et al., 1999; Sharkey and Kroese, 2001). It is a very complex process where virtually all tissue elements within the microenvironment, neurons, enteric glia, connective tissue elements, neuroendocrine and epithelia cells, smooth muscle cells, immune system cells, interstitial cells of Cajal are "players". It involves multiple interactions of these elements through putative mediators- (neurotransmitters, neurotrophic factors, cytokines, eicosanoid etc) receptor interactions.

The gut contains a substantial population of resident inflammatory cells that contribute to a physiological state of basal inflammation. However, once overt inflammation is initiated, it causes selective activation of the gut neurons in distinct neuronal pathways (which correspond to the level of the insult/degree of inflammation i.e. activity-dependent) that result into structural and functional changes in the innervation of the gut. Consequently, the pattern of innervation and the interactions of nerves and their target tissues is disrupted (Palmer and Koch, 1995, Sharkey and Kroese, 2001; **Papers V, VI**). The activity-dependent changes in the ENS which are induced by inflammation include both up and down regulation of transmitter expression as well as induction of new genes (Collins SM, 1996; Giaroni, et al., 1999; Sharkey and Kroese, 2001). It has been hypothesised that probably, neurotrophic factors for instance nerve growth factor released by the ENS serve as messengers of plasticity through modulation of the expression of neuropeptides (Giaroni et al., 1999). Existing data from inflammatory bowel diseases in humans and animal models and other inflammatory diseases in the gut show that during inflammation the ENS system is activated and respond by

releasing neuropeptides (Sharkey and Kroese, 2001). According to Sharkey and Kroese (2001), neuropeptides may prime immune system cells to respond to changes such as inflammatory stimulus, and hence, they are able to modulate the functional capacity of the immune system. Major work in this area has focused on mainly SP, VIP, calcitonin gene related peptide and to some extent nitric oxide and onco genes (Collins, 1996, Shanahan, 1998; Holzer, 1989; Giaroni et al, 1999; Sharkey and Kroese, 2001; **Papers V, IV**). For instance, local release of the neuropeptides, most notably SP and calcitonin gene related peptide can modulate or initiate inflammatory response which involves vasodilatation, extravasation of plasma, degranulation of mast cell and secondary effects of mast cell mediators on tissue function.

On the other hand, mediators released by immune system have direct activating effect on neurons in the ENS and cause potentiation of neurochemical mediators. Pro-inflammatory cytokines from activated immune cells suppress release and interfere with the biosynthesis of neurotransmitters partly through stimulation of prostaglandin synthesis in the myenteric plexus of rat (Hurst and Collins, 1994). Chemical mediators from macrophages inhibit release of acetylcholine causing impairment of cholinergic enteric nerves (Galeazzi et al., 2000). Increased neuronal substance P activity requires release of cytokines such as interleukin-1β (IL-1β) from lymphocytes (Hurst et al., 1993). The "cross-talk" or bi-directional neuro-immune interactions between the ENS and the immune system cells which is well described in the reviews by Collins, (1996) and Giaroni, et al., (1999) is considered as an important facet of structural and functional innervation of the gut in health and disease. During inflammation, intestinal hypersensitivity, and other related conditions, mast cells play a major role in the neuro-immune signalling cascades (Bienenstock et al., 1987a, b; Suzuki et al., 1999). It has been realised that nerve-mast cell "cross-talk" is a prototypic neuro-immune interaction that can occur in the absence of an intermediary transducing cell and that SP, operating via NK-1 receptors, is an important mediator of this communication (Suzuki et al., 1999). Constant nerve-mast cell communication is suggested to be structural and conceptual framework whereby the nervous system may communicate with inflammatory events. Mast cells are also essential for nerve growth and repair of nerves (Bienenstock et al., 1987a, b; Suzuki et al., 1999, Kobayashi et al., 1999). The mechanisms of neuro-immune communication are not known entirely.

Enteric glial cells play a role in the transfer of information between neurons and the surroundings as demonstrated by their response to a variety of neuroligands with Ca^{2+} signalling (Sarosi et al., 1998) and dye coupling (Maudlejet and Hanani, 1992). They are also suggested to play immunosuppressive and anti-inflammatory roles possibly via neurotransmitter and or interleukin regulated mechanisms and thus, protection of neurons against injury by noxious agents (Bush et al., 1998). For instance, in the central nervous system astrocytes have been observed to protect neurons

though VIP-regulated uptake of glutamate (Brown, 2000). Enteric glial cells in the myenteric plexus of guinea pig have been shown to be a potential source of IL-6 and cytokine production which can be regulated by cytokines. These findings strongly support the suggestion that enteric glial cells act as immunomodulators (including neuronal survival) in the enteric nervous system. It has been suggested that during intestinal inflammation, there may be a regulatory interplay between different classes of cytokines (interelukins (IL-) 6 and the soluble IL-6 receptor, IL-1beta and IL-10) modulating peripheral nerve regeneration (Ruhl et al., 2001a, b). Clearly, from the discussion above, it is apparent that studies on the extent of damage to the ENS and neuro-immune interactions during schistosomosis deserve more attention in the future.

3.4 Alterations in the nervous system in Schistosomosis

3.4.1 Central nervous system

In recent years, it has been observed that during schistosoma infection, although far less common, via embolisation of eggs and anomalous migration of adult worms schistosomes may reach the central nervous system (Pittella, 1997; Aloe and Fiore, 1998). The presence of eggs in the central nervous system induces a cell-mediated periovular granulomatous reaction. The heavy concentration of eggs and the presence of large granulomas in circumscribed areas of the brain cause the signs and symptoms of increased intracranial pressure and focal neurological signs. In the spinal cord they cause, the signs and symptoms of rapidly progressing transverse myelitis, usually affecting the lumbosacral segments of the spinal cord. Neuroschistosomosis cause severe neuropsychiatric and neuropathological disorders, low work productivity, poor cognitive performances (Aloe and Fiore, 1998). Brain granulomas are associated with a significant alteration in the constitutive expression of nerve growth factor, a neurotrophic factor that plays an essential role in the growth and differentiation and in preventing neuronal damage. Neuropsychiatric and neuropathological disorders may be linked to alterations in the basal levels and or activity of neurotrophic factors by local formation of granulomas (Aloe and Fiore, 1998). Compared to the central nervous system, the extent of damage and neuropathophysiology of the brain-in-the-gut where hundreds to thousands of granulomas form depending on severity of infection is probably greater but, less studied.

3.4.2 Enteric nervous system

A few studies have been conducted to evaluate changes in the structure and neurochemical contents in the ENS during *S. mansoni* infections in mice (Varilek et al., 1991, Bogers et al., 2000; Van Nassau et al., 2001) and *S. bovis* in cattle (Balemba et al., 2000). The principal findings were (a) alterations in the neurochemical contents including increased VIP and dihydronicotinamide adenine

dinucleotide (NADH) (Varilek et al., 1991) and increased VIP but, reduced staining for NF (Balemba et al., 2000). Van Nassauw et al., (2001) observed a significant increase in the number of 3-nitrotyrosine-immunoreactive neurons (a biomarker of reactive nitrogen species) and very few active caspase-3, (a key executioner of apoptosis) positive neurons in both the submucous and myenteric plexuses in the ileum of mouse. (b) Varilek et al., (1991) and Balemba et al., (2000) showed that intestinal granulomas focally destroyed enteric ganglia, neurons and nerves. They extent of injury was related directly to the number of granulomas. However, Bogers et al. (2000) and Van Nassau et al. (2001) did not observe significant apototic neurons in the myenteric plexus in the ileum of mice. They observed ganglionitis with few apototic cells indicating damage in a significant number of enteric neurons but, rare neuronal cell death.

In intestinal anaphylaxis, infection and inflammation, neuronal activation and plasticity (structural and neurochemical changes) cause an imbalanced function of peptidergic neurons, and are suggested to contribute to motor, secretory, vascular and immunological disturbances (Belai et al., 1997; Holzer, 1998; Shanahan, 1998; Giaroni et al, 1999; Sharkey and Kroese, 2001). Injury to the ENS caused by granulomatous inflammation has been suggested to impairs its regulatory functions and partly account for clinical and pathological features seen in schistosomosis (Varilek et al, 1991; Balemba et al., 2000; Bogers et al, 2000; Van Nassauw et al., 2001). Studies of neuronal plasticity in the ENS in terms of release and expression of neurotransmitters, structural changes and cell death during schistosomosis are limited. The time of infection, duration and challenge infections might also influence the activity. These observations prompted the current study (**Papers V, IV**).

3.5 Objectives of the study

-To study changes in the neurochemical contents of the (a) intrinsic non-cholinergic excitatory (SP-containing) and (b) non-adrenergic, non-cholinergic inhibitory (VIP- and nitric oxide (NO) containing) neural pathways in the large intestine of the pig during granulomatous inflammation induced by *S. japonicum* infections. Compare changes seen in postnatally infected pigs with those in prenatally infected pigs with or without postnatal challenge re-infections.

Correlate observations with the severity of pathological lesions.

-To compare responses between plexuses by determining the numerical densities of NOS IR neurons.

-To study structural changes in the ganglia of the ENS by using different routine staining procedures.

-What was accomplished with respect to these objectives is shown in papers IV-VI.

CHAPTER 4: OVERVIEW DISCUSSION OF RESULTS AND PERSPECTIVES

4.1 Organisation of the enteric nervous system

In the pig, immunohistochemistry for VIP and NF was used to study the neural elements in wholemounts, chopped and paraffin sections (**Paper I**). In addition, the VIP and SP immunohistochemistry was used to clarify the organisation of the mucous plexus wholemounts, and paraffin sections (**Paper II**). VIP and NOS were used in the stereological (methodological) study to establish the unbiased sampling scheme for morphometry in the ENS as well as for the EC and Peyer's patches (**Paper IV**). VIP, SP, NOS and NADPH-d were used to investigate plasticity of the respective neurochemical contents during *S. japonicum* infection (**Papers V, VI**). In the goat, S-100 protein, NF, and SP, VIP and NOS were used to study the ENS mainly in wholemounts. Paraffin sections were also used to complement observations in wholemounts. However, a slightly more extensive study involving the whole intestinal tract was undertaken in the goat with respect to that intra-plexus variations between compartments and inter-plexus variations with respect to the length and width of ganglia and S-100 protein IR neurons, and width of nerve strands. The arrangement of the enteric ganglia and nerve fibre plexuses in the pig (**Papers I, II**) and goat (**Paper II**) was very much similar and a detailed comparison has been made in **Paper III**. The comparisons between the pig and goat suffered one major drawback because in the goat, VIP antibody did not reveal the organisation of the ENS and IR neurons clearly as in the pig and the polyclonal rabbit anti rat cerebellar NOS antibody did not stain the nervous tissue at all. Different methods (citrate buffer pH 6.1; Tris buffer pH 8.4 with or with out heating at high temperatures, ~ 90 °C) for antibody retrieval were tried without much success. This is probably, because the antibodies used did not cross-react fully with the goat antigens. Since, the goat is less studied, it was very difficult to obtain a suitable antibody. Substance P also showed some problems with cross reactivity, however, upon antibody retrieval by incubating tissue in citrate buffer pH 6.1, overnight at room temperature substantial staining was obtained.

The organisation of the myenteric plexus was similar to that described by Furness and Costa, (1987) with the primary, secondary and the tertiary components. However, a broad mesh of type II tertiary nerve strands intimately related and oriented perpendicular to the outer surface of the ICM was observed in the whole intestinal tract. This observation confirms previous observation in the small intestine of calves (Balemba et al., 1999). However, type two tertiary nerve strands interconnected primarily the secondary nerve strands whereas in calves (Balemba et al., 1999) they interconnected

ganglia. Their orientation resembles that of large shunt fascicles observed in the rectum and distal colon in the pig, opossum, sheep, goat and cat (Christensen et al., 1984).

The organisation of the enteric ganglia and nerve strands in submucous layer of pig and goat was very similar and complex compared to that of the myenteric plexus. In the intestine of both the pig and goat (**Papers I, III**), the ganglia of the outer submucous plexus (OSP) and inner submucous plexus (ISP) were situated at different topographical locations, being clearly demarcated by the submucosal vascular arcades. Ganglia were distributed at different topographical levels showing differences in structure, orientation, compactness, branching patterns of nerve strands, size of neurons and staining patterns. This observation is in accordance with other reports in the, pig sheep and goat (Gunn, 1968), pig (Scheuermann et al., 1987a,b; Timmermans et al., 1990, 1992, 1997, 2001; Wedel et al., 1999), horse (Pearson, 1994) and cattle (Balemba et al., 1999). A study in the goat (**Paper III**), showed new features for the OSP. Large ganglia and primary nerve strands could be seen by naked eyes when stained for NF and S-100 proteins IR. Primary strands were oriented perpendicular to the ICM while the major axis of large ganglia and S100 and NF IR neurons was oriented parallel to the ICM. Viewed from the serosal side, primary strands appeared beneath the main body of the larger ganglia. These new features showed close morphologic resemblance between the OSP and the myenteric plexus compared to previous data from other species. They enhance further, the differences between the OSP and ISP.

However, in each of the two plexuses, the ganglia were further located at different topographical levels (**Paper I, III**). In the OSP, small sized ganglia were observed mainly in the network closely associated with the ICM on its inner side. The large ganglia network was located closer to the vascular arcades. Therefore, the OSP was subdivided into the outer OSP subplexus (the meshwork similar to *Plexus submucous extremus)* and inner OSP subplexus (Schabadasch's plexus) formed by a meshwork of larger ganglia (**Paper III**). This observation, supports similar finding in small intestine of cattle (Balemba et al., 999) and the observation of the *Plexus submucous extremus* by Stach (1972) in the colon of rat and guinea pigs and by Hoyle and Burnstock (1989a) and by Wedel et al. (1999) in the human colon. The staining for NOS and NADPH-d, SP, VIP and NF showed clear differences between the OSP and ISP plexuses but, not between the outer and inner OSP subplexuses (**Papers I, III-VI**). Apparently, functional differences between the OSP (Schabadasch) and *Plexus submucous extremus* have not been reported. In the present study, segmental variations of the outer and inner OSP subplexuses were not investigated separately.

In the present study, two, topographically different but closely interconnected outer and inner ISP subplexuses were also observed both in the pig and goat (**Paper III**). In the goat, further differences in the size, shape and outlines of ganglia and nerve strands and size of neurons were

revealed. In the large intestine of the pig, NOS and NADPH-d staining revealed a slightly different staining pattern between OSP and ISP and between the outer and inner ISP subplexuses especially in the pigs infected with *S. japonicum* with intensely stained neurons being observed in the inner ISP subplexus compared to the outer ISP subplexus (**Papers IV, VI**). However, in the goat differences in the staining for VIP, SP, NF and NOS IR between the ISP subplexuses were not studied. The differences observed between two ISP meshworks are similar to findings of the intermediate and Meissner's plexuses in the intestine of pig (Gun, 1968). They support the proposition for the third intermediate plexus in larger mammals other than man (Gun, 1968; Christensen and Rick, 1987). The third intermediate plexus has been confirmed in intestine of humans (Timmermans et al., 2001, for review) and it resembles phenotypically the ISP in the small intestine (Dhatt and Buchan, 1994) and OSP in the large intestine (Crowe et al., 1992). Studies on neurochemical coding and projections of neurons (Porter et al., 1999; Hens et al., 2000) corollary with morphometric analysis are required before the outer OSP subplexus and the outer ISP subplexus in the goat and pig are considered as different distinct plexuses namely the *Plexus submucosus extremus*, and the intermediate plexuses respectively. However, the problem associated with further subdivisions of the OSP and ISP into distinct plexuses is that as there are no clear-cut morphological demarcations and the ganglia networks in the OSP and ISP are intimately linked. Therefore, the level of precision when assigning individual ganglia to their respective plexuses might be low and this is likely to be influenced by the level of experience, the intestinal segment of interest, and the staining technique and/or antibodies. It is possible to dissect the submucous layer into two and thereby enhancing the possibility to differentiate the submucosal plexuses (Pearson, 1994; Wedel et al., 1999). The problem here is that, the ganglia especially in the outer ISP subplexus (intermediate plexuses) and inner OSP subplexus are subjected to damage and displacement of ganglia and hence, creation of the so called "lost caps" (Hedreen, 1998).

The organisation of the ISP in the Peyer's patches was different from other parts of the gut without follicles. The ISP formed a continuous mesh of 3 ganglionated subplexuses namely the subepithelial, interfollicular and coronary subplexuses around the follicles (**Papers I, III**). The observations on the organisation of the OSP and ISP in the Peyer's patches are similar to those of Kulkarni-Narla et al. (1999) in the small intestine of the pig and Balemba et al. (1999) in small intestine of cattle. However, the need for new terminologies instead of those advanced by Balemba et al. (1998) (**Paper I**) was realised. Therefore, new terms above were suggested by Balemba et al. (2001) (**Paper III**) to clarify the subplexuses in the ISP surrounding the follicles of Peyer's patches and the mucous plexus in conformity to the nomenclature proposed by (Timmermans et al., 1997, 2001) and based on the topographical locations of the subplexuses. It is apparent from the review (see

chapter 1) that there is great controversy with respect to the naming of the submucosal plexuses (Scheuermann et al., 19787b; Hoyle and Burnstock, 1989; Crowe et al., 1992; Pearson, 1994). In the present study, an attempt has been made to use the appropriate descriptive terminologies to name the plexuses in the submucosa and lamina propria based on the locations (**Papers I-IV**).

In the present study (**Papers I-IV**), it was established that the mucous plexus in the intestine of both the pig and goat contains many small ganglia and isolated neurons (**Paper I-VI**). In the pig (**Paper II**), they were many and comparably larger in the caecum and colon, few in ileum, and fewer and smaller in the jejunum. In the goat (**Paper III**), morphometric evaluation for numerical densities of ganglia showed higher density in caecum followed by ileum and colon, rectum, duodenum and lastly the jejunum. Surprisingly, the total number of intramucosal VIP IR neurons in the pig jejunum was comparable to that observed in the OSP and greater than that observed in the myenteric plexus (**Paper IV**). Similarly, qualitative assessment in the mucous plexus in the intestine of goat showed many SP IR neurons in the mucosa compared to the myenteric plexus (**Paper III**). Although, these findings are in agreement with previous studies (**Papers II, III**), they provide an insight on the extent of ganglia and isolated neurons in the mucous plexus. The observation of the highest number of intramucosal ganglia and neurons in the caecum is supported by the occasional finding of neurons in the lamina propria of the appendix of normal humans and during neurogenic appendicopathy (Papadaki et al., 1983; Naik et al., 1999).

Studies on the organisation of the mucous plexus in the pig revealed a 'new subplexus', the inner propria plexus (**Paper I**) and therefore subdivision of the mucous plexus into 4 plexuses. In the course of the study, the subdivision was revisited and 7-8 subplexuses were observed in the mucous plexus. Viewed from serosal side they are lamina muscularis mucosa subplexus (LMMP), outer proprial (OPP), interglandular proprial (IGPP), inner proprial (IPP), perivascular (PVP), villous (VP) and subepithelial subplexuses (SEP) (**Papers II-VI**). This classification is different from others reports (Furness and Costa, 1980; Furness et al., 1988; Costa and Brookes, 1994), but it is based on the location and simplicity as stated earlier. Intramucosal ganglia and isolated neurons were situated at different topographical levels in the LMMP, OPP and IGPP. The majority occurred in the basal region of the mucosa in the OPP. The PVP, IPP, VP and SEP were aganglionic. These subplexuses varied with respect to the amount, sizes and shapes of ganglia and neurons, sizes and orientation of nerve strands and their respective immunoreativities (**Paper II**). In the present study, VIP IR nerve fibres from ISP innervated the dome (**Paper I**). A dense nerve fibre meshwork was revealed by SPIR in the dome in the goat (**Paper III**). The observation of SP IR in the dome is similar to that of (Kulkarni-Narla et al., 1998) in the pig. These findings signify the importance of neuropeptides in the ENS in modulating immunity in the Peyer's patches.

The estimation of sizes of the ganglia (**Paper III**) showed the longest ganglia in the caecum and broadest in the colon. The mean values of the size of ganglia and nerve strands between these two compartments did not differ significantly but, were significant different from the rest of the intestinal tract. The sizes of ganglia and nerve strands in the rectum and small intestine did not differ significantly. However, in the decreasing order, ganglia and nerve stands in the duodenum, rectum and ileum were larger than those in the distal, proximal and middle jejunum where the ganglia and nerve strands were the smallest. In general, in all plexuses, larger ganglia, primary and secondary nerve strands as well as S-100 IR neurons were found in the caecum and colon. They were medium sized in the duodenum, rectum, ileum and distal jejunum and relatively smaller in the proximal and middle jejunum. These findings support the observation of Gabella, 1990 in the small intestine of mouse, guinea pig and sheep.

Staining for neurofilament proteins revealed types II, IV and VI neurons in the small intestine of the pig (**Paper I**). In the goat they showed type II neurons only (**Paper III**). The reasons for the differences are not clearly apparent. They show species variations in reactivity to the antibody used and support to the concept that in the gastrointestinal tract, some neurons in the ganglia cannot be stained by antibodies to neurofilament proteins (Krammer and Kühnel, 1992a; **Paper I**). The observations on the location, size and shape and staining of Schwann cells and enteric glia by S-100 protein IR in the intestine of goat correspond with the observation of Scheuermann et al. (1989) in the small intestine of the pig and Albuerne et al. (1998) in the intestine of goat and other mammals. The observation of S-100 protein IR in enteric neurons supports similar observation by Albuerne et al. (1998) in the myenteric and submucous plexus of cow and goat by using paraffin sections. However, in the present study, type II and the rounded S-100 protein IR neurons were identified in all segments and all ganglionated plexuses in the goat.

4.2 Morphometry of the ENS, EC cells and Peyer's patches

In the present study, we have highlighted the problems associated with previous studies and emphasised the need for using the absolute (total) number of neurons in a defined unit of the gut *vs* numerical densities whenever dealing with number of neurons. In the example (**Paper IV**), a morphometric study in the jejunum of the pig showed that the total number of NOS IR neurons was highest in the myenteric, medium in the ISP and lowest in the OSP. These results correspond to those of Van Ginneken et al. (1998) in the 1cm long pieces of tissue from the oral and aboral duodenum of 4-6 weeks old pigs. The majority of investigations on NOS and NADPH-d in the ENS of the adult pig and other species have focused more on the myenteric and OSP (Krammer et al., 1992b; Barbiers et al., 1993, 1994, 1995; Timmermans et al., 1994; Bogers et al., 1994). This may be due to few

intense NOS neurons which are normally seen in the ISP. However, the present study showed many NOS IR neurons (total number) in the ISP in weaner pigs which is due to the highest number of ganglia in the ISP and the presence of many moderately to weakly stained neurons (**Paper IV**). It signifies the importance of morphometry to complement qualitative observation (Ferri, 1988). The total number of VIP IR neurons in all plexuses in the jejunum was 68,4 x 10^6. This amount reflects a very large total number of neurons in the jejunum and indeed, in the whole gut. It shows clearly that the ENS is the brain-in-the-gut (Wood, 2000; Grundy et al., 2000) or the second brain with respect to the number of neurons. In any mammalian species the ENS contains vast neuronal populations (10^7-10^8) approximating to the number of neurons in the spinal cord (Furness and Costa, 1980). The number of neurons in the colon of the guinea pig is larger than the total number of neurons in the jejunum ileum (Karaosmanoglu et al., 1996). Assuming that the number of VIP IR neurons represented about 2/3 of the total number of neurons in the jejunum, the total number of neurons in the jejunum would be approximately 10^7. Therefore, the total number of neurons in the whole gastrointestinal tract of pig would approximately be10^8-10^9 neurons.

In addition, we have shown that the sampling sampling scheme presented could also be used to estimate the total number of enterochromaffin and the surface area of the Peyer's patches. The finding that most of the EC cells reached intestinal lumen by narrow cytoplasmic extensions suggest that the majority of EC cells were of the "open" type. These findings are in accordance to those of Cetin et al. (1994) in the intestine of the guinea pig and Totzauer (1991) in the duodenum of cattle that the majority of EC cells are bipolar. The observations of the total number of EC cells as well as the total surface area in the whole jejunum of 8 weeks old pigs are new information. The method described here which gives very good estimates is based on the use of a simple and cheap, unbiased sampling design which will be useful in further investigations of importance in understanding the ENS as well as neuroendocrine cells, Peyer's patches and other structures during normal and pathological states.

4.3 The ENS in schistosomosis

The effects of granulomatous inflammation against migrating *S. japonicum* eggs on the enteric nervous tissue in the caecum and colon were studied in the pig model. Ganglia situated within or near granulomas showed ganglionitis, and necrosis of neurons as well as infiltration by eosinophils, mast cells, lymphocytes, plasma cells, neutrophils and macrophages. The inner submucous and mucous plexuses were the most damaged. These findings are similar to those of Balemba et al. (2000) in calves infected with *S. bovis*, and Varilek et al. 1991 and Bogers et al. (2000) in mice infected with *S. mansoni*. However, in the ileum of mice infected with *S. mansoni*, neuronal cell death was rarely

observed and was not significant (Bogers et al., 2000; Van Nassau et al., 2001). The difference could be due to variation in severity of infection. In the present study it was established that the staining of VIP in inflamed tissues was reduced. That of SP, NOS and NADPH was increased at lower levels of inflammation and decreased in severe lesions. The alterations of the staining of VIP, SP, NOS and NADPH-d correlated with severity of inflammation. The observations of increased NOS and NADPH-d staining supports those of Varilek et al. (1991) in mice infected with *S. mansoni*. However, finding of reduced VIP in all types of inflamed tissues and that of reduced NOS and NADPH-d in very severely inflamed tissues are different from the findings of Varilek et al. (1991) and Balemba et al. (2000) but, the reasons are not entirely apparent. The finding of more intensely stained neurons and varicosities in tissue from prenatally and pre-/postnatally challenge infected pigs compared to postnatally infected pigs is probably due to differences in immunity following low levels of prenatal infection. A study comparing postnatally with or without challenge infection with prenatally/postnatally challenge infected pigs might shed more light to this aspect.

In the present study, the number of NOS IR neurons increased significantly as shown by the numerical density in the ISP followed by the myenteric plexus and OSP. There were also differences between caecum and colon. In both compartments, the highest numerical densities were recorded in the postnatally infected pigs. These findings show differences in the pattern of response exhibited by the enteric plexuses to schistosome egg induced granulomatous inflammation. These findings are in accordance with the concept that during inflammation, there is up and down regulation of neurotransmitters. That, alterations occur in selective pathways in the ENS and they are activity dependent i.e. dependent to the level of inflammation (Collins, 1996, Shanahan, 1998; Giaroni et al, 1999; Sharkey and Kroese, 2001). The changes observed could be have been caused by chemical mediators from inflammatory cells (Durack, et al., 1979; Sunoraha, et al., 1989; Hurst et al., 1994; Palmer and Koch, 1995; McCormick et al., 1996; Galeazzi et al., 2000; Van Nassau et al., 2001) as complex neuroimmune interactions occur during inflammation and/or by toxic excretions from schistosome eggs (Semuguruka, 1992). The observations show alterations of VIP, SP and nitric oxide synthase contents in the local microenvironment in the VIP-, nitric oxide- and SP-mediated reflex pathways that regulate intestinal motility, epithelial transport and modulate immunity. These changes may cause alterations in bowel motility, electrolyte and fluid secretion, vascular and neuroimmune functions. They may influence the pathobiology of migration and egress of schistosome eggs, trapping of eggs in granulomas as well as tissue repair during dissolution of granulomas.

4.4 Future perspectives

-The organisation of the submucous plexuses in large mammals has been further elucidated, but, is still unclear particularly with respect to the number of distinct plexuses. Therefore, the existence of *plexus submucous (entericus) extremus* and the third intermediate plexus in large mammals other than man need to be re-examined and segmental variations elucidated.

-Studies on functional implications for the variation in the size of ganglia and topographical locations amongst the OSP and ISP subplexuses as well as morphological criteria to differentiate them need to be clarified before they are identified as distinct plexuses.

-Further studies to establishing the microcircuits between the mucous, the submucous and the myenteric plexuses are suggested to elucidate the regulatory mechanisms of importance in mucosal functions and consideration of the mucous plexus in the intestine of the large mammals to be one of the major ganglionated plexuses. Therefore, further studies with neurochemical coding and 1,1′-didodecyl-3,3,3′, 3′-tetramethyl indocarbocyanine perchlorate labelling to elucidated projections of neurons are suggest to unravel the intricate organisation of the enteric nervous system in the submucous and mucous plexuses. Complementation of qualitative studies with morphometric analysis may be mandatory to elucidate what may seen to be minor differences in qualitative studies.

-Small ganglia and isolated neurons have been reported in *tunica muscularis* (Furness and Costa, 1987). Morphometric studies are suggested to clarify their amount and significance for regulation of muscle activity and functioning.

-The total number of neurons in ENS in different mammals as well as the total populations of neuroendocrine cells are not well studied. Further studies using the simple, cheap and unbiased sampling design described in the present study are recommended to establish data during normal state which can be used as the basis for evaluating pathophysiological changes.

-Further investigation on neuroplasticity associated with schistosoma infections in the acute and chronic forms are suggested. These will shed light on the mechanisms of adaptation by the ENS. There is also need to explore the neuro-immune interactions to understand the impact of the ENS on the regulatory mechanisms of immunity in the gut.

4.5 References

Albuerne, M., Mammola, C.L., Naves, F.J., Levanti, B., Germana, G., Vega J.A., 1998. Immunohistochemical localization of S100 proteins in dorsal root, sympathetic and enteric ganglia of several mammalian species, including man. *J. Peri. Nerv. Syst.* 3(4), 243-53.

Aloe L., Fiore, M., 1998. Neuroinflammatory implications of *Schistosoma mansoni* infection: New information from the mouse model. *Parasitol. Today* 14(8), 314-318.

Amiri, P., Locksley, R.M., Parslow, T.G., Sadick, M., Rector, E., Ritter, D., McKerrow, J.H., 1992. Tumour necrosis factor alpha restores granulomas and induces parasite egg-laying in schistosome-infected SCID mice. *Nature* 356(6370), 604-607.

Argenzio RA., 1997. Neuro-immune pathobiology of infectious enteric disease. *Adv. Exp. Med. Biol.* 412, 21-29.

Auerbach, L., 1962 Über einen Plexus gangliosus myogastricus. 39. *Jahres-Bericht und Abhandlungen der Schlesischen Gesellschaft für vaterlandische Cultur.* (1961), 103-104.

Auerbach, L., 1964 Fernere vorlaufige Mitteilung über den Nervenapparat des Darmes. *Arch. Pathol. Anat. Physiol. Klin. Med.* 30, 457-460.

Balemba, O.B., Mbassa, G.K., Assey, R.J., Kahwa, C.K.B., Makundi, A.E., Hay-Schmidt, A., Dantzer V., Semuguruka, W.D., 2000. Lesions of the enteric nervous system and the possible role of mast cells in the pathogenetic mechanisms of migration and egress of schistosome eggs in the small intestine of cattle during *Schistosoma bovis* infection. *Vet. Parasitol.* 90, 57-71.

Balemba, O.B., Mbassa, G.K., Semuguruka, W.D., Assey, R.J., Kahwa C.K.B., Hay-Schmidt, A., Dantzer V., 1999. The topography, architecture and structure of the enteric nervous system in the jejunum and ileum of cattle. *J. Anat.* 195, 1-9.

Barbiers M., Timmermans, J-P, Scheuermann, D.W., Adriaensen, D., Mayer, B., De Groodt-Lasseel, M.H.A., 1994. Nitric oxide synthase-containing neurons in the pig large intestine: topography, morphology, and visceralfugal projections. *Microsc. Res. Tech.* 29, 72-78.

Barbiers, M., Timmermans, J-P., Adriaensen, D., De Groodt-Lasseel, M.H.A., Scheuermann D.W., 1995. Projections of neurochemically specified neurons in the porcine colon. *Histochem. Cell Biol.* 103, 115-120.

Barbiers, M., Timmermans, J-P., Scheuermann, D.W., Adriaensen, D., Mayer, B., De Groodt-Lasseel, M.H.A., 1993. Distribution and morphological features of nitrigenic neurons in the porcine large intestine. *Histochem.* 100, 27-34.

Barman, N.N., Bianchi, A.T.J., Zwart, R.J., Pabst, R., Rothkötter, H.J., 1997. Jejunal and ileal Peyer's patches in pigs differ in their postnatal development. *Anat. Embryol.* 95, 41-50.

Bayliss, W.M., Starling., E.H., 1899. The movements and innervation of the small intestine. *J. Pysiol.* 24, 100-143.

Bayliss, W.M., Starling., E.H., 1900a. The movements and innervation of the large intestine. *J. Pysiol.* 26, 107-118.

Bayliss, W.M., Starling., E.H., 1900. The movements and innervation of the small intestine. *J. Pysiol.* 26, 125-138.

Belai, A., Boulos, P.B., Robson T., Burnstock, G., 1997. Neurochemical coding in the small intestine of patients with Crohn's disease. *Gut*, 40(6), 767-764.

Bienenstock, J., Tomioka, M., Matsuda, H., Stead, R.H., Quinonez, G., Simon, G.T., Coughlin, M.D., Denburg, J.A., 1987b.The role of mast cells in inflammatory processes: evidence for nerve/mast cell interactions. *Int. Arch. Allergy Appl. Immunol.* 82(3-4), 238-243.

Bienenstock, J., Tomioka, M., Stead, R., Ernst, P., Jordana, M., Gauldie, J., Dolovich, J., Denburg, J., 1987a. Mast cell involvement in various inflammatory processes. *Am. Rev. Respir. Dis.* 35(6 Pt 2), S5-S8.

Blum, A.M., Metwali, A., Crawford, C., Li, J., Qadir, K., Elliott, D.E., Weinstock, J.V., 2001. Interleukin 12 and antigen independently induce substance P receptor expression in T cells in murine schistosomiasis mansoni. *FASEB J.* 5(6), 950-7.

Blum, A.M., Metwali, A., Mathew, R.C., Elliott, D., Weinstock, J.V., 1993. Substance P and somatostatin can modulate the amount of IgG2a secreted in response to schistosome egg antigens in murine schistosomiasis mansoni. *J. Immunol.* 151(12), 6994-7004.

Bogers, J., Moreels, T., De Man, J., Vrolix, G., Jacobs, W., Pelckmans, P., van Marck, E., 2000. *Schistosoma mansoni* infection causing diffuse enteric inflammation and damage of the enteric nervous system in the mouse small intestine. *Neurogastroenterol. Motil.* 12, 431- 440.

Bogers, J.J., Timmermans J-P., Scheuermann, D.W., Pelckmans, P.A., Mayer, B., van Marck, E.A.,

1994. Localization of nitric oxide synthase in enteric neurons of the porcine and human ileo-caecal junction. *Anat. Anz.* 176(2), 131-135.

Brehmer, A., Beleites B., 1996. Myenteric neurons with different projections have different dendritic tree patterns: a morphometric study in the pig ileum. *J. Auton. Nerv. Syst.* 7;61(1), 43-50.

Brehmer, A., Schrodl, F., Neuhuber, W., 1999. Morphological classification of enteric neurons-100 years after Dogiel. *Anat. Embryol.* 200, 125-135.

Brehmer, A., Stach, W., Addicks, K., 1994. Fine structural distinction between ganglia of the outer and inner submucosal plexus in the porcine small intestine. *Acta Anat.* 151, 188-193.

Brehmer, A., Stach. W., 1998. Regional structural differences in the neuronal composition of myenteric ganglia along the pig small intestine. *Anat. Rec.* 250(1), 109-116.

Bridges, R.J., Rack, M., Rummel, W., Schreiner, J., 1986. Mucosal plexus and electrolyte transport across the rat colonic mucosa. *J. Physiol.* 376, 531-542.

Brown, D.R., 2000. Neuronal release of vasoactive intestinal peptide is important in astrocytic protection of neurons from glutamate toxicity. *Mol. Cell Neurosci.* 15(5), 465-475.

Burns, G., Cummings, J.F., 1993. Neuropeptide distributions in the colon, caecum and jejunum of the horse. *Anat. Rec.* 236, 341-50.

Bush, T.G., Savidge, T.C., Freeman, T.C., Cox, H.J., Campbell, E.A., Mucke, L., Johnson, M.H., Sofroniew, M.V., 1998. Fulminant jejuno-ileitis following ablation of enteric glia in adult transgenic mice. *Cell.* 93, 189-201.

Cetin, Y., Kuhn, M., Kulaksiz, H., Mägert, H.J., Hill, O., Zuchit, H.D., Bargsten, G., Grube., D., Forssmann, W.G., 1994. Enterochromaffin cells of the digestive system: cellular source of guanylin, a guanylate cyclase-activating peptide. *Proc. Ntl Acad. Sci. USA.* 91;2935-2939.

Cheever, A.W., 1981. Schistosomiasis and colon cancer. *Lancet*, 1(8234),1369-1370.

Chen, M.C., Wang, S.C., Chang, P.Y., Chuang, C.Y., Chen, Y.J., Tang, Y.C., Chou, S.C., 1978. Granulomatous disease of the large intestine secondary to schistosome infection. A study of 229 cases. *Chin. Med. J.* 91, 371-378.

Ching-Fan, C., 1957. Schistosomiasis japonica of the colon complicated with carcinoma. *Chin. Med. J.* 75, 500-508.

Christensen, J., Rick, G.A., 1987. Intrinsic nerves in the mammalian colon: confirmation of the a plexus at the circular muscle-submucosa interface. *J. Aut. Nerv. Sys.* 21, 223-231.

Christensen, J., Stiles, M.J., Rick, G.A., Sutherland, J., 1984. Comparative anatomy of the myenteric plexus of the distal colon in eight mammals. *Gastroenterol.* 86, 706-713.

Chu, R.M., Liu, C.H., 1984. Morphological and functional comparisons of Peyer's patches in different parts of swine small intestine. *Vet. Immunol. Immunopathol.* 6(3-4), 391-403.

Collins, S.M., 1996. The immunomodulation of the enteric meuromuscular function: implications for motility and inflammatory disorders. *Gastroenterol.* 111(6), 1683-1699.

Costa, M., Brookes, S.J., 1994. The enteric nervous system. *Am. J. Gastroenterol.* 89(suppl. 8),129-137.

Costa, M., Furness, J.B., Llewellyn-Smith, I.J., 1987. Histochemistry of the enteric nervous system. In: L.R., Jonson, J.,Christensen, M.J., Jackson, E.D., Jacobson, J.H., Walsh, (Eds.), *Physiology of the gastrointestinal tract*, Raven Press, New York, 1-39 pp.

Crowe, R., Kamm, M.A., Burnstock, G., Lennard-Jones, J.E., 1992. Peptide-containing neurons in different regions of the submucous plexus of human sigmoid colon. *Gastroenterol.* 102, 461-467.

de Miranda Neto, M.H., Molinari, S.L., Natali, M.R., Sant'Ana, D.M., 2001.Regional differences in the number and type of myenteric neurons of the ileum of rats: a comparison of techniques of the neuronal evidentiation. *Arq. Neuropsiquiatr.* 59(1), 54-59.

de Souza, R.R., Moratelli, H.B., Borges, N., Liberti, E.A., 1993. Age-induced nerve cell loss in the myenteric plexus of the small intestine in man. *Gerontorology* 39, 183-188.

Dhatt, N., Buchan, A.M.J., 1994. Colocalization of neuropeptides with calbindin D28K and NADPH diaphorase in the enteric nerve plexuses of normal human ileum. *Gastroenterol.* 107, 680-

690.
Doenhoff, M.J., 1997. A role for granulomatous inflammation in the transmission of infectious disease: schistosomiasis and tuberculosis. *Parasitol.* 115 Suppl, S113-125.
Doenhoff, M.J., Hassounah, O., Murare, H., Bain. J., Lucas, S., 1986. The schistosome egg granuloma: Immunopathology in the cause of host protection or parasite survival? *Trans. Roy. Soci. Trop. Med.Hyg.* 80, 503-514.
Drasch, O., 1881. Beiträge zur Kenntniss des feineren Baues des Dünndarms, inbesondere über die Nerven desselben. Sitzber Akad Wiss Wien 82, 3rd div, 168 -198.
Durack, D.T., Sumi, S.M., Klebanoff S.J., 1979. Neurotoxicity of human eosinophils. *Proc. Natl. Acad. Sci. USA* 76, 1443-1447.
Fang, S.Y., Wu, R.W., Christensen, J., 1993. Intramucosal nerve cells in human small intestine. *J. Aut. Nerv. Sys.* 44, 129 - 136.
Faust, E.C., 1946. The effects of cold temperatures on the eggs of *Schistosoma japonicum. Am. J. Trop. Med.* 33, 134-137.
Faust, E.C., Russell, P.F., 1964. Craig and Faust's Clinical Parastology. Henry Kimpton, London.
Ferri, G.-L., 1988. Human gut neuroanatomy: methodology for quantitative analysis of nerve elements and neurotransmitter diversity in the human enteric nervous system. *Bas. Appl. Histochem.* 32, 117-144.
Fregonesi, C.E.P.T., de Miranda-Neto, M.H., Molinari, S.L., Zanoni, J.N., 2001. Quantitative study of the myenteric plexus of the stomach or rats with Streptozocin-induced diabetes. *Arq. Neuropsiquiatr.* 59(1),50-53.
Furness, J.B., Costa, M., 1980. Commentary: Types of nerves in the enteric nervous system *Neurosci.* 5, 1-20.
Furness, J.B., Costa M., 1987. *The enteric nervous system.* Churchill, Livingstone, Edinburgh, 1-286 pp.
Furness, J.B., Costa M., Keast J.R., 1984. Choline acetyltransferase- and peptide immunoreactivity of the submucous neurons in the small intestine of the guinea-pig. *Cell and Tissue Res.* 237, 329-336.
Furness, J.B., Li Z.S., Young, H.M., Förstermann U., 1994. Nitric oxide synthase in the enteric nervous system of the guinea pig: a quantitative description. *Cell and Tissue Res.* 277, 139-149.
Furness, J.B., Llewellyn-Smith, I.J., Bornstein, J.C., Costa, M., 1988. Chemical neuroanatomy and the analysis of neuronal circuitry in the enteric nervous system. In: Bjørklund, A., Hökfelt, T., (Eds.), *Handbook of chemical neuroanatomy*, Elsevier science publishers, Amsterdam, 161-218 pp.
Gabella, G., 1971. Neuron size and number in the myenteric plexus of the newborn and adult rat. *J. Anat.* 109 (1), 81-95.
Gabella, G., 1976. Structure of the autonomic nervous system. Wiley, New York.
Gabella, G., 1979. Innervation of the gastrointestinal tract. In: G.H., Bourne, J.F., Danielli, (eds) *International Review of Cytology.* Academic Press, New York. 129-193 pp.
Gabella, G., 1987. The number of neurons in the small intestine of mice, guinea-pigs and sheep. Neurosci. 22, 737-752.
Gabella, G., 1989. Fall in the number of myenteric neurons in ageing guinea pigs. *Gastroenterol.* 96, 1487-93.
Gabella, G., 1990. On the plasticity and structure of the enteric ganglia. *J. Aut. Nerv. Syst.* 30, S59-S66.
Galeazzi, F., Haapala, E.M., Van Rooijen, N., Bruce, A. Vallance, B.A., Collins, S.M., 2000. Inflammation-induced impairment of enteric nerve function in nematode-infected mice is macrophage dependent *Am. J. Gastrointest. Liver Physiol.* 278(2), G259-G265.
Giaroni, C., De ponti, F., Cosentino, M., Lecchini, S., Frigo, G., 1999. Plasticity in the enteric nervous system. *Gastroenterol.* 117, 1438-1458.

Grundy, D., Schemann, M., Wood, J., 2000. A tale of two brains, one little and one big. *Neurogastroenterol. Mot.* 12, 105-111.

Gundersen, H.J.G., 1986. Stereology of arbitrary particles: A review of unbiased number and size estimators and the presentation of some new ones, in memory of William R. Thompson. *J. Microsc.* 143, 3-45.

Gundersen, H.J.G., Bagger, P., Bendtsen, T.F., et al. 1988.The new Stereological tools: Disector, fractionator, nucleator, and point sampled intercepts and their use in pathological research and diagnosis. *APMS.* 96, 857-881.

Gunn, M.,1968. Histological and histochemical observations on the myenteric and submucous plexuses of mammals. *J. Anat.* 102(2), 223-239.

Hansen, M.B., Skadhauge, E. 1995. New aspects of the pathophysiology and treatment of secretory diarrhoea. *J. Physiol. Res.* 44, 61-78.

Hass, W., Gui, M., Haberl, B., Ströbel, M., 1991. Miracidia of *Schistosoma japonicum*: approach and attachment to the snail host. *J. Parasitol.* 77, 509-513.

He, Y.X., 1993. Biology of *Schistosoma japonicum* from cercariae penetrating into host skin to producing egg. *Chin. Med. J.* 106(8), 576-583.

He, Y.X., Hu, Y.Q., Yu, Q.F., Tang, Z.J., 1991. Characteristics of different isolates of *Schistosoma japonicum* from China in the final host. *South East Asian J. Trop. Med. Publ. Health* 23, 240-244.

He, Y.X., Yang, H.H., 1980. Physiological studies on the post-cercarial development of *Schistosoma japonicum. Acta Zoologica Sinica* 26, 32-39.

Hedreen, J.C. 1998. Lost caps in histological counting methods. *Anat. Rec.* 250, 366-372.

Hens, J., Schrödl, F., Brehmer, A., Adriaensen, D., Neuhuber, W., Scheuermann, D.W., Schemann, M., Timmermans, J.-P., 2000. Mucosal projections of enteric neurons in the porcine small intestine. *J. Comp. Neurol.* 421, 429 - 436.

Hesse, M., Cheever, A.W., Jankovic, D., Wynn, T.A., 2000. NOS-2 mediates the protective anti-inflammatory and anti-fibrotic effects of the Th1-inducing adjuvant, IL-12, in a Th2 model of granulomatous disease. *Am. J. Pathol.* 157(3), 945-955.

Hirata, M., Kage, M., Hara, T., Yoneda, Y., Zhang, M., Fukuma, T., 2001. Schistosoma japonicum egg granuloma formation in the interleukin-4 or interferon-gamma deficient host. *Parasite Immunol.* 23(6), 271-280.

Holzer, P., 1998. Implications of tachykinins and calcitonin gene-related peptide in inflammatory bowel disease. *Digestion* 59(4), 269-283.

Howard, C.V., Reed, M.G., 1998. Unbiased Stereology: Three dimensional measurement in microscopy. BIOS Scientific Publishers, Oxford, London, pp 1-123.

Hoyle, C.V., Burnstock, G., 1989a. Galanin-like immunoreactivity in enteric neurons of human colon. *J. Anat.* 166, 23-33.

Hoyle, C.V., Burnstock, G., 1989b. Neuronal populations in the submucous plexus of the human colon. *J. Anat.* 166, 7-22.

Hunter, J.M., Rey, L., Chu, K.Y., Adekulu-John, E.O., Mott, K.E. 1993. Parasitic Diseases in Water Resources development. The need for intersectorial negotiation. World Health Organisation, Geneva.

Hurst, M.H., Lee Willingham III A., Lindberg, R., 2000. Tissues responses in experimental schistosomiasis japonica in the pig: a histopathologic study of different stages of low- or high-dose infections. *Am. J. Trop. Med. Hyg.* 62(1), 45-56.

Hurst., S.M., Collins S.M., 1994. Mechanisms underlying tumour necrosis factor-alpha suppression of norepinephrine release from rat myenteric plexus. *Am. J. Physiol.* 266, G1123-1129.

Hurst SM, Stanisz AM, Sharkey KA, Collins SM. 1993. Interleukin 1 beta-induced increase in substance P in rat myenteric plexus. *Gastroenterol.* 105(6),1754-1760.

Iburg, T., Balemba, O.B., Dantzer, V., Leifsson, P.S., Johansen, M.V., 2001. A note on pathogenesis of congenital infection with *Schistosoma japonicum* in pigs. Proceedings of International

Symposium on Schistosomiasis. Shanghai, China (4-6 July, 2001). 134 pp.
Imbert-Establet, D., Mone, H., Coulson, P.S., Wilson, R.A., 1998. Schistosome-induced portacaval haemodynamic changes in *Rattus rattus* are associated with translocation of adult worms to the lungs. *Parasitol.* 116(Pt 3), 237-241.
Johansen, M.V., Bøgh, H.O., Giver, H., Eriksen, L., Nansen, P., Stephenson, L., Knudsen, K.E.B., 1997. *Schistosoma japonicum* and *Trichuris suis* infections in pigs fed diets with high and low protein. *Parasitol.* 115, 257-264.
Johansen, M.V., Iburg, T., Bøgh, H.O., Christensen N.Ø., 2001. Postnatal challenge infections of congenitally *Schistosoma japonicum* infected piglets. *J. Parasitol.* (In press).
Karaosmanoglu, T., Aygun, B., Wade, R., Gershon, M., 1996. Regional differences in the number of neurons in the myenteric plexus of the guinea pig small intestine and colon: An evaluation of markers used to count neurons. *Anat. Rec.* 244, 470-480.
Keast, J.R., Furness, J.B., Costa, M., 1984. Somatostatin in human enteric neurons. *Cell Tissue Res.* 237, 299-308.
Kobayashi, H., Yamataka, A., Fujimoto, T., Lane, G.J., Miyano, T., 1999. Mast cells and gut nerve development: implications for Hirschsprung's disease and intestinal neuronal dysplasia. *J. Pediatr. Surg.* 34(4), 543-548.
Krammer, H., Kühnel, W., 1992a. Immunohistochemistry of intermediate filaments in the enteric nervous system of the porcine small intestine. *Annals Anat.* 174, 275-278.
Krammer, H., Stach, W., Kühnel, W., Meyer, B., 1992b. Occurrence and distribution of nitric oxide synthase-immunoreactive neurons in the submucosal plexus of the porcine small intestine. *Brain Res.* 577, 337-342.
Krammer, H.-J., Kühnel, W., 1993. Topography of the enteric nervous system in the Peyer's patches of the porcine small intestine. *Cell Tissue Res.* 272, 267-272.
Krause, W.J., Yamada, J., Cutts, J.H., 1984. Quantitative distribution of endocrine cells in the gastrointestinal tract of the adult opossum, *Didelphis virginiana*. *J. Anat.* 140(4), 591-605.
Kuba, N., 1963. Histopathological study on mechanisms of extrusion of schistosome ova from blood vessels. *Jap. J. Vet. Sci.* 25, 289-297.
Kulkarni-Narla, A., Bertz A.J., Brown, D.R., 1999. Catecholaminergic, cholinergic and peptidergic innervation of the gut-associated lymphoid tissue in the porcine jejunum and ileum. *Cell and Tissue Res.* 298, 273-286.
Langley, J.N., 1889. On the local paralysis of the peripheral ganglia and on the connection of different classes of nerve fibres with them. *Proc. R. Soc. Lond.* 46, 423-431.
Lassmann, G., 1975. Vorkommen von Ganglienzellen im Schleimhaustroma von Colon, sigma und Rectum. *Virch. arch. A: Pathol. Anat. Histol.* 365, 257-261.
Lawrence, J.A., 1978. The pathology of *Schistosoma matthei* infection in ox. 2. Lesions attributable to the adult parasites. *J. Comp. Pathol.* 88, 15-29.
Leaming, D.B., Cauna, N., 1961. A qualitative and quantitative study of the myenteric plexus of the small intestine of the cat. *J. Anat.* 95(2), 160-169.
Lenzi, H.L., Lenzi, J.A., Sobral, A.C.L., 1987. Eosinophils favour the passage of eggs to the intestinal lumen in Schistosomiasis. *Braz. J. Med. Biol. Res.* 20, 433-435.
Liberti, E.A., Gaspar, L.P., de Carvalho, C.A., Fujimura, I., de Souza, R.R., 1998. A morpho-quantitative study of the myenteric ganglia throughout the human digestive tract. *Rev. Hosp. Clin. Fac. Med. Sao Paulo*, 53(2), 55-60.
Lowden, S., Heath, T., 1994. Ileal Peyer's patches in pigs: Intercellular and lymphatic pathways. *Anat. Rec.* 239, 297-305.
Maifrino, L.,B., Liberti, E.A., Watanabe, I., and De Souza, R.R., 1999. Morphometry and acetylcholinesterase activity of the myenteric neurons of the mouse colon in the chronic phase of experimental *Trypanosoma cruzi* infection. *Am. J. Trop. Med. Hyg.* 60(5), 721-725.
Mannl, A., Pospischil, A., Dahme, E., 1986. The submucosus plexus (Meissner's and Schabadasch's) in the pig gut: I. Light and Electron Microscopy of the normal structure. *J. Vet. Med.* A. (33),

647-659.

Matthew, R.C., Cook, G.A., Blum, A.M., Metwali, A., Felman, R., Weinstock, J.V., 1992. Vasoactive intestinal peptide stimulates T lymphocytes to release IL-5 in murine schistosomiasis mansoni infection. *J. Immunol.* 148(11), 3572-3577.

Maudlej, N., Hanani, M., 1992. Modulation of dye coupling among glial cells in the myenteric and submucosal plexuses of the guinea pig. *Brain Res.* 578, 94-98.

McCormick, M.L., Metwali, A., Railsback, M.A., Weinstock, J.V., Britigan, B.E., 1996. Eosinophils from schistosome-induced hepatic granulomas produce superoxide and hydroxyl radical. *J. Immunol.* 157(11), 5009-5015.

Meciano-Filho, J., Carvalho, V.C., and de Souza, R.R., 1995. Nervous cell loss in the myenteric plexus of the human oesophagus in relation to age: a preliminary investigation. 1995. *Gerontol.* 41, 18-21.

Meissner, G., 1957. Über die Nerven der Darmwand. *Henle und Pfenfer Z. Ration Med.* 8, 364-366.

Mestres, P., Diener, M., Rummel, W., 1992a. Histo- and immunocytochemical characterization of the neurons of the mucosal plexus in the rat colon. *Acta Anat.* 143, 268-74.

Mestres, P., Diener, M., Rummel, W., 1992b. Electron Microscopy of the mucosal plexus of the rat colon. *Acta Anat.* 143, 275-82.

Metwali, A., Blum, A., Matthew, R., Sandor, M., Lynch, R.G., Weinstock, J.V., 1993. Modulation of T-Lymphocyte proliferation in mice infected with schistosoma mansoni: VIP suppresses mitogen-and antigen-induced T cell proliferation possibly by inhibiting IL-2 production. *Cell Immunol.* 149(1), 11-23.

Ming-Chai C., Shan-Chi, C.W., 1957. Acute colonic obstruction in schistosomiasis japonica. A clinical study of 40 cases-14 associated with carcinoma. *Chin. Med. J.* 75(7), 517-532.

Ming-Hsin, H., Shao-Chi, C., Cheng-Wei, L., Kuo-Juei, Y., Juei-P`eng, P., Ju-Sun, P. Pnag-Fu, K., 1957. Schistosomiasis dwarfism. *Chin. Med. J.* 75, 448-461.

Miyagawa, Y., Takemoto, S. 1921. The mode of infection of *Schistosoma japonicum* and the principal route of its journey from skin to the portal vein in the host. *J. Pathol. Bacteriol.* 24, 168-174.

Naik, R., Baliga, P., Pai, M.R., 1999. Neurogenic appendicopathy--role of enterochromaffin cells in its pathogenesis. *Indian J. Pathol. Microbiol.* 42(3), 279-281.

Nai-Kuang, C., Pen-Chung, C. 1957. Pyloric obstruction and sigmoidal fistula due to schistosomiasis. *Chin. Med. J.* 75, 324-327.

Newson, B., Ahlman, H., Dahlström, A., Das Gupta, T.K., Nyhus, L.M., 1979. Are there sensory neurons in the mucosa of the mammalian gut? *Acta Physiol. Scand.* 105, 521-523.

Oshima, S., Fujimura, M., Fujimiya, M., 1999. Changes in number of serotonin-containing cells and serotonin levels in the intestinal mucosa of rats with colitis induced by dextran sodium sulphate. *Histochem. Cell Biol.* 112, 257-263.

Oswald, I.P., Dozois, C.M., Barlagne, R., Foumout, S., Johansen, M.V., Bogh, H.O., 2001. Cytokine mRNA expression in pigs infected with *Schistosoma japonicum*. *Parasitol.* 122, 299-307.

Ozaki, T., Inaba, T., Sato, H., Nargis, M., Chisty, M., Kamiya, H., 1997. *Schistosoma mansoni*: relocation of parasites to lungs from hepatic portal system in rodents. *South East Asian J. Trop. Med. Publ. Health* 28(3), 581-587.

Palmer, J.M., Koch T.R., 1995. Altered neuropeptide content and cholinergic enzymatic activity in the inflamed guinea pig jejunum during parasitism. *Neuropeptides* 28, 287-297.

Papadaki, L., Rode, J., Dhillon, A.P., Dische, F.E., 1983. Fine structure of a neuroendocrine complex in the mucosa of the appendix. *Gastroenterol.* 84(3), 490-497.

Pearson, G.T., 1994. Structural organisation and neuropeptide distributions in the equine enteric nervous system: an immunohistochemical study using whole-mount preparations from the small intestine. Cell Tissue Res. 276(3), 523-534.

Pearson, G.T., Thompsen, L., Tindholdt, T.T., Skadhauge, E., 1997. Synaptic communication between external and internal submucosal plexus neurons in the jejunum of the newborn pig?

Comp. Biochem. Physiol. A. Physiol. 118(2), 355-357.

Pittella, J.E., 1997. Neuroschistosomiasis. *Brain Pathol.* 7(1), 649-62.

Porter, A., Wattchow, D.A., Brookes, S.J.H., Costa, M., 1999. Nitric oxide synthase and vasoactive intestinal polypeptides in the human colon: Projections of nitric oxide synthase and vasoactive polypeptide-reactive submucosal neurons in the human colon. *J. Gastroenterol. Hepatol.* 14, 1180-1187.

Pothoulakis, C., Castagliuolo, I., LaMont, T., 1998. Nerves and intestinal mast cells modulate responses to enterotoxins. *News Physiol. Sci.* 13, 58-63.

Powel D.W., 1994. New paradigms for the pathophysiology of infectious diarrhea. *Gastroenterol.* 106(6), 1705-1707.

Rantala, I., Paronen, I., Kainulainen, H., Ala-Kaila, K., 1996. Enterochromaffin cell density in the gastric mucosa of patients with chronic renal failure. *APMIS* 104(5), 362-366.

Read, N.W., 1991. The role of motility in diarrheal diseases in: M., Fiels (eds) *Diarrheal Diseases.* Elsevier, New York. pp 173-190.

Rothkötter, H.J., Zimmermann, H.J., Pabst, R., 1990. Size of jejunal Peyer's patches and migration of lymphocyte substets in pigs after sesection or transposition of the continuous ileal Peyer's patch. *Scand. J. Immunol.* 31(2), 191-197.

Ruhl, A., Franzke, S., Collins, S.M., Stremmel, W., . 2001a. Interleukin-6 expression and regulation in rat enteric glial cells. *Am. J. Physiol. Gastrointest. Liver Physiol.* 280(6), G1163-171.

Ruhl, A., Franzke, S., Stremmel, W., 2001b. IL-1beta and IL-10 have dual effects on enteric glial cell proliferation. *Neurogastroenterol Motil.* 13(1), 89-94.

Saad, A.M., Hussein, M.F., Dargie,J.D., Taylor,M.G., Nelson, G.S., 1980. *Schistosoma bovis* in calves: The development and clinical pathology of primary infections. *Res. Vet. Sci.* 28, 105-111.

Sarosi, G.A., Barnhart, D.C., Turner, D.J., Mulholland, M.W., 1998. Capacitative Ca2+ entry in enteric glia induced by thapsigargin and extracellular ATP. *Am. J. Physiol.* 275, G550-G555.

Scheuermann, D.W., Krammer, H.-J., Timmermans, J.-P., Stach, W., Adriaensen, D., De Groodt-Lasseel, M.H., 1991. Fine structure of morphologically well-defined type II neurons in the enteric nervous system of the porcine small intestine revealed by immunorectivity for calcitonin Gene- related peptide. *Acta Anat.* 142, 236-241.

Scheuermann, D.W., Stach, W., Timmermans, J.-P., 1986. Three dimensional organisation and topographical features of the myenteric plexus (Auerbach) in the porcine small intestine: Scanning electron microscopy after enzymatic digestion and Hcl-hydrolysis. *Acta Anat.* 127, 290-295.

Scheuermann, W.D., Stach, W., Timmermans, J.-P., 1987*a*. Topography, architecture and structure of the plexus submucousus internus (Meissner) of the porcine small intestine in scanning electron microscopy. *Acta Anat.* 129, 96-104.

Scheuermann, W.D., Stach, W., Timmermans, J.-P., 1987*b*. Topography, architecture and structure of the plexus submucousus externus (Schabadasch) of the porcine small intestine in the Scanning Electron microscopy. *Acta Anat.* 129, 105-115.

Scheuermann, D.W., Stach, W., Timmermans, J.-P., Adriaensen, D., De Groodt-Lasseel, M.H., 1989. Neuron-specific enolase and S-100 protein immunohistochemistry for defining the structure and topographical relationship of the different enteric nerve plexuses in the small intestine of the pig. *Cell and Tissue Res.* 256(1), 65-75.

Semuguruka, W.D., 1992. Intestinal lesions associated with transmucosal migration of eggs in calves and hamsters infected with *Schistosoma bovis*: A light and electron microscopic study. *PhD Thesis* RVAU, Copenhagen, Denmark.

Shanahan, F., 1998. Enteric neuropathophysiology and inflammatory bowel disease. *Neurogastroenterol. Motil.* 10, 185-187.

Sharkey, K.A., Kroese, A.B.A., 2001. Consequences of intestinal inflammation on the enteric nervous system: Neuronal activation induced by inflammatory mediators. *Anat. Rec.* 262, 79-90.

Sjöqvist, A., Cassuto, J., Jodal, M., Lundgren, O., 1992. Actions of serotonin antagonists on cholera-toxin induced intestinal fluid secretion. *Acta Physiol. Scand.* 145, 229-237.

Stach, W. 1972. Der Plexus entericus extremus des Dickdarm und seine Beziehungen zu den interstitiellen zellen (Cajal). *Z. Mikrosk. Anat. Forsch.* 85, 245-272.

Stach, W. 1977. Der Plexus submucosus externus (Schabadasch) im Dünndarm des Schweins. I. Form, Struktur und Verbindindungen der Ganglien und Nervenzellen. *Z. Mikrosk. Anat. Forsch.* 91, 737-755.

Stach, W. 1989. A revised morphological classification of neurons in the enteric nervous system. In Singer, M.V., Goebell, H., (eds), *Nerves and the Gastrointestinal Tract.* MTP Press, Dordecht. 29-45 pp.

Stöhr, P., 1934. Mikroscopische studien zur Innervation des Magen-Darmkanales III. *Z. Zellforsch. Mikrosk. Anat.* 21, 243-278.

Stöhr, P., 1944. Mikroscopische studien zur Innervation des Magen-Darmkanales V. *Z. Zellforschung mikrosk. Anat.* 34, 1-54.

Sunoraha, N., Furukawa,, S., Nishio, T., Mukoyama, M., Satayoshi E., 1989. Neurotoxicity of eosinophils towards peripheral nerves. *J. Neurol. Sci.* 92 (1), 1-7.

Suzuki, R., Furuno, T., McKay, D.M., Wolvers, D., Teshima, R., Nakanishi, M., Bienenstock, J., 1999. Direct neurite-mast cell communication in vitro occurs via the neuropeptide substance P. *J. Immunol.* 163(5), 2410-2415.

Thomsen, L., Pearson, G.T., Larsen, E.H., Skadhauge, E., 1997. Electrophysiological properties of neurons in the internal and external submucous plexuses of newborn pig small intestine. *J. Physiol.* 498(Pt 3), 773-785.

Thuneberg, L., 1989. Intestitial cells of Cajal. In: Wood, J.D., (ed), *Handbook of Physiology: The gastrointestinal System,* Sect. 6, Vol. 1, Part 1, Bethesda, MD: American Physiology Society, Chapter 10; 349-386 pp.

Timmermans, J.-P., Adriaensen, D., Cornelissen, W., Scheuermann, D.W., 1997. Structural organisation and neuropeptide distribution in the mammalian enteric nervous system, with special attention to those components involved in mucosal reflexes. *Comp. Biochem. Physiol.* 118A (2), 331-340.

Timmermans, J.-P., Barbiers, M., Scheuermann, D.W., Bogers, J.J., Adriaensen, D., Mayer, B., De Groodt-Lasseel, M.H.A., 1994. Distribution pattern, neurochemical features and projections of nitrigenic neurons in the pig small intestine. *Ann. Anat.* 176, 515-525.

Timmermans, J.-P., Hens, J, Adriaensen, D., 2001. Outer submucous plexus: An intrinsic nerve network involved in both secretory and motility processes in the intestine of large mammals and human. *Anat. Rec.* 262, 71-78.

Timmermans, J.-P., Scheuermann, D.W., Stach, W., Adriaensen, D., De Groodt-Lasseel, M.H.A., 1990. Distinct distribution of CGRP-, enkephalin-, somatostatin-, substance P-, VIP- and serotonin - containing neurons in the two submucosal ganglionic neural networks of the porcine small intestine. *Cell Tissue Res.* 260, 367-379.

Timmermans, J.-P., Scheuermann, D.W., Stach, W., Adriaensen, D., De Groodt-Lasseel, M.H.A., 1992. Functional morphology of the enteric nervous system with special reference to large mammals. Eur. J. Morphol. 30 (2), 113-122.

Totzauer, I., 1991. Development of the bovine duodenum with reference to enterochromaffin cells. *Anat Histol. Embryol.* 20;54-65.

Van Ginneken, C., Van Meir, F., Sommereyns, G., Sys, S., Weyns, A., 1998. Nitric oxide synthase expression in enteric neurons during development in the pig duodenum. *Anat. Embryol.* 198 (5), 399-408.

Van Nassauw, L., Bogers, J., Van Marck, E., Timmermans, J.-P., 2001. Role of reactive nitrogen species in neuronal cell damage during intestinal schistosomiasis. *Cell Tissue Res.* 303(3), 329-336.

Varilek, G.W., Weinstock, J.V., Williams, H., Jew, J., 1991. Alterations of the intestinal innervation

in mice infected with *Schistosoma mansoni*. *J. Parasitol.* 77, 472-478.

Vau E., 1932. Über die subglandulären Ganglienzellen in der Magenwand einiger Haussäugetiere. *Anat. Anz.* 73, 380-385.

Wallis, T.S., Vaughan, A.T.M., Clarke, G.J., Qi, G.-M., Worton, K.J., Candy, D.C.A., Orsborne, M.P., Stephen J., 1990. The role of leukocytes in the induction of fluid secfretion by *Salmonella typhimurium*. *J. Med. Microbiol.* 31, 27-35.

Warren, K.S., 1969. Intestinal obstruction in murine schistosomiasis japonica. *Gastroenterol.* 57(6), 697-702.

Wedel, T., Roblick, U., Gleiss, J., Schiedeck, T., Bruch, H.P., Kühnel, W., Krammer, H.J. 1999. Organisation of the enteric nervous system in the human colon demonstrated by wholemount immunohistochemistry with special reference to the submucous plexus. *Anat. Anz.* 181(4), 327-337.

Weinstock, J.V., 1991. Production of neuropeptides by inflammatory cells within the granulomas of murine *Schistosomiasis mansoni*. *Eur. J. Clin. Invest.* 22 (2), 145-153.

Weinstock, J.V., 1996. Vasoactive intestinal peptide regulation of granulomatous inflammation in murine schistosomiasis mansoni. *Adv Neuroimmunol.* 6(1), 95-105.

Weinstock, J.V., Blum, A.M., 1990. Detection of vasoactive intestinal polypeptide and localization if its mRNA within granulomas of murine schistosomiasis. *Cellular Immunol.* 125, 291-300.

Weinstock, J.V., Elliott, D., 1998 The substance P and somatostatin interferon-gamma immunoregulatory circuit. *Ann N Y Acad Sci.* 1(840), 532-539.

Weinstock, J.V., Elliott, D., 2000.The somatostatin immunoregulatory circuit present at sites of chronic inflammation. *Eur J Endocrinol.* 143(Suppl 1), S15-19.

Wilks, N.E., 1967. Lung to liver migration of schistosomes in the laboratory mouse. *Am. J. Trop. Med. Hyg.* 16, 599-605.

Willingham, A.L., 3rd, 1996. Experimental *Schistosoma japonicum* infection in the pig: The host regulatory response and other aspects of the host-parasite relationship. *PhD Thesis*, RVAU, Copenhagen, Denmark.

Willingham, A.L., 3rd, Johansen, M.V., Bogh, H.O., Ito, A., Andreassen, J., Lindberg, R., Christensen, N.O., Nansen, P., 1999. Congenital transmission of *Schistosoma japonicum* in pigs. *Am. J. Trop. Med. Hyg.* 60(2), 311-312.

Wood, J.D., 1994. Gastrointestinal neuroimmune interaction. In: G., Holle, J.D., Wood, J (eds) *Advances in the Innervation of the Gastrointestinal Tract*. Elsevier, Amsterdam. PP 607-615.

Wood, J.D., 2000. Neuropathy in the brain-in-the-gut. *Eur. J. Gastroenterol. Hepatol.* 12, 597-600.

Wu, T.S., Chen, T.C., Chen, R.J., Chiang, P.C., Leu, H.S., 1999. *Schistosoma japonicum* infection presenting with colon perforation: case report. *Changgeng Yi Xue Za Zhi* 22(4), 676-81.

Wu, Z.W. Liu, Z.D., Pu, K.M., Hu, G.H., Zhou, S.Y., Zhang, S.J., Yuan, H.C., 1992. Role of human and domestic reservoir hosts of schistosomiasis japonica in Dongting and Boyang Lake regions. *Chin. J. Parasitol. and Parasit. Dis.* 10, 194-197.

Xiong, S., Puri, P., Nemeth, L., O`Briain, D.S., Reen, D.J., 2000. Neuronal hypertrophy in acute appendicitis. *Arch. Pathol. Lab. Med.* 124(10), 1429-1433.

Yamamoto, Y., Kitamura, N., Yamada, J., Atoji, Y., Suzuki, Y., Yamashita, T., 1994. Structure of the enteric nervous system in sheep omasum as revealed by neurofilament protein-like immunoreactivity. *J. Anat.* 184, 399-405.

Yason, C.V., Novilla, M., 1984. Clinical and pathological features of experimental *Schistosoma japonicum* infection in pigs. *Vet. Parasitol.* 17, 47-64.

Young, H.M., Furness, J.B., Sewell, P., Burcher, E.F., and Kandiah, C.J., 1993. Total numbers of neurons in myenteric ganglia of the guinea-pig small intestine. *Cell Tissue Res.* 272, 197-200.

Yunker, A.M., Paupore, E.J., Galligan, J.J., 1999. C-Fos in enteric nerves after extrinsic denervation of guinea pig ileum. *J. Surg. Res.* 82(2), 324-330.

Paper I

J. Anat. (1998) 192, pp. 257–267, with 5 figures Printed in the United Kingdom

The organisation of the enteric nervous system in the submucous and mucous layers of the small intestine of the pig studied by VIP and neurofilament protein immunohistochemistry

O. B. BALEMBA[1], M. L. GRØNDAHL[2], G. K. MBASSA[1], W. D. SEMUGURUKA[3], A. HAY-SMITH[2], E. SKADHAUGE[2] AND V. DANTZER[2]

[1] *Department of Veterinary Anatomy, Faculty of Veterinary Medicine, Sokoine University of Agriculture, Chuo Kikuu-Morogoro, Tanzania,* [2] *Institute for Anatomy and Physiology, Royal Veterinary and Agriculture University, Copenhagen, Denmark, and* [3] *Department of Veterinary Pathology, Faculty of Veterinary Medicine, Sokoine University of Agriculture Chuo Kikuu Morogoro, Tanzania*

(*Accepted 3 December 1997*)

ABSTRACT

The arrangement of the enteric ganglia and nerve fibre plexuses was examined in the submucous and mucous layers and around Peyer's patches of the porcine small intestine to clarify their organisation. Immunohistochemistry of vasoactive intestinal peptide (VIP) and neurofilament proteins in wholemounts, chopped or paraffin sections was used to locate the neural elements. The ganglia of the internal and external submucous plexuses were situated at 2 different topographic locations, being clearly demarcated by the submucosal vascular arcades and differing in neuronal composition. The internal submucous plexus was the only contributor to the plexus surrounding the follicles of Peyer's patches as a continuous mesh of 3 ganglionated nerve subplexuses. VIP-immunoreactive fibres from this mesh innervated the dome. The mucosal plexus, which was subdivided into 4 subunits—the outer proprial, inner proprial, pericryptal and villous plexuses—contained a few solitary neuronal perikarya. Labelling for neurofilament proteins revealed Dogiel types II, IV and VI neurons. The observations reveal several new features in the enteric nervous system of the pig and clarify its nomenclature.

Key words: Small intestine; neurofilament protein; vasoactive intestinal peptide.

INTRODUCTION

In large animal species, the enteric nervous system (ENS) comprises 3 ganglionic plexuses: the myenteric plexus (MP), the internal submucous plexus (ISP) and the external submucous plexus (ESP) (Stach, 1988; Timmermans et al. 1992; Pearson, 1994). The ISP is also termed Meissner's plexus and the ESP is called Henle's or Schabadasch's plexus (Scheuermann et al. 1987*b*).

In the small intestine of the pig, the 2 submucous plexuses are situated at 2 different topographic levels. They differ in number, shape and size of ganglia, number and size of neurons and number and diameter of nerve fibres (Mannl et al. 1986; Scheuermann et al. 1987*a*, *b*). The glial cell mass is more abundant in the ESP than the ISP, and the ESP meshwork is wider than that of the ISP (Thomsen et al. 1997). In the ISP, numerous small ganglia are located at the intersections of the fibre mesh (Scheuermann et al. 1987*a*, *b*; Krammer & Kühnel, 1992). Neuropeptides show a distinct distribution between the 2 submucosal plexuses. Neuropeptide Y, somatostatin and enkephalin immunoreactive neuronal perikarya appear solely in the ESP, whereas those immunoreactive to neuromedin U are abundant in the ISP (Timmermans et al. 1990).

In view of these differences between the 2 submucous plexuses in the small intestine of pig, Timmermans et al. (1990) proposed that they perform

Correspondence to Dr vet. sci. Vibeke Dantzer, Institute for Anatomy and Physiology, The Royal Veterinary and Agricultural University, Bülowsvej 13, DK-1870 Frederiksberg C, Copenhagen, Denmark. Tel: 4535282543; fax: 4535282547; e-mail: Vibeke.Dantzer@iaf.kvl.dk

different functions. This proposition has been supported by differences in electrophysiological properties between these plexuses as recorded by Pearson et al. (1996) and Thomsen et al. (1997).

Despite this information, there are contradictory descriptions of morphology and function between the submucous plexuses in the small intestine of the pig. For instance, there are reports of a third (intermediate) plexus in the submucous layer (Gunn, 1968). Scanning electron microscopy (SEM) shows that ISP ganglionic clusters and nerve fibre strands are situated at 2 topographic levels. The smallest ganglia are situated close to and associated with the lamina muscularis mucosae (Scheuermann et al. 1987*a*). In some respects, these observations support the existence of an intermediate plexus. In the small intestine of pig the ISP and ESP are separated by the submucosal vascular arcades with the ISP on the mucosal and the ESP on the serosal side (Scheuermann et al. 1987*a*, *b*; Thomsen et al. 1997). These arcades have been observed to underlie the lymphoid follicles (Lowden & Heath, 1994). In contrast, the EPS ganglia in Peyer's patches have been reported to be situated close to the base of the lymphoid follicles and those of the ISP are in the interfollicular region (Krammer & Kühnel, 1993). Because of these contradictions we re-examined the morphological organisation of the ISP and ESP in the jejunum and ileum of pig.

According to Furness & Costa (1980), the mucous plexus is composed of fine nerve bundles and axons. The mucous plexus can be subdivided into subglandular, periglandular and villous components.

Peyer's patches play a central role in the uptake of antigens, induction of immune responses, proliferation of B lymphocytes and synthesis of immunoglobulin (Pabst, 1987). VIP modulates T-cell proliferation and regulates their function (Metwali et al. 1993). We have observed that VIP outlines organisation of the ENS in the small intestine of pig.

Pooled antisera against neurofilament proteins (NF 200, 70 and 160 kDa) have been used to visualise the structure of the ENS in the sheep omasum (Yamamoto et al. 1994). Antibodies against NF 200 kDa NF have also been used to visualise its organisation in the pig small intestine but reactivity to this antibody was only displayed in type II neurons (Krammer & Kühnel, 1992).

In the last 3 decades, the organisation of the ENS in the small intestine of pig has been studied mainly by histochemistry (Timmermans et al. 1990, 1992; Krammer & Kühnel, 1992) and SEM (Scheuermann et al. 1987*a*, *b*). The most recent study by conventional light microscopy is that of Mannl et al. (1986). These authors used toluidine blue and safranin staining to reveal topographic and neuronal differences between the 2 submucosal plexuses.

In this study, we have used histochemical staining for VIP- and NF-like immunoreactivity (IR) and histological staining by haematoxylin-eosin to elucidate the organisation of the ENS in the jejunum and ileum of pig. Emphasis has been placed on the organisation of the ENS in the tela submucosa, Peyer's patches and tunica mucosa. We also aimed to describe clearcut criteria to differentiate the 2 submucosal plexuses and thereby establish an appropriate nomenclature.

MATERIALS AND METHODS

Sampling and fixation

Seven Danish Landrace/Yorkshire cross bred weanling piglets aged 6–8 wk (13–15 kg) fed on a standard commercial diet (N.A.G. Svine foder 5, Helsinge, Denmark) and 1 2-d-old piglet, were used. The 2 age groups were employed so as to compare the ease in microdissection. During the 12 h before anaesthesia, the piglets were allowed access to sterile drinking water containing D-glucose (55 g/l) only. Animals were sedated by an intramuscular injection of azaperone (5 mg/kg) (Stresnil, Jenssen Pharmaceutica, Belgium) 20 min before anaesthesia. This was induced by the intravenous injection of pentobarbitone sodium (10 mg/kg) and maintained by 2% halothane in oxygen via a semiclosed circuit.

A midline laparotomy was performed in the anaesthetised pigs and 2 (2–3 cm) pieces of intestinal tissue were obtained from the jejunum and ileum. Tissues were immersed in 0.01 M phosphate buffered saline (PBS, pH 7.3) in a Petri dish, opened along the mesenteric border and gently washed with PBS to remove faecal contents. They were pinned onto polystyrene and fixed by immersion in 4.5% buffered formalin at room temperature. After 1 h, biopsies were transferred into fresh fixative after removal from the polystyrene and trimming 1 piece into a 1 cm × 0.5 cm block for embedding. Tissues for embedding were fixed for 7 d at 4 °C; those for microdissection for 24 h at room temperature.

Embedding, sectioning and staining

Two 1 cm × 0.5 cm tissue blocks were dehydrated, cleared in xylene and embedded in paraffin wax. Two blocks of similar size were embedded in 5% molten Becto agar (50 °C) and chopped into 100 μm pieces by

using a McIlwain tissue chopper (Mickle Laboratories, UK). Chopped sections were collected and processed as free floating sections in 0.01 M PBS + 0.5% Triton X-100 (washing buffer). They were washed in washing buffer while shaking on a HS 250 shaker (Janke and Kunkel, IKA, Labortechnik, Germany) at 200 cycles/min for 1 h. The washing buffer was changed every 20 min. Tissues were then kept in this buffer at 4 °C overnight.

Three 5 and 25 μm sections were cut from each paraffin block. The 5 μm sections were stained with haematoxylin-eosin-phloxine (HE). The 25 μm sections were collected in glass vials containing 0.5 ml xylene for clearing and subsequent rehydration. They were washed and thereafter kept in the washing buffer at 4 °C overnight.

Microdissection

The 1 cm × 2 cm formalin-fixed tissues were trimmed (1 cm × 1 cm), washed, and pinned stretched out in washing buffer on Sylgaard (silicone rubber), mucosal surface uppermost, and viewed under a stereo microscope (Olympus, SZH. Japan; × 64 max. magn.). The mucosa was removed by scraping carefully using pair of blunt tissue forceps. Tissue wholemounts bearing the myenteric, internal and external submucous plexuses were teased apart using very fine tissue forceps and a scalpel blade to sever the tight interconnections (Pearson, 1994). Wholemount tissue was collected in 0.5 ml washing buffer contained in glass vials, washed and kept in the same buffer at 4 °C overnight.

Immunohistochemical staining

Wholemounts, deparaffinised (25 μm) and chopped (100 μm) free floating sections were rinsed in washing buffer for 20 min and then quenched against endogenous peroxidase reactivity using 3% aquous hydrogen peroxide (Merck, Germany) for 20 min.

Sections were immunolabelled overnight at 4 °C either with a rabbit anti-VIP (Fahrenkrug, Denmark) diluted 1:4000 or a mouse antihuman neurofilament protein (NF) (Sigma) antibody diluted 1:20. In both cases, a biotin-streptavidin-HRP revealing system was used. For VIP labelling, a biotinylated swine anti-rabbit antibody (Dako, Denmark) diluted 1:500 and for NF labelling a biotinylated rabbit antimouse antibody (Zymed, USA) at 1:500 were used. For the third layer, an avidin-biotin complex conjugated to HRP (Dako, Denmark) was used in both cases. DAB in 1:500 washing buffer was employed as a chromogen for 1 h without hydrogen peroxide, then 5–15 min with 0.01% hydrogen peroxide. All incubations were carried out in PBS with 0.5% Triton X-100 and at the blocking step and antibody incubations there was additional 5% nonimmune serum (swine or rabbit). Tissues from mouse brain and sheep omasum were used as positive controls for VIP and NF-like immunoactivities respectively to check reaction specificity. The reaction was stopped by rinsing tissues in distilled water for 30 min with the water being changed after every 10 min.

During each trial, half of the chopped tissues labelled for VIP were subdivided into 2 groups. One group was embedded in paraffin wax and another in Historesin (Leica, Heidelberg, Germany). These were sectioned and counterstained by HE.

Tissue processing for mounting

Wholemounts and chopped sections were dehydrated by graded passages in methanol followed by one step in isopropanol. They were then cleared in 1,2,3,4-tetrahydronapthalene (THN) (Aldrich, Germany) and thereafter in 20, 30 and 50% benzyl benzoate (Merck, Germany) in THN for 10 min at each step except the last in which they were left overnight. Paraffin sections were dehydrated in ethanol and brought to xylene. All tissues were mounted in DPX (Poole, UK).

RESULTS

ENS organisation in the submucosa and tunica muscularis

In the present study, 3 major plexuses of the ENS, namely the myenteric and external (ESP) and internal (ISP) submucous plexuses, were identified in sections and wholemounts (Figs 1*a*, *b*; 2*a–d*). Wholemounts and sections gave the same results, namely that ISP ganglia are situated at 2 different topographic levels, with the internal and external ISP ganglia being separated by a thin connective tissue layer (Fig. 1*c*). The ganglia and interganglionic nerve strands were intertwined and large interganglionic nerve strands and nerve fibres projecting into the submucous layer and lamina propria firmly attached the ISP to the lamina muscularis mucosae.

The ESP ganglia were also observed to be situated at 2 different topographic locations. They were seen to be situated a few micrometres from the inner circular smooth muscle layer of the tunica muscularis and occasionally very close to or between bundles of this muscle layer (Figs 1*b*, 4*b*). The connective

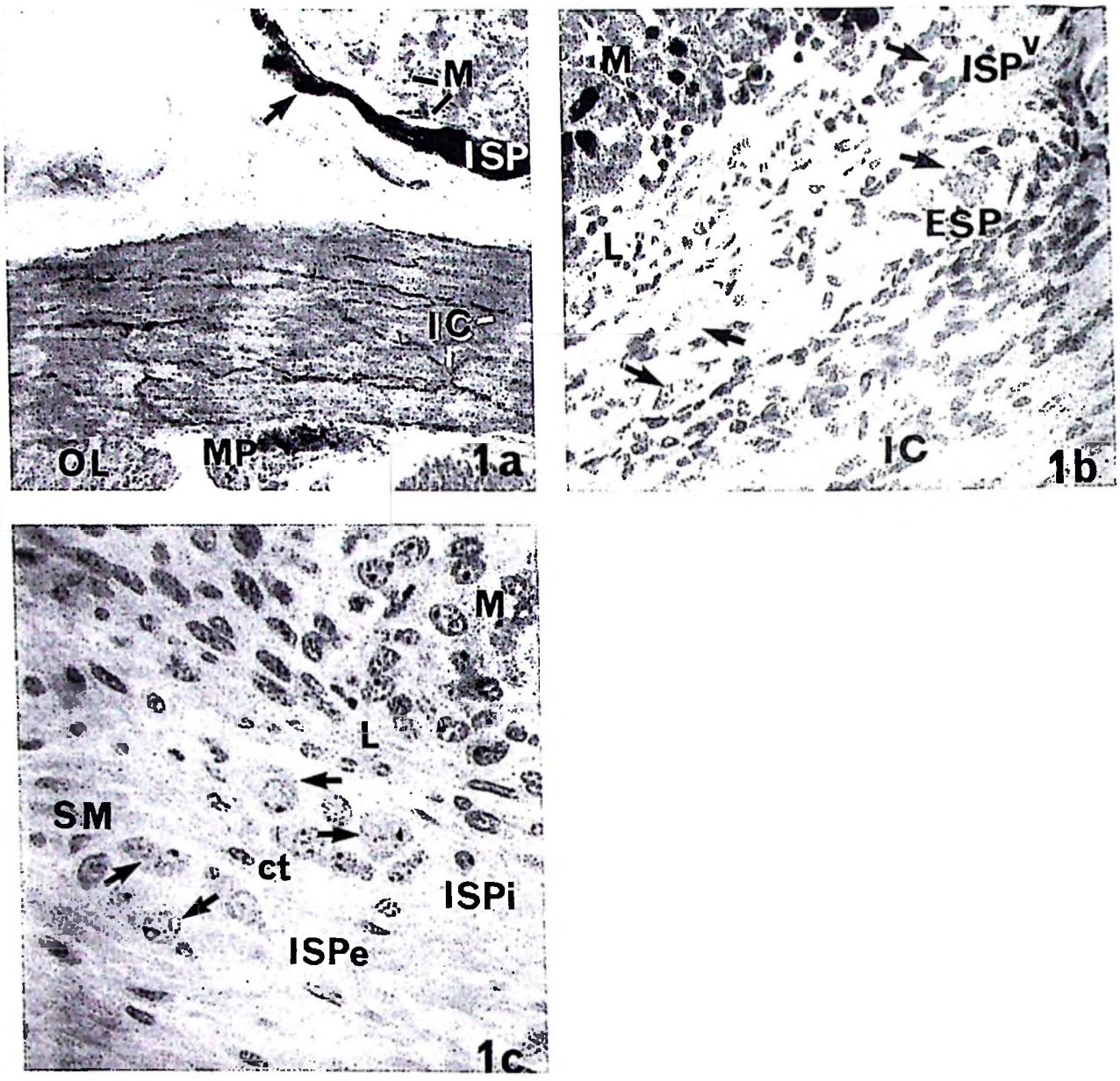

Fig 1. The topographic features of the ENS in the jejunum, of the pig. (*a*) VIP-like immunoreactivity in a 25 μm paraffin section. Note ISP ganglion (ISP) with many immunoreactive neurons (arrow), intensely stained VIP-like positive nerve fibres in the inner circular muscle layer (IC). Weak reactivity is seen in the tunica mucosa (M). MP, myenteric plexus; OL, outer longitudinal smooth muscle layer. ×900. (*b*) HE stained, 5 μm paraffin section. Both the ESP ganglion (ESP) and its neurons (arrows) are larger than the ISP ganglion (ISP) and its neurons (arrow). The ESP is situated close to the inner circular muscle layer (IC) on the serosal side and to submucosal vascular arcades (v), close to the ISP ganglia (ISP). The tunica mucosa (M) with the lamina muscularis mucosae (L) is also seen. ×840. (*c*) HE, 2.5 μm Historesin section. Two ISP ganglia in the submucous layer (SM); ganglia of the external ISP (ISPe) and internal ISP (ISPi) plexuses are located at 2 different topographic levels, and separated by a thin connective tissue layer (ct). The internal ISP is situated adjacent to the lamina muscularis mucosae (L) of the tunica mucosa (M). Neurons are marked by arrows. ×4200.

tissue around ESP ganglia was more dense when compared with that around those of the ISP. Connective tissue around the submucosal vascular arcades was less in comparison with the adjacent areas.

These observations imply that both the ISP and ESP ganglia are subdivided and situated at different topographic levels. However, ISP and ESP were clearly demarcated by the submucosal vascular arcades. The ISP was situated on the luminal and the ESP on the serosal side of these arcades. Wholemounts showed that the ESP meshwork is wider with larger ganglia, neurons and interconnecting nerve strands and thus fewer ganglia per unit area compared with ISP ganglia, which were abundant.

The perikarya with VIP-like IR were abundant in the inner submucous plexus, scarce in the outer submucous plexus and very infrequent in the

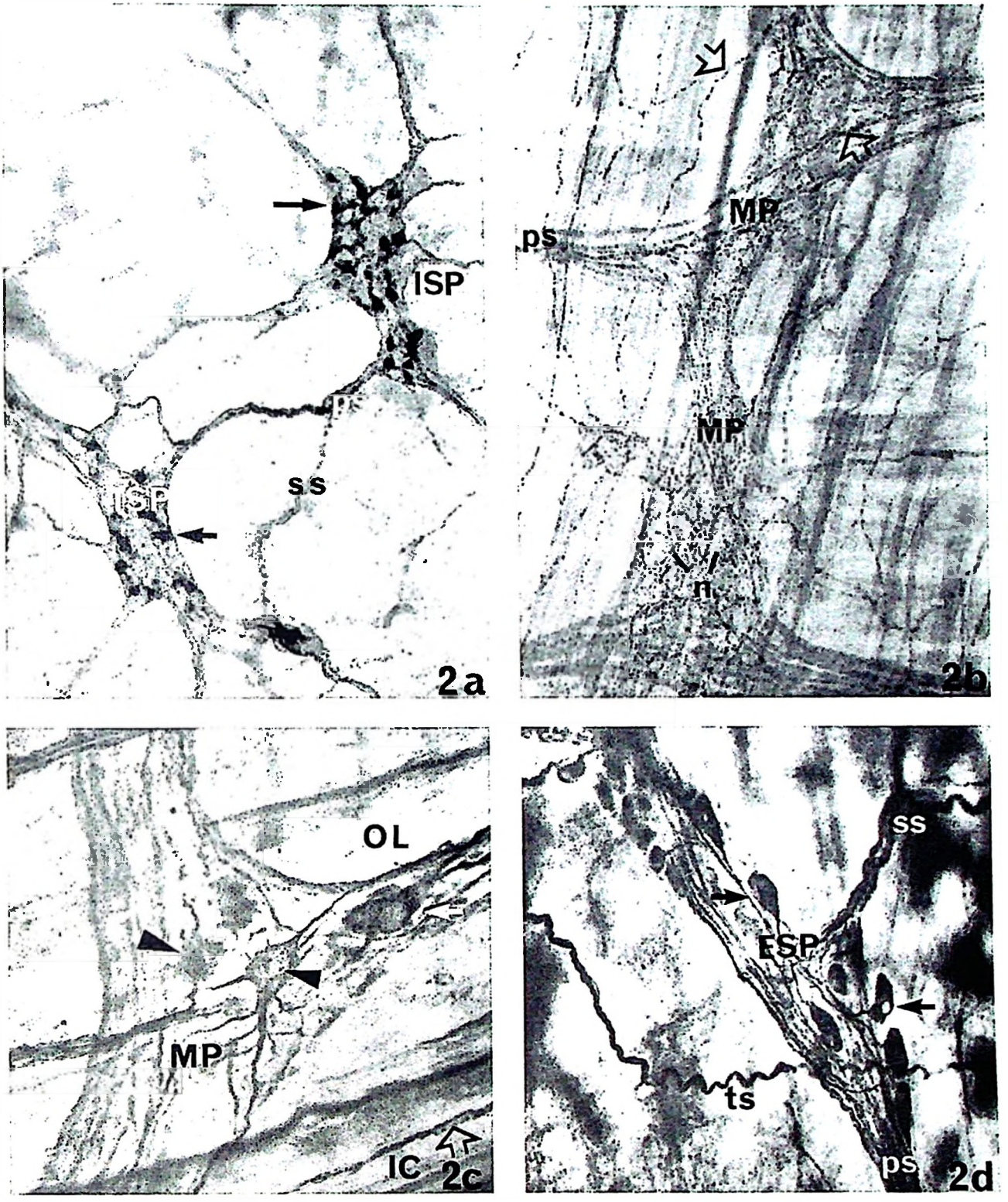

Fig. 2. VIP- and NF-like IR in wholemounts. (*a*) VIP-like IR in the ISP of a jejunal wholemount. The ISP ganglia (ISP) contain many VIP-like immunopositive neurons (arrows) and nerve fibre varicosities. Primary (interganglionic) nerve strands (ps) are larger but less wavy than secondary strands (ss). × 400. (*b*) Large myenteric plexus ganglion (MP) from an ileal wholemount. Shown are interganglionic nerve strands (ps), and many varicose nerve fibres (open arrow) which are also seen outside the ganglia as tertiary nerve strands. Nonimmunoreactive neurons (n). × 400. (*c*) Myenteric plexus ganglion (MP) from a jejunal wholemount showing NF-like IR. The inner circular muscle layer (IC) overlies the ganglion, whereas the outer longitudinal muscle underlies the ganglion. A positive nerve fibre (open arrow) can be identified in the circular muscle layer. Type IV neurons (arrowheads) are more abundant than type II neurons (arrow) which predominate in the ESP. × 400. (*d*) ESP ganglion (ESP) from a jejunal wholemount. Note NF-like IR Dogiel type II neurons (arrows), primary strands (ps), secondary strands (ss) and tertiary strands (ts). × 400.

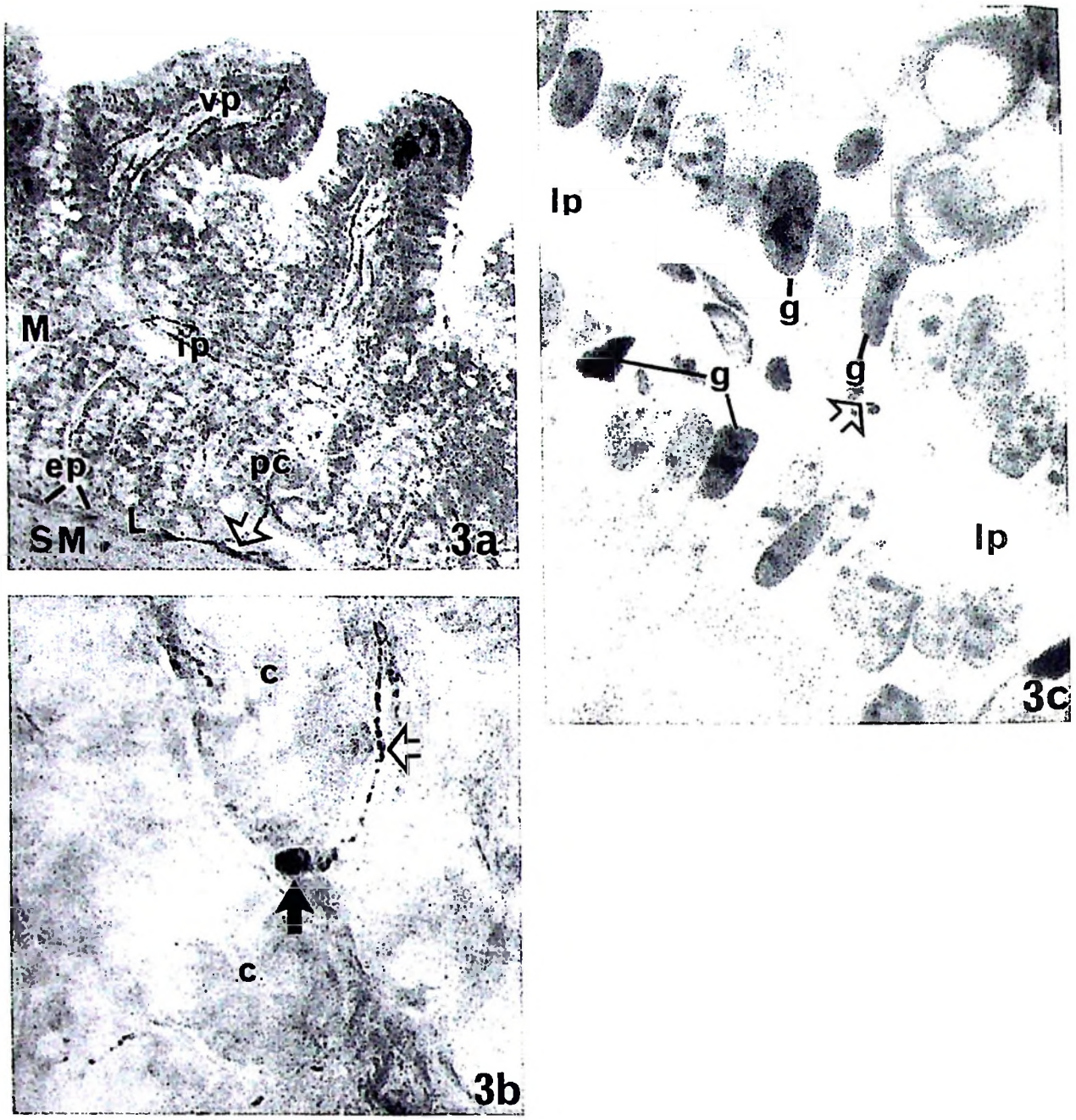

Fig. 3. VIP-like IR in the tunica mucosa of pig jejunum. (*a*) The 4 identifiable nerve plexuses in the tunica mucosa (M) are seen: the external propria (ep), the pericryptal (pc), the internal propria (ip) and the villus (vp) plexuses. L, lamina muscularis mucosae; ISP, open arrow. × 350. (*b*) VIP-like immunopositive neuron (arrow) in the pericryptal plexus and its positive nerve fibre (open arrow); c, intestinal crypt. × 1690. (*c*) HE counterstained 2.5 μm section from a Historesin-embedded chopped section initially labelled for VIP-like IR. Close to the base of a goblet cell (g) in the lamina propria (lp) are VIP-like positive varicosities (open arrow). × 4200.

myenteric plexus. The staining intensity in labelled perikarya decreased in the same order (Fig. 2*a*, *b*). The VIP-like IR nerve fibres were more abundant in the lamina propria and inner circular muscle than in the outer longitudinal muscle layer of the tunica muscularis.

Labelling for NF-like IR in strippings revealed clearly Dogiel type II, IV and VI neurons (Fig. 2*c*, *d*). However, it was not possible to correlate these to VIP-like IR neurons as double labelling was not done. In the ISP and ESP, neurons were intensely stained by VIP antibody and appeared to be Dogiel type II (Fig. 2*a*) neurons, whereas in the myenteric plexus, they showed weaker VIP immunoreactivity, and appeared to be different from those in the ISP and ESP.

ENS organisation in Peyer's patches

Chopped, paraffin and Historesin sections revealed that in Peyer's patches the ISP and ESP were separated

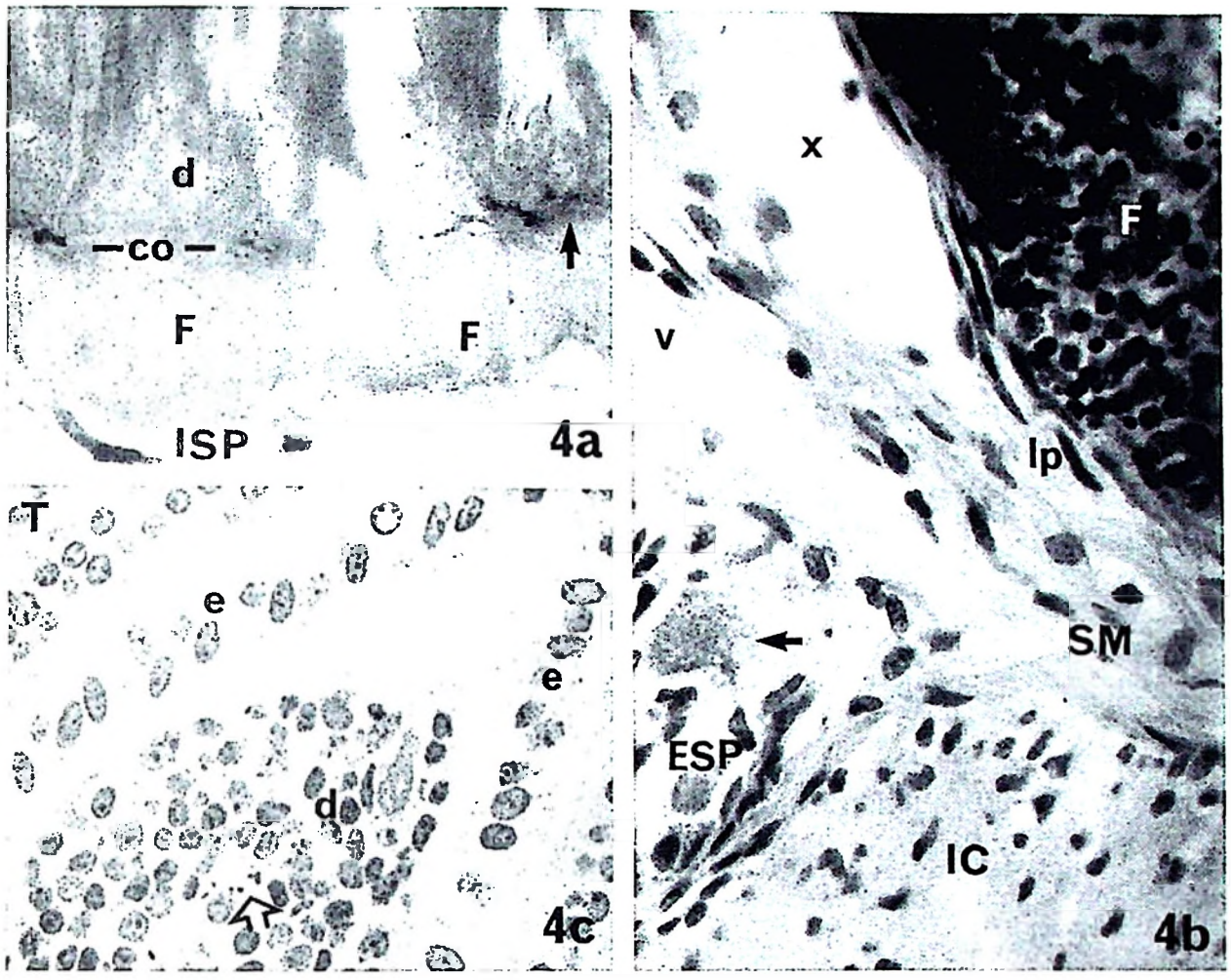

Fig. 4. VIP-like IR at Peyer's patches from the ileum. (*a*) Chopped section (100 μm) showing ISP ganglia (ISP) containing many positive neurons, under the base of the follicles (F) and in the corona (co). A dense mesh of positive fibres containing few immunopositive neurons (arrow) is seen in the corona (co) between the dome (d) and follicle proper (F). ×400. (*b*) HE stained 5 μm paraffin section, pig ileum. The ESP ganglion (ESP) in the ileal submucosa (SM) underlies a Peyer's patches follicle (F) and is situated remote from the base of the follicle. This ganglion lies between muscle bundles of the inner circular muscle layer (IC). The ganglion has large neurons (arrow) and is situated below the level of the submucosal vascular arcades denoted by the vessel (v). The lamina propria (lp) is thin and has in an area been detached from the tela submucosa leaving an artefactual open space (x) under the follicle. ×840. (*c*) HE counterstained 2.5 μm section from a chopped tissue labelled for VIP before Historesin embedding and sectioning. VIP-like positive reactivity in the apex of the dome (d) is seen as nerve fibre varicosities (open arrow); e, dome epithelium. ×1690.

by the submucosal vascular arcades with the ESP being situated on the serosal side. The ISP was always seen on the luminal side of the arcades and formed a continuous mesh around the follicles of Peyer's patches (Fig. 4*a*, *b*). This nerve meshwork appeared as 3 ganglionated plexuses, subdivisions of the ISP, around the follicles of Peyer's patches. Of the ISP subdivisions, the first plexus was situated between the base of the follicles and the submucosal vascular arcades, the second in the interfollicular zone, and the third in the corona. Ganglia in these plexus subdivisions contained many VIP-like immunoreactive perikarya. The first 2 subdivisions had a wider mesh, larger ganglia and larger perikarya when compared with the third plexus. The latter was composed of smaller ganglia containing smaller perikarya and numerous fine nerve fibres forming a very dense nerve meshwork. VIP-like IR nerve fibres from the ISP meshwork innervated the dome but not the follicles proper (Fig. 4*c*). Observations that Peyer's patches follicles are enclosed by ganglionated ISP meshwork were achieved by staining for VIP-like IR only.

ENS in the lamina propria

Labelling for VIP-like reaction product in chopped and paraffin sections revealed 4 distinct nerve plexuses formed by nerve fibres ascending into the lamina propria from the submucosa (Fig. 3*a*). We have applied simple terms to name these plexuses. The first 2 are the external propria plexus (EPP) (plexus lamina muscularis mucosae) which overlies the lamina mus-

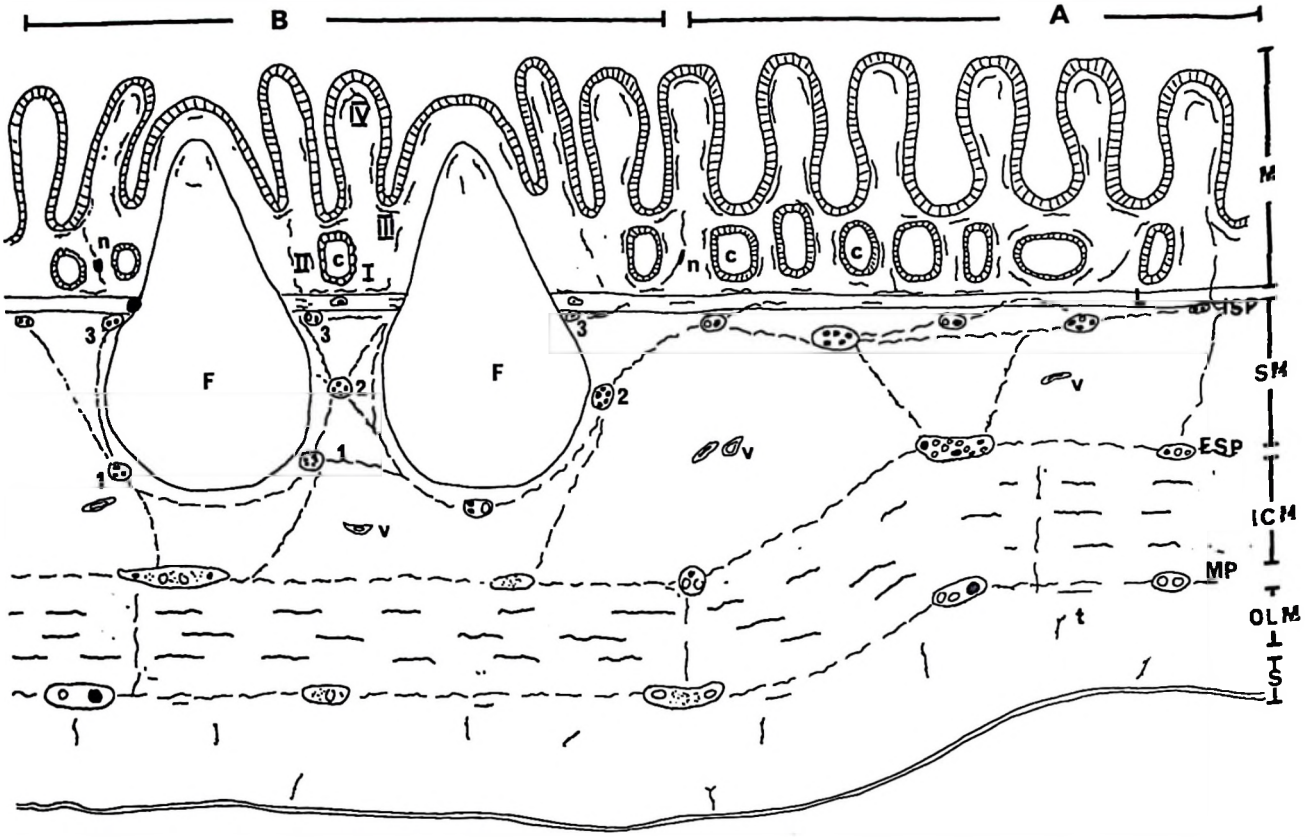

Fig. 5. Schematic presentation (not to scale) of the identifiable plexuses in the ENS in the wall of the jejunum and ileum of the pig as revealed by VIP-like IR. The ENS in areas without and with Peyer's patches follicles are shown by A and B respectively. The myenteric plexus (MP) is situated between the inner circular (ICM) and the outer longitudinal (OLM) muscle layers of the tunica muscularis. In the tela submucosa (SM) the ganglionated plexus is subdivided into the inner (ISP) and external submucosal (ESP) plexuses, this being demarcated by the submucosal vascular arcades (v). At the follicles of Peyer's patches the ISP is subdivided into 3 subunits surrounding the follicles, seen at the base of the follicles (ISP1) (1), in traffic areas (ISP2) (2) and at the corona (ISP3) (3). The VIP-like IR neurons (dark profiles) are frequent in the ISP, infrequent in the ESP and very scarce in the myenteric plexus. Nonreactive neurons are denoted by open profiles. In the lamina propria, 4 plexuses, the external propria (I), the pericyptal (II), the inner propria (III) and the villus plexuses (IV) are shown in the tunica mucosa (M), where also a few solitary neurons (n) are seen. The tertiary aganglionic plexus (t) underlying the myenteric plexus and the subserosa plexus of the tunica serosa (S), although not discussed in the present work, is also visualised by staining for VIP-like IR.

cularis mucosae and the internal propria plexus (IPP) located at the base of the intestinal villi. These 2 meshworks were oriented parallel to the luminal surface being almost perpendicular to the villus/crypt axis. A third, the pericryptal plexus (PCP) or the periglandular plexus surrounded the intestinal crypts. The PCP and EPP gave rise to the fourth component, the villus plexus (VP). Solitary neuronal perikarya in the lamina propria were also revealed (Fig. 3*b*). These immunoreactive cells gave rise to varicose nerve fibres projecting towards the serosal and luminal side of the lamina propria.

Chopped sections labelled with VIP-like antibodies and Historesin sections counterstained by HE showed varicose nerve fibres in the villus plexus running in the lamina propria between the core of the villi and the epithelial basement membrane. These fibres were related to terminal arterioles and the luminal epithelium. They were sometimes in close proximity to goblet cells (Fig. 3*c*).

Labelling for NF-like immunogen did not demonstrate nerve fibres of the proprial plexuses in paraffin and chopped sections although fibres were labelled clearly in wholemounts, which were all parallel to the lumen.

The general organisation of the ENS in the small intestine of pig as revealed by staining for VIP is summarised in Figure 5.

DISCUSSION

The ENS in the tela submucosa and tunica muscularis

Our finding that the external (ESP) and internal (ISP) submucous plexuses are topographically, structurally, and architecturally different is in agreement with the observations of Scheuermann et al. (1987*a*, *b*), Mannl et al. (1986) and Thomsen et al. (1997). Our findings using wholemounts and sections on ISP topography

and its attachment to the lamina muscularis mucosae confirm those of Scheuermann et al. (1987*a*, *b*), who used SEM on tissue wholemounts in contrast to our observations made in wholemounts stained by immunohistochemical methods and sections stained by HE. In conformity with Gunn (1968) we observed that the ISP ganglia of the pig were subdivided into external and internal ganglia; however, as we did not observe major morphological differences among the ISP ganglia at these 2 levels, we do not advocate the subdivision of this plexus.

Our findings that ESP ganglia are situated at 2 topographic levels support the results of Christensen & Rick (1987) and Hoyle & Burnstock (1989), who described them in the submucosa of the opposum and human colon, respectively. We however observed them to be in the submucosa of the pig jejunum and ileum.

The observation that the ISP and ESP are demarcated by the submucosal vascular arcades supports earlier findings by Scheuermann et al. (1987*a*, *b*) and Thomsen et al. (1997). The submucosal vascular arcades are landmarks for topographic differences between the ISP and ESP, and the 2 plexuses can also be considered as different entities morphologically. The presence of thin bands of connective tissue in the area of the submucosal vascular arcades in comparison with adjacent areas is in agreement with the observations of Scheuermann et al. (1987*a*). This explains the ability to separate the tela submucosa by microdissection into ISP and ESP containing tissue laminae (wholemounts).

Our finding that VIP-like IR neurons were abundant in the ISP, infrequent in the ESP and very scarce in the myenteric plexus is in agreement with that of Timmermans et al. (1990). According to Scheuermann et al. (1987*c*), type II neurons are immunoreactive with antibodies to calcitonin gene related polypeptide (CGRP) and can be identified by their round, oval or triangular shaped cell bodies, with a smooth outline, from which long processes extend. The processes vary in calibre and divide into different branches at a fair distance from the perikaryon. Depending on the type of plexus, these neurons may contain substance P, VIP, galanin, and/or dynorphin (Timmermans et al. 1991). The abundance of VIP-IR nerve fibres in the ganglia, and the thickness of the wholemounts made it difficult to visualise the axons and dendrites to aid proper morphological identification. Nevertheless the VIP-like IR neurons appeared, from their shape, to be Dogiel type II neurons. In the myenteric plexus, VIP-containing neurons had the morphology of Dogiel type I, which receive cholinergic synaptic inputs (Costa et al. 1988). The VIP-IR neurons in the myenteric plexus were very sparse and stained less intensely. Whether they were Dogiel type I is uncertain but they appeared to be different from the neurons identified as Dogiel type II in the ISP and ESP.

According to Krammer & Kühnel (1992), NF (200 kDa)-like IR identifies adendritic, pseudounipolar to multiaxonal Dogiel type II neurons. The pooled NF antibody (200, 160 and 70 kDa), in addition, revealed the uniaxonal, multidendritic type IV and the uniaxonal multidendritic axodendritic type VI neurons. The NF 200 intermediate filaments are thought to exist in a high concentration and close arrangement in type II neurons and this is why antisera against the 200 kDa intermediate filaments 'recognise' type II neurons (Krammer & Kühnel, 1992). It may be considered that binding to type IV and VI neurons was displayed either by 70 or 160 kDa or both types of antineurofilament protein antibodies and that these neurons have higher concentrations either of 70 or 160 kDa, or both types of intermediate filaments.

The observed variation in the number of neurons as revealed by labelling for both VIP- and NF-like immunoreactivity supports the finding by Timmermans et al. (1990) that the submucous plexuses differ in neurochemical and neuronal contents. The fact that immunoreactivity to pooled antisera was not detected in all perikarya is in agreement with the finding by Björklund et al. (1984) and Krammer & Kühnel (1992) that, in the gastrointestinal tract, a small number of ganglion cells cannot be stained by antibodies to neurofilament protein.

ENS organisation in Peyer's patches

According to Krammer & Kühnel (1993), the ESP is situated close to the base of the follicles in the Peyer's patches of the small intestine of pig. Our results by labelling for VIP-like antigens and HE staining revealed that ISP surrounds follicles of Peyer's patches as a continuous mesh of the 3 subdivisions (subplexuses) of the ISP nerve meshwork. This is in accordance with the general view that Peyer's patches intrude into the submucosa and therefore will most likely be closely related to the ISP. The differences between our observations and those of Krammer & Kühnel (1993) could be due to the markers (protein gene product 9.5, neuron-specific enolase, neurofilament 200, S-100 protein and the glial fibrillary acidic protein) used by Krammer & Kühnel. They could not demonstrate neurons in the third ISP subdivision in Peyer's patches. Therefore there is a

need to use other ENS markers to study this complexity.

In Peyer's patches, nerve fibres are found in the dome but not in the follicle proper (Krammer & Kühnel, 1993). The VIP-like IR nerve fibres were also detected in the dome only. This indicates that a particular subset of lymphocytes in the dome is innervated by VIP immunoreactive fibres. The functional significance of this observation requires identification of cells specifically innervated by these fibres.

The ENS in the tunica mucosa

Our results on VIP-like IR showed that nerve fibre meshes in lamina propria form 4 distinct nerve plexuses. We propose for them the following nomenclature: (1) the external propria plexus (EPP), (2) the internal propria plexus (IPP); (3) the pericryptal plexus (PCP) and (4) the villus plexus (VP). According to Furness & Costa (1980) and Costa & Brookes (1994), the ENS in the mucosa plexus is composed of fine nerve bundles and axons and can be subdivided into subglandular, periglandular and the villous components. Except for the description of the IPP which is new, our findings are consistent with their description of the EPP, PCP and VP.

We detected the presence of solitary neuronal perikarya in the porcine pericryptal plexus. These perikarya are immunoreactive to antisera used in staining for VIP-like proteins and give rise to positively stained varicose nerve fibres extending towards both serosal and luminal surfaces. Probably they act as integration centres of impulses in the mucosal reflexes which do not involve relay neurons of the submucosal and myenteric plexuses.

The fact that we did not observe similar cells in sections labelled with NF-like antisera may be due to poor penetration or that the antibody was unable to bind to filaments in these cells.

The observation of abundant VIP-like IR varicose nerve fibres close to the luminal epithelium and goblet cells signifies the importance of VIP in regulating epithelial transport and possibly to stimulate secretion in goblet cells.

CONCLUSIONS

Our results have shown that in the pig jejunum and ileum the ESP is subdivided at 2 different topographic levels, that the pericryptal plexus contains solitary neuronal perikarya and that a 'new plexus', the internal propria plexus, is well developed. In the areas of Peyer's patches our results show that it is the inner submucosal plexus, ISP, alone, that contributes to the plexus surrounding the follicles and that it is subdivided into 3 compartments.

The controversy over the names of submucosa plexuses (Scheuermann et al. 1987*b*; Hoyle & Burnstock 1989; Pearson, 1994) has been clarified and we have used the most appropriate descriptive terminology to name the plexuses in the submucosa and lamina propria as indicated above and schematised in Figure 5.

Further studies using supplementary histochemical staining combined with laser scanning confocal microscopy might contribute to elucidation of fine details of the innervation and organisation of the enteric nervous system in the small intestine of the pig and other animals.

ACKNOWLEDGEMENTS

The authors thank the Danish International Development Agency for financial support, and are grateful to Professor Poul Hyttell for putting all the facilities needed at our disposal. Technical assistance from J. Dennis, H. Holm, G. Holden and I. Bjerring, is highly appreciated. We also thank Dr C. J. P. Jones for language corrections. We are thankful to all those who contributed towards the success of this work.

REFERENCES

Björklund H, Dahl D, Seiger A (1984) Neurofilament and glial fibrillary acidic protein-related immunoreactivity in rodent enteric nervous system. *Neuroscience* **12**, 277–287.

Christensen J, Rick GA (1987) Intrinsic nerves in the mammalian colon: confirmation of the a plexus at the circular muscle-submucosa interface. *Journal of Autonomic Nervous System* **21**, 223–231.

Costa M, Furness JB, Gibbins IL, Morris JL, Bornstein C, Llewellyn-Smith IJ et al. (1988) Colocalization of VIP with other neuropeptides and neurotransmitters in the autonomic nervous system. *Annals of the New York Academy of Sciences* **527**, 103–108.

Costa M, Brookes SJ (1994) The enteric nervous system. *American Journal of Gastroenterology* **89** (Suppl. 8), 129–137.

Furness JB, Costa M (1980) Types of nerves in the enteric nervous system. *Neuroscience* **5**, 1–20.

Gunn M (1968) Histological and histochemical observations on the myenteric and submucous plexuses of mammals. *Journal of Anatomy* **102**, 223–239.

Hoyle CH, Burnstock G (1989) Neuronal populations in the submucous plexus of the human colon. *Journal of Anatomy* **166**, 7–22.

Krammer H-J, Kühnel W (1992) Immunohistochemistry of intermediate filaments in the enteric nervous system of the Porcine small intestine. *Annals of Anatomy* **174**, 275–278.

Krammer H-J, Kühnel W (1993) Topography of the enteric nervous system in the Peyer's patches of the porcine small intestine. *Cell and Tissue Research* **272**, 267–272.

Lowden S, Heath T (1994) Ileal Peyer's patches in pigs: intercellular and lymphatic pathways. *Anatomical Record* **239**, 297–305.

MANNL A, POSPISCHIL A, DAHME E (1986) The plexus submucous (Meissner's and Schabadasch's) in the pig gut: I. Light and electron microscopy of the normal structure. *Journal of Veterinary Medicine* A(33), 647–659.

METWALI A, BLUM A, MATTHEW R, SANDOR M, LYNCH RG, WEINSTOCK JV (1993) Modulation of T lymphocytes proliferation in mice infected with Schistosoma mansoni: VIP suppresses mitogen- and antigen-induced T cell proliferation possibly by inhibiting IL-2 production. *Cell Immunology* **149**, 11–23.

PABST R (1987) The anatomical basis for the immune function of the gut. *Anatomy and Embryology* **176**, 135–144.

PEARSON GT (1994) Structural organization and neuropeptide distributions in the equine enteric nervous system: an immunohistochemical study using whole-mount preparations from the small intestine. *Cell and Tissue Research* **276**, 523–534.

PEARSON GT, THOMSEN L, SKADHAUGE E (1996) Synaptic communication between external and internal submucosal plexus neurons of the porcine jejunum. *Journal of Comparative Biochemistry and Physiology*, in press.

SCHEUERMANN WD, STACH W, TIMMERMANS J-P (1987*a*) Topography, architecture and structure of the plexus submucosus internus (Meissner) of the porcine small intestine in scanning electron microscopy. *Acta Anatomica* **129**, 96–104.

SCHEUERMANN WD, STACH W, TIMMERMANS J-P (1987*b*) Topography, architecture and structure of the plexus submucosus externus (Schabadasch) of the porcine small intestine in the scanning electron microscopy. *Acta Anatomica* **129**, 105–115.

SCHEUERMANN DW, STACH W, DE GROODT-LASSEEL MHA, TIMMERMANS J-P (1987*c*) Calcitonin gene-related peptide in morphologically well-defined type II neurons of the enteric nervous system in the porcine small intestine. *Acta Anatomica* **129**, 325–328.

STACH W (1988) A revised morphological classification of neurones in the enteric nervous system. In *Nerves and the Gastrointestinal tract* (ed. Singer, MV, Goebell H), pp. 29–45. *Proceedings of the 50th Falk symposium, Tirisee, FRG, June 2–4, 1988*. Lancaster: MTP Press.

THOMSEN L, PEARSON GT, SKADHAUGE E, HVIID LARSEN E (1996) Electrophysiological properties in neurones in the internal and external submucosal plexuses of newborne pig small intestine. *Journal of Physiology* **498**, 773–785.

TIMMERMANS J-P, SCHEUERMANN DW, STACH W, ADRIAENSEN D, DE GROODT-LASSEEL MHA (1990). Distinct distribution of CGRP-, enkephalin-, somatostatin-, substance P-, VIP- and serotonin-containing neurons in the two submucosal ganglionic neural networks of the porcine small intestine. *Cell and Tissue Research* **260**, 367–379.

TIMMERMANS J-P, ADRIAENSEN D, SCHEUERMANN DW, STACH W (1991) Morphological features of the enteric nervous system of an omnivorous animal, the domestic pig. *Journal of the Autonomic Nervous System* **33**, 193–194.

TIMMERMANS J-P, SCHEUERMANN DW, STACH W, ADRIAENSEN D, DE GROODT-LASSEEL MHA (1992). Functional morphology of the enteric nervous system with special reference to large mammals. *European Journal of Morphology* **30**, 113–122.

YAMAMOTO Y, KITAMURA N, YAMADA J, ATOJI Y, SUZUKI Y, YAMASHITA T (1994) Structure of the enteric nervous system in sheep omasum as revealed by neurofilament protein-like immunoreactivity. *Journal of Anatomy* **184**, 399–405.

Paper II

An immunohistochemical study of the organisation of ganglia and nerve fibres in the mucosa of the porcine intestine.

O.B. Balemba[1], A. Hay-Schmidt[4], R.J. Assey[1], C.K.B. Kahwa[1], W.D. Semuguruka[2], V. Dantzer[3]

Addresses:

Departments of [1]Veterinary Anatomy and [2]Veterinary Pathology, Sokoine University of Agriculture, Morogoro, Tanzania. [3]Department of Anatomy and Physiology, The Royal Veterinary and Agricultural University and [4]Institue of Medical Anatomy, Copenhagen University, Copenhagen, Denmark.

Address for correspondence:

Dr. Vet. Sci. V. Dantzer.

Department of Anatomy and Physiology, RVAU, Grønnegårdsvej 7, 1870 Frederiksberg C, Copenhagen, Denmark. Tel: 4535282543; Fax 4535282547;

e-mail: Vibeke.Dantzer@iaf.kvl.dk

Abstract

Mucosal subplexuses are defined and named differently among authors and the description of their topographical and architectural organisation is inadequate. It is unclear whether the ganglia in mucous plexus are ectopic or not. Therefore, the organisation of mucous plexus was studied in six pigs by vasoactive intestinal peptide, substance P, nitric oxide synthase and neurofilament proteins immunohistochemistry. The mucous plexus of both large and small intestine contained ganglia and isolated neurons. They were many and comparably larger in the caecum and colon, few in ileum, and fewer and smaller in the jejunum. The mucous plexus was subdivided into the lamina muscularis mucosae, outer proprial, interglandular proprial, inner proprial, perivascular, villous and subepithelial subplexuses to give identity to the most ganglionated outer proprial subplexus and a dense clearly oriented inner proprial subplexus. These subplexuses varied with respect to the amount, sizes and shapes of ganglia and neurons, sizes and orientation of nerve strands and their respective immunoreativities. Ganglia were situated at different topographical levels in the lamina muscularis mucosae, outer proprial and interglandular proprial subplexuses. Isolated neurons situated at the centre of the nodes were immunoreactive to substance P, vasoactive intestinal peptide and nitric oxide synthase. The perivascular, inner proprial, villous and subepithelial subplexuses were aganglionic. We propose mucous plexus in the intestine of the pig to be one of the major ganglionated plexuses, others being the inner submucous, outer submucous and myenteric plexuses. Further studies to establishing the microcircuits between this plexus, the submucous and myenteric plexuses and its role in functional regulation of the mucous membrane are suggested.

Key words: *Porcine, intestine, mucous plexus, vasoactive intestinal peptide, substance P, nitric oxide synthase, neurofilament proteins.*

Introduction

The mucous plexus in the enteric nervous system (ENS) is a dense network of fine interconnecting nerve bundles found through out the lamina propria (LP) and is divided into 3- 4 different subplexuses: a subglandular plexus, a periglandular plexus, vascular plexus and a villous subepithelial plexus (Furness and Costa, 1980; Furness et al., 1988). Costa and Brookes, (1994) described 5 subplexuses by subdividing the vascular plexus into the perivascular plexus as fine anastomosing nerve strands which supplies the arterial innervation and the paravascular nerves which followed the arterioles. Keast et al. (1984) proposed subdivision of nerve fibre meshwork in the LP into a subepithelial plexus being adjacent to mucosal epithelium and close to the crypts, and a loose network in the LP. Balemba et al. (1998) proposed 4 subplexuses namely: the external proprial plexus (EPP) which overlay the *lamina muscularis mucosae* (LMM), the pericryptal plexus (PCP) which surround

the intestinal crypts, the internal propria plexus (IPP) located at the base of the intestinal villi and the villous plexus (VP) which is located around the core of the villi.

The reports of presence of neurons in the LP in the mucosal layer in the gut goes back many years ago as shown for instance by Drasch (1881) and Vau (1932) in cattle, Stöhr (1934, 1944) in the stomach and intestine of man, Lassmann (1975) in the colon and rectum of cows and Newson et al. (1979) in rat ileum. Many observations have recently been published on ganglia and isolated nerve cell bodies in the LP, for instance, VIP IR neurons in the ileum of rat and rectum of the guinea-pig (Schultzberg et al., 1980), VIP- and SP- IR neurons in the LMM and LP in the small intestine and colon (Korman et al., 1989) and peptide histidine methionine/VIP mRNA- positive neurons in the LMM and LP in the ileum (Bredkjær et al., 1994) of the human. Others are on VIP IR neurons in the large intestine of the Hedgehog (Vittoria et al., 1992), acetylcholinesterase and neurofilament protein IR in the colon of rat (Mestres et al., 1992a, b) and nicotinamide adenine dinucleotide diaphorase and acetylcholinesterase IR neurons in the small intestine of humans (Fang et al., 1993). Existence of intramucosal ganglia and isolated neurons have also been showed by VIP and neurofilament protein (NF) IR in the small intestine of pig and cattle respectively (Balemba et al., 1998, 1999) and protein gene product 9.5 in the colon of humans (Wedel et al., 1999). Nevertheless, mucosal ganglia and isolated neurons are considered to be ectopic from the submucous plexus (Stöhr 1934, Lassmann 1975). There appear to be lesser studies of the organisation of the mucous plexus which are based on the use of wholemounts compared to the myenteric, outer and inner submucous plexuses. Our objective was to elucidate and describe the organisation of the ganglia, neurons and nerve fibre network in the mucous plexus in the intestine of the pig in order provide histological data which might be used in other studies to elucidate further functions of the mucous plexus.

Materials and methods

Three 8 week, fully weaned (13-15 kg) male and three female, 18 - 19 week old Danish Land race -Yorkshire crossbred pigs were euthanised by captive bolt and exsanguination. Immediately after death, the stomach and intestine were exposed and tissues (~ 4 x 3 cm in size) were collected from each of the proximal, middle and distal part of jejunum, ileum as well as caecum and colon respectively, cut open along the mesenteric attachment and rinsed thoroughly using cold (4 °C) 0.1 M PBS (pH 7.3). Each tissue was subdivided into two pieces, which were placed on polystyrene with the serosal surface down, pinned while being maximally stretched and subsequently fixed in 4.5 % buffered formaldehyde. After 1 hr, they were freed from the polystyrene, the fixative replaced by fresh 4.5 % buffered formaldehyde and fixed for 47 hrs, stored in cold 0.1M PBS until processed for microdissection of wholemounts for the mucous, submucous and myenteric plexuses

as described by Balemba et al. (1998).

Freshly dissected wholemounts were stored in 0.1% sodium azide in 0.1M PBS containing 0.5% triton X-100, pH 7.3, at 4 °C. Prior to staining, tissues were washed 3 x 20 minutes each in PBS containing 0.5% triton X-100 and thereafter overnight at 4 °C. Staining for vasoactive intestinal peptide (VIP), substance P, (SP), nitric oxide synthase (NOS) and neurofilament protein (NF) immunoreactivities (IR) was done by the two step indirect streptavidin-ABComplex/HRP immunoenzymatic method described by Balemba et al. (1998). The specificity and sources of background staining were controlled by replacing the primary and secondary antibodies, and streptavidin-ABComplex/HRP with 5% non-immune swine serum. Monoclonal rabbit anti swine-VIP (VIP 8084-4; 1:1400) and monoclonal rabbit anti-swine SP (SP 250-2; 1:2000) were kindly donated by Dr. J. Fahrenkrug, of Bispebjerg Hospital and Dr. P.J. Larsen of Panum institute, Copenhagen University, Denmark respectively. The neuronal polyclonal rabbit anti-rat nitric oxide synthase B 220-1 (Eurodiagnostica) was used at 1:1000 dilution. Wholemounts were evaluated and photographs taken. For each of the peptides studied, two wholemounts representing each segment were embedded in paraffin with the mucosal surface being oriented in either upright or horizontal positions. From each block, 5 serial sections of 10 and 5 μm each were taken respectively. The sections were counterstained by Meyer's Haematoxylin for 30 seconds, dehydrated by graded passages in alcohol and xylene and mounted in DPX. Lamina muscularis mucosae was used as a landmark to differentiate mucosal from submucosal neurons. Sizes of neurons and nerve strand were estimated using a calibrated eye piece, while the criteria described by Scheuermann et al. (1987 *a, b*) was used to classify nerve strands.

The semi-quantification was done based on the occurrence of the following structures in a wholemount as: (+++) fairly many ganglia, isolated neurons and primary and secondary nerve strands; (++) few ganglia, isolated neurons and primary and secondary nerve strands; (+) scarce occurrence of ganglia, isolated neurons and primary and secondary nerve strands and (-) ganglia and isolated neurons not observed, and primary and secondary nerve strands not distinguished.

Results

The organisation of the myenteric plexus, outer submucous plexus (OSP), inner submucous plexus (ISP) and mucous subplexuses in the caecum and colon was in many ways similar to that of the jejunum and ileum. VIP, SP, NOS and NF IR revealed ganglia and isolated neurons in primary nerve strands in the mucous plexus being situated at different topographical levels (Fig.1; Tables 1, 2). Mucosal ganglia and neurons were abundant in the caecum, many in colon and ileum and few in the jejunum. Large, mostly elongated ganglia were seen in caecum and colon whereas, smaller ovoid or

rounded ganglia were common in the ileum and jejunum.

In the present study, the mucous plexus was subdivided into the (1) lamina muscularis mucosae (LMMP), (2) outer proprial (LPP), (3) interglandular proprial (IGPP), (4) perivascular (PVP), (5) inner proprial (IPP), (6) villous (VP) and (7) subepithelial (SEP) subplexuses. The criteria for the subdivision was based on differences in the location, presence and amount of ganglia and neurons, sizes and shapes of ganglia, sizes of nerve strands, density and orientation of meshworks, VIP, SP, NOS and NF IR (Tables 1, 2; Figs.1; 2 a - f; 3a-c; 4a-c; 5a-e). Nerve fibre strands in the LMMP, OPP, IGPP and IPP were differentiated into large primary (PS), medium sized secondary (SS) and tertiary nerve strands (TS) (mainly nerve axons) (Table 1). Primary strands were more obvious and generally abundant in the LMMP, OPP, IGPP and IPP (Figs. 2b-f; 4a, c; 5e). There was no marked difference between the two age groups studied and the possible variation of IR along segments was not studied.

Lamina muscularis mucosae subplexus (LMMP)

The LMM layer had an outer longitudinal layer and an inner circular layer of almost equal thickness. The LMMP was made up of a nerve meshwork containing sparse ganglia and isolated neurons located in thin connective tissue layer between the two layers and small nerves fibres situated in the two muscle layers having a similar course as the muscle fibres (Figs. 1; 2a; 3c, 4a). Large paravascular nerve strands originating from the submucosal layer which traversed the LMM into the mucosa without any interruption were not considered as part of the LMMP. In the LMMP there were many and intense VIP, moderate SP and NOS nerve fibre varicosities and sparse NF IR nerve fibres.

The outer proprial subplexus (OPP)

The OPP is a ganglionated nerve meshwork which was observed at the base of the crypts in the subglandular region. The major axis of ganglia, isolated neurons and nerve strands situated immediately against the inner side of the LMM was oriented parallel to inner circular layer of LMM (Figs. 1; 2b-c). At the base of the crypts, ganglia and large nerve fibres were oriented parallel to blood vessels surrounding a group of crypts showing a honeycomb-like network (Figs. 2d-f). The OPP had many and larger ganglia and nerve strands, and a more dense meshwork compared to LMMP and IGPP. In the Peyer's patches the OPP was a subplexus in the corona of the follicles in which there were small ganglia with VIP, SP, NOS and NF IR neurons. Ganglia, VIP, SP, NF, and NOS IR neurons as well as nerve fibres varied in sizes (Table 1). Large ganglia had up to 3-9 IR neurons whereas, the smallest ganglia had 1 - 3 IR neuron(s) (in a cross section). There were many and intense VIP and SP IR neurons and nerve fibre varicosities (Figs. 2b-f; 5a). A few SP IR neurons

were observed very close to LMM gave rise to a nerve fibre of ~ 3 μm which projected towards the submucosa and another fibre (dendrite) of ~ 2 μm projecting towards the luminal surface. NF IR neurons (Fig. 3a) were also many but, NF IR was seen in large nerve fibres only. NOS IR neurons and nerve fibre varicosities were sparse.

The interglandular proprial subplexus (IGPP)

The IGPP was formed by a ganglionated nerve meshwork composed of the nerve meshwork coursing without any specific orientation in the LP starting from the base of the crypts up into the connective tissue between the crypts to level of the IPP. Ganglia and isolated neurons in the primary strands in IGPP were few and situated at different topographical levels (Figs.1; 3b, 4b-c, 5b-d). The majority of ganglia were located in the basal region of the IGPP. Large ganglia were elongated or ovoid whereas, the small ganglia were often rounded. In the inner parts of the mucosa, ganglia were very scarce and small in size.

VIP, SP and NF IR neurons were observed in the ganglia and as isolated neurons in primary strands showing variation in sizes (Table 1). The largest VIP IR neurons were commonly seen in the caecum. Large neurons were common in the caecum and colon whereas, the medium sized and smallest VIP IR neurons were encountered in all segments. The majority of VIP, SP and NF IR neurons had smooth surfaces and elongated or ovoid outlined. They were uniaxonal, bipolar, a few were multipolar, Dogiel type II neurons (Figs. 3a-b, 4b, 5b). There were extremely few SP IR neurons which were multipolar, multiaxonal, multidendritic Dogiel type III neurons some of which innervated blood vessels (Figs. 5d). The NF IR revealed ganglia, neurons, primary nerve strands and a few secondary nerve strands in the IGPP (Fig. 3b). NOS IR was seen only in extremely few large nerve strands in the IGPP in the basal lamina propria (not shown).

The inner proprial subplexus (IPP)

The IPP is an aganglionic meshwork situated at the base of the villi/crypt openings whose major axis is oriented perpendicular to the vertical axis of the villi/crypts (Figs. 1; 5e). The IPP was stained intensely and revealed well by VIP IR. SP IR was moderate and showed mainly large nerve strands. The nerve fibre meshwork in the IPP was finer, shorter and denser than that of the OPP and IGPP. NOS and NF IR were not observed.

The perivascular subplexus (PVP)

The PVP was revealed mainly by VIP and SP IR which showed a few large varicose nerve fibres coursing around blood vessels mainly terminal arterioles, capillaries and lacteals. The PVP had more

intense and dense VIP IR varicosities and a finer and shorter mesh than that of the IGPP (Figs. 1; 2d; 4b, 5d). SP IR varicosities were intense in large nerve strands, moderate or weak in small nerve fibres. The VIP and SP IR varicosities were observed close to pericytes, smooth muscles cells and endothelial cells (Fig. 5d). NOS- and NF IR were not observed. In the large intestine, the PVP around capillaries and terminal arterioles close to the opening of the crypts was closely interconnected to the IPP.

The villous subplexus (VP)

This subplexus was best revealed by VIP IR as fine nerve fibre meshwork located in the loose connective tissue in the LP between the core of the villi and SEP starting at the level of the IPP (Fig.1). It was formed by nerve fibre branches from the IPP, and nerve fibres extending into the villi from the IGPP. Varicose nerve fibres interconnected it to the PVP around terminal arterioles, capillaries and lacteals and to SEP. NOS- and NF IR were not observed.

Subepithelial subplexus (SEP)

The subepithelial plexus was composed of fine nerve fibre meshwork underlying the intestinal epithelium (Figs. 1; 2d; 4c). The glandular SEP was revealed clearly by VIP IR as varicose nerve fibres which partly surrounded the crypts especially in the basal regions or coursed obliquely and/or around the crypts for shorter distances while ascending up into the mucosa. The dense glandular SEP meshworks were seen at the base of the crypts and near their openings. The SP IR varicosities in the glandular SEP were sparse. NF and NOS IR were absent. The SEP underlying the luminal epithelium was formed by fine nerve fibre branches from the IGPP, IPP, VP and PVP and was best revealed by VIP IR. SP IR varicosities were scarce and NF and NOS IR were absent.

Nodes and interconnections

Architectural cross linkages of nerve strands in the mucosa being interconnected at nodes was similar to the classic organisation in the myenteric and submucous plexuses. Nerve fibre branches from the OPP coursed into the LP interconnecting the OPP with IGPP, PVP and SEP, others interconnected it to the LMMP and overlying major plexuses. The subplexuses in the mucosa were interconnected by small nerve fibre branches forming a complex nerve fibre meshwork.

Peptide IR outside the ENS

SP IR was localised simultaneously in the ENS and a few "open" and "closed" types of enterochromaffin (EC) cells (Fig. 2e).

Discussion

The observations on the nerve fibre meshworks, presence of ganglia and isolated neurons in the mucous subplexuses were in accordance to what has been reported earlier (Drasch, 1881; Ströhr, 1934, 1944; Lassmann, 1975; Furness and Costa, 1980, 1987; Keast et al. 1984; Costa et al. 1987; Furness et al. 1988; Korman et al., 1989; Mestres et al., 1992a, b; Fang et al., 1993; Costa and Brookes, 1994; Balemba et al., 1998, 1999; Wedel et al., 1999). However, the present study, revealed new observations and some differences compared to previous findings.

In the present study, we have demonstrated for the first time the presence of many ganglia and isolated neurons in the mucous plexus in the intestine of the pig. The present study, showed that ganglia and neurons were situated at different topographical levels in three subplexuses namely in the LMMP, OPP and IGPP and isolated neurons in the IPP (Fig. 1b). The observation of the highest amount of ganglia and isolated neurons in the caecum and that of ganglia and nerve strands in the outermost meshwork in the OPP which is closely apposed to the LMM is oriented perpendicular to the inner circular LMM muscle layer are new information. We have clarified the differences between the ganglionated and aganglionic subplexuses (LMMP, OPP and IGPP) in the mucous plexus (Table 1, 2).

Previous studies revealed very few ganglia/neurons in the mucosa and these ganglia and neurons were considered to be ectopic from the submucous plexus (Stöhr, 1934, 944; Lassmann, 1975) and the mucous plexus of both large (pig, man, ruminants) and small animal species (rat, mice and guinea-pig) to be aganglionic (Schultzberg et al., 1980; Costa et al., 1987; Timmermans et a., 1990; Burns and Cummings, 1993). Many ganglia and isolated neurons were seen regularly in the caecum and colon, followed by ileum while fewer ganglia and isolated neurons were seen in the jejunum. The reason for such a distribution and implications on intestinal function need to be clarified. Our findings support those of Mestres et al. (1992b) in the human colon by transmission electron microscopy which shows clearly that intramucosal ganglia are not ectopic. We therefore suggest the mucous plexus in the intestine of the pig to be considered as one of the major ganglionated plexuses others being ISP, OSP and the myenteric plexus (Timmermans et al., 1997; Balemba et al., 1998). However, when compared to the major ganglionated plexuses (Timmermans et al., 1997; Balemba et al., 1998) the meshwork of the ganglia and isolated neurons in the mucous plexus is very wide and with highly variable spatial distribution along intestinal segments and being composed of smaller ganglia and neurons than the other three major plexuses.

In the present study, the LMMP was considered as part of the mucous plexus which is different from other reports (Furness and Costa, 1980; Furness et al., 1988). The observation of two

layers of LMM was similar to that of Costa et al. (1980) in the ileum of guinea pig. The observation that LMM was moderately innervated by SP IR nerves are similar to those of Hens et al. (2000) in the small intestine of the pig. The findings on NOS IR in the present study, support those of Barbiers et al., (1993) in the large intestine of the pig.

The term outer proprial plexus was used instead of the subglandular plexus (Wedel et al., 1999) or external proprial plexus (Balemba et al., 1998). The term interglandular proprial subplexus (IGPP) was introduced to replace the terms paravascular subplexus (Furness et al., 1988, Costa and Brookes, 1994), periglandular (Wedel et al., 1999) and pericryptal subplexuses (Balemba, et al., 1998). These suggestions aimed at emphasising the distinction of the IPP which was well described by Balemba, et al. (1998), the location of ganglia and isolated neurons and the use of the nomenclature which is similar to that suggested for the submucous plexuses (Timmermans et al., 1997). Our observations on the topography and orientation of the IPP are similar to our earlier reports in the pig and cattle (Balemba et al., 1998, 1999). The close association of the IPP with terminal arterioles and capillaries in the large intestine correlates morphologically and functionally to blood vessels and nerves in the villi.

Our observations on variation in the size of ganglia and VIP, SP, NOS and NF IR neurons in the mucous plexus in the intestine of the pig are described for the first time (Tables 1, 2). However, they correspond to variations reported between the MP, OSP and ISP (Scheuermann et al., 1987a, b; Timmermans et al., 1990, 1997; Balemba, 1998). The observations of NOS and NF IR neurons and that of SP and NOS IR in the corona of Peyer's patches in the pig are new information. The observation of large neurons being common in the caecum and colon whereas, the medium sized and smallest VIP IR neurons were encountered in all segments is new as well and shows segmental variations. The morphology of the majority of VIP and SP IR neurons type II neurons corresponded to the description of type II neurons (Brehmer et al., 1999) and small multipolar neurons seen in the human colon mucosa (Stöhr, 1934). The observation of type III neurons in the mucosa is apparently new. Our observation that SP IR neurons in the OPP projected their axons though the LMM into the submucosa is opposite to that reported by Burns and Cummings, (1993) in the horse. Probably, we observed a different type of SP IR neurons which probably perform different function(s). In the present study, we observed intense and abundant VIP IR varicosities in the PVP around the terminal arterioles and capillaries being close to pericytes, smooth muscle cells and endothelial cells and moderate to scarce VIP IR around larger lacteals. These findings are similar to those in the intestine of the rat, cat and guinea pig (Fehèr and Burnstock, 1986). In a way, they support the suggestion by Schultzberg et al. (1980) that VIP- evoked vasodilatation could be due to direct action on vascular smooth muscle cells. The observation of moderate to weak SP IR nerve fibres associated with blood

vessels is similar to those of Hens at al. (2000) in the pig. Our observation of very few NOS IR neurons and sparse IR in large nerve fibres in the OPP and IGPP supports the report of NOS IR varicosities in large nerve fibres in the mucosa in the pig (Barbiers et al., 1993).

Mucosal functions are primarily regulated by neurons in the ISP (Timmermans et al., 1997; Hens et al., 2000). It has been shown that in the colon of rat, intramucosal neurons participate in regulating electrolyte transport (Bridges et al., 1986). The observation of fairly many neurons in the porcine intestinal mucosa reported here supports the proposition that mucosal neurons in the intestine contribute to mucosal innervation (Mestres al., 1992a; Fang et al., 1993). Studies to clarify the projection of mucosal neurons in combination with chemical coding which have been useful in elucidating neuronal functions (Porter et al., 1999; Hens et al., 2000) could provide an insight on the functional significance of mucosal neurons.

SP- containing endocrine cells are believed to be absent in the intestine of the pig (Schmidt et al., 1991). However, in the present study, SP IR was also localised in a few "open" and "closed" types of EC cells, which is new information.

Conclusions

- Mucosal ganglia and isolated neurons are not ectopic, they exist at different topographic levels in the LMMP, OPP and IGPP. The majority of them occur in the basal region of the mucosa.
-There are marked segmental variations in the amount of intramucosal ganglia and isolated neurons. They are abundant in the caecum, many in colon and ileum and few in the jejunum.
- Mucosal subplexuses show variation in the sizes and shapes of ganglia and sizes, shapes and types of IR neurons, and the staining pattern and intensity to VIP, SP, NOS and NF IR.
- The new observations presented here, calls for a re-examination of the mucous plexus to elucidate the regulatory mechanisms of importance in mucosal functions and consideration of the mucous plexus in the intestine of the pig to be one of the major ganglionated plexuses.

Acknowledgements

The authors are grateful to the Danish International Development Agency for financial support. The kind donation of the monoclonal rabbit anti-swine VIP by Dr. J. Fahrenkrug and monoclonal rabbit anti-SP by Dr. P. J. Larsen, is warmly acknowledged. Technical assistance by H. Holm, G. Holden, A.M. Thomsen, O. Mwangalimi, B. Makata and M. Mukama is highly appreciated.

References

Balemba, O.B., Grøndahl, M.-L., Mbassa, G.K., Semuguruka, W.D., Hay-Schmidt A., Skadhauge,

E., Dantzer, V., 1998. Organisation of the enteric nervous system in the submucous and mucous layers of the small intestine of the pig studied by VIP and neurofilament proteins immunohistochemistry. *J. Anat.* 192, 257-267.

Balemba, O.B., Mbassa, G.K., Semuguruka, W.D., Assey, R.J., Kahwa C.K.B., HAY-Schmidt, A., Dantzer V., 1999. The topography, architecture and structure of the enteric nervous system in the jejunum and ileum of cattle. *J. Anat.* 195, 1-9.

Barbiers, M., Timmermans, J.P., Scheuermann, D.W., Adriaensen, D., Mayer B., De Groodt-Lasseel, M.H.A., 1993. Distribution and morphological features of nitrigenic neurons in the porcine large intestine. *Histochem.* 100(1), 27-34.

Bredkjær, H.E., Wulff, B.S., Emson P.C., Fahrenkrug, J., 1994. Location of PHM/VIP mRNA in human gastrointestinal tract detected by in situ hybridisation. *Cell Tissue Res.* 276, 229-238

Brehmer, A., Schrodl, F., Neuhuber, W., 1999. Morphological classification of enteric neurons-100 years after Dogiel. *Anat. Embryol.* 200, 125-135.

Bridges, R.J., Rack, M., Rummel, W., Schreiner, J., 1986. Mucosal plexus and electrolyte transport across the rat colonic mucosa. *J. Physiol.* 376, 531-542.

Burns, G.A., Cummings, J.F., 1993. Neuropeptide distributions in the colon, caecum, and jejunum of the horse. *Anat. Rec.* 236, 341-350.

Costa, M., Brookes, S.J., 1994. The enteric nervous system. *Am. J. Gastroenterol.* 89(suppl. 8), 129-137.

Costa, M., Furness, J.B., Buffa, R., Said, S,I., 1980. Distribution of enteric nerve cell bodies and axons showing immunoreactivity for vasoactive intestinal polypeptide in the guinea-pig small intestine. *Neurosci.* 5, 587-596.

Costa, M., Furness, J.B., Llewellyn-Smith, I.J., 1987. Histochemistry of the enteric nervous system. In: Jonson, L.R., Christensen, J., Jackson, M.J., Jacobson, E.D., Walsh, J.H., (Eds.), *Physiology of the gastrointestinal tract*, Raven Press, New York, 1-39 pp.

Drasch, O., 1881. Beiträge zur Kenntniss des feineren Baues des Dünndarms, inbesondere über die Nerven desselben. Sitzber Akad Wiss Wien 82, 3rd div, 168-198.

Fang, S.Y., Wu, R.W., Christensen, J., 1993. Intramucosal nerve cells in human small intestine. *J. Auton. Nerv. Syst.* 44, 129-136.

Fehèr, E., Burnstock, G., 1986. Ultrastructural localisation of substance P, vasoactive intestinal polypeptide, somatostatin and neuropeptide Y immunoreactivity in perivascular nerve plexuses of the gut. *Blood Vessels* **23(3)**, 125-136.

Furness, JB., Costa, M., 1980. Types of nerves in the enteric nervous system; commentary. *Neurosci.* 5, 1-20.

Furness, J.B., Costa M., 1987. *The enteric nervous system.* Churchill, Livingstone, Edinburgh, 1-286 pp.

Furness, J.B., Llewellyn-Smith, I.J., Bornstein, J.C., Costa, M., 1988. Chemical neuroanatomy and the analysis of neuronal circuitry in the enteric nervous system. In: *Handbook of chemical neuroanatomy.* In: Bjørklund, A., Hökfelt, T., (Eds.), Elsevier science publishers, Amsterdam, 161-218 pp.

Hens, J., Schrödl, F., Brehmer, A., Adriaensen, D., Neuhuber, W., Scheuermann, D.W., Schemann, M., Timmermans, J.-P., 2000. Mucosal projections of enteric neurons in the porcine small intestine. *J. Comp. Neurol.* 421, 429-436.

Keast, J.R., Furness, J.B., Costa, M., 1984. Somatostatin in human enteric neurons. *Cell Tissue Res.* 237, 299-308.

Korman, L.Y., Sayid, H., Bass, B., Moody, T.W., Harmon, J.W., 1989. Distribution of vasoactive intestinal polypeptide and substance P receptors in human colon and small intestine. *Dig. Dis. Sci.* 34(7), 1100-1108.

Lassmann, G., 1975. Vorkommen von Ganglienzellen im Schleimhaustroma von Colon, sigma und Rectum. *Virch. arch. A: Pathol. Anat. Histol.* 365, 257-261.

Mestres, P., Diener, M., Rummel, W., 1992a. Histo- and immunocytochemical characterization of

the neurons of the mucosal plexus in the rat colon. *Acta Anat.* 143, 268-274.

Mestres, P., Diener, M., Rummel, W., 1992b. Electron Microscopy of the mucosal plexus of the rat colon. *Acta Anat.* 143, 275-282.

Newson, B., Ahlman, H., Dahlström, A., Das Gupta, T.K., Nyhus, L.M., 1979. Are there sensory neurons in the mucosa of the mammalian gut? *Acta Physiol. Scand.* 105, 521-523.

Porter, A., Wattchow, D.A., Brookes, S.J.H., Costa, M., 1999. Nitric oxide synthase and vasoactive intestinal polypeptides in the human colon: Projections of nitric oxide synthase and vasoactive polypeptide-reactive submucosal neurons in the human colon. *J. Gastroenterol. Hepatol.* 14, 1180-1187.

Scheuermann, W.D., Stach, W., Timmermans, J.-P., 1987*a*. Topography, architecture and structure of the plexus submucousus internus (Meissner) of the porcine small intestine in scanning electron microscopy. *Acta Anat.* 129, 96-104.

Scheuermann, W.D., Stach, W., Timmermans, J.-P., 1987*b*. Topography, architecture and structure of the plexus submucousus externus (Schabadasch) of the porcine small intestine in the scanning electron microscopy. *Acta Anat.* 129, 105-115.

Schmidt, P., Poulsen, S.S., Rasmussen, T.N., Bersani, M., Holst, J.J., 1991. Substance P and neurokinin A are co-distributed and co-localised in the porcine gastrointestinal tract. *Peptides* 12, 963-973.

Schultzberg, M., Hökfelt, T., Nilsson, G., Terenius, L., Rehfeld,, J.F., Brown, M., Eldie, R., Goldstein, M., Said, S., 1980. Distribution of peptide- and catecholamine- containing neurons in the gastro-intestinal tract of rat and guinea-pig: Immunohistochemical studies with antisera to substance P, vasoactive intestinal polypeptide, enkephalins, somatostatin, gastrin/cholecystokinin, neurotensin and dopamine β-hydroxylase. *Neurosci.* 5, 689-744.

Stöhr, P., 1934. Mikroscopische studien zur Innervation des Magen-Darmkanales III. *Z. Zellforsch. Mikrosk. Anat.* 21, 243-278.

Stöhr, P., 1944. Mikroscopische studien zur Innervation des Magen-Darmkanales V. *Z. Zellforsch. Mikrosk. Anat.* 34, 1-54.

Timmermans, J.-P., Scheuermann, D.W., Stach, W., Adriaensen, D., De Groodt-Lasseel, M.H.A., 1990. Distinct distribution of CGRP-, enkephalin-, somatostatin-, substance P-, VIP- and serotonin - containing neurons in the two submucosal ganglionic neural networks of the porcine small intestine. *Cell Tissue Res.* 260, 367-379.

Timmermans, J.-P., Adriaensen, D., Cornelissen, W., Scheuermann, D.W., 1997. Structural organisation and neuropeptide distribution in the mammalian enteric nervous system, with special attention to those components involved in mucosal reflexes. *Comp. Biochem. Physiol.* 118A (2), 331-340.

Vau E., 1932. Über die subglandulären Ganglienzellen in der Magenwand einiger Haussäugetiere. *Anat. Anz.* 73, 380-385.

Vittoria,, A., La Mura E., Cocca, T., Castaldo, L., 1992. Vasoactive intestinal polypeptidergic innervation and gastroenteropancreatic system: An immunocytochemical study in the hedgehog *Erinaceus europaeus. Acta Anat.* 143, 84-88.

Wedel, T., Roblick, U., Gleiss, J., Schiedeck, T., Bruch, H.P., Kühnel, W., Krammer, H.J., 1999. Organisation of the enteric nervous system in the human colon demonstrated by wholemount immunohistochemistry with special reference to the submucous plexus. *Anat. Anz.* 181(4), 327-337.

Table 1. Summary of findings on the components of the subplexuses in the mucous plexus.

Subplexuses		LMMP	OPP	IGPP	IPP	PVP	VP	SEP
Ganglia	Presence	+[1]	+++[2]	++[3]	+/-?	-[4]	-	-
	Large size	NS[5]	135 - 337µm long, 18 - 95µm width	33 - 47µm long, 29µm width	-			
	Small size	NS	13.5 - 25µm long, 27µm width	16µm long, 6.5µm width	-	-	-	-
Isolated neurons		++	+++	+++	++	-	-	-
Nerve strands	PS (7 - 13µm)	+++	+++	++	++ (4 - 7µm)	-	-	-
	SS (3.5 - 7µm)	++	++	++	++ (3 - 4µm)		-	-
	TS (≤ 3.5µm)	++	++	++	++ (≤3µm)	++	++	++
VIP like IR neurons	Presence	+	+++	++	+	-	-	-
	Large size	NS	54µm long, 35 - 42µm width; 34 - 54µm long, 6 - 11µm width	20-30 µm long, 12-20 µm width	-	-	-	-
	Medium size	NS	30 – 33µm long, 7 - 7.5µm width	NS	-	-	-	-
	Small size	NS	18 – 27µm long, 12 - 13.5µm width	NS	-	-	-	-
SP IR nerons	Presence	+	+++	++	+	-	-	-
	Large size	NS	39 – 42µm long, 8 - 10µm width	40 - 45µm long	-	-	-	-
	Small size	NS	NS	20 - 45µm long, 8 - 13.5µm width	-	-	-	-
NF IR	Neurons	+	+++	++	-	-	-	-
NOS IR	Neurons	+	++	-	-	-	-	-

[1]Scarce ganglia/isolated neurons/nodal cells/primary/secondary/nerve strands seen in a wholemount
[2]Few ganglia/isolated neurons/nodal cells/primary/secondary nerve strands seen in a wholemount
[3]Fairly many ganglia/isolated neurons/nodal cells/primary/secondary nerve strands seen in a wholemount.
[4]Ganglia/isolated neurons/nodal cells not observed/primary/secondary nerve strands not seen wholemount.
[5]Specified item not studied.

Table 2. Variations of the VIP, SP, NF and NOS IR in the subplexuses of the mucous plexus.

Subplexuses	Immunoreactivities in the subplexuses			
Name	VIP	SP	NOS	NF
Lamina muscularis mucosae subplexus (LMMP)	+++[1]	++	++	+
Outer proprial subplexus (OPP)	+++	++(+)[2]	++[3]	+++
Interglandular proprial subplexus (IGPP)	+++	++(+)	+[4]	+
Inner proprial subplexus (IPP)	+++	++	-[5]	-
Villous subplexus (VP)	+++	+	-	-
Perivascula subplexus (PVP)	+++	++	-	-
Subepithelial subplexus (SEP)	++	+	-	-

[1]Immunoreactivity in the subplexus was abundant.

[2]Many immunoreactive varicosities seen in the subplexus.

[3]Immunoreactivity in subplexus was moderate.

[4]Immunoreactivity in the subplexus was sparse.

[5]Immunoreactivity was absent in the subplexus..

Figures and legends

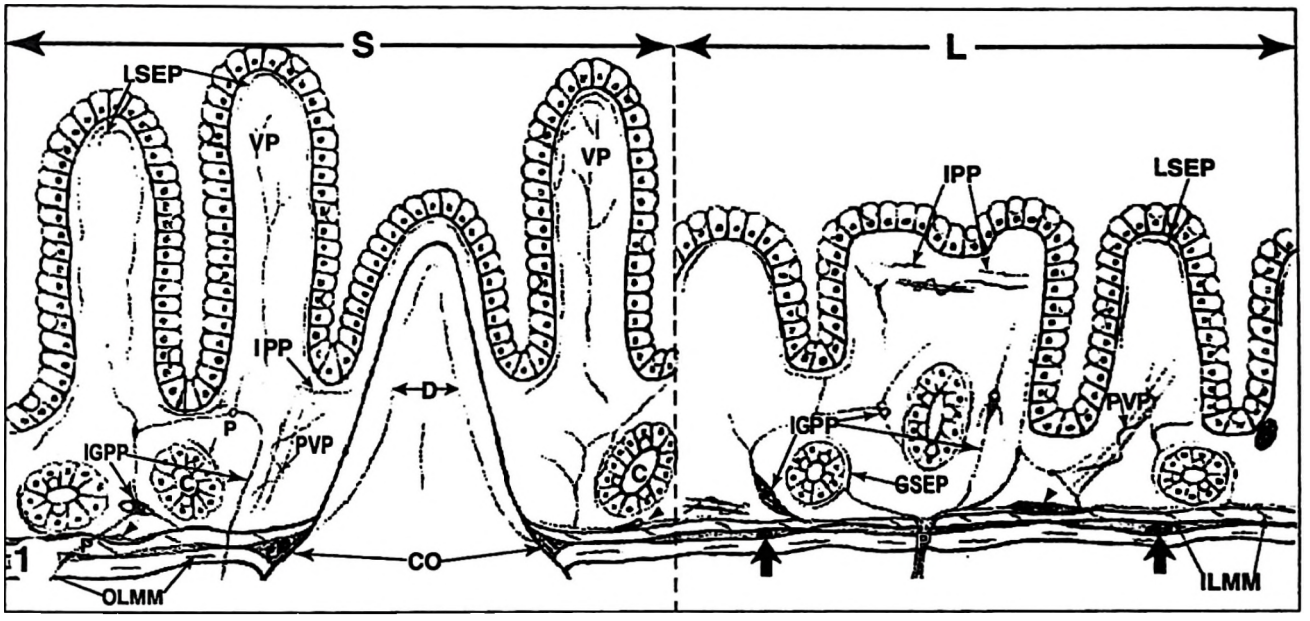

Fig. 1. Schematic drawing (not to scale) showing subplexuses in the mucous plexus both in the small (S) and large (L) intestine. In the following text (*) denotes ganglionated subplexuses. Viewed from serosal side they are (1) lamina muscularis mucosae subplexus (LMMP *) showing nerve fibres (small arrows) in the OLMM and ILMM and ganglia between the two layers (large arrows), (2) outer proprial subplexus (OPP *) (arrow heads) and (3) interglandular propria subplexus (IGPP *). Others are (4) the perivascular subplexus (PVP), (5) inner proprial subplexus (IPP), (6) villous subplexus (VP) which is absent in the large intestine and (7) the subepithelial subplexus (SEP). The glandular subepithelial subplexus is labelled GSEP and the subepithelial plexus underlying luminal epithelium by LSEP. A part of a follicle of the Peyer's patches showing nerves and ganglia in the corona (CO) and the dome (D) is also shown. P shows nerve strands traversing the LMM interconnecting underling major plexuses and higher centres to the mucous plexus.

Fig. 2a. Caecum, paraffin section of submucosal wholemount stained for SP IR, and counterstained by Mayer's Haematoxylin. Notice SP IR nerve fibres (large arrows) in the LMMP. Smooth muscle cells are shown by (small arrows). x 460. Figs. 2b-f. Mucosal wholemounts. Figs. 2b-c. Show the outermost meshwork of the outer proprial plexus (OPP) which has specified orientation. Fig. 2b.VIP IR in the ileum with the OPP overlying the base of the crypts (C). (G) shows a ganglion, (P) a primary nerve strand and (S) a secondary nerve strand. x 460. Fig. 2c.VIP IR staining of colon showing nerve strands (arrows) and ganglia (G) in the OPP. (Arrow heads) show the glandular subepithelial subplexus (SEP) close to the base of the crypts which are labelled (C). x 115. Fig. 2d. VIP IR staining of caecum showing dense nerve meshwork in the innermost part of the OPP at the base of the crypts in the subglandular proprial connective tissue. (G) shows ganglia, (small arrows) the perivascular subplexus (PVP), (open arrows) paravascular nerves in the IGPP, (V) shows the vascular arcades and (arrow heads) show the glandular subepithelial subplexus (SEP). x 115. Fig. 2e. Caecum, showing SP IR. Notice 7 ganglia (G) situated close the base of the crypts (C) with unipolar SP IR neurons emphasising their numerical density in the OPP. (Thick arrows) shows SP IR EC cells simultaneously stained with the nervous tissue. x 115. Fig. 2f. Caecum, VIP IR, notice a large ganglion (G) in the OPP meshwork at the base of the crypts (C). (P) and (S) shows primary and secondary nerve strands respectively. (Arrow head) shows the glandular subepithelial subplexus (SEP). x 230.

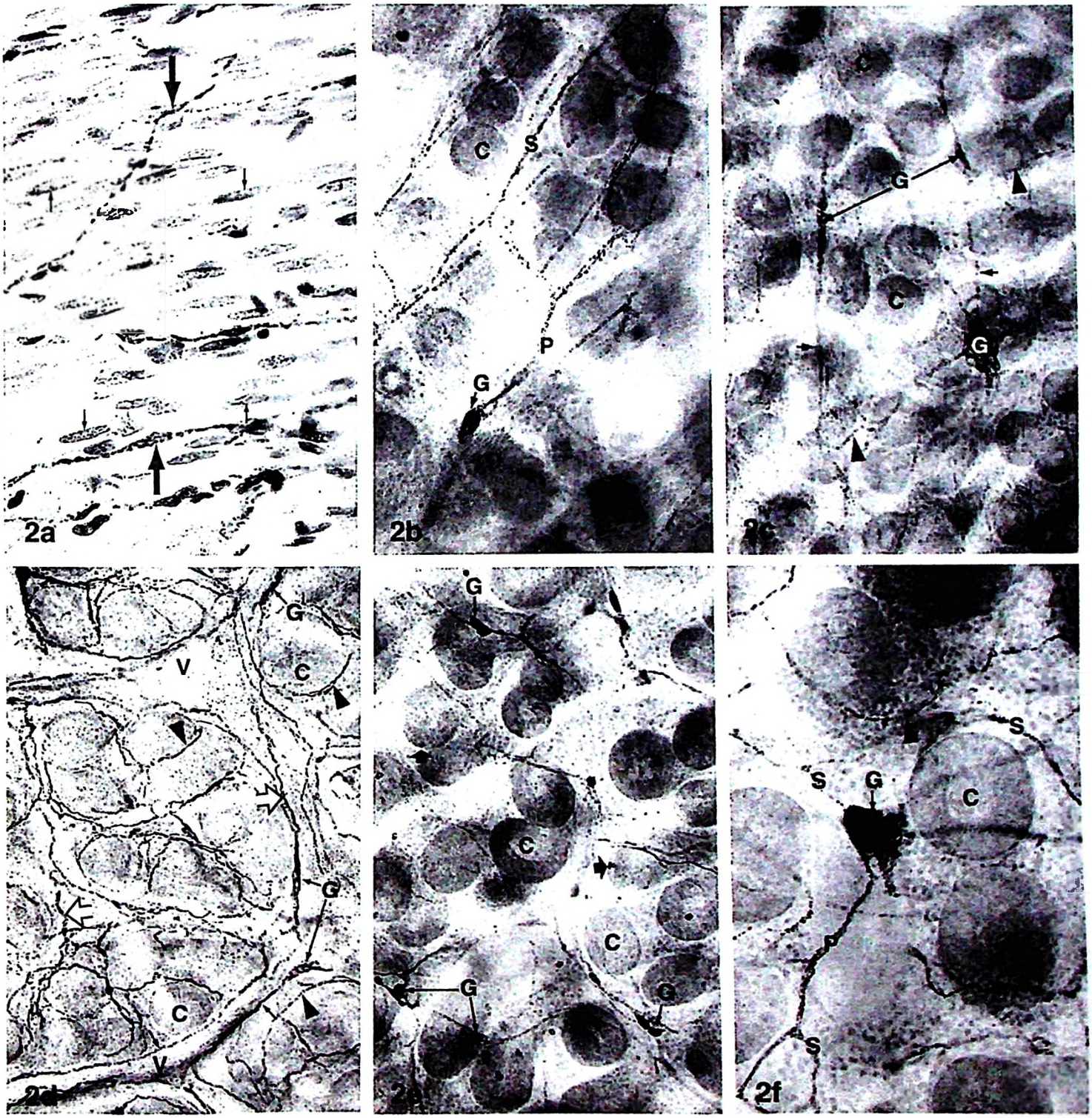
2a
C
S
P
G
2b
G
C
G
2c
V
C
G
C
V
2d
G
C
C
G
G
2e
S
S
G
C
P
S
2f

Fig. 3a-b. Colon, mucosal wholemounts stained for NF IR. 3a, notice a fairly large ganglion (G) with ovoid, smooth outlined NF IR neurons (arrows) predominantly of Dogiel type II in the OPP. (C) intestinal crypt. x 466. 3b. NF IR multipolar, uniaxonal Dogiel type II neuron (arrow) in the IGPP. (C) intestinal crypt. x 690.

Figs. 3c; 4a-b; 5a-h. Mucosal wholemount stained for either VIP or SP or NOS IR, embedded in paraffin, cut at 10 μm or 5 μm and counterstained by Mayer's Haematoxylin for 30 seconds.
Fig. 3c. Caecum, 10 μm section of mucosal wholemount stained for NOS IR. Notice two IR neurons (thick arrows) in LMMP, a satellite cell (open arrow), fibrocyte (arrow head) and a smooth muscle cell (thin arrow). x 1700.

Fig. 4a. Caecum, (10 μm) section of mucosal wholemount. Notice SP IR in the ISP revealing a neuron (large arrow) and a nerve strand (open arrows) close to LMM (small arrows). Large nerve strands (P) are traversing LMM interconnecting the mucosal subplexuses such as OPP and the underlying ISP, OSP and myenteric plexuses. (Arrow heads) show IR nerve fibres in the lamina muscularis mucosae subplexus. (C) intestinal crypt. x 1020. Fig. 4b. Caecum, SP IR, 10 μm section cut perpendicular to the major axis of the crypts and close to the base of the crypts (C). Noticed a ganglion (G) in the IGPP which has intensely stained Dogiel type II neurons (arrow heads). (Arrows) show the PVP close to a large lymphatic vessel (V). x 680. Fig. 4c. Caecum, VIP IR, 10 μm section showing the IGPP close to the base of the crypts (C). Notice an isolated VIP IR neuron in a node (arrow). (Arrowhead) shows glandular subepithelial plexus. x 1020.

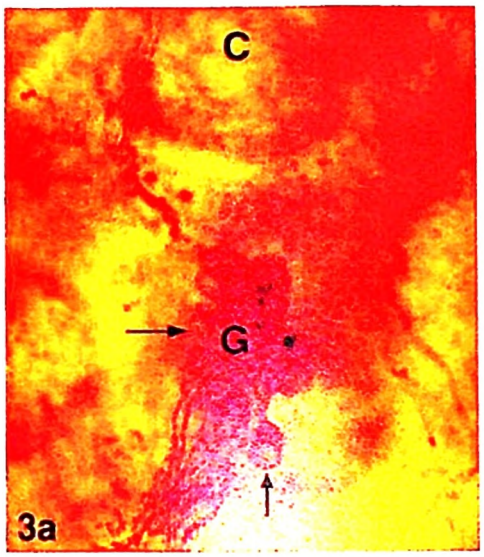

3a

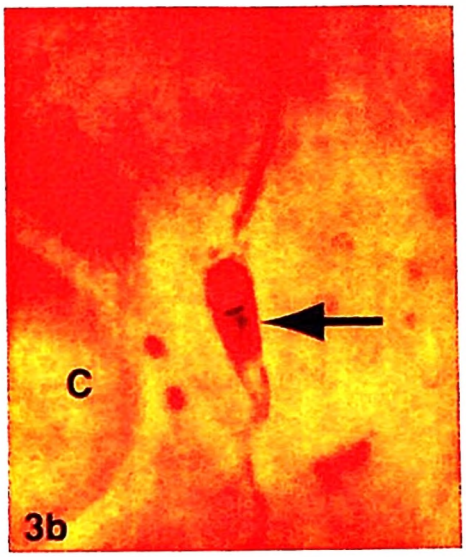

3b

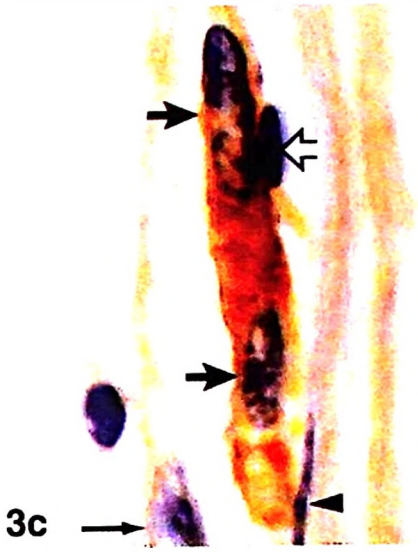

3c

4a

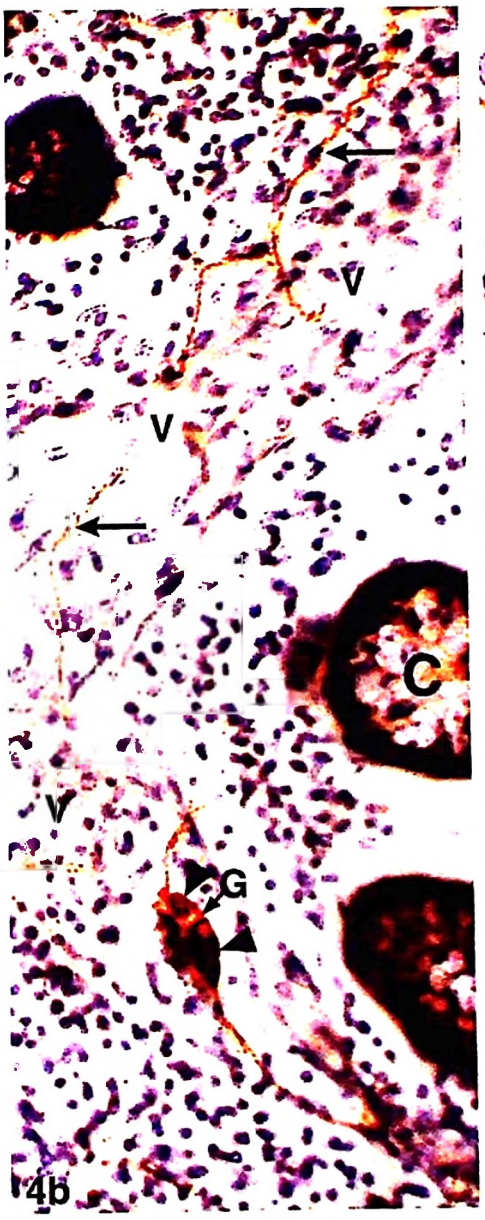

4b

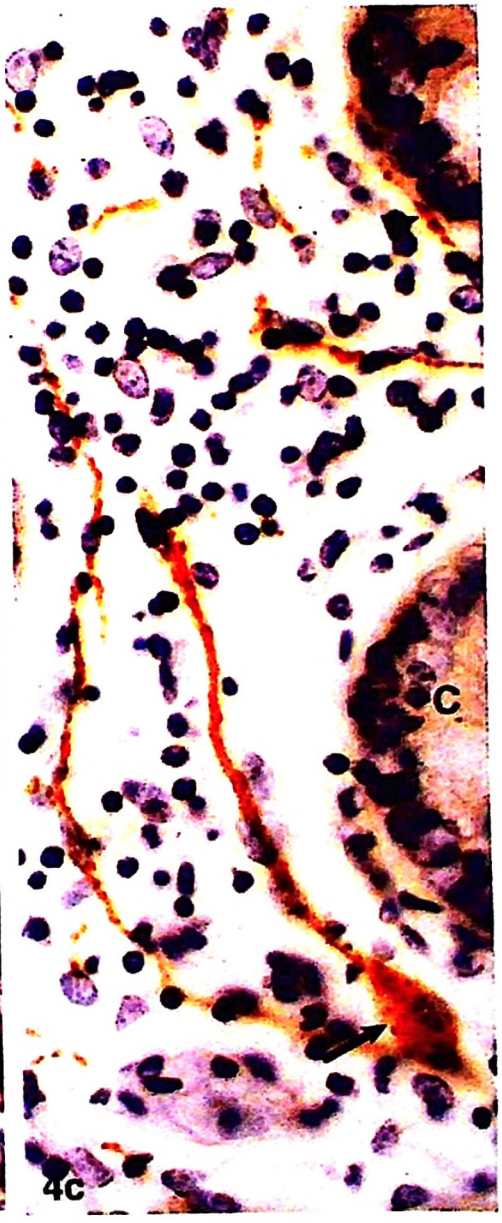

4c

Fig. 5a. Caecum, SP IR, 10 μm section. Notice mucosal ganglion with two IR unipolar neurons (large arrows), gliocytes (open arrows) and a primary nerve strand (P). The ganglion was localised in the OPP very close to LMM (not shown). (V) is a venule. x 1700.

Fig. 5b. Same tissue as in Fig. 5c showing an isolated, an ovoid (unipolar, uniaxonal) neuron with a smooth outline (arrow) in the IGPP, localised at ½ level of the mucosal height. A gliocyte (open arrow) is seen close to the neuron. x 1700.

Fig. 5c. Caecum, 5 μm section showing a 30 μm long, 19.5 μm in wide, bipolar SP IR neuron (arrow) localised in the IGPP close to the base of the crypts (C). Small arrows show the origin of neuronal processes. x 690. Fig. 5d. Colon, 5 μm section, SP IR in the IGPP showing part of a multipolar, multiaxonal Dogiel type III neuron (large arrow) with nerve fibres (small arrows) innervating a blood capillary (V). Also shown are a perivascular nerve (medium size arrow) in the PVP and another nerve (open arrow) probably in the IGPP. Endothelial cell (arrow head). x 1700.

Fig. 5e. Caecum,10 μm section, VIP IR varicosities in nerve meshwork in the IPP (arrows) and IGPP (arrow heads). The IPP is located closer to the lumen (LU) and oriented perpendicular to the vertical axis of the crypts (C). The epithelium lining the luminal surface was sloughed of during processing. x 170.

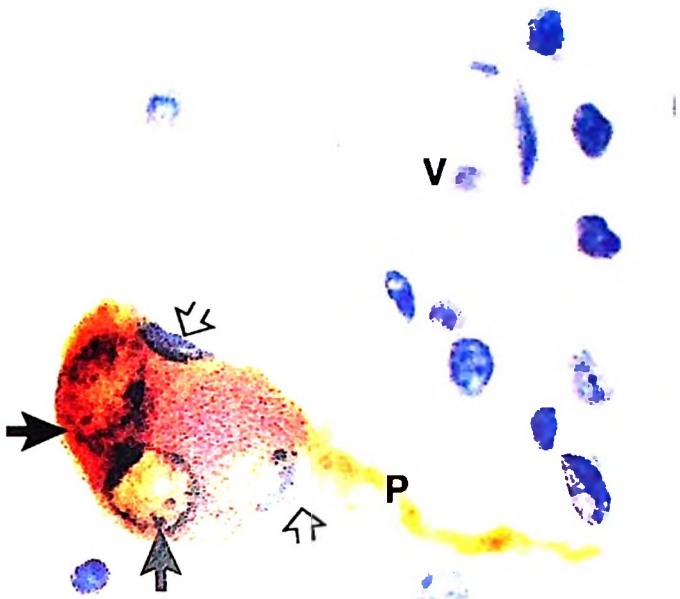

5a

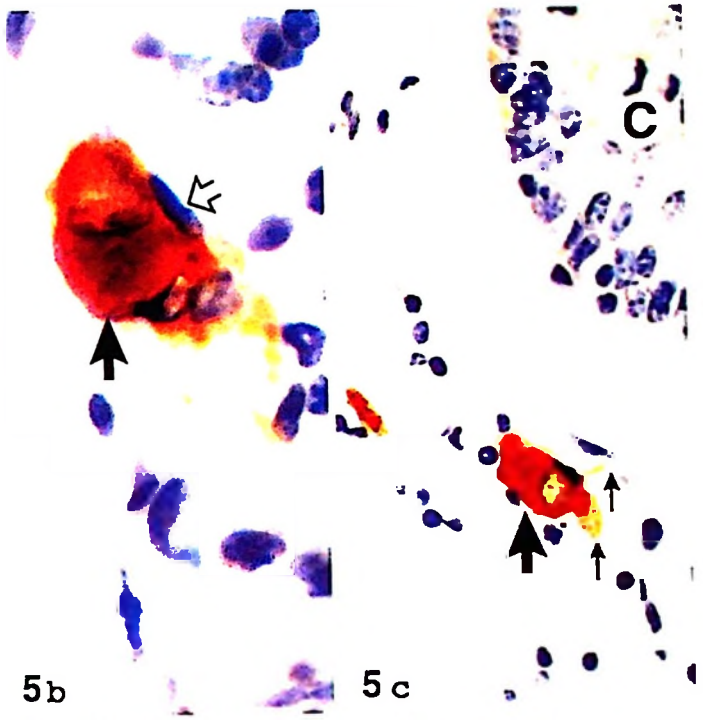

5b

5c

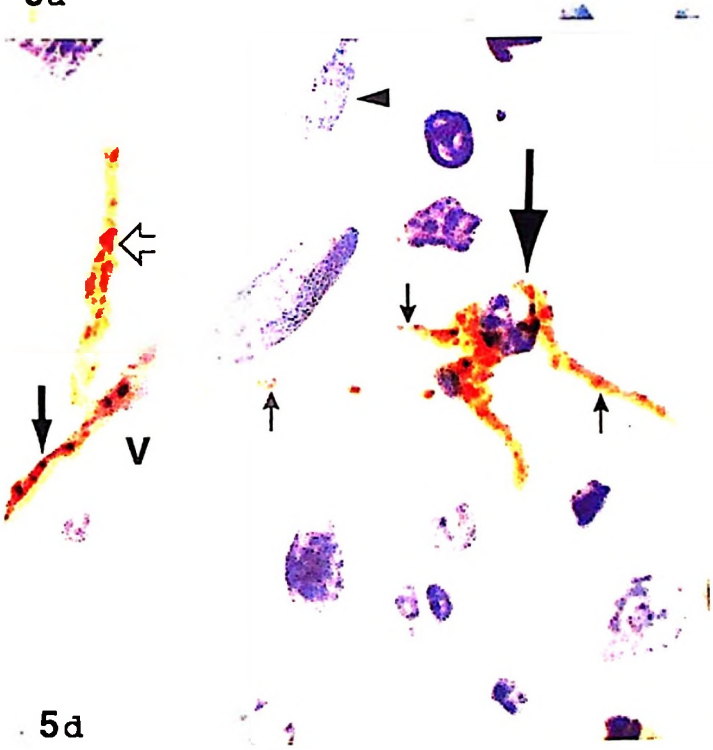

5d

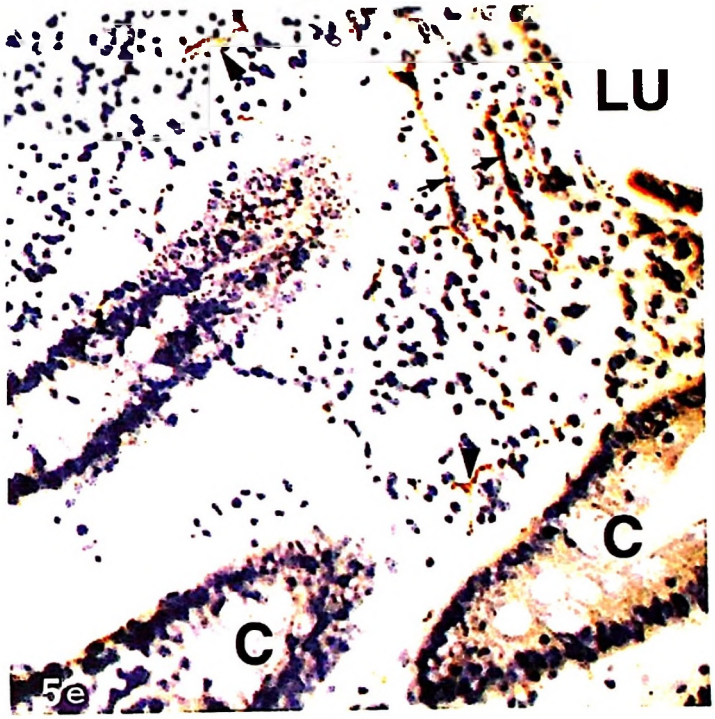

5e

Paper III

The organisation and variations of ganglionated plexuses of the enteric nervous system in the goat.

O.B. BALEMBA[1], W.D. SEMUGURUKA[2], A. HAY-SCHMIDT[3] AND V. DANTZER[4]

Departments of Veterinary Anatomy [1], Veterinary Pathology [2], Sokoine University of Agriculture, P.O. Box 3016 Morogoro, Tanzania. Institute of Anatomy, Panum building, Copenhagen University [3], Department of Anatomy and Physiology, RVAU [4], Copenhagen, Denmark.

Address for correspondence:

Dr. Vet. Sci. Vibeke Dantzer

Department of Anatomy and Physiology, RVAU, Grønegärdsvej 7, 1870 Frederiksberg C, Copenhagen, Denmark. Telephone: 4535282543; Telefax: 4535282547;

E-mail: Vibeke.Dantzer@iaf.kvl.dk

ABSTRACT

The number of distinct ganglionated plexuses and their organisation in the submucous layer as well as features to differentiate the outer from the inner submucous plexuses in the intestine of large mammals and the extent of ganglia in the mucous plexus are not yet clear. The enteric nervous system in the entire intestinal tract of eight, adult goats was studied using S-100 protein, neurofilament proteins, substance P and vasoactive intestinal peptide immunohistochemistry. Morphometry was used to evaluate the distribution of intramucosal ganglia. In the outer submucous plexus, complex and large ganglia and primary nerve strands showed coarse texture and were seen by naked eyes. The main axis of the majority of ganglia, primary nerve strands and neurons showed polarisation with respect to the circular muscle layer. Viewed from the serosal side, primary strands appeared beneath the main body of the larger ganglia. The new features seen in the outer submucous plexus show further the differences between the outer and inner submucous plexuses. Throughout the intestinal tract of the goat, the outer and inner submucous plexuses were distinct and were separated by the submucous vascular arcades. Within each plexus, ganglia and nerve strands appeared at different topographical levels and differed in the size, shape, outline and the density of meshworks as well as the size of neurons. These findings show features which support the existence of four plexuses in submucous layer. However, differences in neuronal phenotypes and projections, and functions are required before the subplexuses can be considered as distinct plexuses. Therefore each plexus was subdivided into the inner and outer subplexuses. In the mucous plexus, many ganglia and isolated neurons were seen along the entire intestinal tract. The highest numerical density was seen in the caecum, ileum and colon. The presence of many ganglia in the mucous plexus of the goat as well as in other mammals suggests a functional significance which need to be elucidated. In all plexuses, segmental and inter-plexus variations in the size of ganglia, nerve strands and S100 protein immunoreactive neurons showed close similarities between caecum and colon, between duodenum, rectum, ileum and distal jejunum, and between proximal and distal jejunum. This clarification, might explain variations in the total number and densities of neurons as well as functional differences between compartments.

Key words: *S-100 protein; neurofilament protein; substance P; vasoactive intestinal peptide; enteric nervous system, mucosal ganglia, goat.*

INTRODUCTION

To date, the existence of two interconnected but morphologically and functionally distinct submucous plexuses in the intestine of large mammals namely the outer submucous plexus (OSP) and the inner

submucous plexus (ISP) has been confirmed based on their variability in topography, ultrastructure, size and shape of ganglia and neurons, size of nerve strands, neurochemical coding and projection of neurons (Timmermans et al., 1997, 2001 for review). However, there are reports showing two more ganglionated plexuses. One, is a delicate ganglionated network closely associated with the inner circular muscle at its inner side, the *Plexus submucous (entericus) extremus* observed first by Stach (1972) in the colon of rat and guinea pigs which recently has been confirmed in the human colon (Hoyle and Burnstock, 1989a; Wedel et al., 1999). The observations of the OSP ganglia at different topographical levels in small intestine of the pig and cattle (Balemba et al.., 1998, 1999) gives further support to the existence of the *Plexus submucous extremus*. But, it is not clear whether this is a distinct plexus or part of the OSP. Two, is an intermediate plexus located between the OSP and ISP which was reported in the inner submucous layer in the small intestine of the pig (Gunn, 1968) and the colon of opossum (Christensen and Rick, 1987). The third intermediate plexus has also been confirmed throughout the intestine of humans (Timmermans et al., 1997, 2001, for review). In the small intestine of the pig (Scheuermann et al., 1987a; Balemba et al.,1998) and cattle (Balemba et al., 1999) the ISP ganglia and nerve fibre strands were observed at two topographic levels. The smallest ganglia were situated close to and associated with lamina muscularis mucosae whereas, larger ganglia were located close to the vascular arcades. Due to these observations, the ISP was subdivided into the outer and inner subplexuses (Balemba et al., 1998, 1999). Clearly, the intricate organisation of ganglionated meshworks in the submucous plexus of large mammals has not been clarified. Therefore, structural and architectural features which might ease the differentiation of submucosal plexuses need to be described. Although existence of marked species differences in the ENS of mammals has been emphasised (Timmermans et al., 1997; Brehmer, 1999), there is apparently only one report of the ENS in the goat using silver impregnation and histochemical staining for cholinesterase (Gunn, 1968).

The presence of small ganglia in the mucous plexus was first reported about 120 years ago by Drasch (1881) and Vau (1932) in cattle. Thereafter, similar observations were reported by Stöhr (1934, 1944) in the stomach and intestine of man, Lassmann (1975) in the colon and rectum of cows and Newson et al. (1979) in rat ileum. Since then, a number of similar observations have appeared and it is now clear that mucosal ganglia and isolated neurons are not ectopic from the submucous plexus (Mestres et al., 1992a, b; Fang et al., 1994; Wedel., 1999; Balemba et al., 2001a). However, the density and distribution pattern of intramucosal ganglia along the whole intestinal segments is not well established.

S-100 protein allows delineation of superimposed submucous plexuses and has been recommended for defining structural and topographical relationship of different subplexuses in the

small intestine of the pig (Scheuermann et al., 1989). Neurofilament proteins (NF) have also been proven to be useful to visualise the structure of the enteric nervous system (ENS) in the omasum of sheep (Yamamoto *et al.*, 1994) and small intestine of cattle (Balemba et al., 1999). Substance P (SP) and vasoactive intestinal peptide (VIP) revealed clearly the submucous plexuses (Timmermans et al., 1990), and ganglia and isolated neurons in the mucous plexus in the pig (Balemba et al., 2001a). Therefore, S-100 protein, NF, SP and VIP immunohistochemistry was used to elaborate organisation of ENS plexuses in whole intestinal tract of the goat, clarify segmental and inter-plexus variations, elaborate differences between the OSP and ISP and the extent of distribution of intramucosal ganglia.

MATERIALS AND METHODS

Eight male, Tanzanian local goats aged 1½ - 2 ½ years, (8-12 kg) were euthanised by exsanguination and the stomach and intestine were exposed. Two ligatures each were applied at the pylorus and the distal part of the terminal rectum. The entire intestine tract was removed from the carcass and put into cold (~ 4 °C), 0.01M phosphate buffered saline (PBS), pH 7.3 (5L). Extra ligatures were applied at the aboral end at the duodeno-colica ligament, at the oral end of ileo-caecal ligament and ileo-caeco-colical junction to mark the duodenum, jejunum and ileum. The small intestine was carefully freed from the mesentery and its total length was estimated to the closest centimetre. Tissues samples (n = 2 , ~ 3- 4 cm long each) were collected from the proximal, middle and distal jejunum, ileum as well as caecum and proximal part of the ascending colon. One sample each was collected from the duodenum and rectum. They were cut open along the mesenteric attachment and washed thoroughly using cold (4 °C), 0.01M PBS, pH 7.3. Each sample was cut (by width) into two pieces and each piece was pinned mucosal surface up on polystyrene plastic while being maximally stretched. Of the two pieces cut from the same sample, one was fixed in Stephanini/Zambooni and the other in 4.5% buffered formaldehyde (BF) for 1 hr. Thereafter, tissues were freed from polystyrene, fixed in fresh fixatives for 48 hrs at 4 °C, washed with PBS and thereafter dissected as described by Balemba et al., (1998).

Freshly dissected wholemounts were stored in 2ml of 0.01M PBS, pH 7.3 containing 0.5% triton X-100 and 0.1% sodium azide in plastic tubes at 4 °C. Tissues were washed and thereafter stained for S-100 protein, NF, SP and VIP immunoreactivities (IR) by the two step indirect streptavidin-ABComplex/HRP method described by Balemba et al., (1998). The polyclonal rabbit anti-cow S-100 protein (Z 0311) (1:400 dil.) was kindly donated by Dako, Glostrup, Denmark. Pooled monoclonal mouse anti-human neurofilament proteins (Cat. no. 168) was obtained from Immunotech, France. Monoclonal rabbit anti-swine SP (SP 250- 2; 1:2000) and monoclonal rabbit

anti swine-VIP (VIP, 8084-4; 1:1400) were kindly donated by Dr. P.J. Larsen of Panum institute, Copenhagen University, and Dr. J. Fahrenkrug, of Bispebjerg Hospital, Copenhagen, Denmark respectively. The specificity of immunostaining, dehydration and tissue mounting was done using the method described earlier (Balemba et al., 1998). Mucosal tissues were mounted serosal surface up. Wholemounts were evaluated and photographs taken. Mucosal wholemounts stained for S-100 protein IR from each of the segments studied (n = 2 goats) were embedded in paraffin, serosal surface down. From each block, 10 serial sections of 10 and 4 μm each respectively were cut, counterstained by Harri's Haematoxylin for 30 seconds, dehydrated in ethanol, cleared in xylene and mounted in DPX. These tissues were used to clarify and complement the topographical, architectural and structural features revealed by wholemounts. Lamina muscularis mucosae was used as a landmark to demarcate the mucous plexus from inner submucous plexus. The average sizes of ganglia were arbitrarily estimated based on that the boundary of a ganglion is where the ganglion narrows to form the internodal strands (Young et al, 1993). The nerve strands were classified based on the interconnections between ganglia and other nerve strands, size, shape and tortuousness as described by Scheuermann et al. (1986, 1987 *a, b*). Tissues stained for S-100 protein IR (three goats) were used to estimate sizes of ganglia, primary (PS) and secondary (SS) nerve strands and IR neurons using a calibrated eye piece at 10x, 20x and 40x objectives using an Olympus BH-2 microscope. In each plexus in a given segment, ganglia were classified into complex, large and small ganglia prior to estimating their length and width, data were added together to calculate the means. Five replications were considered enough for each of the structures measured in each of the specific plexuses in an individual wholemount representing a given segment.

Quantification of intramucosal ganglia was done on mucosal wholemounts (3 goats) stained for S-100 protein IR. A set of field of vision were examined under projection onto a table using a Leica DMLB microscope fitted with a projection arm at 20x objective (x333 total magnification). The counting was done using the unbiased counting frame (Gundersen, 1978). With a random start, each field of vision was systematically randomly sampled using a predetermined fraction of an 18cm^2 sampling frame. The selected fraction of the frame was used as an unbiased sampling frame: ganglia completely inside and those only intersecting the "inclusion" edges were sampled, provided they in no way intersected the "exclusion" edges. Numerical densities were calculated based on the sampling fractions, the results were analysed for variance using Statistical Analysis Systems (1987; edition 6) and significance was assumed at $P<0.05$.

RESULTS

Overall

Staining for S-100 protein, NF, SP and VIP IR revealed ganglia and nerve strands in the myenteric, outer submucous, inner submucous and mucous plexuses (Figs.1a-f; 2a-g; 3a-f; 4a-l). There were many small ganglia in the mucous plexus (Fig. 5) along the whole intestinal tract. All antisera revealed clearly IR neurons except the one for VIP which showed IR varicosities in a subset of nerves in the ganglia and nerves strands (Figs. 3f, 4g). Topographical, architectural and structural features of the ganglia and nerve strands were revealed best by S-100 protein IR. Structural features of neuronal surfaces were best demonstrated by NF IR (Figs. 1e; 2g) followed by S100 protein IR (Figs. 1d, 2e, 3b-d, 4l). NF IR showed lesser staining intensity in the ISP and the mucous plexus compared to the OSP and myenteric plexus. Compared to other plexuses, the VIP and SP IR predominated in the ISP.

All the four plexuses showed marked variations in the size and structure of the ganglia and nerve strands, and size and amount of neurons (Figs. 6a-b; 7a-b). Complex ganglia formed by fusion of neighbouring ganglia were polygonal being either rounded, often with an open space at the centre, or elongated and were seen in all plexuses (Fig.1c; 3b; 4e). Large ganglia were ovoid or elongated and showed clear demarcations from primary nerve strands. Small ganglia were rounded, ovoid or elongated, and in the myenteric plexus, OSP and ISP, they were either found at the intersections between PS and SS or between SS or between SS and tertiary nerve strands (TS). The smallest ganglion contained at least two neurons in a well defined node. Individual neurons located in nerve strands were considered as isolated neurons. In all four plexuses, S-100 protein, SP and NF IR neurons differed in size and shape. The majority of S-100 protein, and NF IR neurons were ovoid or elongated, had smooth outlines and peripherally located nuclei. They were adendritic, pseudo- or uniaxonal or multiaxonal being very much similar to Dogiel type II neurons (Figs. 1d-e; 2e, g; 3b; 4a, l). S-100 protein IR showed also rounded, adendritic, bipolar neurons (Fig. 3c). SP IR neurons were ovoid or rounded and their neuronal processes were hardly revealed. Dense pericellular SP and VIP IR varicosities were commonly seen around non reactive neurons (Figs. 1f-g; 3f). Antibodies against S-100 protein stained Schwann cells and enteric glia which were compressed between neurons. Schwann cells were small, spindle shaped with elongated, cork screw-like or indented nuclei with very little cytoplasm (Figs. 3d; 4a, i). Nerves and Schwann cells in the perivascular plexus were distinctly stained with S-100 protein IR so that it was possible to trace the outline of the vascular arcades in all layers (Figs. 2b; 3d). NF IR showed clearly the vascular arcades in the submucous layer.

Myenteric plexus

In the myenteric plexus (MP), S-100 protein and NF IR showed macroscopically the complex and large ganglia, and primary nerve strands (PS). Their surfaces were coarse with their main axis being oriented perpendicular to the inner circular muscle layer (ICM) whereas, secondary nerve strands were mainly oriented parallel to the ICM (Figs. 1a-c). Tertiary nerve strands, were classified into: (a) type one tertiary strands (TI) which were abundant, large, short and oriented parallel to the ICM and OLM giving fine branches into these muscle layers. They formed a network of nerve fibres in the tertiary plexus. (b) Type two tertiary strands (TII) were few, slender, long and oriented perpendicular to the ICM (Fig. 1c). TII were located on the outer side of the ICM. They coursed parallel to each other and often branched to give rise to a few branches each, which either, interconnected with SS or linked the MP to the ICM. Isolated neurons were identified within PS, SS and type one tertiary nerve strands. There were many NF-, few S-100 protein and very few SP IR neurons in the myenteric plexus (Figs. 1d-e).

Segmental variations

Ganglia in the caecum and colon were significantly longer compared to those in the rectum and in the small intestine (Figs. 1a-c). Ganglia, PS and SS in the colon, caecum, duodenum and rectum were significantly broader than those in the jejunum and ileum (Fig. 6a). Presence of smaller ganglia between the main mesh was a typical observation in the colon followed by duodenum and ileum. Complex ganglia were many in the colon, frequently seen in the duodenum, caecum, ileum and rectum and few in the jejunum. The meshwork formed by ganglia and PS was widest in the rectum, wide in the caecum, ileum and distal jejunum, less wide in the duodenum, proximal and middle jejunum and narrow in the colon. In the small intestine, the majority of S-100 protein and NF IR Dogiel type II were oriented in the direction of the ICM. Polarisation of ganglia and nerve strands with respect to the musculature was not entirely clear in the caecum and colon. Type II tertiary nerve strands were sparse and small in the jejunum and ileum, few in the duodenum and rectum and many and large in the caecum and colon. Larger S-100 IR neurons were commonly seen in the large intestine and duodenum. The largest S-100 protein IR neurons were seen in caecum (Fig. 6b).

The outer submucous plexus (OSP)

Viewed from serosal surface, the OSP was situated on the inner side of the ICM above the submucous vascular arcades (SVA). Both ganglia and nerve strands varied in size and were situated at different topographical levels (Figs. 2a-e). Small ganglia and isolated neurons were frequently seen

at the intersections between nerve strands underlying closely the ICM and thus constituted the outer OSP subplexus (Fig. 2d). Larger ganglia with very few small ganglia at the intersections between the PS and SS, SS, and SS and tertiary strands were situated closer to the SVA than to the ICM and were considered as the inner OSP subplexus. Complex and large ganglia and large PS were coarse and could be seen macroscopically in tissues stained for S-100 protein and NF IR. The PS formed the major axis which was oriented perpendicular to the ICM and appeared mostly beneath the body of larger ganglia (Figs. 2a; 2c). The majority of these large ganglia, and S-100 protein and NF IR neurons were elongated and oriented parallel to the ICM and neurons were loosely arranged in the ganglia. The majority of TS from both subplexuses were very long and coursed immediately under and parallel to ICM and gave fine branches that linked the OSP to the muscular plexus in the ICM (Figs. 2c-d). These strands and SS interconnecting the OSP to the myenteric plexus firmly attached the OSP to the ICM. Many S-100 protein and NF and few SP IR neurons were observed in the ganglia and as isolated neurons in nerve strands (Figs. 2e-g).

Segmental variations

Ganglia, PS and SS in the caecum, colon and rectum were significantly larger than in the rest of the intestine. Ganglia in the ileum, and rectum were broader and shorter in comparison to other segments. Smallest ganglia were seen in the duodenum (Figs. 6a). Complex ganglia were most common in caecum, colon and ileum. Polarisation of the major axis was most pronounced in the duodenum and jejunum. Larger S-100 protein IR type II neurons were found in the caecum, colon and rectum. The smallest neurons were most common in the duodenum (Figs. 6b).

The internal submucous plexus (ISP)

Viewed from serosal side the ISP was situated between the SVA on the outer side and lamina muscularis mucosae (LMM) on the inner side (Figs. 2b; 3d). The ISP ganglia and nerve strands varied in size, shape and outlines, and were situated at different topographical levels (Figs. 3a; 3e). Complex and large ganglia slighter coarser in the outline and less compact, were located in a broader mesh, had tortuous fibre tracts, contained larger neurons and were interconnected to the OSP by SS. These features were more prominent in the large intestine (Figs. 3a, e). They were situated close to the SVA and were described as the outer ISP subplexus. Smaller, rounded, ovoid or polygonal, narrow meshed, smoothly outlined, compact ganglia with relatively smaller nerve strands and neurons were situated very close to the LMM being interconnected to the outer ISP subplexus by SS and were described as the inner ISP subplexus (Figs. 3a, e). However, the two ISP subplexuses although with differences in morphological features, were closely interconnected without a clear-cut demarcation.

There were abundant SP, many S-100 protein and NF IR neurons (Figs. 2f; 3b-d; 4c, l).

Segmental variations

Ganglia in the caecum and colon were significantly longer and broader than those in the rest of the intestinal tract. The width of ganglia and nerve strands did not differ significantly between other segments (Fig. 6a). Complex ganglia were most common in the caecum, colon and duodenum, and few in the jejunum, ileum and rectum. The meshwork of ganglia and PS was dense in the small intestine and colon and broad in the caecum and rectum. The largest type II S-100 protein IR neurons were common in the caecum. The smallest neurons were mostly seen in the duodenum (Fig. 6b). In the Peyer's patches, both the OSP and ISP were situated under the base of the follicles and were clearly separated by the SVA. The ISP formed a mesh of three sub-plexuses around the follicles namely the (a) subfollicular ISP subplexus which was situated beneath the base of the follicles, (b) interfollicular ISP subplexus which was located in the interfollicular (traffic) areas and the coronary ISP subplexus located in the corona.

Mucous plexus

Many intramucosal ganglia and isolated neurons were observed in the mucous plexus being situated at different topographical levels (Figs. 4a-l). There were sparse ganglia and isolated neurons in the lamina muscularis mucosae subplexus (LMMP) (Fig. 4a), many in the outer proprial subplexus (OPP) in subglandular region (Figs. 4b-c, e, g-i). In the interglandular/cryptal proprial subplexus (IGPP) (Figs. 4d, f, l), they were few close to the base of the crypts and very few high up close to luminal side. S-100 protein and SP IR neurons were seen in ganglia and as isolated neurons in the LMMP, OPP and IGPP. NF IR was seen in nerve fibres and few IR neurons in the ganglia and large nerve strands in the OPP and IGPP. Intense SP IR varicosities were seen in the dense nerve fibre network in the dome and in the very sparse nerve fibres in the lymphoid follicles (Fig. 4j). VIP IR revealed varicosities in ganglia and nerve strands and both S-100 protein and VIP IR showed nerve fibres in all subplexuses in the mucosa (Figs. 4g, k-l).

Segmental variations

The LMMP was highly developed in the rectum where the inner circular lamina muscularis mucosae layer was thick. The meshwork of the mucous plexus was shorter in the small intestine and colon, broad in the caecum and rectum following the "honey-comb" organisation pattern of mucosal vascular arcades around the crypts. The highest numerical density of intramucosal ganglia and the highest number of neurons were encountered in the caecum, followed by ileum, colon, distal jejunum, rectum, duodenum, middle jejunum and the proximal jejunum (Fig. 5). The largest ganglia and PS

were observed in the caecum followed by colon, rectum, ileum and duodenum. Complex ganglia were observed in the caecum, colon and rectum. They were not seen in the small intestine. In the large intestine the ganglia were mainly elongated with the major axis being clearly oriented parallel to the vascular arcades. The majority of ganglia in the small intestine were smaller, round or ovoid and sometimes elongated (Figs. 6a-b). Large neurons were mostly seen in the large intestine whereas the smallest neurons were frequently seen in the duodenum.

Variation of plexuses along serosal-mucosal axis

Compared to other plexuses the myenteric plexus was composed of the most coarse, irregularly shaped and largest ganglia, PS, SS and IR neurons and with the most dense meshwork of TS. Their sizes decreased progressively from the MP to the OSP, ISP and mucous plexus being smallest in the mucous plexus (Figs. 7a-b). Type II tertiary strands were observed only in the MP. The OSP formed the widest nerve meshwork with PS and SS being clearly oriented perpendicular to ICM whereas, most of S-100 protein and NF IR neurons and many tertiary nerve strands were oriented parallel to the ICM. The PS appeared mostly beneath the main body of the large and complex ganglia. The ISP formed the most narrow meshed irregular network without specified orientation. Compared to OSP, the existence of ganglia and nerve strand at different topographical levels was appreciably seen in the ISP. The ISP and mucosal ganglia were compact and with smooth outlines. The majority of intramucosal ganglia were located in the OPP. There were many S-100 protein in the OSP and ISP, few in MP and the mucous plexus. There were many NF IR neurons in the MP, OSP and ISP and few in the mucous plexus. SP IR neurons were abundant in the ISP, few in the OSP and the mucous plexus, and very few in the MP. The IR neurons in the ISP and the mucous plexus were not polarised.

DISCUSSION

The overall organisation of the MP, OSP, ISP and the mucous plexus in the intestine of the goat was in many ways similar to previous observations in the pig, sheep and goat (Gunn, 1968; Gabella, 1987), pig (Stach, 1977a,b; Scheuermann et al., 1986, 1987*a, b*; Timmermans et al., 1990; Krammer and Kühnel, 1992; Brehmer et al., 1994, 1999; Balemba et al., 1998, 2001b), horse (Pearson, 1994), man (Hoyle and Burnstock, 1989a, b) and in calves (Mannl et al., 1984, Balemba et al., 1999). Morphological features observed for the OSP and ISP and type II neurons correspond well to those described in reviews by Timmermans et al. (1997, 2001) and Brehmer et al. (1999) respectively. However, (a) the present study of the whole intestinal tract of the goat is apparently, the first detailed description of the organisation of the ENS in the goat. (b) In the present study, complex ganglia were

observed in all plexuses studied and were common in the large intestine and duodenum. In the MP, type two tertiary nerve strands interconnected primarily the SS whereas in calves (Balemba et al., 1999) they interconnected ganglia. (c) In the goat, the OSP was well developed throughout the whole intestinal tract with clear differences between the OSP and ISP which is different from the findings of Gun, (1968) in the small intestine of sheep and goat. The OSP ganglia differed in their sizes, structure, topography, density of meshworks and size of neurons and hence, the OSP was subdivided into the outer and inner OSP subplexuses. (d) In the OSP, large ganglia and PS were polarised and could be seen macroscopically. The TS, S-100 protein and NF IR neurons were also polarised. The PS appeared mostly beneath the main body of larger ganglia. These new observations add to the criteria for differentiating the OSP from ISP in large mammals. (e) The present study provides additional evidence for the existence of two subplexuses in the ISP namely the outer and inner ISP subplexuses which differed in topography, density of meshworks and in sizes of ganglia and neurons as shown earlier by studies in pigs and cattle (Scheuermann et al., 1987*a*; Balemba et al., 1998, 1999). (f) Many intramucosal ganglia and isolated neurons were observed in the mucous plexus and the numerical density of the intramucosal ganglia were estimated and segmental variations elucidated (Fig. 5). (g) In present study, the variations between intestinal compartments and between plexuses were elaborated and showed that in all plexuses, larger ganglia, PS, SS as well as S-100 protein IR neurons were found in the caecum and colon whereas, they were medium sized in the duodenum, rectum, ileum and distal jejunum and relatively smaller in the middle and proximal jejunum (Figs. 6a-b). (h) The observed variations in the distributions of the NF, S-100 protein and SP IR neurons in the MP, OSP, ISP and the mucous plexus with SP IR being seen more frequently in the mucous plexus than in the myenteric plexus are new information. The observation of two types of S-100 protein IR neurons and their presence in the mucous plexus are apparently reported for the first time. However, our observations on S-100 protein IR in enteric neurons supports the localisation of S-100 protein IR in a subset of neurons in the myenteric and submucous plexuses in paraffin sections from the intestine of cow and goat by Albuerne et al. (1998).

The failure of VIP IR to reveal IR neurons is probably because the VIP antibody used did not cross-react fully with VIP antigens in the goat. The findings that S-100 protein IR showed the organisation of enteric plexuses as well as revealing the submucous vascular arcades very well, thereby giving a good delineation of the OSP and ISP are in accordance to observations of Scheuermann et al. (1989) in the intestine of the pig. Our observations on the location, size, shape and staining of Schwann cells and enteric glia cells by S-100 protein IR correspond with the observation of Scheuermann et al. (1989) and Krammer and Kühnel (1993) in the pig,

Krammer et al. (1994) in the human colon, and Albuerne et al. (1998) in dorsal root, sympathetic and enteric ganglia of several mammalian species. The NF IR revealed Dogiel type II as well as types IV and VI neurons in the intestine of the pig (Balemba et al., 1998) and types II and IV in the intestine of cattle (Balemba et al., 1999) but, as shown here, it revealed only Dogiel type II neurons in the goat. The reason for the difference is not apparent. However, it suggests species variation in the molecular composition of NF in intestinal neurons. The observation is also in agreement with the findings by Krammer and Kühnel (1992) and Balemba et al. (1998) that in the gastrointestinal tract of the pig, some neurons in the ganglia cannot be stained by antibodies to neurofilament proteins.

In the present study, all plexuses showed a similar pattern of variations in the sizes of ganglia, nerve strands and S-100 protein IR along compartments. Our observations on segmental variations in the size of ganglia correlates well with the observed segmental variations of neurons per unit of ganglionic area and of more neurons in the myenteric plexus of the colon compared to small intestine of the guinea pigs (Karaosmanoglu et al., 1996). The reasons for the observed pattern of variation, and the close similarity of the rectum to the duodenum and ileum are not apparent. Therefore, the observations may explain differences in the total number and numerical densities (distributions) of neurons as well as functional differences between intestinal compartments and their ability to react and adapt differently during pathophysiological conditions. In addition, the measurements of sizes showed clearly the differences between the MP, OSP, ISP and the mucous plexus (Figs. 7a-b). Although ganglia are not regarded as distinct anatomical entities (Gabella, 1987), estimation of their relative sizes could still be useful in comparative morphology of different plexuses and relative distribution of neurons (Karaosmanoglu et al., 1996) as well as to functional studies of the ENS. The observations of coarse, large and irregularly shaped ganglia and PS in the myenteric plexus are similar to those of Gabella (1987) in the intestine of sheep. However, the tendency of the large proportion of S-100 protein and NF IR to spread in the direction of the ICM is slightly different from that of Gabella, (1987) and probably shows that the tendency for polarisation of neurons differ among subsets of neuronal phenotypes. The lesser degree of polarisation of ganglia and nerve strands recorded in the caecum and colon show segmental differences.

The findings on the sizes, coarseness, orientation ganglia and nerve strands and arrangement of neurons in the ganglia in the OSP give further support to the concept that the OSP is more similar to myenteric plexus than to the ISP (Gunn, 1968; Timmermans et al., 2001). The observation of the outer OSP subplexus comprised of small ganglia located close to ICM nerve network coursing parallel to ICM provide support to a *Plexus submucous extremus* described earlier in the colon of rat and guinea pigs (Stach, 1972) and in the human colon (Hoyle and Burnstock 1989a;

Wedel et al., 1999). This finding also supports the observations of OSP ganglia at different topographical levels in small intestine of the pig and cattle by Balemba et al. (1998, 1999). However, morphological and functional differences between the OSP and *Plexus submucous extremus* are not well established. The observation that the majority of TS linked the OSP to the ICM gives morphological evidence for the involvement of the OSP in regulating the ICM (Timmermans et al., 2001). The observation of PS emerging beneath larger ganglia in the OSP supports the observation of large nerve strands on the luminal side of the OSP in sections from the intestine of calves (Mannl et al., 1984; Balemba et al., 1999). Our findings show that in the goat, bodies of large OSP ganglia are more elevated compared to ganglia in the small intestine of the pig (Scheuermann et al., 1987b).

The observation of the two topographically different but closely interconnected outer and inner ISP subplexuses is similar to previous observations in the small intestine of the pig (Scheuermann et al., 1987a; Balemba et al., 1998) and calves (Balemba et al., 1999). This finding supports the proposition for the third intermediate plexus in larger mammals other than man (Gun, 1968; Christensen and Rick, 1987). The intermediate plexus in intestine of humans (Timmermans et al., 2001 for review) resembles phenotypically the ISP in the small intestine (Dhatt and Buchan, 1994) and OSP in the large intestine (Crowe et al., 1992). Studies on neurochemical coding and projections of neurons (Porter et al., 1999; Hens et al, 2000) as well as functions are required before the OSP subplexus which is equivalent to the *Plexus submucosus extremus*, and the outer ISP, equivalent to the intermediate plexus could be considered as distinct plexuses. The observations on the organisation of the OSP and ISP in the Peyer's patches are similar to those of the pig (Balemba et al., 1998; Kulkarni-Narla et al., 1999). However, in the present study, new terminologies were suggested to clarify the subplexuses in the ISP and the mucous plexus in conformity to that proposed by (Timmermans et al., 1997, 2001) and based on the topographical locations of the subplexuses. The observation of SP IR nerves in lymphoid follicles is similar to that of Kulkarni-Narla et al. (1999) and provides anatomical evidence to signify the importance of the ENS (SP-mediated) in modulating immune responses (Stanisz et al., 1987).

The observation of intramucosal ganglia and isolated neurons are consistent with those reported earlier in colon of rats (Mestres et al., 1992a, b), small intestine (Fang et al., 1993) and colon (Wedel et al., 1999) of humans and in the intestine the pig (Balemba et al.., 2001a,b). However, in the present study the whole intestinal tract was investigated and segmental variations of numerical densities of intramucosal ganglia were clarified. The observed higher numerical density of intramucosal ganglia in the caecum, ileum, colon and duodenum compared to the rectum and jejunum could explain some functional differences between these segments. The observation of many ganglia

and isolated neurons in caecum mucosa is supported by the occasional finding of neurons in the lamina propria of the appendix of normal humans and during neurogenic appendicopathy (Papadaki et al., 1983; Naik et al., 1999) and signifies the importance of mucosal neurons in the pathogenesis of neurogenic appendicopathy. Our finding of many ganglia in the ileum compared to colon is different from that of Balemba et al. (2001a) in the pig. Observation of the smallest S-100 protein IR neurons in the duodenum are different from those of Fang et al. (1993) in the duodenum and ileum of humans.

Our observation of the largest neurons in the myenteric plexus of caecum supports those of Gabella, (1971) in the caecum of rats. It is not very clear here why smaller neurons were commonly seen in the duodenum and almost in all plexuses. Our observations on variation of the size of ganglia and IR neurons between plexuses show direct relationship between the size of ganglia and neurons and supports the observation of Gabella, (1987) in the intestine of mouse, guinea pig and sheep, that larger neurons aggregate in larger ganglia.

CONCLUSIONS

The present study in the goat, revealed the following features:

- The OSP ganglia, PS and TS as well as neurons are polarised and PS appear mostly beneath larger ganglia. These new informations might be added to the morphologic criteria for differentiating the OSP from the ISP.

-Based on the topography, density of meshworks, size of ganglia and neurons, both the OSP and ISP were subdivided into two, the outer and inner subplexuses. In the OSP, outer OSP subplexus is equivalent to the *Plexus submucous extremus* whereas the inner OSP subplexus is the Schabadasch's plexus. In the ISP, the outer ISP is equivalent to the third intermediate plexus and the inner ISP subplexus is the Meissner's plexus. Further morphological and functional studies are suggested to clarify if these subplexuses might be considered as different distinct plexuses.

-There were many ganglia and isolated neurons in the mucosa through out the intestinal tract of the goat with the highest densities in the caecum, ileum and colon. We therefore propose the mucous plexus to be considered among the major ganglionated plexuses.

- In all plexuses, the largest ganglia, PS, SS as well as S-100 protein IR neurons were found in the caecum and colon. They were medium sized in the duodenum, rectum, ileum and distal jejunum and relatively smaller in the middle and proximal jejunum.

ACKNOWLEDGEMENTS

The authors wish to thank the Danish International Development Agency for financial support. The kind donation of the polyclonal rabbit anti-cow S-100 protein by Dako, Glostrup, Denmark and monoclonal rabbit anti-swine vasoactive intestinal peptide by Dr. J. Fahrenkrug is sincerely acknowledged. Excellent technical assistance by O. Mwangalimi, M. Mukama, B. Makata, J. Mbessa, K. Mluge, M. Balisidya, Y. Noah and H. Holm is highly appreciated. We thank Prof. B. Pakkenberg, and Dr. T. Bock for use of the Leica, DMLB microscope and Prof. H.J.G. Gundersen for consultations.

REFERENCES

ALBUERNE M, MAMMOLA CL, NAVES FJ, LEVANTI B, GERMANA G, VEGA JA (1998) Immunohistochemical localisation of S100 proteins in dorsal root, sympathetic and enteric ganglia of several mammalian species, including man. *Journal of Peripheral Nervous System* **3(4)**, 243-53.

BALEMBA OB, GRØNDAHL ML, MBASSA GK, SEMUGURUKA WD. HAY-SCHMIDT A, SKADHAUGE E, DANTZER, V (1998) Organisation of the enteric nervous system in the submucous and mucous layers of the small intestine of the pig studied by VIP and neurofilament proteins immunohistochemistry. *Journal of Anatomy* **192**, 257-267.

BALEMBA OB, HAY-SCHMIDT, A, ASSEY RJ. KAHWA CKB, SEMUGURUKA WD, DANTZER V (2001a) An immunohistochemical study of the organisation of ganglia and nerve fibres in the mucosa of the porcine intestine. *Autonomic Neuroscience: Basic and Clinical* (Submitted).

BALEMBA OB, MBASSA GK, SEMUGURUKA WD, ASSEY RJ, KAHWA CKB, HAY-SCHMIDT A, DANTZER V (1999) The topography, architecture and structure of the enteric nervous system in the jejunum and ileum of cattle. *Journal of Anatomy* **195**, 1-9.

BALEMBA OB, SEMUGURUKA WD, HAY-SCHMIDT A, JOHANSEN MV, DANTZER V (2001b) Vasoactive intestinal peptide and substance P- like immunoreactivities in the enteric nervous system of the pig correlate with the severity of pathological changes induced by *Schistosoma japonicum*. *International Journal for Parasitology*. (In press).

BREHMER A, STACH W, ADDICKS K (1994) Fine structural distinction between ganglia of the outer and inner submucosal plexus in the porcine small intestine. *Acta Anatomica* **151**, 188-193.

BREHMER A, SCHRÖDL F, NEUHUBER W (1999) Morphological classifications of enteric neurons--100 years after Dogiel. *Anatomy and Embryology (Berl)* **200(2)**,125-35.

CHRISTENSEN J, RICK GA (1987) Intrinsic nerves in the mammalian colon: confirmation of the a plexus at the circular muscle-submucosa interface. *Journal of the Autonomic Nervous System* **21**, 223-231.

CROWE R, KAMM MA, BURNSTOCK G, LENNARD-JONES JE (1992) Peptide-containing neurons in different regions of the submucous plexus of human sigmoid colon. *Gastroenterology* **102**, 461-467.

DHATT N, BUCHAN AMJ (1994) Colocalization of neuropeptides with calbindin D28K and NADPH diaphorase in the enteric nerve plexuses of normal human ileum. *Gastroenterology* **107**, 680-690.

DRASCH O (1881) Beiträge zur Kenntniss des feineren Baues des Dünndarms, inbesondere über die Nerven desselben. *Sitzber. Akad. Wiss. Wien.* 82, 3rd div, 168-98.

FANG S, WU R, CHRISTENSEN J (1993) Intramucosal nerve cells in human small intestine. *Journal of Autonomic Nervous System* 44(2-3):129-36.

GABELLA G (1971) Neuron size and number in the myenteric plexus of the new-born and adult rat. *Journal of Anatomy* **109 (1)**, 81-95.

GABELLA G (1987) The number of neurons in the small intestine of mice, guinea pigs and sheep. *Neuroscience* **22(2),** 737-752.

GUNDERSEN HJG (1978) Estimators of the number of objects per area unbiased by edge effects. *Microscopica Acta* **81(2)**, 107-117.

GUNN M (1968) Histological and histochemical observations on the myenteric and submucous plexuses of mammals. *Journal of Anatomy* **102**, 223-239.

HENS J, SCHRÖDL F, BREHMER A, ADRIAENSEN D, NEUHUBER W, SCHEUERMANN DW, SCHEMANN M, TIMMERMANS J.-P (2000) Mucosal projections of enteric neurons in the porcine small intestine. *The Journal of Comparative Neurology* **421,** 429-436.

HOYLE CV, BURNSTOCK G, (1989a) Galanin-like immunoreactivity in enteric neurons of human colon. *Journal of Anatomy* **166**, 23-33.

HOYLE CHV, BURNSTOCK G (1989b) Neuronal populations in the submucous plexus of the human colon. *Journal of Anatomy* **166**, 7-22.

KARAOSMANOGLU T, AYGUN B, WADE PR, GERSHON MD (1996) Regional differences in the number of neurons in the myenteric plexus of the guinea pig small intestine and colon: an evaluation of markers used to count neurons. *The Anatomical Record* **244,** 470-480.

KRAMMER HJ, KARAHAN ST, SIGGE W, KÜHNEL W (1994) Immunohistochemistry of markers of the enteric nervous system in whole-mount preparations of the human colon. *European Journal of Pediatric Surgery* **4(5)**, 274-8.

KRAMMER H-J, KÜHNEL W (1992) Immunohistochemistry of intermediate filaments in the enteric nervous system of the porcine small intestine. *Annals of Anatomy* **174**, 275-278.

KRAMMER H-J, KÜHNEL W (1993) Topography of the enteric nervous system in the Peyer's patches of the porcine small intestine. *Cell and Tissue Research* **272**, 267-272.

KULKARNI-NARLA A, BERTZ AJ, BROWN DR (1999) Catecholaminergic, cholinergic and peptidergic innervation of the gut-associated lymphoid tissue in the porcine jejunum and ileum. *Cell and Tissue Research* **298**, 273-286.

LASSMANN G (1975) Vorkommen von Ganglienzellen im schleimhaustroma von colon, sigma und rectum. *Virchows archives A: Pathol. Anat. Histolo.* **365**, 257-261.

MANNL VA, POSPISCHIL A, DAHME E (1984) The plexus submucous (Meissner) in the calf. 1. Light and electromicroscopic study of normal structure. *Zeitblatt für Veterinarie Medizin* **A(31)**, 585-600.

MESTRES P, DIENER M, RUMMEL W (1992a) Histo- and immunocytochemical characterization of the neurons of the mucosal plexus in the rat colon. *Acta Anatomica* **143,** 268-274.

MESTRES P, DIENER M, RUMMEL W (1992b) Electron Microscopy of the mucosal plexus of the rat colon. *Acta Anatomica* **143,** 275-282.

NAIK R, BALIGA P, PAI MR, (1999) Neurogenic appendicopathy--role of enterochromaffin cells in its pathogenesis. *Indian Journal of Pathology and Microbiology* **42(3)**, 279-281.

NEWSON B, AHLMAN H, DAHLSTRÖM A, DAS GUPTA TK, NYHUS LM (1979) Are there sensory neurons in the mucosa of the mammalian gut? *Acta Physiologica Scandinavica* **105,** 521- 523.

PAPADAKI L, RODE J, DHILLON AP, DISCHE FE (1983) Fine structure of a neuroendocrine complex in the mucosa of the appendix. *Gastroenterology*. **84(3)**, 490-497.

PEARSON GT (1994) Structural organisation and neuropeptide distributions in the equine enteric nervous system: an immunohistochemical study using whole-mount preparations from the small intestine. *Cell and Tissue Research* **276**, 523-534.

PORTER A, WATTCHOW DA, BROOKES SJH, COSTA M (1999) Nitric oxide synthase and vasoactive intestinal polypeptides in the human colon: Projections of nitric oxide synthase and vasoactive polypeptide-reactive submucosal neurons in the human colon. *Journal Of Gastroenterology and Hepatology* **14**, 1180-1187.

SCHEUERMANN DW, STACH W, TIMMERMANS JP, ADRIAENSEN D, DE GROODT-LASSEEL MH (1989) Neuron-specific enolase and S-100 protein immunohistochemistry for defining the structure and topographical relationship of the different enteric nerve plexuses in the small intestine of the pig. *Cell and Tissue Research* **256(1)**, 65-75.

SCHEUERMANN DW, STACH W, TIMMERMANS J.-P (1986) Three dimensional organisation and topographical features of the myenteric plexus (Auerbach) in the porcine small intestine: Scanning electron microscopy after enzymatic digestion and Hcl-hydrolysis. *Acta Anatomica* **127**, 290-295.

SCHEUERMANN WD, STACH W, TIMMERMANS J-P (1987*a*) Topography, architecture and structure of the plexus submucosus internus (Meissner) of the porcine small intestine in scanning electron microscopy. *Acta Anatomica* **129**, 96-104.

SCHEUERMANN WD, STACH W, TIMMERMANS J-P (1987*b*) Topography, architecture and structure of the plexus submucosus externus (Schabadasch) of the porcine small intestine in the scanning electron microscopy. *Acta Anatomica* **129**, 105-115.

STACH W, (1972) Der Plexus entericus extremus des Dickdarm und seine Beziehungen zu den interstitiellen zellen (Cajal). *Z. Mikrosk.-Anat. Forsch.* **85**, 245-272.

STACH W (1977a) Neuronstruktrur und -architektur im Plexus submucosus externus (Schabadasch) des Duodenums. *Vehr. Anat. Ges.* **71**, 867-871.

STACH W (1977b) Der Plexus submucosus externus (Schabadasch) im Dünn-darm des Schweins. I. Form, Struktrur und Verbindungen der Ganglien und Nervenzellen. *Z. mikrosk.-anat. Forsch.* **91**, 737-755.

STANISZ A, SCICCHITANO R, STEAD R, MATSUDA H, TOMIOKA M, DENBURG J, BIENENSTOCK J (1987) Neuropeptides and immunity. *American Review of Respiratory Diseases* **136(6 Pt 2)**, S48-51.

STÖHR P (1934) Mikroscopische studien zur Innervation des Magen-Darmkanales III. *Z. Zellforsch mikrosk. Anat.* **21**, 243-278.

STÖHR P (1944) Mikroscopische studien zur Innervation des Magen-Darmkanales V. *Z. Zellforschung mikrosk. Anat.* **34**, 1-54.

TIMMERMANS J.-P, ADRIAENSEN D, CORNELISSEN W, SCHEUERMANN DW (1997) Structural organization and neuropeptide distribution in the mammalian enteric nervous system, with special attention to those components involved in mucosal reflexes. *Comparative Biochemistry and Physiology* **118A (2)**, 331-340.

TIMMERMANS J.-P, HENS J, ADRIAENSEN D (2001) Outer submucous plexus: An intrinsic nerve network involved in both secretory and motility processes in the intestine of large mammals and human. *The Anatomical Record* **262**, 71-78.

TIMMERMANS J.-P, SCHEUERMANN DW, STACH W, ADRIAENSEN D, DE GROODT-LASSEEL MHA (1990) Distinct distribution of CGRP-, enkephalin-, somatostatin-, substance P-, VIP- and serotonin-containing neurons in the two submucosal ganglionic neural networks of the porcine small intestine. *Cell and Tissue Research* **260**, 367-379.

VAU E (1932) Über die subglandulären Ganglienzellen in der Magenwand einiger Haussäugetiere. *Anatomischer Anzeiger* **73**, 380-385.

WEDEL T, ROBLICK U, GLEISS J, SCHIEDECK T, BRUCH HP, KÜHNEL W, KRAMMER HJ (1999) Organization of the enteric nervous system in the human colon demonstrated by

wholemount immunohistochemistry with special reference to the submucous plexus. *Annals of Anatomy* **181(4)**, 327-337.

YAMAMOTO Y, KITAMURA N, YAMADA J, ATOJI Y, SUZUKI Y, YAMASHITA T (1994) Structure of the enteric nervous system in sheep omasum as revealed by neurofilament protein-like immunoreactivity. *Journal of Anatomy* **184,** 399-405.

YOUNG HM, FURNESS JB, SEWELL P, BURCHER EF, KANDIAH CJ, (1993) Total numbers of neurons in myenteric ganglia of the guinea-pig small intestine. *Cell Tissue Research* **272(1)**,197-200.

FIGURES AND LEGENDS

Figs. 1 *a-g*. The S-100 protein, NF and SP IR in the myenteric plexus. Fig. 1a. The S-100 protein IR, distal jejunum showing complex (Gc) and large (G) ganglia, PS (P), SS (S), and type one tertiary strands (TI) (arrows). PS are oriented perpendicular to ICM. TI are mainly oriented parallel to ICM (not shown). The OLM (OL) is seen in the background. x 42. Fig.1b. S-100 protein IR, caecum showing large (G) and small (g) ganglia, primary (P), secondary (S) and type one (arrrows) tertiary nerve strands, and OLM (OL). SS are oriented parallel to ICM (IC). x 42. Fig. 1c. S-100 protein IR, colon showing complex (Gc) ganglia, primary (P), secondary (S), type I (small arrows) and type II (arrow heads) tertiary nerve strands. Type II tertiary nerve strands are oriented perpendicular to ICM shown by remnant nerves (large arrows). x 42. (Compare variation among segments in the blending and sizes of ganglia, nerve strands and orientation in Figs. 1a-c). Fig. 1d. Ileum, a higher magnification of a small ganglion. Note the shape of the S-100 protein IR neurons (arrows). They have smooth outline, are principally adendritic, pseudo-uniaxonal to multiaxonal. x 413. 1e. NF IR, caecum showing adendritic, pseudo-uniaxonal to multiaxonal IR neurons (arrows) in a ganglion and the primary (P) and secondary (S) nerve strands. x 250. Figs. 1f-g. SP IR, rectum. Fig. 1f. Shows clusters of intense, pericellular, IR varicosities around non reactive neurons (arrows) in a ganglion (G). x 103. Fig. 1f. Close up of pericellular IR varicosities around a non reactive neuron. x 413.

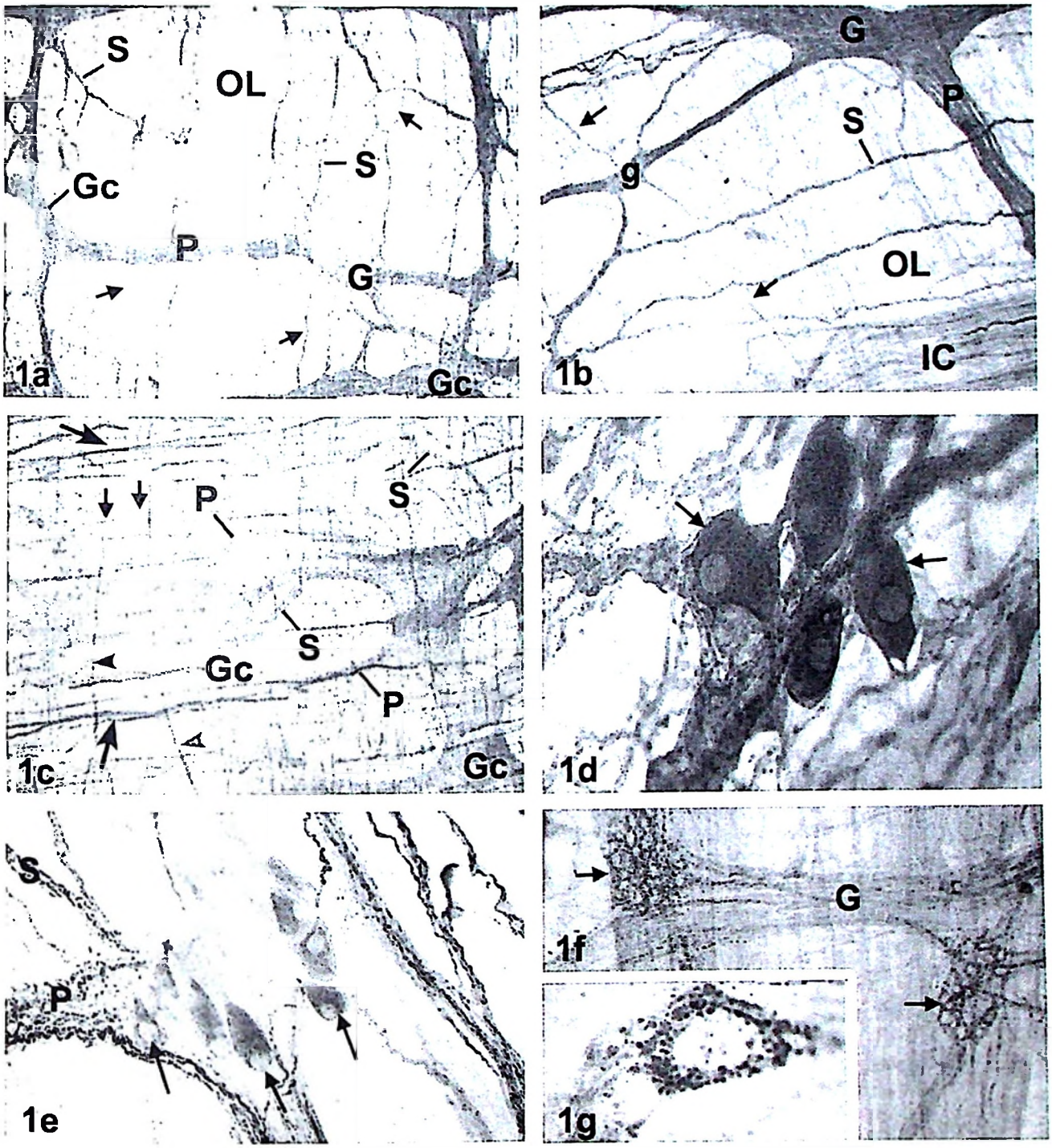
S
OL
S
Gc
P
G
Gc
1a
G
P
S
g
OL
IC
1b
P
S
S
Gc
P
Gc
1c
1d
S
P
1e
G
1f
1g

Figs. 2*a-g*. The S-100 protein, NF and SP IR in the OSP. Fig. 2a. Duodenum, S-100 protein IR viewed from the serosal side. The OSP is shown by two parallel, clearly oriented PS (P) and a part of the ganglion (Go) overlying the ISP. Large ISP ganglia (arrow heads) in the outer ISP subplexus are located close to OSP. Small ISP ganglia (arrows) in the inner ISP subplexus are located close to lamina muscularis mucosae (not shown). IC shows an area with remnant nerves of the ICM. x 42. Fig. 2b. S100 protein IR, Middle jejunum viewed from the serosal side. The inner OSP (Go) and outer ISP subplexuses (Gi) (not in focus) ganglia at different topographical levels are demarcated by the submucous vascular arcades (V). A few S-100 protein IR neurons are shown by arrows. x 103. Fig. 2c. Proximal jejunum, S100 protein IR, a large ganglion in the inner OSP subplexus, viewed from serosal side. The PS (P) emerging beneath the body of the ganglion (G) are oriented perpendicular to ICM which is shown by remnant nerves (arrows). The major axis of the ganglion, IR neurons (not in focus) and tertiary nerve strands (arrow heads) coursing into the ICM are oriented almost parallel to ICM.. x 103. Fig. 2d. Duodenum, S-100 protein IR. A small, polygonal OSP ganglion (G) in the outer OSP subplexus located very close to the ICM (IC). Tertiary nerve strand (arrow heads) course in the same direction as nerve fibres in the ICM to innervate ICM. A tortuous secondary nerve strand in the inner OSP subplexus is shown by an arrow. x 103. Fig. 2e. Middle jejunum, S-100 protein IR, a close up of a large ganglion of the inner OSP subplexus showing ovoid, smooth outlined, adendritic, type II neurons (arrows). x 400. Fig. 2f. Caecum, showing many SP IR neurons in two polygonal outer ISP ganglia (Gi) located close to a large, elongated inner OSP subplexus ganglion (Go) with abundant SP IR varicosities but, few IR neurons (arrow). x 103. 2g. Colon, NF IR in the inner OSP subplexus ganglion (G) showing many, intense, elongated, smooth outlined adendritic, pseudo-uniaxonal to multiaxonal type II IR neurons (arrows). x 400. Compare sizes of the OSP ganglia in Figs. 2b-d; f.

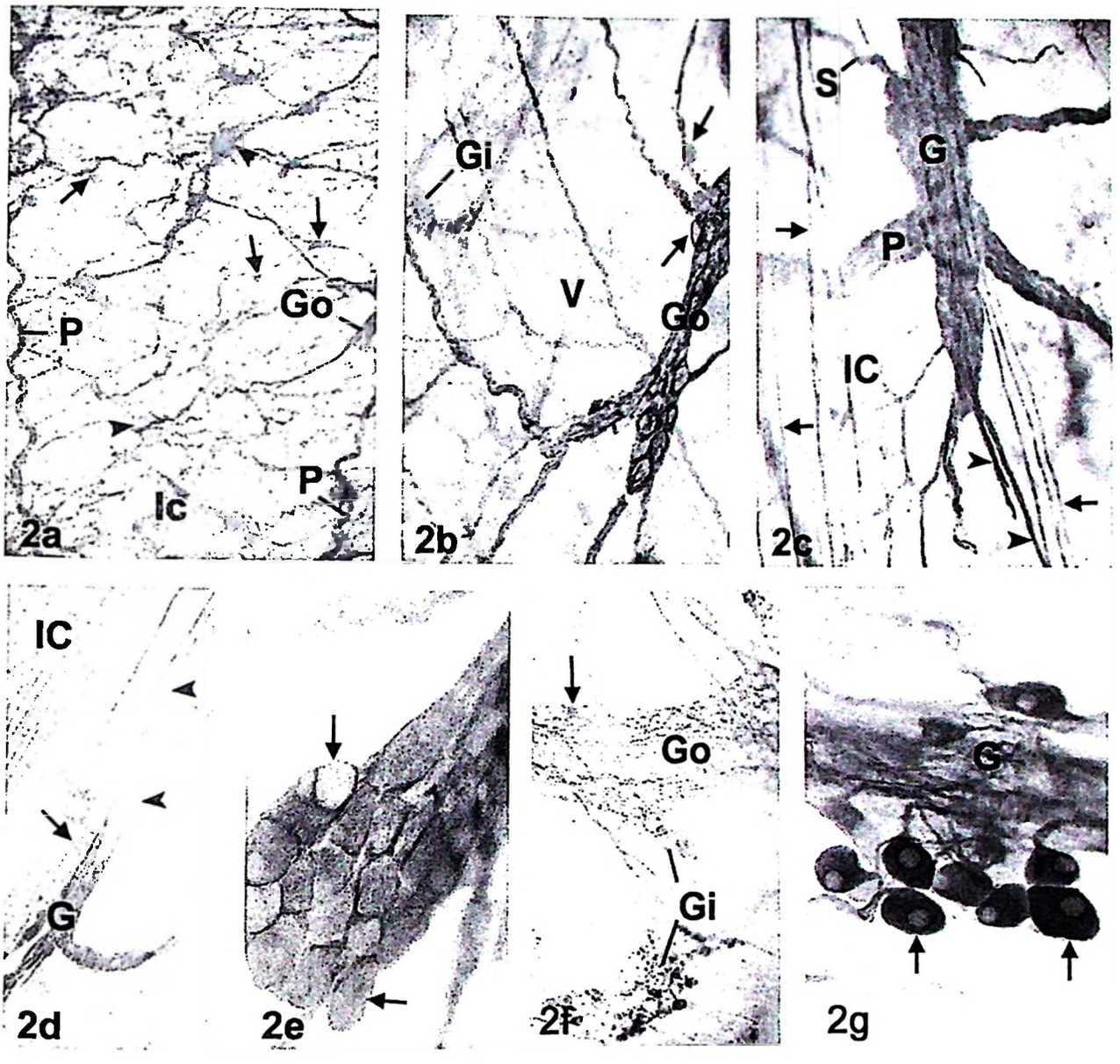
P
Go
P
Ic
2a
Gi
V
Go
2b
S
G
P
IC
2c
IC
G
2d
2e
Go
Gi
2f
G
2g

Figs. 3a-f. The S-100 protein, NF, SP and VIP IR in the ISP. Fig. 3a. Proximal jejunum, S-100 protein IR. Notice the density of the meshwork of ganglia (G) and nerve strands variation in the size and shape of ganglia, and lack of specified orientation. x 103. Fig. 3b. Duodenum, S-100 protein IR, showing a complex ganglion (Gc), PS (P), SS (S) and IR neuron (arrow). x 206. Fig. 3c. Duodenum, close up of a rounded S-100 protein IR neuron in the ISP. x 413. Fig. 3d. Middle jejunum, S-100 protein IR, showing an outer ISP subplexus ganglion viewed from the serosal side, IR neurons (small arrow) and enteric glia cells (large arrows), a vessel (V) is overlying the PS (P) and a Schwann cell (arrow head) in the perivascular plexus. x 413. Fig. 3e. Rectum, S-100 protein IR in the ISP focussed from the luminal side. Two small ISP ganglia (g) in the inner ISP subplexus are overlying two large ganglia (G) in outer ISP subplexus. The submucous vascular arcade is labelled V. x 206. Fig.3f. Caecum, VIP IR in the ISP ganglia (G) and nerve strands. Notice absence of the IR neurons. x 100.

Figs. 4*a- l*. S-100 protein, NF, SP and VIP IR in the mucous plexus in wholemounts and sections. Only sections will be mentioned in the text. Fig. 4a. Caecum, S-100 protein IR showing an isolated neuron (arrow) in the LMMP and Schwann cells (arrow heads). x 403. Fig. 4b. Middle jejunum, S-100 protein IR in the ganglia (G) and an isolated neuron (arrow) in the OPP in the subglandular region. x 206. 4c-d. Ileum, S-100 protein IR. Fig. 4c. Notice IR in a ganglion (G) and IR neurons (arrow) in the OPP. (C) show intestinal crypts. x 206. Fig. 4d. Paraffin section of the wholemount in Fig. 4c counter stained by H & E showing a ganglion (G) and isolated neurons (arrows) in the interglandular proprial plexus (IGPP). (C) show intestinal crypts. x 413.

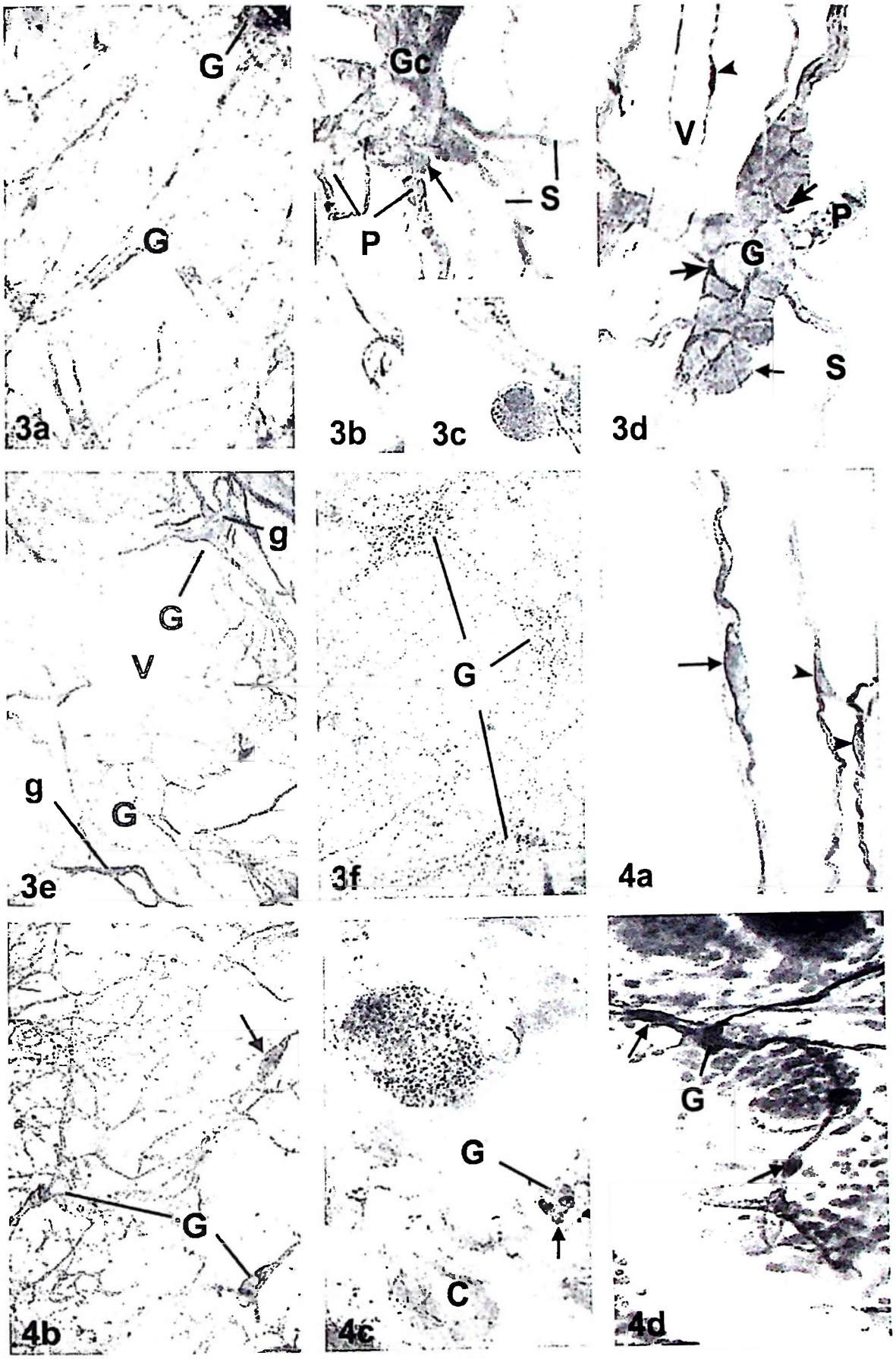
G
G
3a
Gc
P
S
3b
3c
V
P
G
S
3d
g
G
V
g
G
3e
G
3f
4a
G
G
4b
G
C
4c
G
4d

Fig. 4e-f. Caecum, S-100 protein IR. Fig. 4e. Notice IR in an elongated ganglion (G), a complex ganglion (Gc) , PS (P) and other strands in the OPP. Intestinal crypts (C) are very lightly stained. x 206. Fig. 4f. Paraffin section cut from a wholemount in Fig. 4e and counter stained by H & E. Notice two small ganglia (G) and IR neurons (arrows) in IGPP. (C) show intestinal crypts. x 403. Fig. 4g. Caecum, VIP IR in nerve strands (small arrows) and one isolated IR neuron (large arrow) in a node in the OPP. (C) show intestinal crypts. x 200. Fig. 4h. Colon, S100 protein IR in the ganglia (G) and an isolated neuron (arrow) in the OPP. Intestinal crypts (C) are very lightly stained. x 206. Fig. 4i. Rectum, S-100 protein IR, showing a ganglion (G) in the OPP immediately underlying the LMM which is revealed by nerve fibres (arrows). (C) shows crypts. x 206. Fig. 4j. Distal jejunum showing dense SP IR (arrow) in the dome in a lymphoid follicle. x 206. Fig. 4k. Distal jejunum, showing S-100 protein IR in the villous plexus (arrows). x 206. 4l. Duodenum, paraffin section from mucosal wholemount which was stained for S-100 protein IR counter stained by H & E showing an isolated neuron (arrow) in the IGPP. C, shows part of an intestinal crypt. x 1030.

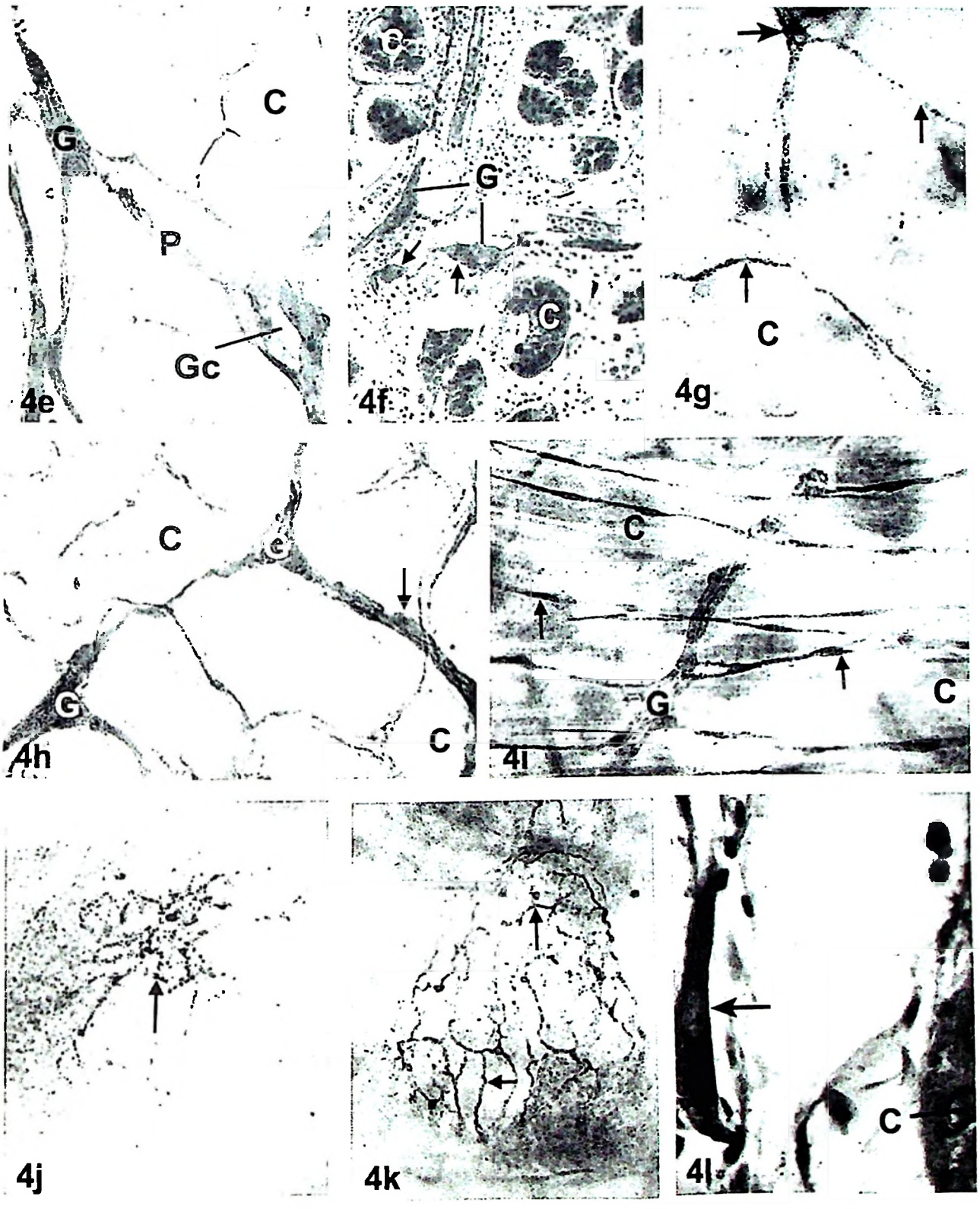
C
G
P
Gc
4e
G
C
4f
C
4g
C
G
C
4h
G
C
4i
4j
4k
4l
C

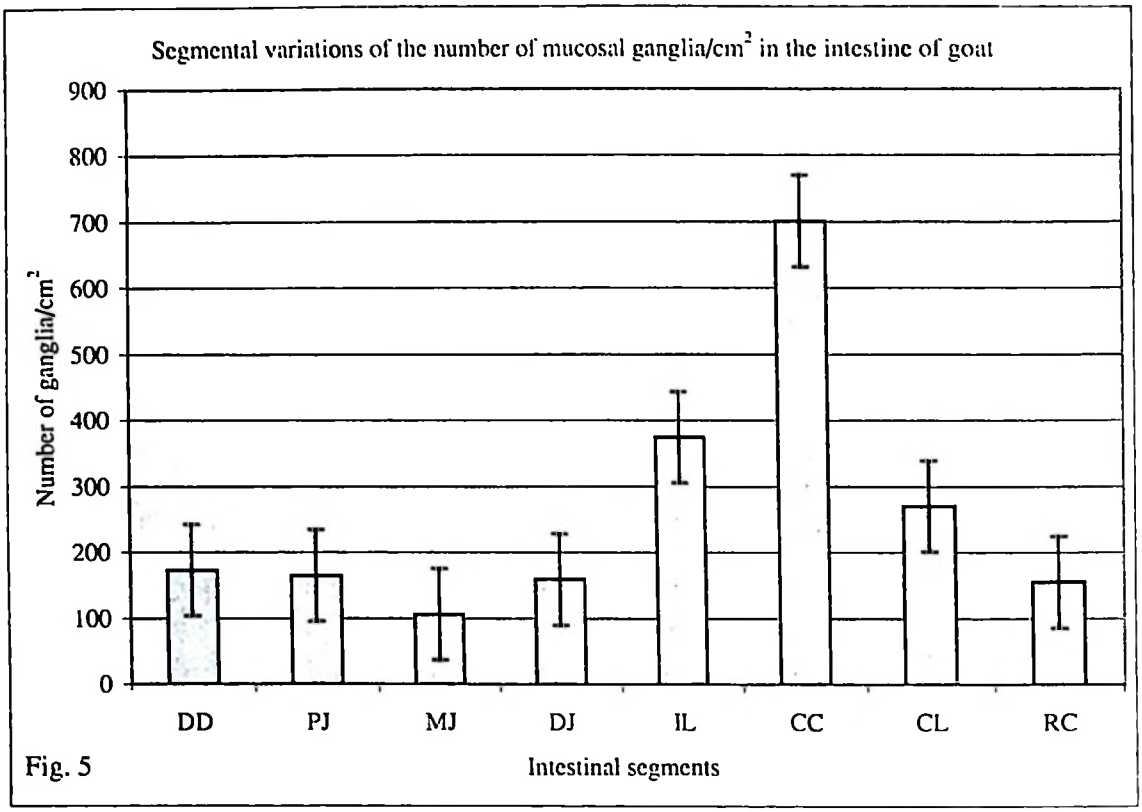

Fig. 5

The differences between caecum and the rest were highly significant. *** P<0.(X)1

The differences between caecum, ileum and colon and the rest were highly significant. *** P<0.(X)1

The differences between ileum and colon, and between both ileum and colon,

and the rest were highly significant. *** P<0.001

The differences between middle and distal jejunum and colon and the rest were highly significant. *** P<0.(X)1

The differences between proximal and middle jejunum and rectum as well as between

proximal and middle jejunum, distal and middle jejunum were significant . ** P<0.05

The differences between duodenum, proximal and distal jejunum, and rectum were not significant. P> 0.05

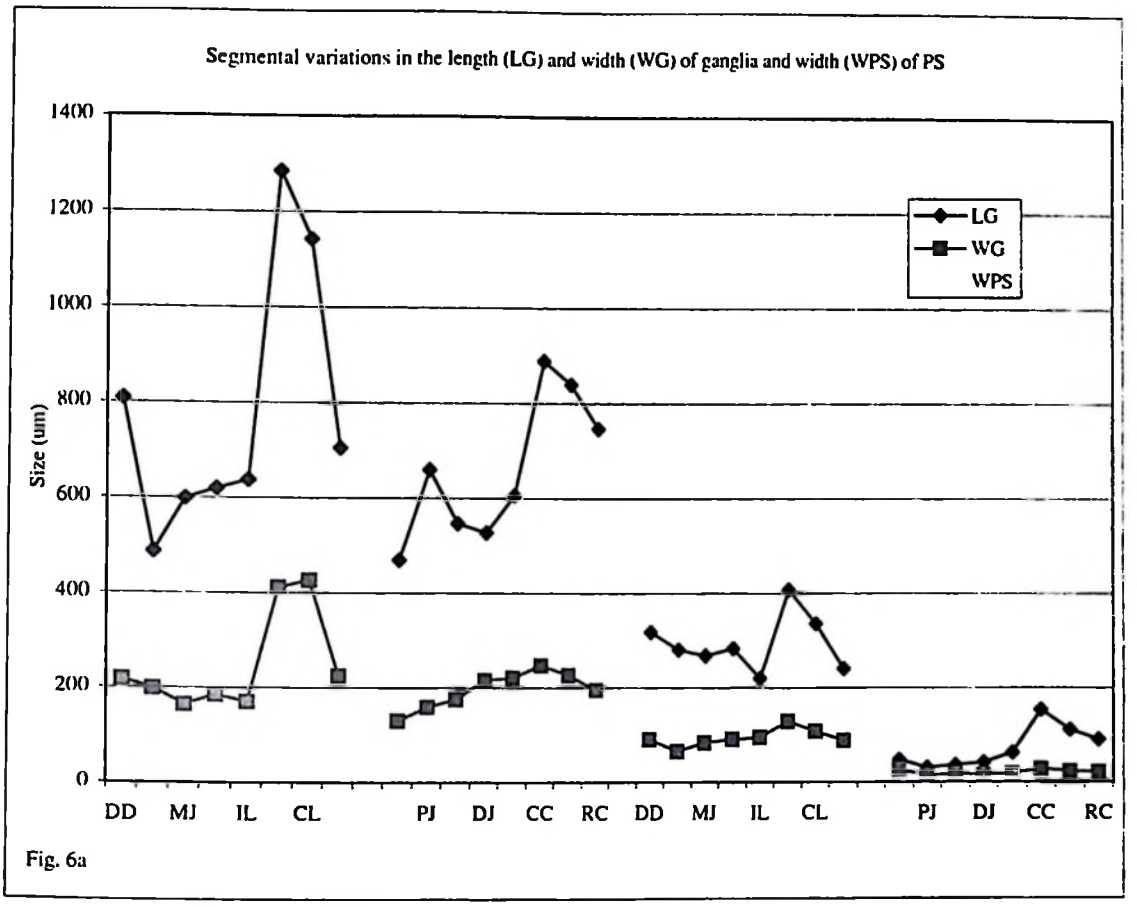
Segmental variations in the length (LG) and width (WG) of ganglia and width (WPS) of PS
1400
1200
1000
800
600
400
200
0
Size (um)
LG
WG
WPS
DD MJ IL CL PJ DJ CC RC DD MJ IL CL PJ DJ CC RC

Fig. 6a

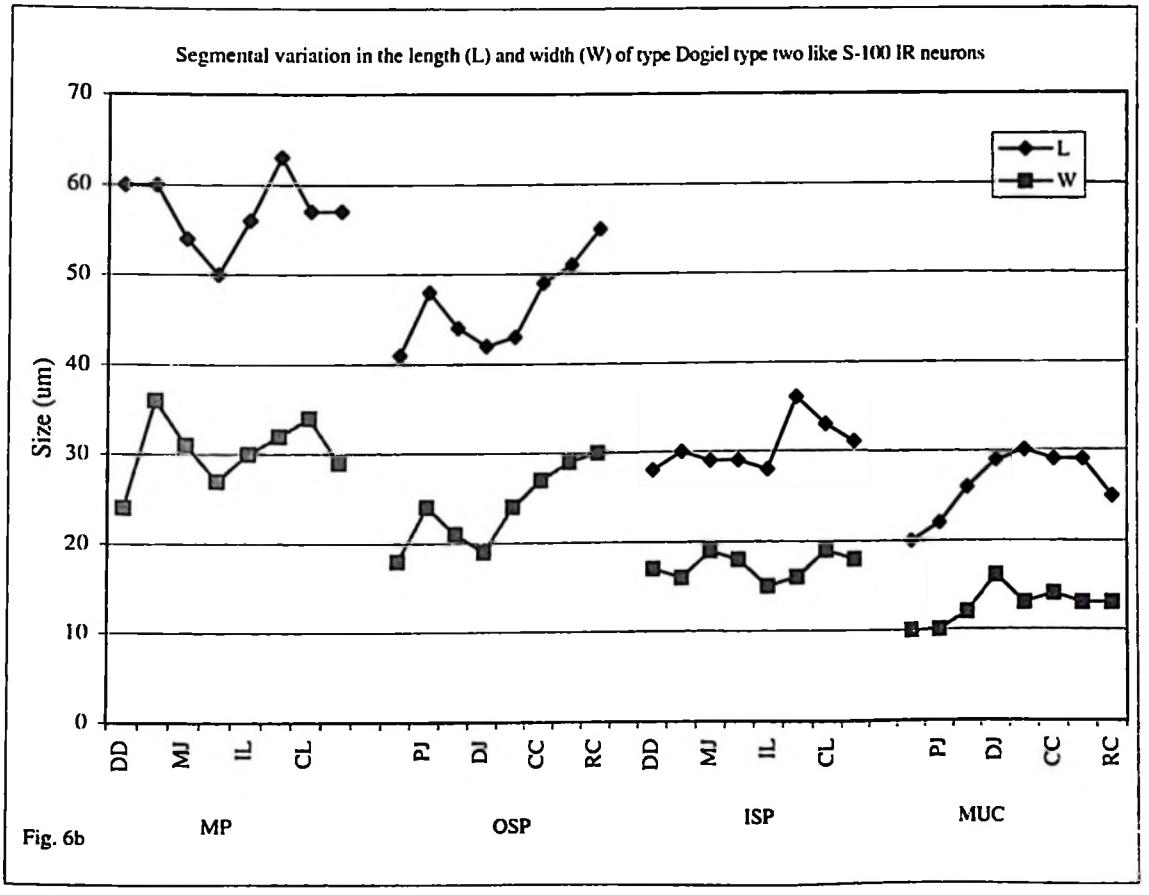
Segmental variation in the length (L) and width (W) of type Dogiel type two like S-100 IR neurons
70
60
50
40
30
20
10
0
Size (um)
L
W
DD MJ IL CL PJ DJ CC RC DD MJ IL CL PJ DJ CC RC
MP
OSP
ISP
MUC

Fig. 6b

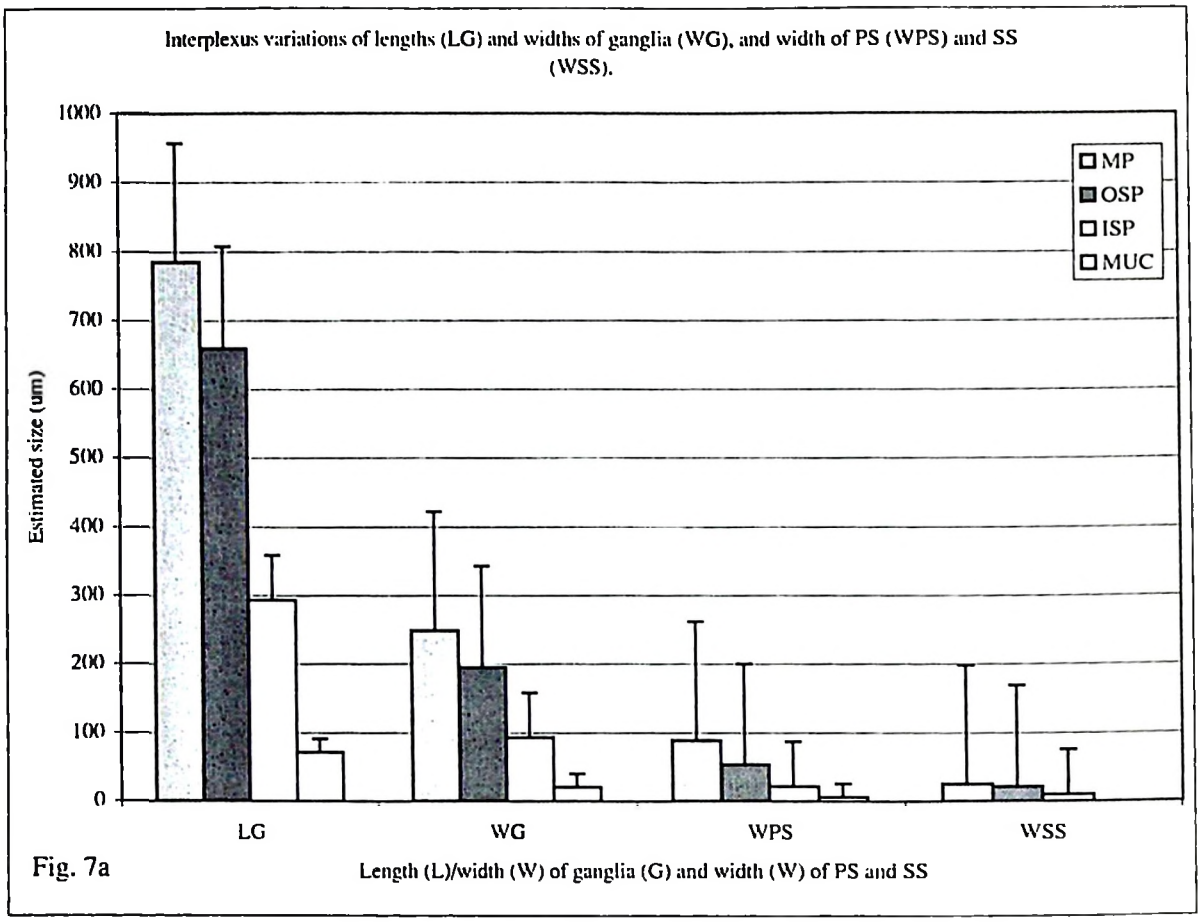
Interplexus variations of lengths (LG) and widths of ganglia (WG), and width of PS (WPS) and SS (WSS).
Estimated size (um)
1000
900
800
700
600
500
400
300
200
100
0
MP
OSP
ISP
MUC
LG
WG
WPS
WSS
Length (L)/width (W) of ganglia (G) and width (W) of PS and SS

Fig. 7a

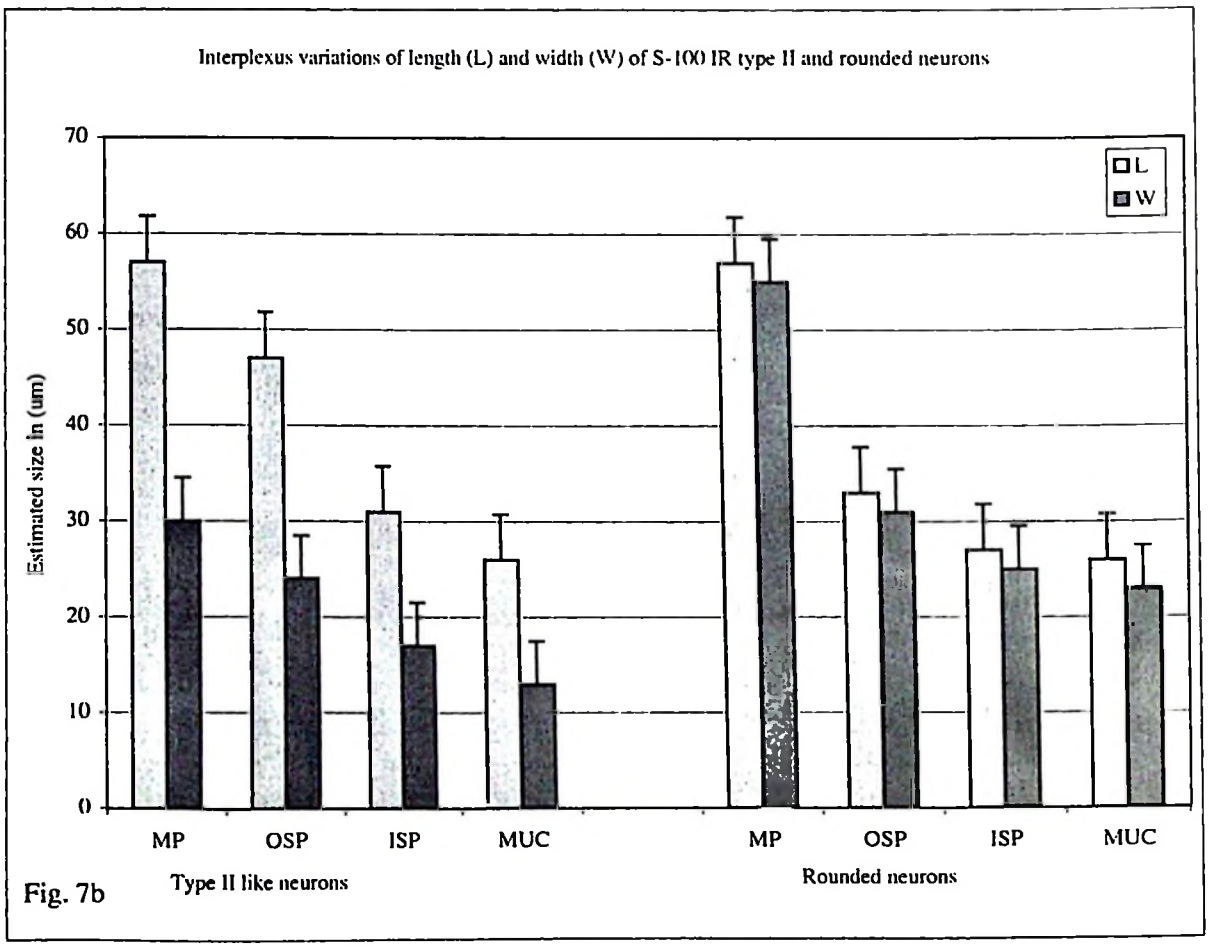
Interplexus variations of length (L) and width (W) of S-100 IR type II and rounded neurons
Estimated size in (um)
70
60
50
40
30
20
10
0
L
W
MP
OSP
ISP
MUC
MP
OSP
ISP
MUC
Type II like neurons
Rounded neurons

Fig. 7b

Paper IV

A very simple and efficient stereological sampling scheme for large mammalian gut, with estimation of the total number of specific neurons in distinct plexuses using unbiased principles.

OB Balemba[1], A Hay-Schmidt[2], V Dantzer[3], HJG Gundersen[4]

Addresses:

[1]*Department of Veterinary Anatomy, Sokoine University of Agriculture, Morogoro, Tanzania.* [2]*Institute of Anatomy, Panum Building, Copenhagen University,* [3]*Department of Anatomy and Physiology, The Royal Veterinary and Agricultural University Copenhagen.* [4]*Stereological Research Laboratory, University of Aarhus, Denmark.*

Address for correspondence:

Dr. Vet. Sci. Vibeke Dantzer

Institute for Anatomy and Physiology, RVAU, Grønnegårdsvej 7, 1870 Frederiksberg C, Copenhagen, Denmark. Tel: 4535282543; Fax 4535282547;

E-mail: Vibeke.Dantzer@iaf.kvl.dk

Abstract

Background—There are many studies providing numerical densities of specific enteric neurons in various parts of the gut, their variations among plexuses and during ageing, inflammatory bowel diseases and other disorders in the gut. A more meaningful measure of local specific innervation is the absolute (total) number of specific neurons in a unit length of gut. But, studies of the total number of neurons are scarce and were mostly done by using distended organs without properly randomised sampling.

Aim— To establish a simple and efficient stereological sampling scheme for estimation of the total number of specific neurons in the enteric plexuses as well as enterochromaffin (EC) cells and Peyer's patches in a large mammal using unbiased principles.

Methods—Jejunum from three male, 8 weeks old pigs were freed from the mesentery and their lengths measured. Each organ was uniformly randomly sampled into sub-samples of known dimensions and ultimately dissected into mucosal, submucosal and myenteric plexuses. Neurons were studied by nitric oxide synthase (NOS) and vasoactive intestinal peptide (VIP), and EC cells were studied by 5-hydroxytryptamine (5-HT) immunohistochemistry respectively. A set of fields of vision selected by systematic randomly X- and Y-step lengths using a low-tech stepping device were projected onto a table using an ordinary Leica DMLB microscope fitted with a projection arm. In each field of vision, a set of predetermined counting frames in a grid fixed on the table, were used to systematically randomly sample and count neurons and EC cells using the optical fractionator. The surface area of Peyer's patches was measured by superposing the unbiased point sampling grid and counting points hitting the Peyer's patches and the whole tissue. The total number of neurons and EC cells and the surface area of Peyer's patches were computed based on the known sampling fractions.

Results—In the jejunum of the pig, the total number of NOS IR neurons was 11.2×10^6, 1.84×10^6 and 6.79×10^6 in the myenteric, outer submucous and inner submucous plexuses respectively. The total number of VIP IR neurons was 17.4×10^6, 1.15×10^6, 48×10^6 and 1.82×10^6 in the myenteric, outer submucous, inner submucous and mucous plexuses respectively. The total number of EC cells was 3.038×10^9 and the surface area of the Peyer's patches was 403.725 cm^2.

Conclusions—The simple and cheap sampling scheme described here, suffices most quantitative aspects in the gut such as total number and area profiles of ganglia, neurons, neuroendocrine cells as well other epithelial cells, and nerve length density and the extent of the territory of enervation. Such information is important to understand differences between various plexuses, morphogenesis, neuroplasticity and the interaction between the nervous and target tissues.

Key Words: *Sampling scheme, stereology, fractionator, VIP, NOS, 5-HT, enteric nervous system, enterochromaffin cells, Peyer's patches, jejunum, gut, pig.*

Introduction

There have been many studies in which ganglia, neurons, neuronal and nuclear profiles, nerve length density in the enteric plexuses of various compartments, in different animals were quantified (See, Tables 1, 2, 3; Brehmer et al., 1996; Liberti et al., 1998; Yunker et al., 1999; Xiong et al., 2000; Fregonesi et al., 2001). However, there are very few reports dealing with the absolute (total) number of neurons in the gut (Table 1). Studies of the total number of neurons in a well defined part of the gut have appeared in the guinea pig (Karaosmanoglu et al., 1996) and in the pig duodenum (Van Ginneken et al., 1998). The majority of previous studies were aimed at determining either the numerical density expressed as neurons/cm^2 of serosal surface area of the gut or as neurons/cm^2 of ganglion area or area profiles of specific neurochemically defined neurons in specified plexuses during normal, ageing and pathological conditions (Tables 2). In many other studies neurons were counted in the ganglia and presented in percentages relative to total counts or numerical density (number/cm^2) using the established ganglia density/cm^2 (Furness et al., 1984; Young et al., 1993; Furness et al., 1994; Burns and Cummings, 1993; Brehmer and Stach, 1998). Estimation was done using fully distended compartments or stretched wholemounts. Neuronal packing density expressed in terms of number of neurons per cm^2 of stretched serosal surface area is greatly influenced by how much the wall is stretched during the preparation (Gabella, 1987; Karaosmanoglu et al., 1996). Stretching of tissues from human colon increased their lengths by up to 200% (Wedel et al., 1999). In the human colon and small intestine, it increased serosal surface area by 32% and reduced the numerical density by 19% to 31% (Karaosmanoglu et al., 1996).

Different methods were used to count neurons in order to establish both the total number (Gabella, 1971, 1987, 1989; Ali and McLelland, 1979; Karaosmanoglu et al., 1996; Van Ginneken et al., 1998) and densities (Timmermans et al., 1990; Young et al., 1993; de Souza et al., 1993; Meciano-Filho et al., 1995) of enteric neurons. The technique that was used widely in the past, was that of counting on photographic montages while checking cell by cell in the original preparation under the microscope (Gabella, 1971, 1987, 1989). Ali and McLelland, (1979) counted all nicotinamide adenine dinucleotide phosphatase-diaphorase stained neurons in each wholemount from the chicken gut by using a light microscope. Karaosmanoglu et al. (1996) used computerised stereological software and a video camera attached to a microscope to project images at 40X onto a 512 by 480 pixel array to estimate the total number and the density of neurons in the colon and small intestine of guinea pig. Measurements were obtained from 30

non-overlapping rectangular windows (0.052mm^2) projected onto each specimen. The outline of each ganglion was traced with a cursor and the areas of these ganglia were computed. All neurons in all focal planes in each of the measuring windows were traced and counted.

Apparently, the vast majority of the previous studies suffer from several limitations. (a) Sampling of tissues was biased to specific sites within the specified compartments. Sampling was not randomised either while sampling tissues from animals or during counting or both (Gabella, 1971, 1987, 1989; Karaosmanoglu et al., 1996). (b) Samples were obtained from distended organs and measurements of sizes of organs and tissues to obtain serosal surface areas were done mostly after distension and fixation of tissues. The influence of stretching and shrinkage during fixation and subsequent procedures were not considered. (c) The majority of studies were done on the myenteric plexus of smaller mammals and were limited to short segments (Tables 1, 2, 3). Variations along the oral-aboral axis such as those reported between the oesophagus, stomach, duodenum, ileum and distal colon (Furness et al., 1994), duodenum and ileum (Karaosmanoglu et al., 1996) in the guinea pig and the small intestine in the pig (Brehmer and Stach, 1998) were not considered. Variations along and the mesenteric-antimesenteric axis (Table 3) were also not considered. (d) Numerical densities (neurons/cm^2 referred to serosal surface area or ganglion area) or percentages per total number of neurons in the ganglia and can only be referred to specific tissue preparations. (e) Data from different laboratories can hardly be compared (Table 2). (f) Counting in tissues has been time consuming and in some studies not randomised.

The counting of EC cells (Krause et al., 1984; Rantala et al., 1996; Oshima et al., 1999) and morphometry of Peyer's patches (Chu and Liu, 1984; Barman et al., 1997) are usually done by using paraffin sections and have had limitations.

A more meaningful measure of local specific innervation for drawing biological conclusions regarding the functional capacity might therefore be the absolute (total) number of specific neurons/neuroendocrine cells per unit length of intact gut.

A sound morphometric analysis must be founded on unbiased efficient systematic sampling design (Gundersen and Jensen, 1987; Howard and Reed, 1998). The fractionator is the simplest and the most powerful sterological sampling scheme which is based upon uniform random sampling with a known and predetermined probability. The total number in the reference space is derived from the number in the sample and the sampling probability (Gundersen, 1986). A three dimensional (3-D) probe, the optical disector is beneficial and efficient to count differentially stained cells in semi-transparent volumes (Gundersen, 1986; Gundersen et al., 1988). Attempts to count the total number of neurons in the enteric nerve plexuses have been limited by lack of a stain that could virtually specifically stain all the neurons (Karaosmanoglu et

al., 1996). Therefore, the axiom of the present study was to establish a simple, cheap and efficient stereological sampling scheme for estimation of the total number of specific neurons in a distinct plexus, the total number of EC cells and the surface area of Peyer's patches in the jejunum of a large mammal using unbiased principles.

Materials and methods

ANIMALS, SAMPLING AND STAINING

Three, male, Danish Landrace/Yorkshire crossbred, 8 week, fully weaned (13-15 kg) pigs were used in the present study. The animals were euthanised by captive bolt pistol and exsanguination. Immediately after death, the stomach and intestine were exposed. The jejunum was defined from the aboral end of the duodeno-colica ligament (ligament of Treitz) to the oral end of the ileo-caecal-colical ligament, at which points is was ligated and cut free from the rest of the intestine. It was carefully and gently freed from the mesentery very close to the mesenteric attachment so as to get rid of folds. The freed part was always kept into cold (4°C) 0.1M phosphate buffered saline (PBS) (pH 7.3).

The total length of jejunum, ***L(jej)*** was estimated using 1metre ruler. The total number, ***n(ps)*** = 7, the length, ***l(ps)*** = 15 cm of primary samples ***(ps)*** and therefore the sampling period, ***period(ps)*** = ***L(jej)/n(ps)*** were fixed. The number of samples ***n(ps)*** = 7 was considered to be sufficient to represent the jejunum. The length ***l(ps)*** = 15 cm was chosen because it allows a reasonably precise estimate of the area of Peyer's patches. With a uniform random start, ***rand***, looked up in a table of random numbers, in the first ***period(ps)***, the ***n(ps)*** primary samples of length ***l(ps)*** were cut from the gut (Fig. 1).

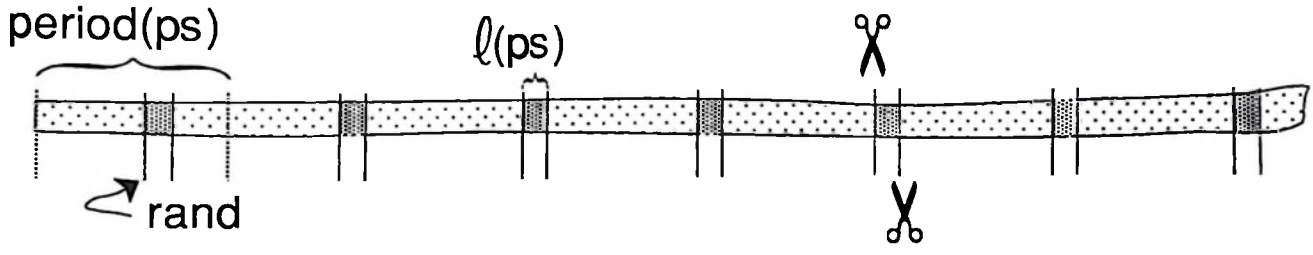

Fig. 1. Schematic drawing (not to scale) showing the uniformly random sampling of a fixed number of primary samples from a whole, unopened jejunum.

Each primary sample was cut open along the mesenteric attachment and washed thoroughly in cold (4 °C) PBS. The orientations of primary samples and subsequent sub-samples were always marked by pinning the oral and aboral ends by using pins with different colours. Each primary sample was spread out on a wax plate with the mucosal surface up, and the exact dimensions of each piece ***l(ps)*** and ***w(ps)*** (Fig. 2) were measured. The secondary sample ***(ss)*** (3

cm long) was cut from a random end (selected by tossing a coin) from each of the ***n(ps)*** primary samples (Fig. 2).

The set of secondarily sampled pieces constituted a sampling fraction of $f_1 = 3$ ***cm/period(ps)*** of the whole jejunum.

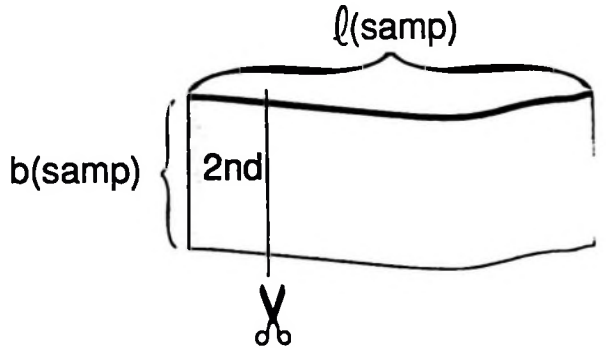

Fig. 2. The predetermined length of one primarily sampled piece, ***l(ps)***, and the local width, ***w(ps)***, of the jejunum is indicated. The secondary sample ***(ss)*** was cut from a random end of all primarily sampled pieces. The heavy line at the top shows the mesenteric attachment. (An improved sampling scheme is shown in Fig. 2.5).

Each secondary sample was washed thoroughly in cold PBS, spread out gently on polystyrene plastic, mucosal surface up, and its length and width were measured. Each secondary sample had precise dimensions ***w(ss)*** by ***l(ss)*** and area $a(ss) = w(ss) \times l(ss)$. The primary and the secondary samples shared one dimension: $w(ps) = w(ss)$ (Figs. 2; 3a). The area for cutting a tertiary sample ***(ts)*** was randomly selected with respect to the oral-aboral as well as mesenteric anti-mesenteric positions by tossing a coin twice. Thereafter, two pins with different colours were as close as possible, fixed to the randomly selected mesenteric edge with an interval of ~ 1.2 cm in between them. Another set of pins with matching colours was fixed on the opposite side slightly beyond the oral-aboral midline axis (Fig. 3, left). The exact dimensions of each selected unstretched ***ts*** sample were measured. The unstretched ***ts*** had dimensions ***w(ts)*** by ***l(ts)*** and an area $a(ts) = w(ts) \times l(ts)$.

Thus the tertiary samples constituted a fraction of $f_2 = a(ts)/a(ss)$ of the secondary samples.

The tertiary sample was carefully and gently stretched maximally upon the same polystyrene while taking care to retain the pins in their original positions in the tissues. Stretched tissues (Fig. 3, right) were fixed in 4.5% buffered formaldehyde for 1 hr, freed from polystyrene while keeping the pins marking the specific orientation, transferred into fresh 4.5% buffered formaldehyde where they were fixed for 47 hrs at 4 °C.

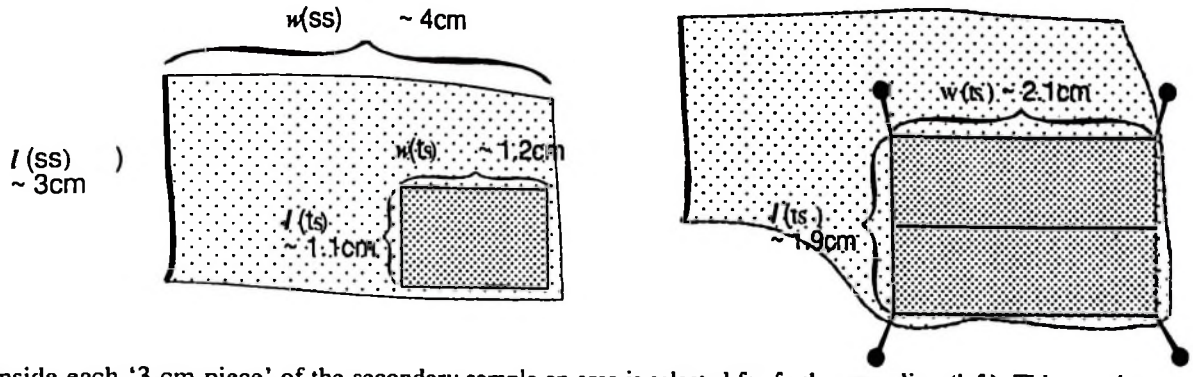

Fig. 3. Inside each '3 cm-piece' of the secondary sample an area is selected for further sampling (left). This area is stretched by pins on a polystyrene (right), fixed and subsequently split along the mesenteric-antimesenteric axis into two approximately equal pieces, each of which is dissected into 3 wholemounts.

Tertiary samples were washed 3 x 20 minutes each in PBS, cut perpendicular to the mesenteric-antimesenteric axis into two, equal quarternally samples *(qs)* (Fig. 3 right) each, and dissected to obtain the mucous, submucous and myenteric plexuses (Figs. 6; 7a-g) using the method described by Pearson (1994) and Balemba et al. (1998).

Therefore, each wholemount constituted a fraction of $f_3 = ½$ of the unstretched tissue, described above.

Wholemounts were stored in 2 ml of 0.01M PBS (pH 7.3) containing 0.1% sodium azide and 0.5% triton X-100 in plastic tubes at 4 °C. Prior to staining, tissues were washed 3 x 20 min. each in 0.01M PBS containing 0.5% Triton X-100 and thereafter overnight at 4 °C. In the mucosal wholemounts (Figs. 7c-e), VIP and 5-HT immunohistochemistry was used to study the mucous plexus and EC cells respectively. The outer submucous (OSP) and inner submucous (ISP) plexuses in the submucous wholemount and the myenteric (MP) plexus were studied by VIP and NOS immunohistochemistry (Figs. 7a-b; 7f-g; 8a-l). For each plexus, the two wholemounts prepared from each of the tertiary sample were randomly assigned (tossing a coin) to the two specific immuno-stains in the two groups above. The staining for VIP, NOS and 5-HT IR was done by the two step indirect streptavidin-ABComplex/Horse radish peroxidase immunoenzymatic method described by Balemba et al. (1998). The specificity of staining was controlled by substituting the primary and secondary antibodies, and streptavidin-ABComplex/HRP by 5% non-immune (swine or rabbit) serum. Monoclonal rabbit anti-swine VIP (1:1400) (VIP 8084-4) was kindly donated by Dr. J. Fahrenkrug of Bispebjerg, Hospital, Copenhagen, Denmark. The polyclonal rabbit anti-rat cerebellar NOS (B220-1) and monoclonal mouse anti-5-HT (M0758) were obtained from Eurodiagnostica, Sweden and Dako, Denmark respectively. Tissues were dehydrated using methanol and isopropanol, cleared in 1,2,3,4-tetrahydroxynapthalene (Aldrich, Germany) and benzylbenzoate (Merck, Germany) as described by Balemba et al. (1998). All tissues were mounted in DPX (Poole, UK). Mucosal wholemounts were mounted serosal surface up. During staining and dehydration for mounting, wholemounts

shrunk and end up with a combined area of $a(2\times who)$, the total area of the two wholemounts. The area shrinkage from unfixed, unstretched gut to fixed, stretched, processed, and stained wholemounts was $shr = 1 - a(2\times who)/a(ts)$.

COUNTING NEURONS AND EC CELLS

Tissues were studied using a Leica DMLB microscope fitted with a projection arm at 20X objective (333X final magnification). Using the sampling device for 2D systematic, uniformly random sampling, a set of fields of vision were examined under projection onto the unbiased sampling grid fixed on the table (Fig. 5a). Using the 'devices' shown in Figs. 5a-b, the basic units for stepping, Δx and Δy, were fixed (but, one is free to select an integer number of units for each wholemount: $dx = i\Delta x$ and $dy = j\Delta y$, where i and j are two integers). The **X**- and **Y**-step lengths were dx and dy, respectively (Fig. 4, left). The corresponding area of sampling for each field was $a(sam) = dx \times dy$. The counting was done using the unbiased counting frame (Gundersen, 1978). With a random start, the projected image was systematically randomly sampled using a predetermined fraction *(fra)* (a set of uniformly distributed small frames shown by dotted frames in Fig. 4 (right) of the large sampling frame. The step lengths dx and dy, and the fraction of the larger frame *(fra)* to be used for counting were predetermined for each wholemount aiming at obtaining a sample of 10 to 15 neurons/EC cells in all of fields of vision *(F)*.

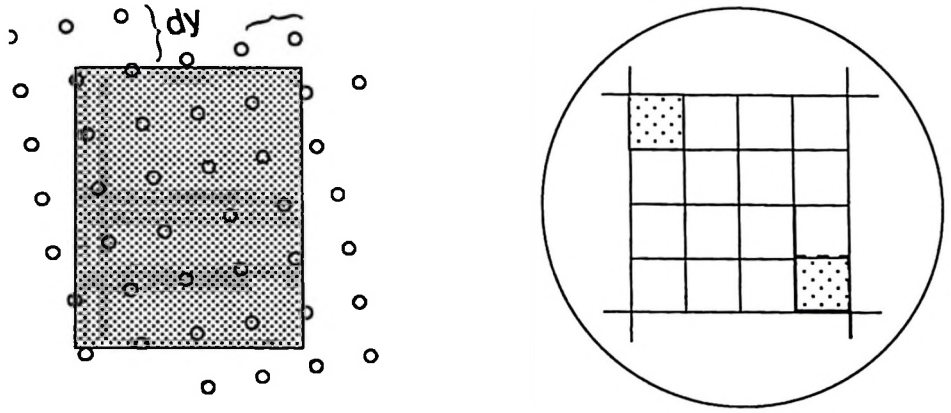

Fig. 4. Schematic (not to scale) drawing showing (to the left) systematic, uniformly random 2D sampling with a 2D period of $a(sam) = dx \times dy$ using an ordinary microscope fitted with a low-tech stepping device at the mechanical stage arm (Figs. 5a-b). In each field of vision (shown to the right), a set of small counting frames was fixed; a predetermined fraction of them *(fra)* (hatched) was used for counting using the optical fractionator (Fig. 7g). Each frame was used as an unbiased sampling frame: neurons completely inside and those only intersecting the dashed 'inclusion' edges were sampled, provided they in no way intersected the full-drawn 'exclusion' edges and their extensions. The four corners of the grid (complete set of frames) were used for counting hits on the tissue.

The counting rules were: a) An IR neuron cell was considered for counting when displayed a brown stained perikaryon and unambiguously visible nucleus. b) The IR neurons completely or

partly inside the frame (Fig. 7g) were counted provided their perikarya did not intersect the fully drawn exclusion zone(s) in any way. c) Similarly, EC cells completely or partly inside the counting frames were counted provided their cytoplasm did not intersected the fully drawn exclusion zone(s) in any way. However, similar to neuronal axons and dendrites, cytoplasmic extensions of the open type EC cells were disregarded in the counting rule.

In each field of vision, the counting frame was focused through the wholemount (Z-axis) so that all neurons/EC within the frames counted. In each field of vision, the number of the 4 corners ***p(cor)*** of the sampling grid which hit tissue were noted. The total area of the set of small frames used were ***a(fra)***.

The final sampling fraction of neurons/EC cells in the wholemount was thus f_4 = ***a(fra)/a(sam)***.

The unbiased estimate of the total number of specific neurons in each plexus and EC cells in mucosal wholemounts (N) were based on the simple total 3D count, ΣQ, of sampled neurons/EC cells obtained from the 7 primary samples:

$$N := (1/f_1)(1/f_2)(1/f_3)(1/f_4)\Sigma Q \qquad (1)$$

ESTIMATION OF THE AREA OF PEYER'S PATCHES

Tissue segments that remained after cutting the 3 cm *ss* from each of the primary sample ***(ps)*** above were kept in 0.01M PBS at 4 °C overnight. Thereafter, they were washed in PBS to free the mucous from mucosal surface. Each sample was spread out on a wax plate mucosal surface up.

The spread jejunal sample ***(js)*** had dimensions ***w(ps)*** by ***l(ps)-3 cm*** and an area ***A(js)*** = ***w(ps)*** $\times$ ***l(ps -3 cm*** and constituted a fraction of ***f(js) = l(ps)-3 cm /period (sample)***.

The total area of the 7 jejunal samples was $\Sigma A(js)$.

The unbiased quadratic (2D) point-sampling grid (Gundersen et al., 1988; Howard and Reed, 1998) slightly larger than the tissue was superimposed over the tissue (Figs. 9a-b). With a random start and an inter-point ***dx(pp)*** = 4 mm, all points hitting the area covered by Peyer's patches (**pp**) were counted. Every fourth point of the grid (***dx(js)*** = 1,6 cm) was used to quantify all points hitting the whole jejunal sample (**pjs**).

The number of points hitting the area covered by Peyer's patches over 7 samples, **Σpp** constituted an area profile, $AP(pp/js) = \frac{1}{4} \times \Sigma pp/\Sigma pjs$ of the whole sample ***(js)***.

The absolute area of the Peyer's patches in the jejunum, $APP(jej) = 1/f(js) \times AP(pp/js) \times \Sigma A(js)$.

Results

ORGANISATION IN THE ENTERIC PLEXUSES, VIP, NOS AND 5-HT IR

The overall organisation of the enteric nervous system (ENS) is shown in Fig. 6. Results of VIP, NOS and 5HT- IR are illustrated by Figs. 7a-g; 8a-i. From the serosal side, the ENS was comprised of the myenteric (Auerbach) plexus (Fig. 7a) and muscular plexuses in the tunica muscularis, the outer submucous (Schabadasch) plexus (OSP) and inner submucous (Meissner) plexus (ISP) in the submucosa (Fig. 7b) and the mucous plexus (Fig.7e). The latter was composed of the sparsely ganglionated lamina muscularis mucosae, outer proprial and interglandular proprial subplexuses and the aganglionic internal proprial, perivascular, villous and subepithelial subplexuses as illustrated in Fig 6. In the submucous layer, the OSP and ISP were distinct with ganglia and nerve strands appearing at different topographical levels being separated by the submucous vascular arcades (not shown). Visualised from serosal side, the OSP was located in the outer submucous layer between the submucous vascular arcades on the inner side and the inner circular muscle layer on the outer side. The ISP was located in the inner submucous layer between the submucous vascular arcades on the outer side and lamina muscularis mucosae on the inner side. The two plexuses, differed in the size, shape and outlines of ganglia and size of nerve strands, size of neurons and density of meshworks, and the staining pattern to VIP and NOS IR, and amount of VIP and NOS IR neurons (Fig. 8a-d). The OSP meshwork was wider with larger ganglia, neurons and interconnecting nerve strands and thus fewer ganglia per unit area compared to the ISP which had smaller, abundant ganglia and neurons and a narrow mesh.

The VIP IR neurons were abundant in the ISP, many in myenteric plexus and sparse in the mucous plexus and OSP (Figs. 7e, f; 8a, c-g). The staining in the perikarya was intense in the ISP and mucous plexus and moderate to weak in the OSP and the myenteric plexus in which intensely stained VIP IR neurons were seen infrequently. VIP IR varicosities were abundant in the myenteric plexus ganglia and the lamina propria in the mucous plexus followed by ISP and moderate in the OSP ganglia. The VIP IR nerve fibres were more abundant and inner circular muscle layer than in the outer longitudinal muscle layer. The staining pattern, intensity and density of NOS IR in the nerves and neurons varied among plexuses. In the ISP, staining intensity was weaker compared to other plexuses (Figs. 7g; 8b, h-i). There were a few intensely stained and many moderate stained neurons (Fig. 8h). The proportion of IR neurons in a ganglion was smaller in the larger ganglia located close to vascular arcades compared to smaller ganglia which were located close to lamina muscularis mucosae. In the OSP, there were many intensely stained NOS IR neurons and varicosities giving a clear overview of ganglia, primary and secondary nerve strands without marked differences in the staining between ganglia (Figs. 8b, i).

In the myenteric plexus (Figs. 7a, g) there were many intensely and a few moderate stained NOS IR neurons and varicosities. In the all plexuses NOS IR neurons varied in sizes (small, medium and large) and staining intensity, with the majority of the small neurons being moderately stained.

In the present study, the vast majority of EC cells were observed at the base of the intestinal crypts. Most of the EC cells reached intestinal lumen by narrow cytoplasmic extensions and were considered as the "open" type. The EC cells without cytoplasmic extensions ("closed" type) were often seen at the base of the intestinal crypts.

The Peyer's patches were continuous in the most distal part of the jejunum and discrete in the middle and proximal jejunum. However, fairly more Peyer's patches were encountered in the proximal part of jejunum close to duodenum compared to middle jejunum.

TOTAL NUMBER OF VIP, NOS IR NEURONS AND ENTEROCHROMAFFIN CELLS, AND SURFACE ARE OF THE PEYER'S PATCHES.

The total number of NOS IR neurons in the pig jejunum was 11.2×10^6 in the myenteric plexus, 1.84×10^6 in the outer submucous plexus and 6.79×10^6 in the inner submucous plexus. The total number of VIP IR neurons in the pig jejunum 17.4×10^6 in the myenteric plexus, 1.15×10^6 in the outer submucous plexus, 48×10^6 in the inner submucous plexus and 1.82×10^6 in mucous plexus. The total number of enterochromaffin cells was 3.038×10^9 and the surface area of the Peyer's patches was 403.725 cm^2.

Discussion

METHODOLOGY

In the present study in the pig, we have demonstrated a simple, efficient, cheap, method to estimate the total number of neurons, EC cells and the surface area of Peyer's patches in the jejunum of large mammals using unbiased principles. In the process of developing and optimising the sampling scheme, it was realised that to cut open the jejunum along the mesenteric attachment jeopardised the uniformity of subsequent sampling. As illustrated in Fig. 3a, the ***ts*** was selected uniformly with respect to the mesenteric attachment for further sampling. This was just an approximation to a 2D uniformly random sampling. For proper sampling, the ***ts*** should have been completely inside the ***ss*** (3 cm piece) and therefore, uniform with respect to its edges. The correct way to cut the gut open for 2D uniformly random sampling procedure is shown by Fig. 2.5.

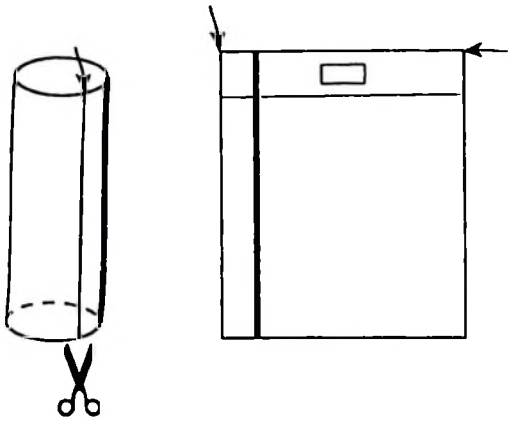

Fig. 2.5. An alternative and more correct (2D uniform) sampling of the secondary samples *(ss)* from the 'unstretched primary samples *(ps)*'. Shown on the left is the unopened 15 cm *ps*. The mesenteric attachment indicated by a heavy line. The upper arrow points to a uniformly random point on the upper edge. The segment is cut open through the random point parallel to the mesenteric attachment as illustrated to the right. From a random end, a 3 cm *ss* is selected randomly from the *ps* (large rectangle). A tertiary sample *(ts)* with precise dimensions (~1.5 cm) (small rectangle) is selected and cut exactly from the middle of the *ss* and stretched as described in Fig. 3b. This area is 2D uniformly random because the edge of the *ps* (horizontal arrow) is uniformly random along the gut axis, and the end of the *ss* (vertical arrow) is uniformly random perpendicular to the gut axis.

The sampling scheme shown resulted in a rather large number of fields (av. 65 fields) per wholemount. This was necessary because all plexuses are rather inhomogeneous with neurons grouped in clusters, almost like small ganglia with pronounced connections to many neighbouring "ganglia". The optical disector is primarily used to count cells in thick tissue sections assuming optimal tissue transparency and counting is done by using a 3D counting frame top and bottom of which are focal planes within the tissue (Gundersen, 1986). The sampling through the plexuses, illustrated in Fig. 7g was complete in the Z-axis (Figs. 8c-f). There was no so-called "height sampling fraction" involved. This has the most unusual consequence that it is not necessary to use oil-immersion optics, ordinarily a must for the optical disector/fractionator. The thickness of wholemounts was not a problem except in areas containing the Peyer's patches because by stretching tissues, neurons almost formed monolayers within the ganglia hence, no neurons were missed because of cellular overlap thus all cells were counted by using the optical disector. Even in mucosal wholemounts which are usually thicker than the submucosal and myenteric plexuses, all cells in one plane were easily counted by focusing through the tissues and there was no need for the so called "guard" space in the Z-direction. The wholemounts are thin enough and can be used to estimate the number of all kinds of cells in a defined layer, within all defined segments of the gut.

For each of the wholemounts, the 2D density, (N_A) of specific neurons/EC cells could be estimated:

$$N_A := \Sigma Q / [F \times a(fra)] \times (1 - shr) \times \Sigma p / 4F \qquad (2)$$

where the summation is over the total fields of vision F in the wholemount, $1 - shr$ is the correction for shrinkage of the tissue area, and $\Sigma p/4F$ is the average number of corner points that hit tissue, a 'compensation' for incomplete fields at the edges of the wholemount. Since the oral-anal sequence of the samples is known, one could study the variation in the local numerical density as a function of position in the gut.

The regression (if significant) is a descriptor of the local architecture of the specific neurons/EC cells in the particular wholemount in question and of its spatial variation. A more informative way of viewing the variation in numerical number through out the gut is provided by the number of neurons per length of gut:

$$N_L := w(sample) \times N_A \qquad (3)$$

where $w(sample)$ is the local circumference at each sampled position (Fig. 3). This function is also unbiased and completely independent of shrinkage and the many deformations occurring during processing of the tissue. The precision of a fractionator sampling scheme is rarely simple to predict, the present design is no exception, reference to smooth. However, since the estimator of the total number of neurons/EC is a sum of $n(sample)$ estimates, one may use the CE among samples as an indication of the precision.

In the previous studies, estimation of sizes of organs and tissues to obtain serosal surface areas was done mainly after distension and fixation of tissues (Gabella, 1971, 1987, 1989). Stretching of tissues increased the surface area and consequently decreased the neurons/cm^2 (Karaosmanoglu et al. 1996). Some investigators tried to avoid the effects of stretch by presenting the numbers of neurons/cm^2 of ganglion area because, ganglion per unit resting length of gut is independent of stretch (Timmermans et al., 1990; Parr and Sharkey 1994; Karaosmanoglu et al. (1996). The limitations of this approach include: stretching deforms the shape of ganglia and therefore alter its dimension (Wedel et al., 1999). Ganglia are heterogeneous in size and shape and there are isolated neurons in the nerve strands, and some neurons are occasionally lying outside the outline of the ganglia (Karaosmanoglu et al., 1996). In the present study, the possible changes in the size of tissues were monitored throughout in the sampling procedure and after staining. Furthermore, all neurons that were IR to specified stains were counted regardless of whether they were located in ganglia or isolated in nerve strands. However, the present method, had an advantage that the total number of neurons and EC cells were independent of the magnification, shrinkage and all other dimensional changes in the tissues that occur during staining and processing for mounting.

The unrecognised or lost elements are traditionally called lost caps (Hedreen, 1998) and constitute the so called "truncation problem" (Gundersen, 1986). In studies using wholemounts, lost caps may be due to several factors: (a) When preparing wholemounts (microdissection),

some of the neurons and ganglia can either be lost or displaced to aberrant positions within the adjacent tissues. For instance, neurons and ganglia may be lost while dissecting the inner circular muscle to expose both the OSP and myenteric plexus. The ISP ganglia and neurons may be displaced to the mucosal wholemounts or *vice versa*. (b) Staining methods. Some stains reveal neurons better than others, others reveal the soma and perikarya. In the present study, NOS IR revealed neurons and their cytoplasmic processes in the myenteric plexus and OSP better as compared to VIP IR. However, some of the stains reveal the dense nerve fibre networks or IR varicosities within the ganglia as shown by VIP IR in the myenteric plexus in this study such that weakly stained neurons may not be counted. Specificity of the antibodies should also to be considered. Any non specific staining of enteric glia is a potential source of false positive identifications of neurons especially because neurons are highly heterogeneous in size and shape, and in the enteric ganglia there are many small sized neurons (Karaosmanoglu et al., 1996). (c) Other factors such as experience, attentiveness, patience of the observer and the observers conscious and unconscious policies to make appropriate decisions on when to count neurons/EC in the border line may have great influence on the results if not held constant (Hedreen, 1998). Experience is particularly important in counting neurons in the submucous plexus because the OSP and ISP are superimposed above each other and closely interconnected by secondary strands. Furthermore, they are both composed of ganglia that are located at different topographical levels, highly heterogeneous in size and shape (Scheuermann et al., 1987a,b; Balemba et al., 1998, 2001; Timmermans et al., 1997; Wedel et al., 1999). The large ganglia in the ISP might easily be confused with the OSP whereas small OSP ganglia might be considered as the ISP ganglia.

Several types of stains have been used to estimate the total number or numerical density in the ENS and their comparison is beyond the scope of the current work. Still, to date there is no single standard stain that reveals all neurons (Gabella, 1987; Young et al., 1993; Karaosmanoglu et al. (1996). However, the recent comparison by Karaosmanoglu et al. (1996) shows that for the purpose of determining the total number of neurons at least in the myenteric plexus, cuprolinic blue and nerve cell antibody could provide almost complete estimate of the total number of neurons. For comparative purposes and uniformity of data between different laboratories, there is need to adopt a common reference stain the "gold stain" wherever the total number (population) of neurons is being sought.

TOTAL NUMBER OF VIP AND NOS IR NEURONS AND EC CELLS, AND SURFACE ARE OF THE PEYER'S PATCHES

The organisation of the enteric plexuses and the nomenclature used are in accordance with previous studies in the pig (Timmermans et al., 1997, 2001). The observation on the staining pattern of VIP IR in the enteric plexuses are similar to those reported earlier in the small intestine of the pig by Timmermans et al. (1990) and Balemba et al. (1998). The observations on NOS IR correspond to the findings by Van Ginneken et al. (1998) in duodenum and Krammer and Kühnel (1993) and Brehmer et al., (1998) in the small intestine of the pig.

The total numbers of the VIP and NOS IR neurons in the individual plexuses in a well defined length of the gut, the jejunum are reported for the first time. In the small intestine of the pig, the numbers of VIP IR neurons/cm^2 were 7,500 in the ISP and 130 in the OSP (Timmermans et al., 1990). These data correlate with the present findings of very high total number of VIP in the ISP compared to the OSP in the jejunum of the pig. The observations of ganglia and isolated neurons in the mucous layer supports the similar findings in small intestine (Fang et al., 1993) and colon (Wedel et al., 1999) of humans and in the intestine the goat (Balemba et al., 2001). However the observation that the mucous plexus contained a surprisingly large number of VIP IR neurons slightly larger than the total number in the OSP is new information. This finding provides additional evidence to support the propositions for the mucous plexus to be considered among the major ganglionated plexuses and the need to elucidate their physiological significance in the regulation of mucosal functions (Balemba et., 2001). The total numbers and numerical densities of the bNOS-expressing neurons were estimated in the ISP, OSP and the myenteric plexuses in 1 cm long pieces of tissues from the oral and aboral duodenum of prenatal, neonatal and weaned pigs (Table 4), (Van Ginneken et al., 1998).

Table 4. Total number (Q) and numerical density (Q_A) of bNOS- expressing neurons in 1cm long tissue from the duodenum of the pig.

Duodenal plexuses		Prenatal (90-115 days)		Weaner pigs(6-8 wk)	
		Total number (Q)	(Q_A)	Total number (Q)	(Q_A)
ISP	Oral	51,900	13,800	36,600	722
	Aboral	55,500	14,700	33,600	611
OSP	Oral	~8,500	~1,200	~11,000	246
	Aboral	~8,500	~1,200	~9,000	173
MP	Oral	~70,000	~17,000	115,000	2,270
	Aboral	~55,000	~12,000	81,500	1,610

(Extracted and modified from Van Ginneken et al., 1998). ~ Shows estimated values from graphs

These results indicated that despite dramatic increase in the size of the gut during development, the total number of neurons increased whereas, numerical densities decreased. These data

illustrate clearly that numerical densities are much to dependent on the volume of the reference space and their relevance in drawing biological conclusions is therefore highly limited (Braendgaard and Gundersen, 1986). Dividing the total number of bNOS IR neurons in the jejunum/total length of jejunum, the average no of neurons/1 cm tissue is ~ 5,434, 1,492 and 9,084 bNOS IR neurons in the ISP, OSP and MP respectively. These values are approximately 10x less than those obtained by Van Ginneken et al. (1998) in the duodenum of 6-8wk pigs (Table 4). The reasons for the variations are not clear. However, it could partly be due to differences between segments. Nevertheless, since Van Ginneken et al. (1998) used distended organs and estimated sizes of tissue segments after fixation and the extent of stretch and shrinkage were not considered our results were expected to be even higher than those of Van Ginneken et al. (1998). In the present study, a large number of moderate NOS IR neurons were observed in the ISP which is similar to the observations by Van Ginneken et al. (1998). In most qualitative studies of NOS, neurons expressing NOS in the ISP are given lesser emphasis compared to the myenteric plexus and OSP (Krammer and Kühnel, 1993; Grozdanovic et al., 1994; Brehmer et al., 1998). The present observations on the total number of NOS IR neurons in the ISP and VIP IR neurons in the mucous plexus signify the importance of complementation of microscopic observations with quantitative approaches (Ferri, 1988).

The finding that most of the EC cells reached intestinal lumen by narrow cytoplasmic extensions suggest that the majority of EC cells were of the "open" type. These findings are in accordance to those of Cetin et al. (1994) in the intestine of the guinea pig and Totzauer (1991) in the duodenum of cattle that the majority of EC cells are bipolar. Apparently, data for the total number of EC cells as well as the total surface area of the Peyer's patches in the jejunum of 8 weeks old pigs is new information. In a few, fully developed disease conditions, it is comparatively easy to qualitatively show clear-cut abnormalities but not when there are minor and diffuse changes (Ferri, 1988). The present sterelogical method is expected to heightened the application of morphometric analysis corollary to immunocytochemical stains in studying various forms of disorders in the gut and thus, expand our understanding of normality of the ENS and its role in diseases and malformations.

Acknowledgements

The authors wish to thank the Danish International Development Agency for financial support. The kind donation of the monoclonal rabbit anti-swine vasoactive intestinal peptide by Dr. J. Fahrenkrug is highly acknowledged. We are grateful to Prof. B. Pakkenberg and Dr. T. Bock for availing us with the microscope, and Mr. D. Mkuki, Mrs H. Holm and Dr. C.D. Pfarrer for excellent technical assistance.

References

Ali HA, McLelland J. Neuron number in the intestinal myenteric plexus of the domestic fowl (Gallus gallus). *Anat Histol Embryol* 1979,8:277-83.

Balemba OB, Grøndahl M-L, Mbassa GK, *et al.* The organisation of the enteric nervous system in the submucous and mucous layers of the small intestine of the pig studied by VIP and neurofilament proteins immunohistochemistry. *J Anat* 1998;(192):257-67.

Balemba OB, Semuguruka WD, Hay-Schmidt A, *et al.* The organisation and variations of ganglionated plexuses of the enteric nervous system in the goat. *J. Anat.* (2001) (submitted).

Barman NN., Bianchi ATJ, Zwart RJ, *et al.* Jejunal and ileal Peyer's patches in pigs differ in their postnatal development. *Anat Embryol* 1997;195: 41-50.

Bor-Seng-Shu E, Chadi G, Bor-Jiun-Shu F, *et al.* Myenteric neurons of the mouse small intestine. Morphometry and acetylcholinesterase activity. *Braz J Med Biol Res* 1994;27(1):101-8.

Braendgaard H, Gundersen HJG. The impact of recent stereological advances on quantitative studies of the nervous system. *J Neurosci Meth* 1986;18:39-78.

Brehmer A, Beleites B. Myenteric neurons with different projections have different dendritic tree patterns: a morphometric study in the pig ileum. *J Auton Nerv Syst* 1996; 7:61(1):43-50.

Brehmer A, Stach W. Regional structural differences in the neuronal composition of myenteric ganglia along the pig small intestine. *Anat Rec* 1998; 250(1):109-16.

Brehmer A, Stach W, Krammer HJ, *et al.* Distribution, morphology and projections of nitrergic and non-nitrergic submucosal neurons in the pig small intestine. *Histochem Cell Biol* 1998; 109(1):87-94.

Burns G, Cummings JF. Neuropeptide distributions in the colon, caecum and jejunum of the horse. *Anat Rec* 1993; 236, 341-50.

Cetin Y, Kuhn M, Kulaksiz H, *et al.* Enterochromaffin cells of the digestive system: cellular source of guanylin, a guanylate cyclase-activating peptide. *Proc. Ntl Acad. Sci. USA* 1994; 91: 2935-39.

Chu RM, Liu CH. Morphological and functional comparisons of Peyer's patches in different parts of swine small intestine. *Vet Immunol Immunopathol* 1984; 6(3-4): 391-403.

Costa M, Furness JB, Llewellyn-Smith IJ. Histochemistry of the enteric nervous system. In: L.R., Jonson, J., Christensen, M.J., Jackson, E.D., Jacobson, J.H., Walsh, (Eds.), *Physiology of the gastrointestinal tract*, Raven Press, New York, 1987; 1-39 pp.

de Souza RR, de Carvalho CA, Liberti EA, et al. A quantitative study on the myenteric plexus of the distal end of the human oesophagus. Gegenbaurs Morphol Jahrb 1988; 134(4):565-74.

de Souza RR, Moratelli HB, Borges N, et al. Age-induced nerve cell loss in the myenteric plexus of the small intestine in man. *Gerontology* 1993; 39:183-188.

Fang S, Wu R, Christensen J. Intramucosal nerve cells in human small intestine. *J Aut Nerv Syst* 1993; 44(2-3):129-36.

Ferri G.-L. Human gut neuroanatomy: methodology for quantitative analysis of nerve elements and neurotransmitter diversity in the human enteric nervous system. *Bas Appl Histochem*1988; 32:117-44.

Filogamo G, Gigliani F. Ricerche sperimentali sulla correlazione tra estensione del territorio di innervazione e grandezza e numero delle cellule gangliari del plesso mienterico (di Auerbach), nel cane. *Riv Patol Nerv Ment* 1954, 75:41-62.

Fregonesi CEPT, de Miranda Neto MH, Molinari SL, *et al.* Quantitative study of the myenteric plexus of the stomach or rats with Streptozocin-induced diabetes. *Arq Neuropsiquiatr* 2001;59(1):50-53.

Furness JB, Costa M. *The enteric nervous system.* Churchill, Livingstone, Edinburgh, 1987;1-286 pp.

Furness JB, Costa M, Keast JR. Choline acetyltransferase- and peptide immunoreactivity of the submucous neurons in the small intestine of the guinea-pig. *Cell and Tissue Res* 1984; 237, 329-36.

Furness JB, Li ZS, Young HM, *et al.* Nitric oxide synthase in the enteric nervous system of the guinea pig: a quantitative description. *Cell and Tissue Research* 1994; 277:139-49.

Gabella G. Neuron size and number in the myenteric plexus of the newborn and adult rat. *J. Anat.* 1971; 109 (1): 81-95.

Gabella G. The number of neurons in the small intestine of mice, guinea-pigs and sheep. *Neurosci* 1987; 22:737-52.

Gabella G. Fall in the number of myenteric neurons in ageing guinea pigs. *Gastroenterol* 1989; 96:1487-93.

Grozdanovic Z, Brüning G, Baumgarten HG. Nitric oxide- A novel autonomic neurotransmitter. *Acta Anat* 1994; 150:16-24.

Gundersen HJG. Estimators of the number of objects per area unbiased by edge effects. *Microsc Acta* 1978; 81(2),107-17.

Gundersen HJG. Stereology of arbitrary particles: A review of unbiased number and size estimators and presentation of some new ones, in memory of William R. Thompson. *J Microsc* 1986;143(1):3-45.

Gundersen HJG, Bagger P, Bendtsen, TF, et al. The new Stereological tools: Disector, fractionator, nucleator, and point sampled intercepts and their use in pathological research and diagnosis. *APMS* 1988;96:857-81.

Gundersen HJG, Jensen EB. The efficiency of systematic sampling in stereology and its prediction. *J. Microsc.* 1987;147(3): 229-63.

Hedreen JC. Lost caps in histological counting methods. *Anat. Rec.* 1998, 250:366-72.

Heinckle EA, Kiernan JA, Wijsman J. Specific, Selective, and complete staining of neurons of the myenteric plexus, using Cuprolinic blue. *J Neurosci Meth* 1987; 21:45-54.

Heminghaus M, Holschneider AM, Jordan P, *et al.* A correlative morphometric and clinical investigation of hypoganglionosis of the colon in children. *Eur J Pediatr Surg* 1999;9(2):67-74.

Howard CV, Reed MG. Unbiased Stereology: Three dimensional measurement in microscopy. BIOS Scientific Publishers, Oxford, London 1998, pp 1-123.

Irwin DA, The anatomy of Auerbach's plexus. *Am J Anat*1931, 9:11-166.

Karaosmanoglu T, Aygun B, Wade PR, *et al.* Regional differences in the number of neurons in the myenteric plexus of the guinea pig small intestine and colon: an evaluation of markers used to count neurons. *Anat Rec* 1996;244(4):470-80.

Krammer HJ, Karahan ST, Mayer B, *et al.* Distribution of nitric oxide synthase-immunoreactive neurons in the submucosal plexus of the porcine small intestine. *Anat Anz* 1993;175(3):225-30.

Krause WJ, Yamada J, Cutts JH. Quantitative distribution of endocrine cells in the gastrointestinal tract of the adult opossum, *Didelphis virginiana. J Anat* 1984;140(4):591-605.

Leaming DB, Cauna N. A qualitative and quantitative study of the myenteric plexus of the small intestine of the cat. *J Anat* 1961;95(2),160-9.

Liberti EA, Gaspar LP, de Carvalho CA, *et al.* A morpho-quantitative study of the myenteric ganglia throughout the human digestive tract. *Rev Hosp Clin Fac Med Sao Paulo*, 1998;53(2): 55-60.

Maifrino LB, Prates JC, De-Souza RR, *et al.* Morphometry and acetylcholinesterase activity of the myenteric plexus of the wild mouse *Calomys callosus. Braz J Med Biol Res* 1997;30(5):627-32.

Matsuo H A. Contribution on the anatomy of Auerbach's plexus. *Jap J med Sci Anat* 1934, 4:417-28.

Meciano-Filho J, Carvalho VC, de Souza RR. Nervous cell loss in the myenteric plexus of the human oesophagus in relation to age: a preliminary investigation. *Gerontology* 1995; 41:18-21.

Meier-Ruge WA, Brunner LA. Morphometric assessment of Hirschsprung's disease: associated hypoganglionosis of the colonic myenteric plexus. *Pediatr Dev Pathol* 2001;4(1):53-61.

Maslennikova LD. On the relation between the motor function of the intestine and the gradient of its nervous elements. *Bull exp Biol Med USSR* 1962; 52:972-6.

Ohkubo K. Studies über das intramurale Nervensytem des Verdauungskanals. II. Die Plexus myentericus and Plexus subserosus des Meerschweichens. *Jap J med Sci Anat* 1936a; 6:19-37.

Ohkubo K. Studies über das intramurale Nervensytem des Verdauungskanals. III. Affe und Mensch. *Jap J med Sci Anat* 1936b; 6:219-247.

Oshima S, Fujimura M, Fujimiya M, Changes in number of serotonin-containing cells and serotonin levels in the intestinal mucosa of rats with colitis induced by dextran sodium sulphate. *Histochem Cell Biol* 1999; 112: 257-263.

Parr EJ, Sharkey KA. The use of constitutive oncoproteins to count neurons in the enteric nervous system of the guinea pig. *Cell and Tiss Res* 1994; 277: 325-31.

Rantala I, Paronen I, Kainulainen H, *et al.* Enterochromaffin cell density in the gastric mucosa of patients with chronic renal failure. *APMIS* 1996;104(5):362-366.

Sant'ana Dd, de Miranda-Neto, MH, Molinari, SL, *et al.* Neuron number in the myenteric plexus of the ascending colon of rats. A comparative study using two staining techniques. *Arq. Neuropsiquiatr.* 1997;55(3A):460-466.

Sauer ME, Rumble CT. The number of nerve cells in the myenteric and submucosal plexuses of the small intestine of the cat. *Anat Rec* 1946; 96:373-81.

Scheuermann WD, Stach W, Timmermans J-P. Topography, architecture and structure of the plexus submucousus internus (Meissner) of the porcine small intestine in scanning electron microscopy. *Acta Anat.* 1987a:129; 96-104.

Scheuermann WD, Stach W, Timmermans J-P. Topography, architecture and structure of the plexus submucousus externus (Schabadasch) of the porcine small intestine in the Scanning Electron microscopy. *Acta Anat.* 1987b:129;105-115.

Tafuri WL. Auerbach's plexus in the guinea pig. I. A quantitative study of the ganglia and nerve cells in the ileum, caecum and colon. *Acta anat*1957;31:522-30.

Tafuri WL, de Almeida Campos F. Der Auerbachsche Plexus bei der Maus. Z Natur-forsch 1958;13:816-819.

Timmermans J-P, Adriaensen D, Cornelissen W, *et al.* Structural organisation and neuropeptide distribution in the mammalian enteric nervous system, with special attention to those components involved in mucosal reflexes. *Comp Biochem Physiol* 1997;118A(2):331-40.

Timmermans J-P, Hens J, Adriaensen D. Outer submucous plexus: An intrinsic nerve network involved in both secretory and motility processes in the intestine of large mammals and human. *Anat Rec* 2001;262:71-8.

Timmermans J-P, Scheuermann DW, Stach W, *et al.* Distinct distribution of CGRP-, enkephalin-, somatostatin-, substance P-, VIP- and serotonin - containing neurons in the two submucosal ganglionic neural networks of the porcine small intestine. *Cell Tissue Res.* 1990; 260,367-79.

Totzauer I. Development of the bovine duodenum with reference to enterochromaffin cells. *Anat Histol Embryol* 1991;20:54-65.

Van Ginneken C, Van Meir F, Sommereyns G, *et al.* Nitric oxide synthase expression in enteric neurons during development in the pig duodenum. *Anat Embryol* 1998;198;399-408.

Wedel T, Roblick U, Gleiss J, *et al.* Organisation of the enteric nervous system in the human colon demonstrated by wholemount immunohistochemistry with special reference to the submucous plexus. *Anat Anz* 1999;181(4): 327-37.

Xiong S, Puri P, Nemeth L, *et al.* Neuronal hypertrophy in acute appendicitis. *Arch. Pathol Lab Med* 2000;124(10): 1429-1433.

Young HM, Furness JB, Sewell, P, et al. Total numbers of neurons in myenteric ganglia of the guinea-pig small intestine. *Cell Tissue Res* 1993;272(1):197-200.

Yunker AM, Paupore EJ, Galligan JJ, C-Fos in enteric nerves after extrinsic denervation of guinea pig ileum. *J Surg Res* 1999;82(2):324-330.

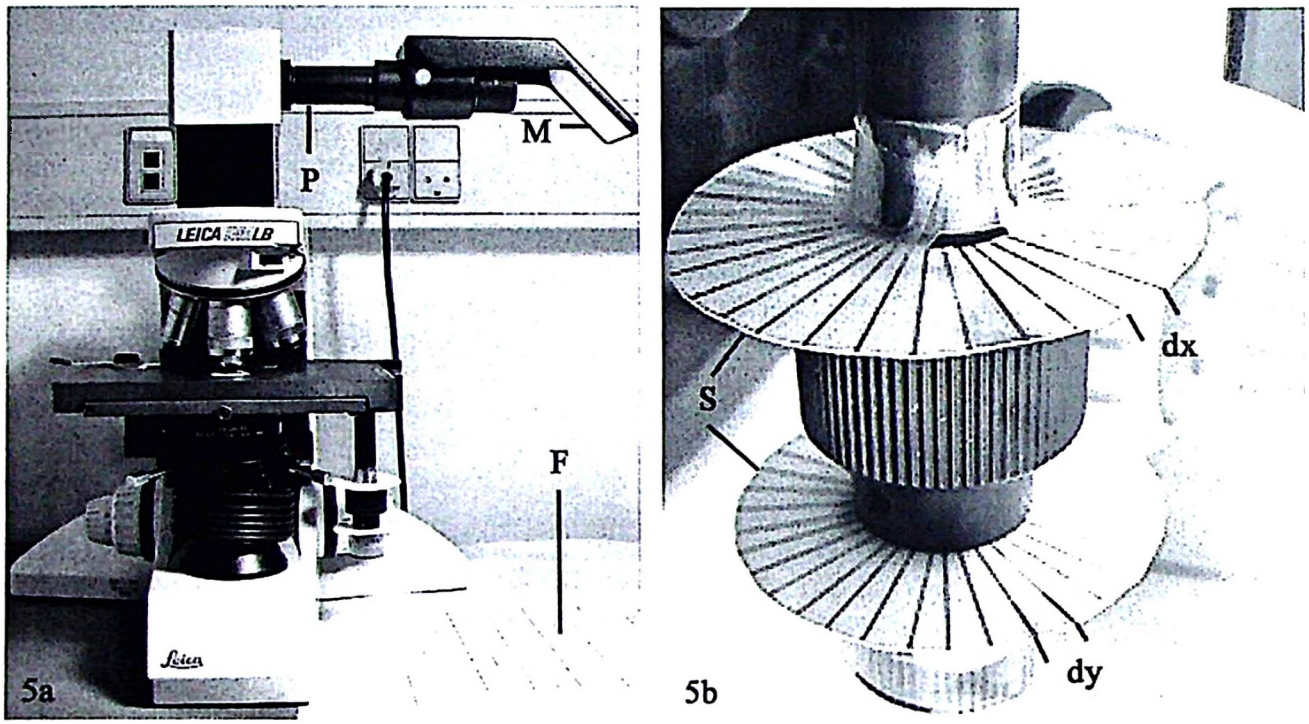

Fig. 5a. Shows a simple light microscope fitted with a projection arm (P) and a mirror (M) for projecting the image on the sampling frame (F) which is fixed on the table. Fig. 5b. Shows a close up of the two, cheap, low tech, stepping devices (S) fitted manually on the side arm for moving the mechanical stage in Fig 5a. The unit step lengths are labelled dy and dx.

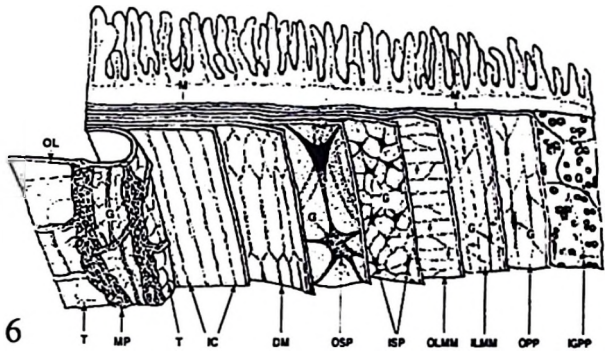

Fig. 6. Fig. 1a. Schematic drawing (not to scale) showing the organisation of ENS plexuses in the intestinal wall. Viewed from serosal side they are the outer longitudinal muscle layer (OL), myenteric plexus (MP), tertiary plexus (T), muscular plexus in the inner circular muscle layer (IC), deep muscular plexus (DM) between the outer and inner laminae of the circular muscle layer, the outer submucous plexus (OSP) and inner submucous plexus (ISP) in the submucous layer. In the mucous layer part of the mucous plexus is shown by the lamina muscularis mucosae subplexus (LMMP) showing nerve fibres (small arrows) in the outer lamina muscularis mucosae (OLMM) layer and inner lamina muscularis mucosae (ILMM) layer with scarce ganglia (G) between them. Others are the outer proprial plexus (OPP) located in the subglandular region and the interglandular proprial plexus (IGPP) located between the crypts. Intestinal crypts are labelled (C), (G) shows ganglia in the four ganglionated plexuses and (M) indicates the rest of the mucous layer. (Modified after illustrations by Furness and Costa, (1987) pg 7, Costa et al. (1987) pg 2 and Timmermans et al. (1990) pg 369).

Figs. 7a-8i. Wholemounts from pig jejunum showing the ENS plexuses as revealed by staining for NOS and VIP IR and enterochromaffin cells (EC) shown by 5HT IR. Fig. 7a. NOS IR, notice ganglia (arrows) and nerve fibre meshwork of the myenteric plexus. x 8.8. Fig. 7b.VIP IR, notice ganglia (arrows) and nerve fibre meshwork in the submucous plexuses. At this magnification individual plexuses can not be identified. Compare sizes of ganglia in Figs. 7a-b. Fig 7c. 5HT IR in the EC cells (arrow) in the intestinal crypt. x 350. Fig 7d. Low power, 5HT IR EC cells (arrow) at the base of the intestinal crypts. x 90. Fig. 7e. VIP IR in the mucous plexus (outer proprial plexus) close to the base of intestinal crypts. Notice IR neurons (lower arrow) in a small ganglion (G), an isolated neuron in a node (arrow head) and IR nerve fibres (upper arrow). C, shows intestinal crypts. x 96. Fig. 7f. Close up of VIP IR neurons (arrows) in a ganglion (G) in the myenteric plexus. x 240. Fig. 7g. Close up of NOS IR neurons (arrow) in a ganglion (G) in the myenteric plexus and a sampling frame illustrating the optical fractionator. In Figs. 7f-g, the black scale bars on the right shows the final magnification of the figure whereas, the left light grey scale bars show the final magnification at which the counting was done (333X).

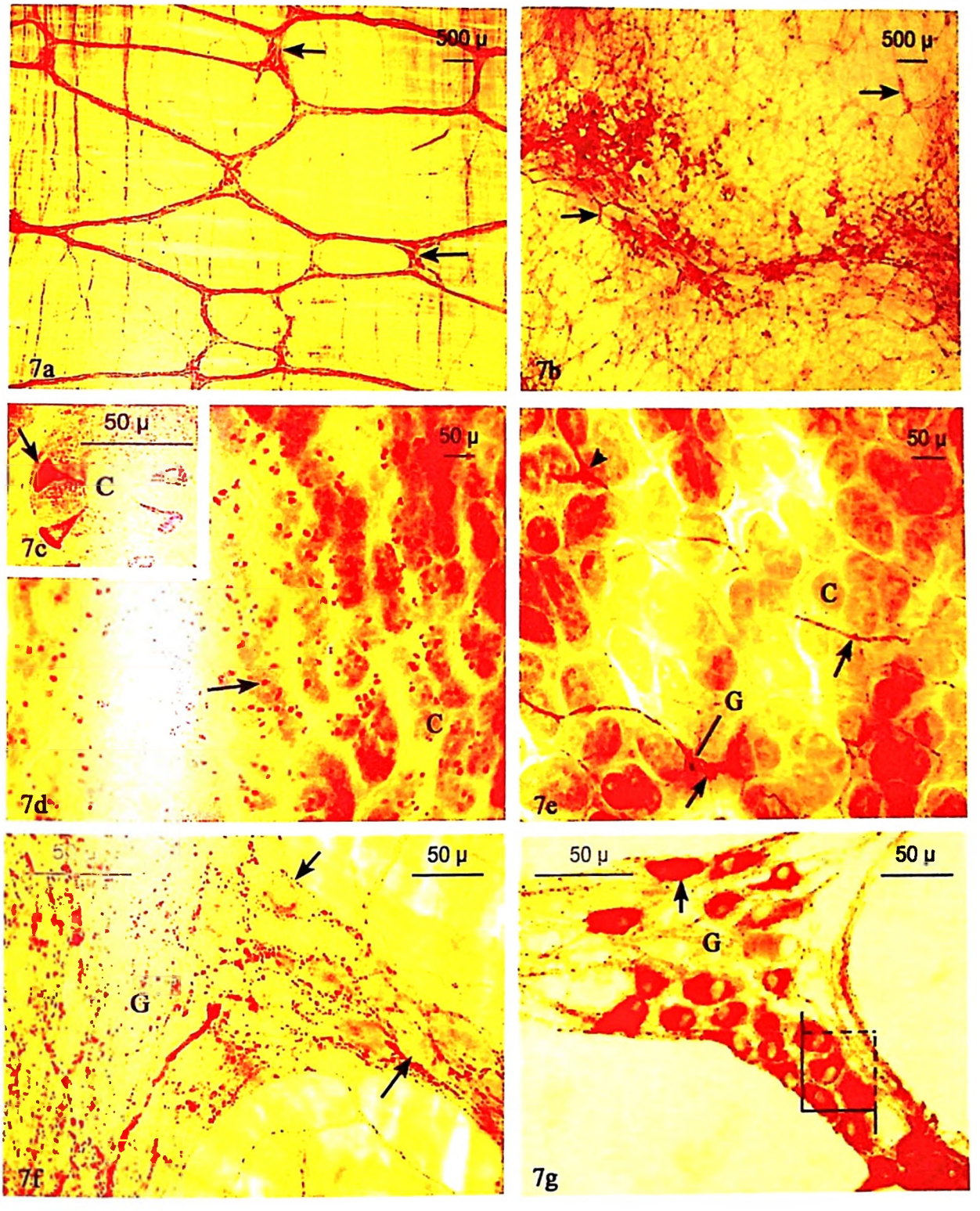
500 µ
7a
500 µ
7b
50 µ
C
7c
50 µ
C
7d
50 µ
C
G
7e
50 µ
G
7f
50 µ
50 µ
G
7g

Fig. 8a. VIP IR, submucous layer, visualised from mucosal side. Notice the ISP (Gi) and OSP (Go) ganglia. Compare the sizes and amount of IR neurons. x 38. Fig. 8b. NOS IR, submucous layer, visualised from serosal side. The OSP ganglia (Go) interconnected by a nerve strand (Po) and ISP ganglion (Gi) which is very lightly stained and slightly out of focus. Compare the sizes and amount of IR neurons. x 38. Notice, in Figs. 8a-b, the ISP and OSP ganglia can easily be identified based on the topography, density of meshworks, size of ganglia and IR neurons. Fig. 8c-d. VIP IR, submucous layer, demonstrating the possibility to visualise the OSP and ISP ganglia, by focusing up and down though the wholemount (Z-axis). x 96. In Fig 8c, The OSP ganglion (Go), a nerve strand (Po) and VIP IR neuron (arrow) are in focus, whereas the ISP ganglion (Gi) and a nerve strand (Pi) are out of focus. In Fig. 8d, the ISP ganglion (Gi), a nerve strand (Pi) and IR neurons (arrow) are in focus whereas the OSP ganglion (Go) and a nerve strand (Po) are out of focus. The depth along the Z-axis at these two focal planes was 99.798µm. Compare the sizes, shapes and amount of IR neurons in the two plexuses. Fig. 8e-f. VIP IR, submucous layer, demonstrating of the ability to visualise the VIP IR neurons in the ISP ganglion (Gi) by focusing up and down on the ganglion (Z-axis). x 384. In Fig. 8e, the VIP IR neurons to the left (arrow head) are in focus, whereas, the those on the right (arrow) are out of focus. In Fig. 8f, the VIP IR neurons to the left (arrow head) are out of focus, whereas, the those on the right (arrow) are in focus. The depth along Z-axis at these two focal planes was 38.105µm. Fig. 8g. Close up of intense (arrow) and weaker (encircled) VIP IR neurons in the OSP ganglion (Go). Compare the amount, sizes and staining intensity of IR neurons in 7e-f; 8e-g. x 240.

Fig. 8h and i Show the close up of NOS IR neurons (arrows) in the ISP ganglion (Gi) (x 350) and in the OSP ganglion (Go) (x 384) respectively. Compare the amount, staining intensity, size and shape of NOS IR in 7g, 8h-i. In Figs. 8g-i, the scale bars on the right show the final magnification of the figure, those on the left show the magnification at which the counting was done (333X).

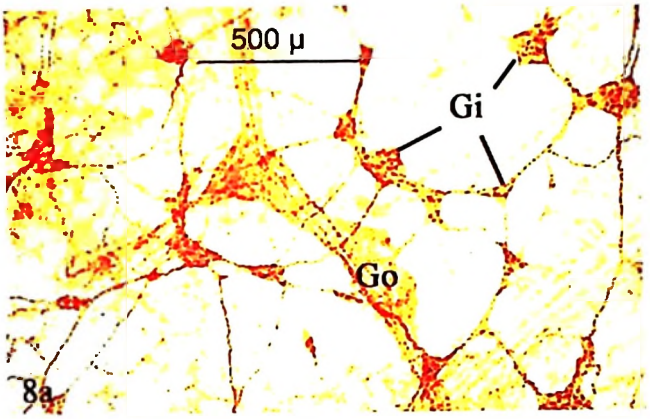
500 µ
Gi
Go
8a

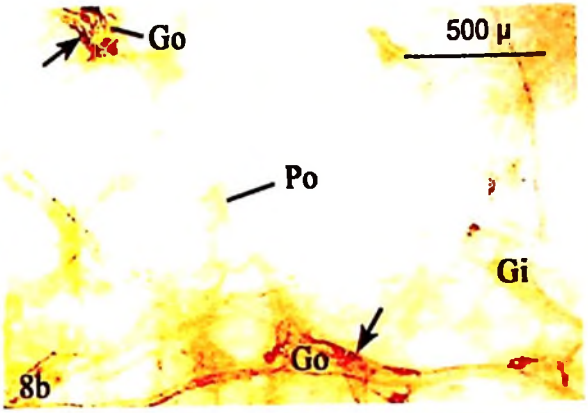
Go
500 µ
Po
Gi
Go
8b

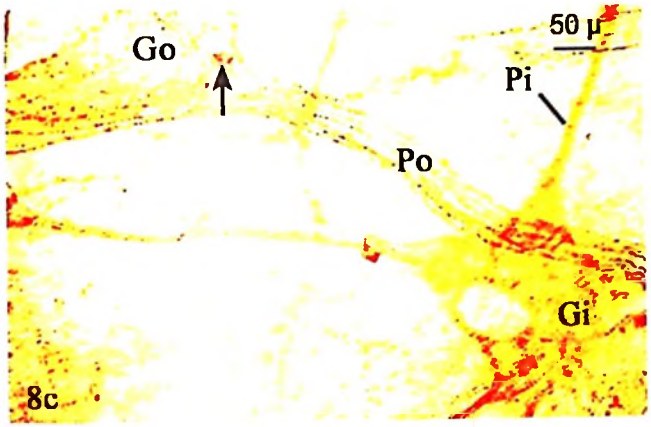
Go
50 µ
Pi
Po
Gi
8c

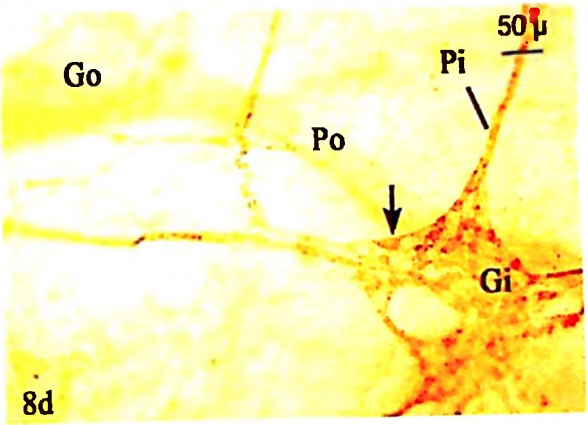
Go
50 µ
Pi
Po
Gi
8d

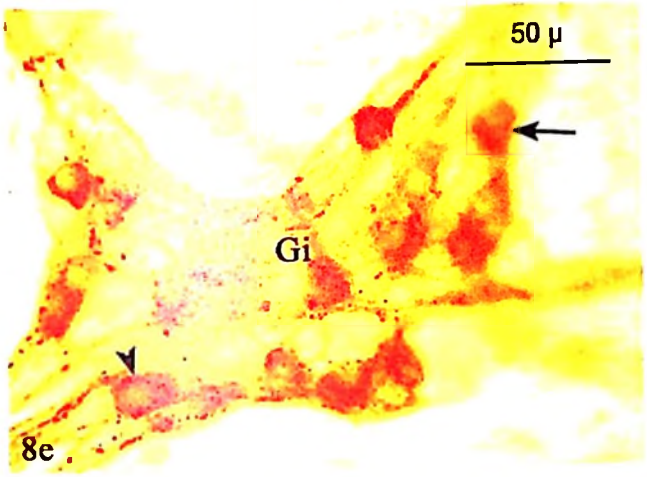
50 µ
Gi
8e

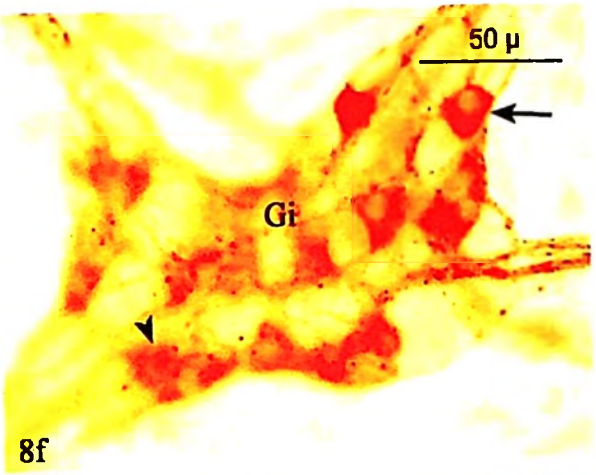
50 µ
Gi
8f

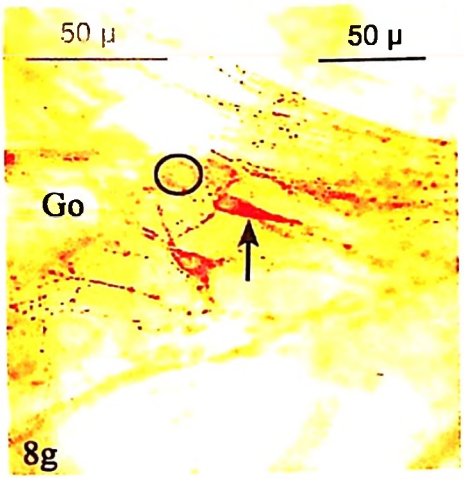
50 µ
50 µ
Go
8g

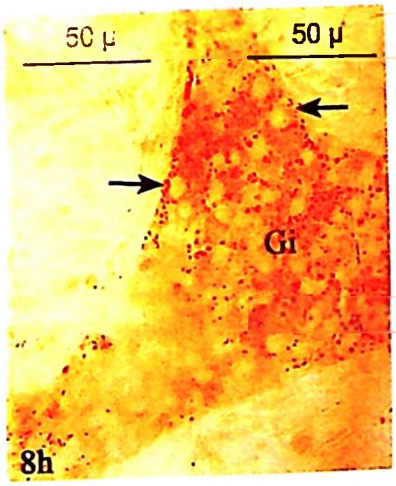
50 µ
50 µ
Gi
8h

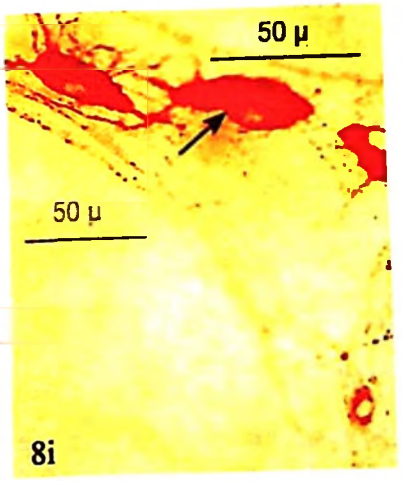
50 µ
50 µ
8i

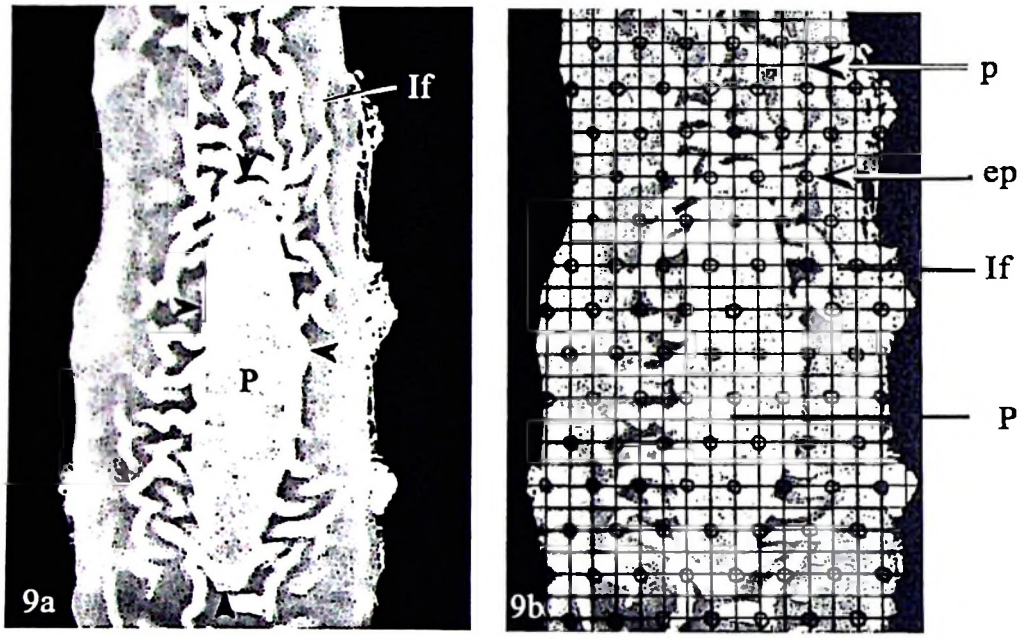

Figs. 9a-b. Show a systematic, uniform random estimation of the surface area of Peyer's patches in the jejunum of the pig. x 1.2. 9a shows a Peyer's patch (p) whose boundaries are marked by arrow heads. (If) show the intestinal folds. In 9b, the sampling grid is superposed above the tissue shown in Fig. 9a. all points (P with arrow) hitting the Peyer's patch **(pp)** are counted as well as encircled points (ep with arrow) hitting whole primary sample **(pjs)** provided those points at the boarders are in no way hitting the patch or the tissue by their exclusions zones only. Notice that although not shown, all points should had the "exclusion" (left half) and "inclusion" zones (right half). (If) show the intestinal folds.

Table 1. Total number of neurons

Animal and location		Total number of neurons		Author
Animal	Segment	Myenteric plexus	Submucous plexus	
Mouse	Small intestine (Distended) (D)	403,000		Gabella, (1987)
Mouse	Small intestine (D)	690,000		Bor-Seng-Shu et al. (1994)
Rat (adult)	Whole intestine (D)	2.5×10^6		Heinickle et al. (1987)
Rat	Small intestine (D)	$\sim 1.85 \times 10^6$		Gabella, (1987)
Guinea pigs (aging)	Small intestine (D)	$1.1 - 1,6 \times 10^6$		Gabella, (1989)
Guinea pigs (adult)	Small intestine (D)	2.75×10^6		Gabella, (1987)
Guinea pigs (adult)	Whole intestine (D)	13.8×10^6		Heinickle et al. (1987)
Guinea pigs (adult)	Small intestine (not distended)	6.5×10^6		Karaosmanoglu et al. (1996)
Guinea pigs (adult)	Colon (not distended)	7.3×10^6		Karaosmanoglu et al. (1996)
Chicken (chicks)	Small intestine (D)	$\sim 1.495 \times 10^6$		Ali and McLelland, (1979)
Chicken (chicks)	Large intestine (D)	$\sim 1.51 \times 10^6$		Ali and McLelland, (1979)
Chicken (adult)	Small intestine (D)	$\sim 2.06 \times 10^6$		Ali and McLelland, (1979)
Chicken (adult)	Large intestine (D)	$\sim 2.76 \times 10^6$		Ali and McLelland, (1979)
Cat	Small intestine (?)	$\sim 5 \times 10^6$		Sauer and Ramble, (1946)
Sheep	Small intestine (D)	31.5×10^6		Gabella, (1987)

Table 2. Number (spatial) densities of neurochemically specified neurons in the myenteric plexus of guinea pig.

Location	Authors					
	Irwin, (1931) (Methylene blue),	Matsuo, (1934) (Methylene blue),	Ohkubo (1936a) Methylene blue,	Tafuri, (1957) Toluidine blue,	Gabella, (1987) NADH, (Distended)	Young et al. (1993), nerve cell antibody, NADPH-d, toluidine blue, methylene blue, (relaxed)
Oesophagus	1,370	1,300				
Stomach-cardia	3,500		2,200			
Stomach-body			9,500			
Stomach-pylorus	20,000	16,500	16,250			
Duodenum	10,000	9,300 (upper) 9,8000 (middle)	6,700			
Ileum	7,500	7,200	5,300	14,211	8,600 (small intestine)	17,300 (small intestine)
Caecum beneath taenia	12,000	4,100		92,920		
Between taenia	4,500					
Colon	15,000	14,800	12,500	35,573		
	19,000	14,800				
Sigmoid	17,000					
Rectum	18,000	16,000	15,600			

Table 3. Number densities of specific neurons

		Stain	Number density/cm^2 serosal surface		Author
Animal	Segment (compartment)	Stain	Myenteric plexus	Submucous plexus	
Guinea pig	Small intestine (D)	NADH-d	8,600	3,000	Gabella, (1987)
Mouse	Small intestine (D)	NADH-d	10,600	8,700	Gabella, (1987)
Mouse	Ileum	Toluidine blue	29,600		Tafuri and De Almeida Campos, (1958)
Wild Mouse	Oesophagus	acetylcholinesterase (AChE), Giemsa	1,500		Maifrino et al. (1997)
Wild Mouse	Stomach	AChE, Giemsa	8,900		Maifrino et al. (1997)
Mouse	Duodenum	AChE, Giemsa	20,212		Bor-Seng-Shu et al. (1994)
Mouse	Jejunum	AChE, Giemsa	9,000		Maifrino et al. (1997)
Mouse	Jejunum	AChE, Giemsa	21,948		Bor-Seng-Shu et al. (1994)
Mouse	Ileum	AChE, Giemsa	25,048		Bor-Seng-Shu et al. (1994)
Mouse	Colon	AChE, Giemsa	13,100		Maifrino et al. (1997)
Rat, Control	Stomach, small curvature	NADH-d	67,707		Fregonesi et al., (2001)
Rat, Control	Stomach, large curvature	NADPH-d	14,345		Fregonesi et al., (2001)
Rat, Diabetic	Stomach, small curvature	NADH-d	45,4200		Fregonesi et al., (2001)
Rat, Diabetic	Stomach, large curvature	NADPH-d	11,026		Fregonesi et al., (2001)

continued ....

Rat	Small intestine (D)	NADH-d	9,405	Gabella, (1971)
Rat	Ascending colon (intermediate region)	NADPH-d	8,798	Santa'na et al. (1987)
Rat	Ascending colon (antimesocolic region)	NADPH-d	12,308	Santa'ana et al. (1987)
Rat	Ascending colon (intermediate region)	Giemsa	30,968	Santa'ana et al. (1987)
Rat	Ascending colon (antimesocolic region)	Giemsa	29,046	Santa'ana et al. (1987)
Cat	Duodenum	Thionine	49,081	Sauer and Rumble, (1946)
Cat	Duodenum (UD)	Methylene blue	12,170	Leaming and Cauna, (1961)
Cat	Duodenum	Thionine	49,081	Sauer and Rumble, (1946)
Cat	Ileum	Thionine	15,411	Sauer and Rumble, (1946)
Cat	Jejunum (UD)	Methylene blue	3,070	Leaming and Cauna, (1961)
Rabbit	Duodenum	Methylene blue	2,280-3,500	Maslenikova, (1962)
Rabbit	Jejunum	Methylene blue	2,088-2,900	Maslenikova, (1962)
Rabbit	Ileum	Methylene blue	2,000-2,500	Maslenikova, (1962)
Rabbit	Caecum	Methylene blue	1,760	Maslenikova, (1962)
Rabbit	Rectum	Methylene blue	2,840-2,940	Maslenikova, (1962)
Rabbit	Anus	Methylene blue	2,640	Maslenikova, (1962)
Dog	Ileum	Thionine	7,786	Filogamo and Vigliani, (1954)

continued ....

Monoky	Duodenum	Methylene blue	1,100-3,500		Ohkubo, (1936b)
	Jejunum		2,700		Ohkubo, (1936b)
	Ileum		2,400		Ohkubo, (1936b)
Sheep	Small intestine (D)	NADH-d	2,500	4,500	Gabella, (1987)
Pig	Small intestine	Substance P		50 (OSP) 7,000 (ISP)	Timmermans et al. (1990)
Pig	Small intestine	Galanin		160 (OSP) 5,800 (ISP)	Timmermans et al. (1990)
Pig	Small intestine	Neuromedin U		70 (OSP) 8,200 (ISP)	Timmermans et al. (1990)
Pig	Small intestine	Calcitonin gene related peptide		100 (OSP) 2,000 (ISP)	Timmermans et al. (1990)
Pig	Small intestine	Vasoactive intestinal peptide		130 (OSP) 7500, (ISP)	Timmermans et al., (1990)
Pig	Duodenum	Nitric oxide synthase			Van Ginneken et al. (1998)
Pig	Duodenum	Nitric oxide synthase			Van Ginneken et al. (1998)
Pig	Duodenum	Nitric oxide synthase	7,506		Van Ginneken et al. (1998)
Pig	Duodenum	Nitric oxide synthase	6,900		Van Ginneken et al. (1998)
Human	Oesophagus	Cresyl Violet	659-3,316		de Souza et al., (1988)
Human	Colon (Hirschsprung's disease)	Lactic dehydrogenase reaction	740		Meier-Ruge and Brunner, (2001)

continued ....

Human	Colon (Hirschsprung's disease)	Lactic dehydrogenase reaction	1,110	Meier-Ruge and Brunner, (2001)
Human	Colon (control)	Lactic dehydrogenase reaction	1,450	Meier-Ruge and Brunner, (2001)
Humans young persons	Duodenum	Giemsa	7,506	de Souza et al., (1993)
Humans young persons	Jejunum	Giemsa	6,900	de Souza et al. (1993)
Humans young persons	Ileum	Giemsa	6,907	de Souza et al. (1993)
Humans elderly persons	Duodenum	Giemsa	4,663	de Souza et al. (1993)
Humans elderly persons	Jejunum	Giemsa	4,583	de Souza et al. (1993)
Humans elderly persons	Ileum	Giemsa	4,376	de Souza et al. (1993)

Paper V

PARA 1646

ELSEVIER

International Journal for Parasitology xx (2001) xxx–xxx

INTERNATIONAL Journal for PARASITOLOGY

www.parasitology-online.com

Vasoactive intestinal peptide and substance P-like immunoreactivities in the enteric nervous system of the pig correlate with the severity of pathological changes induced by *Schistosoma japonicum*

O.B. Balemba[a], W.D. Semuguruka[b], A. Hay-Schmidt[c], M.V. Johansen[d], V. Dantzer[e,*]

[a]*Department of Veterinary Anatomy, Sokoine University of Agriculture, Morogoro, Tanzania*
[b]*Department of Veterinary Pathology, Sokoine University of Agriculture, Morogoro, Tanzania*
[c]*Institute of Medical Anatomy, Panum building, Copenhagen university, RVAU Copenhagen, Denmark*
[d]*Danish Bilharziasis Laboratory, Charlottenlund, Copenhagen, Denmark*
[e]*Institute for Anatomy and Physiology, RVAU, Gronnegaardsvej 7, 1870 Frederiksberg C, Copenhagen, Denmark*

Received 9 May 2001; received in revised form 18 June 2001; accepted 19 June 2001

Abstract

Limited studies have shown that in intestinal schistosomosis, the enteric nervous tissue becomes inflamed, disrupted and destroyed by granulomas and peptides, amines and neurofilaments contents are altered. Therefore, immunoreactivities of vasoactive intestinal peptide and substance P were correlated to pathological lesions in the large intestine from pigs infected with *Schistosoma japonicum*. Ganglia situated within or near granulomas showed ganglionitis, and necrosis of neurons as well as infiltration by eosinophils, mast cells, lymphocytes, plasma cells, neutrophils and macrophages. The inner submucous and mucous plexuses were the most damaged. In all categories of inflamed areas, the vasoactive intestinal peptide-like immunoreactivity was reduced in all plexuses whereas, that of substance P was increased both in the enteric nerve plexuses and enterochromaffin cells in lightly, moderately and severely inflamed tissues. However, both peptides were highly diminished or absent in very severe lesions and areas surrounding schistosome eggs and mature worms laying eggs in the submucosal veins. The alterations of the levels of vasoactive intestinal peptide and substance P were correlated with severity of inflammation. Our observations show alterations of vasoactive intestinal peptide and substance P contents in the local microenvironment in the vasoactive intestinal peptide- and substance P-mediated reflex pathways which regulate intestinal motility, epithelial transport and modulate immunity. These changes could cause alterations in bowel motility, electrolyte and fluid secretion, vascular and immune functions during *S. japonicum* infections in the pig. This may, therefore, partly play a role in the pathobiology of migration and egress of schistosome eggs as well as influence trapping of eggs in granulomas, and account for diarrhoea, loss of body weight and failure to thrive, which are recorded in schistosomosis.

Keywords: Pig; *Schistosoma japonicum*; Enteric nervous system; Histopathology; Vasoactive intestinal peptide; Substance P

1. Introduction

Schistosoma japonicum infections have been suggested to cause severe intestinal disorders, namely that granulomas mainly affecting the large intestine cause proliferation and disruption of the epithelium, fibrosis and thickening of the submucosa, alteration of bowel motility, intestinal distortion, stricture and bleeding (Chen et al., 1978), intestinal obstruction (Ming-Chai and Shan-Chi, 1957; Warren, 1969), pyloric obstruction and sigmoidal fistula (Nai-Kuang and Pen-Chung, 1957). They are also speculated to be a predisposing factor to malignant adenocarcinoma (Ch'ing-Fan, 1957; Cheever, 1981). Schistosomosis exacerbates malnutrition in the host (Johansen et al., 1997) and repeated exposures in early age are suggested to cause dwarfism (Ming-Hsin et al., 1957). The pathology of postnatal infection (Yason and Novilla, 1984; Hurst et al., 2000) and postnatal challenge infection of congenitally infected (Johansen et al., 2001, in press) pigs have been thoroughly described. However, the mechanisms by which granulomatous inflammation causes all the changes stated above are not entirely clear.

In murine schistosomosis mansoni, intestinal granulomas focally destroyed enteric nerves and neurons and in displaced ganglia showed increased staining intensity for vasoactive intestinal peptide and dihydronicotinamide adenine dinucleotide, loss of nuclear definition, chromato-

* Corresponding author. Tel.: +45-35282543; fax: +45-35282547.
E-mail address: vibeke.dantzer@iaf.kvl.dk (V. Dantzer).

0020-7519/01/$20.00
PII: S0020-7519(01)00273-9

lysis and cell death. The extent of injury was related directly to the number of granulomas (Varilek et al., 1991). However, in a similar study in mice, Bogers et al. (2000) did not observe significant apoptotic neurons in the myenteric plexus in the ileum but, recorded ganglionitis with few apoptotic cells in the boundaries of the ganglia. Van Nassauw et al. (2001) observed a significant increase in the number of 3-nitrotyrosine-immunoreactive neurons (a biomarker of reactive nitrogen species) and very few active caspase-3, (a key executioner of apoptosis) positive neurons in both the submucous and myenteric plexuses in the ileum of mouse. These changes indicated damage in a significant number of enteric neurons but, rare neuronal cell death. In bovine *S. bovis*infections (Balemba et al., 2000), neurons and fibres within or close to granulomas showed increased staining for vasoactive intestinal peptide but reduced staining for neurofilament proteins. During inflammation, selective changes occur in specific neurochemical pathways altering specialised neuronal functions. Once neurochemical lesions in one or more of the intestinal microcircuit reflex pathways have developed, neural control of intestinal function is altered (Palmer and Koch, 1995). In intestinal anaphylaxis, infection and inflammation, neuronal activation and plasticity (structural and neurochemical changes) cause an imbalanced function of peptidergic neurons, and are suggested to contribute to motor, secretory, vascular and immunological disturbances (Belai et al., 1997; Holzer, 1998; Shanahan, 1998; Giaroni et al., 1999; Sharkey and Kroese, 2001). Therefore, injury to the enteric nervous system caused by granulomatous inflammation impairs its regulatory functions and may partly account for clinical and pathological features seen in schistosomosis (Varilek et al., 1991; Balemba et al., 2000; Bogers et al., 2000; Van Nassauw et al., 2001). However, studies of lesions inflicted by migrating schistosome eggs and associated inflammatory reactions to the enteric nervous system in mice and cattle are minor. This observation prompted the current study.

In the enteric nervous system, substance P stimulates motility by increased cholinergic activity and influences electrolyte and fluid secretion, vascular and immune functions (Holzer, 1998). Local release of substance P can modulate or initiate an inflammatory response (Shanahan, 1998). Vasoactive intestinal peptide causes relaxation of smooth muscles and dysfunction of vasoactive intestinal peptide-mediated reflexes have been associated with impaired motility in inflammatory bowel diseases (Palmer and Koch, 1995; Collins, 1996; Sigge et al., 1998; Tomita et al., 2000) and enteropathy in mice infected with *Trypanosoma cruzi* (Maifrino et al., 1999). Vasoactive intestinal peptide also stimulates intestinal secretion and plays a role in secretory diarrhoeas (Hansen and Skadhauge, 1995). In the present investigation, immunohistochemistry was therefore used to study changes in the content of intrinsic non-cholinergic excitatory (substance P-containing) and non-adrenergic, non-cholinergic inhibitory (vasoactive intestinal peptide-containing) neural pathways in the large intestine of the pig during granulomatous inflammation caused by *S. japonicum* eggs. The observations were correlated with the severity of pathological lesions.

2. Materials and methods

Samples were obtained from three groups of Danish Landrace–Yorkshire crossbred pigs. The first group comprised five,18 week old pigs, infected i.m. with 1,000 *S. japonicum* cercaria each at 10 weeks old. The second group comprised of six, 19–20 week old pigs, offsprings of sows which were infected with 10,000 *S. japonicum* cercaria each at the 10th week of gestation of which four were challenge infected with 1,000 *S. japonicum* cercaria at 10 weeks of age and two were left unchallenged. Two pigs of the same age, and raised in the same environment, were used in the third group as non-infected controls.

Pigs were sedated by i.m. injection of 3.0 mg/kg Zoletil (zolazepam/tiletamin) and 2.0 mg/kg Narcoxyl (Xylasinum, NFN) and given heparin (500 IU/kg) i.v. Thirty minutes later, they were euthanised by an overdose of i.v. pentorbabitone (30 mg/kg) and immediately perfused to isolate *S. japonicum* worms as described earlier (Bøgh et al., 1997). Immediately after perfusion, the colon and caecum were cut open and examined for pathological lesions. Two pieces of tissue samples of about 4 × 3 cm from each compartment were collected from areas which grossly appeared to be (a) normal (b) lightly, (c) moderately, (d) severely and (e) very severely inflamed from each of the infected animals. They were immediately immersed in cold (4°C) 0.01 M PBS solution of pH 7.3. Each tissue was rinsed thoroughly using cold PBS and trimmed into two pieces of about 2 × 2 cm. Tissues were placed on polystyrene serosal surface down and pinned while being maximally stretched and subsequently fixed by immersion in 4.5% buffered formaldehyde for 1 h and thereafter, freed from polystyrene. One piece was trimmed to obtain two (0.5 × 2 cm) pieces which were transferred into fresh fixative for 7 days at 4°C, embedded in paraffin, sectioned and stained using H & E, Giemsa or toluidine blue stains for histopathological evaluation. The other piece was split further into two (1 × 2 cm) pieces, transferred in fresh fixative at 4°C for 47 h and thereafter processed for microdissection to obtain the mucous, submucous and myenteric plexuses as described earlier (Balemba et al., 1998). Freshly dissected wholemounts were stored in 0.1% sodium azide in 0.01 M PBS (pH 7.3) containing 0.5% Triton X-100, at 4°C. Prior to staining, tissues were washed 3 × 20 min each in 0.01 M PBS containing 0.5% Triton X-100 and thereafter overnight at 4 °C. Wholemounts prepared from the same piece of tissue were allocated for staining with either vasoactive intestinal peptide- or substance P-like immunoreactivities by the two step indirect streptavidin-ABComplex/HRP immunoenzymatic method was carried out as described by Balemba et al. (1998). For each incubation an overlap with tissues from previous incu-

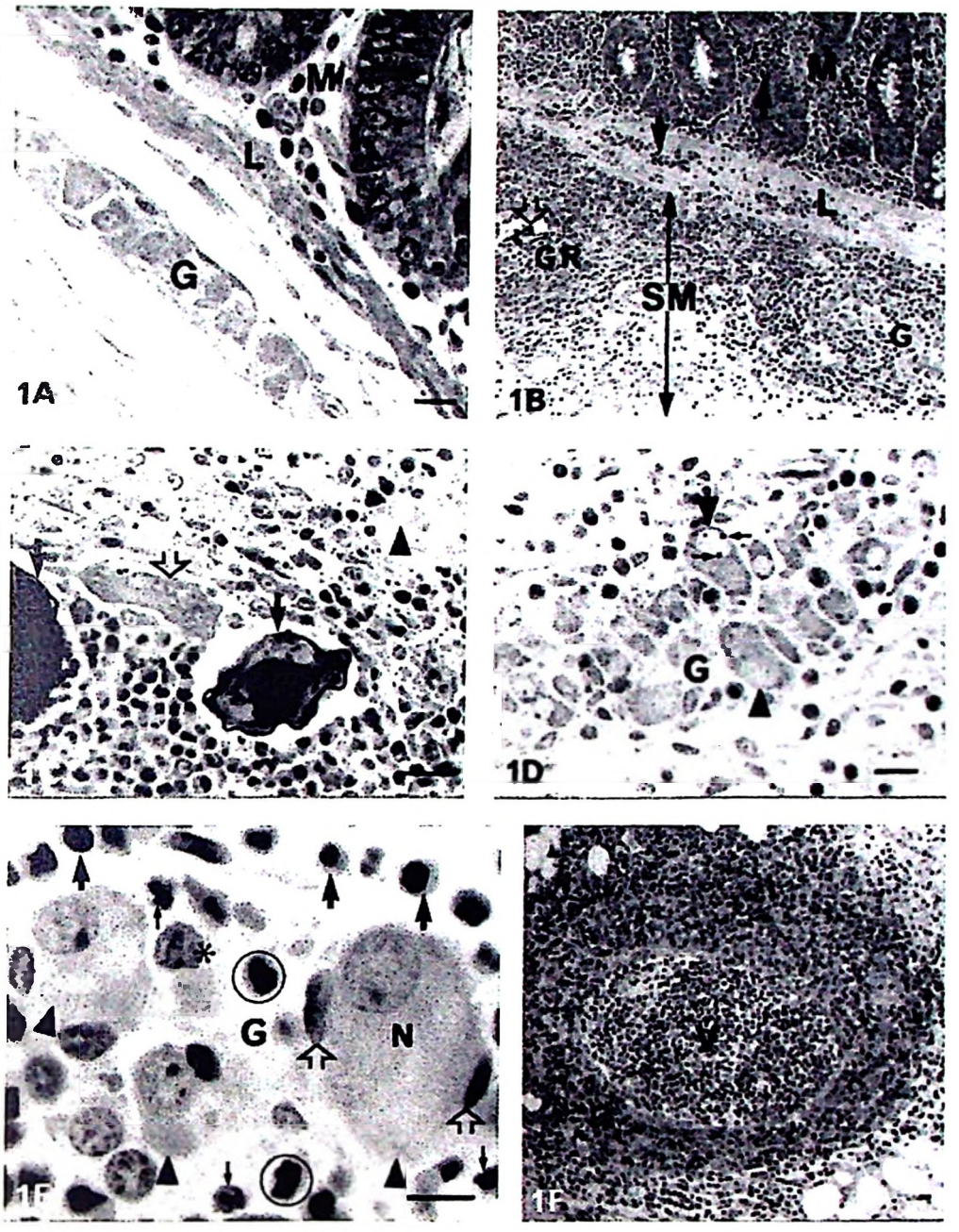

Fig. 1. (A) 5 μm, H & E, paraffin section from the caecum of the control pig showing a normal inner submucous plexus ganglion (G). (L) is lamina muscularis mucosa and (M) tunica mucosa. × 1,400. (B) 5 μm, H & E, paraffin section from the colon of a pig infected with *S. japonicum*. A granuloma (GR) in the submucosal (SM) layer is surrounding a dead egg (open arrow). A nearby inner submucous plexus ganglion (G) is surrounded and infiltrated by inflammatory cells. The mucosa (M) and lamina muscularis mucosa (L) which are thickened have a significantly increased number of inflammatory cells (arrows). × 150. (C) 5 μm, H & E, paraffin section, severely inflamed caecum from an infected pig showing a granuloma in the submucosal layer surrounding two intact *S. japonicum* eggs (arrows), a giant cell (open arrow) and other inflammatory cells (with dark nuclei). The arrow head shows a neuron which is a remnant of a ganglion in the inner submucous plexus that is being destroyed by the granuloma. × 1400. (D) 5 μm, Giemsa, paraffin section, severely inflamed caecum from an infected pig. A close up of the inner submucous plexus ganglion (G) in the periphery of the granuloma shown in (B). The ganglion has no clear cut boundaries and it is infiltrated by eosinophils, mast cells and lymphocytes. Some of the neurons (arrow heads) are enlarged having vacuolated cytoplasm and cramped and marginated chromatin (small arrows).Compare to (A). × 1400. (E) Close up of an inflamed inner submucous plexus ganglion (G) showing enlarged neurons (arrows heads). One neuron (N) is surrounded by satellite cells (open arrows) indicating 'satellitosis'. The ganglion is surrounded by a 'wreath' of inflammatory cells (larger arrows), others eosinophils (smaller arrows), mast cells (encircled) and a macrophage (asterisk) are seen inside a ganglion indicating ganglionitis. × 3000. (F). 5 μm, H & E, paraffin section, caecum of an infected pig. A submucosal vein (V) which is being occluded and destroyed by granulomatous inflammation. × 150.

bations were included in order to obtain the best evaluation. The specificity and sources of background staining were controlled by replacing the primary and secondary antibodies, and streptavidin-ABComplex/HRP with 5% non-immune swine serum. Monoclonal rabbit anti-swine-vasoactive intestinal peptide (1:1400) (VIP 8084-4) and rabbit anti-swine substance P (1:2000) (SP 250- 2) antibodies were kindly donated by Dr J. Fahrenkrug of Bispebjerg and Dr P.J. Larsen of Panum Institute, Copenhagen, Denmark, respectively.

The degree of pathological changes was defined as follows: (a) areas which appeared normal showed no obvious gross pathologic reaction, (b) lightly inflamed areas characterised by small, localised, multifocal haemorrhagic foci within the otherwise grossly normal intestinal mucosa, (c) moderately inflamed areas characterised by small, patchy,

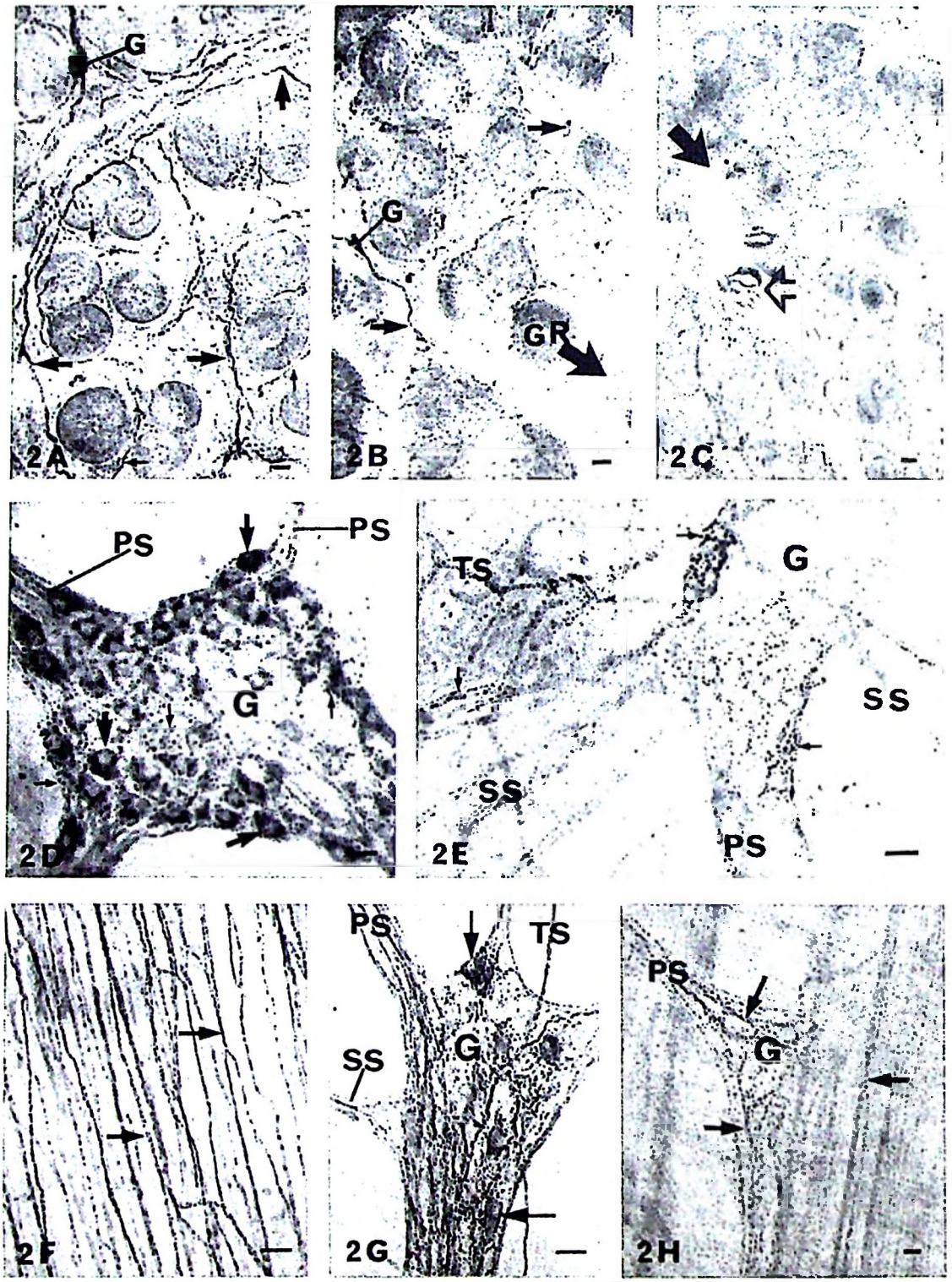

reddened, swollen, thickened and haemorrhagic mucosa, (d) severely inflamed areas were characterised by larger patches of reddened, swollen, thickened and haemorrhagic mucosa with or without necrotised areas and (e) very severely inflamed areas were in addition characterised by isolated blackish, necrotised areas which often exhibited fibrinous exudate and occasionally calcified, sandy-like materials at the centre. In these very severe cases, lesions could affect the entire thickness of the intestinal wall.

3. Results

3.1. Gross and histopathological lesions

There was variation among individual pigs in all groups with respect to severity of gross lesions. However, usually the cecum was the most affected and very severely affected areas covering up to the 2/3 of the mucosa in the caecum were seen in some cases. Within each intestinal segment there was great variation in the severity of changes. Major histopathological changes were recorded in the mucosal and submucosal layers (Fig. 1A–F). They included a significant diffuse increase in the number of eosinophils, lymphocytes and mast cells in all categories of tissues, and localised accumulations of a variable numbers of eosinophils and mast cells around the eggs or egg tracts. Accumulation of eosinophils, mast cells, lymphocytes, macrophages, giant cells and epithelioid cells was seen in the granulomas mainly in the moderately to severely inflamed tissues which were characterised also by oedema, thickening and necrosis of tissues especially in the mucosal, lamina muscularis mucosa and submucosal layers (Fig. 1B,C). Very severely inflamed tissues showed in addition eosinophil cell abscesses and/or composite granulomas. Walls of veins in the submucosa were infiltrated by eosinophils and in severe cases also by mast cells, lymphocytes and macrophages as lesions developed into granulomas which caused thrombosis and occlusion of vessels (Fig. 1F). Some veins had intact worms without signs of inflammation.

Visualised from the serosal side the enteric nervous system was comprised of the myenteric (Auerbach's) plexus and muscular plexuses in the tunica muscularis, the outer submucous (Schabadasch') plexus and inner submucous (Meissiner's) plexus in the submucosa (Fig. 1A,B,D) and the mucous plexus (Figs. 2A,B and 3A). The latter was composed of the sparsely ganglionated lamina muscularis mucosa, outer proprial and interglandular proprial subplexuses and the aganglionic internal proprial, perivascular, villous and subepithelial subplexuses (Balemba, personal observation).

All plexuses in the enteric nervous system were affected by the inflammation. The inner submucous plexus was the most affected followed by the mucous plexus. The outer submucous plexus was lesser affected whereas, the myenteric plexus was the least affected. In both the moderately and severely inflamed tissues, ganglia and nerve fibres in the mucous plexus, inner submucous plexus and the outer submucous plexus meshworks were either displaced or disrupted and or destroyed by granulomas. Lesser affected ganglia were surrounded by inflammatory cells forming a 'wreath' around them whereas, severely affected ganglia were infiltrated by eosinophils, mast cells, lymphocytes, plasma cells, neutrophils and macrophages (Fig. 1B–E). Some of the ganglia in the granulomas lacked the connective tissue and glial sheath and here only one or a few neurons were observed in the ganglia as they had lost some of the neurons (Fig. 1C). Other neurons were enlarged with vacuolated and eosinophilic cytoplasm, enlarged and vacuolated nuclei with marginated clumped chromatin into basophilic masses. Other nuclear reactions seen were central chromatolysis, extremely sparse and less intense chromatin and an increased number or absence of nucleoli all of which indicated early degeneration and/or death (Fig. 1D). Satellite cells surrounded enlarged neurons (satellitosis) whereas necrotic neurons were surrounded by macrophages indica-

Fig. 2. Wholemounts showing vasoactive intestinal peptide-like immunoreactivity in control and inflamed tissues. (A) Control tissue showing the nerve meshwork at the base of the crypts in the mucosal layer, mucosal ganglion (G) and intense and abundant vasoactive intestinal peptide-like immunoreactivity varicose nerves (larger arrows) in the interglandular proprial plexus (IGPP). Vasoactive intestinal peptide-like immunoreactivity varicose nerves in the glandular subepithelial plexus (GSEP) are shown by (smaller arrow). × 300. (B) Severely inflamed tissue from caecum showing a ganglion (G) in the IGPP and scarce interrupted vasoactive intestinal peptide-like immunoreactivity varicosities (smaller arrows) in the IGPP and GSEP. The large arrow points to the core of the granuloma (GR) which is also pointed at in (C). The intensity of vasoactive intestinal peptide-like immunoreactivity varicosities (smaller arrows) increases peripherally from the centre of the granuloma. × 300. (C) Details from the area pointed at in (B). Vasoactive intestinal peptide-like immunoreactivity varicosities are absent in core of and around the granuloma (solid arrow) which contains a cluster of *S. japonicum* eggs (open arrow). Compare (B and C) to (A). × 300. (D,E) Vasoactive intestinal peptide-like immunoreactivity in the inner submucous plexus. (D) Submucosal tissue from caecum of control pig. Vasoactive intestinal peptide-like neurons (larger arrows) and varicosities (smaller arrows) in the inner submucous plexus ganglion (G) are many and abundant. PS shows primary nerve strands. × 600. (E) Submucosal tissue from colon, severely inflamed tissue. Notice paucity of vasoactive intestinal peptide-like immunoreactivity neurons and scarcity of immunoreactivity varicosities which are interrupted (arrows) in the inner submucous plexus ganglion (G), primary (PS), secondary (SS) and tertiary nerve strands (TS). Compare with (D). × 600. (F–H) Vasoactive intestinal peptide-like immunoreactivity in the circular muscle and myenteric plexus. (F) Control tissue, colon showing abundant and intense vasoactive intestinal peptide-like immunoreactivity varicosities in nerve fibres in the inner circular smooth muscle layer (arrows). × 600. (G) Tissue from colon of control pig. Vasoactive intestinal peptide-like neurons (arrows) and abundant varicosities in the ganglion (G). PS shows primary nerve strands, (SS) secondary nerve strands and (TS) tertiary nerve strands. × 600. (H) Colon, very severely inflamed tissue. Notice reduced intensity and density of vasoactive intestinal peptide-like immunoreactivity neurons and immunoreactivity varicosities (arrows) in the ganglion (G) and primary (PS) nerve strand. The staining intensity and density of vasoactive intestinal peptide-like immunoreactivity varicosities in the inner circular smooth muscle layer are highly reduced. Compare with (F,G). × 300.

tive of neuronophagia (Fig. 1E). The myenteric plexus was infiltrated by eosinophils and mast cells.

3.2. *Vasoactive intestinal peptide-like immunoreactivity*

The density and staining intensity of vasoactive intestinal peptide-like immunoreactivities varicosities and neurons in tissues from infected pigs was negatively correlated with the severity of the lesions (Fig. 2A–H). In control pigs, vasoactive intestinal peptide-like immunoreactivity varicosities in nerve fibres and ganglia were intense and abundant in the mucous plexus, inner submucous plexus and outer submucous plexus. Immunoreactivity neurons were intensely stained and abundant in the inner submucous plexus, many in the outer submucous plexus and were sparse in the mucous plexus (Fig. 2A,D). In the myenteric plexus, there were a few immunoreactivity neurons but, abundant and intense nerve fibre immunoreactivity varicosities (Fig. 2G).

In tissues from infected pigs which grossly looked normal, there was no altered staining. In lightly and moderately inflamed tissues, the staining intensity of vasoactive intestinal peptide-like immunoreactivity in nerves and

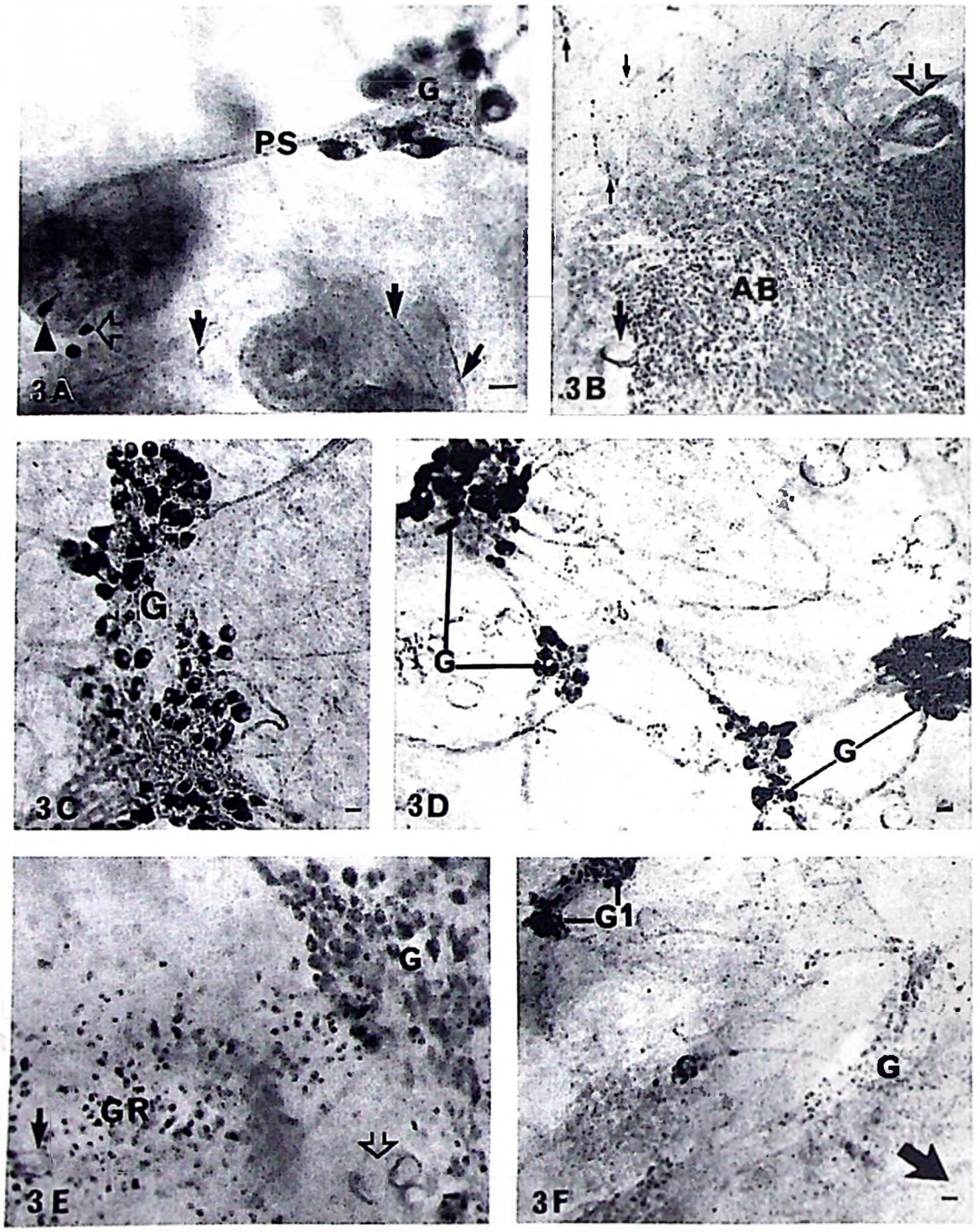

neurons in the mucous plexus, inner submucous plexus and outer submucous plexus was reduced but the density of immunoreactivity nerve fibres varicosities was comparable with that of control tissues (Fig. 2B). In severely inflamed tissues vasoactive intestinal peptide-like immunoreactivity neurons and varicosities in the inner submucous plexus and outer submucous plexus ganglia were greatly reduced (Fig. 2E). In the myenteric plexus there were foci where some ganglia showed depleted and reduced numbers of immunoreactivity neurons, however, nerve fibre varicosities and a few immunoreactivity neurons were intense and clear being similar to those of control tissues.

Within granulomas, eosinophil cell abscesses and areas with clumps of eggs in the severely inflamed tissues, there was absolutely no staining or highly reduced vasoactive intestinal peptide-like immunoreactivity in the mucous plexus, inner submucous plexus and outer submucous plexus (Fig. 2B,C,E). The meshworks of nerve fibres and ganglia in these plexuses were not detectable. The majority of the ganglia showed weak and scarce or isolated clusters of immunoreactivity varicosities and a paucity of immunoreactivity neurons and undetectable interconnecting nerve strands and boundaries. Vasoactive intestinal peptide-like immunoreactivity varicosities in nerve strands were either absent or very scarce and interrupted (Fig. 2B,E). There were scarce and weakly immunoreactivity nerve fibre varicosities and a few detectable ganglia and nerve fibres in the margins of the lesions. However, the staining intensity and abundance of varicosities in nerve strands increased peripherally into area which were less affected by inflammation (Fig. 2B,C). When the mucosal layer overlying the severely inflamed submucosal layer was less affected, there were weak, fairly abundant vasoactive intestinal peptide-like immunoreactivity nerve varicosities in the mucous plexus and the innermost ganglia of the inner submucous plexus. Where the entire intestinal wall was inflamed, immunoreactivity nerve fibre varicosities in the inner circular and outer longitudinal smooth muscle layers and the density and intensity of vasoactive intestinal peptide-like immunoreactivity varicosities and number of immunoreactivity neurons in the myenteric plexus were highly reduced compared with controls (Fig. 2F–H).

3.3. Substance P-like immunoreactivity

The density and staining intensity of substance P-like immunoreactivity varicosities and neurons in tissues from infected pigs correlated with lesion severity (Figs. 3A–H and 4A,B). Tissues from control pigs showed moderate to intense substance P-like immunoreactivity neurons and varicosities in a few ganglia and nerve strands respectively in the mucous plexus (Fig. 3A). In the submucosal layer, substance P-like immunoreactivity in neurons and varicosities were intense and abundant in the inner submucous plexus and many in the outer submucous plexus ganglia. Moderate, less intense immunoreactivity varicosities were seen in the primary and secondary nerve strands and scarce and weak varicosities in tertiary nerve strands which were not clearly apparent (Fig. 3C). In the myenteric plexus, substance P-like immunoreactivity was moderate, characterised by abundant smaller, less intense and fewer, larger, more intense varicosities which surrounded non-reactive neurons and very few and weakly staining immunoreactivity neurons (Fig. 4A).

In the macroscopically normal tissues, substance P-like immunoreactivity neurons and varicosities in the mucous plexus, inner submucous plexus, outer submucous plexus and myenteric plexus were not different from those of control pigs. In the lightly, moderately and severely inflamed tissues there was increased staining intensity and density of substance P-like immunoreactivity neurons and varicosities in the mucous plexus, inner submucous plexus and outer submucous plexus (Fig. 3C,D) as well as in the myenteric plexus where larger varicosities around non-reactive neurons became more prominent (Fig. 4A,B). There was an increase in the number of immunoreactivity small nerve fibres compared with control tissue (Fig. 3A,B). The

Fig. 3. (A,B) Substance P-like immunoreactivity in the mucous plexus. (A) Caecum, control pig. Substance P-like immunoreactivity neurons in a ganglion (G), and its primary nerve strands (PS) in the IGPP in the subglandular space close to the base of intestinal crypts. Arrows show varicose nerve fibres in the glandular subepthelial subplexus (GSEP). The open (arrow head) and closed (open arrow) types of enterochromaffin cell are also positive to substance P-like immunoreactivity. × 600. (B) Colon, severely inflamed tissue. Notice a composite granuloma composed mainly of an eosinophil cell abscess (AB) without any detectable substance P-like immunoreactivity. Fine varicose nerve fibres seen in the periphery (smaller arrows) are usually not detected in normal tissues (C) and lightly inflamed tissues. The open arrow shows an intact egg at the edge of the abscess and (large arrow) a dead egg within the abscess. × 300. (C–H) Substance P-like immunoreactivity in the inner submucous plexus. (C) Caecum, control pig. The inner submucous plexus ganglion (G) contains many intensely stained neurons. Varicosities in nerve fibres are scarce. × 300. (D) Colon, moderately inflamed tissue, inner submucous plexus. Ganglia (G) contain more intensely stained neurons compared to control tissue such that their nuclei are difficult to discern. × 300. (E) Colon, severely inflamed tissue. The inner submucous plexus ganglion (G) has weaker substance P-like immunoreactivity neurons. Small dark stained cells scattered all over and around a granuloma (GR) with some having infiltrated the ganglion are the non specific staining mast cells. The open arrow show a cluster of *S. japonicum* eggs and an arrow shows a dead egg. × 300. (F) Caecum, severely inflamed tissue showing variability in the staining intensity of substance P-like immunoreactivity neurons in the ganglia (G). An arrow points to an area within the core of the granuloma. More peripherally located ganglion (G1) has more intense neurons. × 300. (G) Caecum, very severely inflamed tissue. Notice an eosinophilic abscess (AB) without any substance P-like immunoreactivity, a cluster of *S. japonicum* eggs (open arrow) and highly reduced substance P-like immunoreactivity neurons and varicosities in the ganglia (G) and nerve strands (arrows) around the abscess. × 150. Compare with (C,D). (H) Caecum of prenatally/challenge infected pig, severely inflamed area. A worm in the submucosal vein is shown by thick arrows. Substance P-like immunoreactivity around the worm is highly reduced. A small inner submucous plexus ganglion (G) has very weak immunoreactivity neurons and no varicosities in nerve strands (fine arrows). × 150.

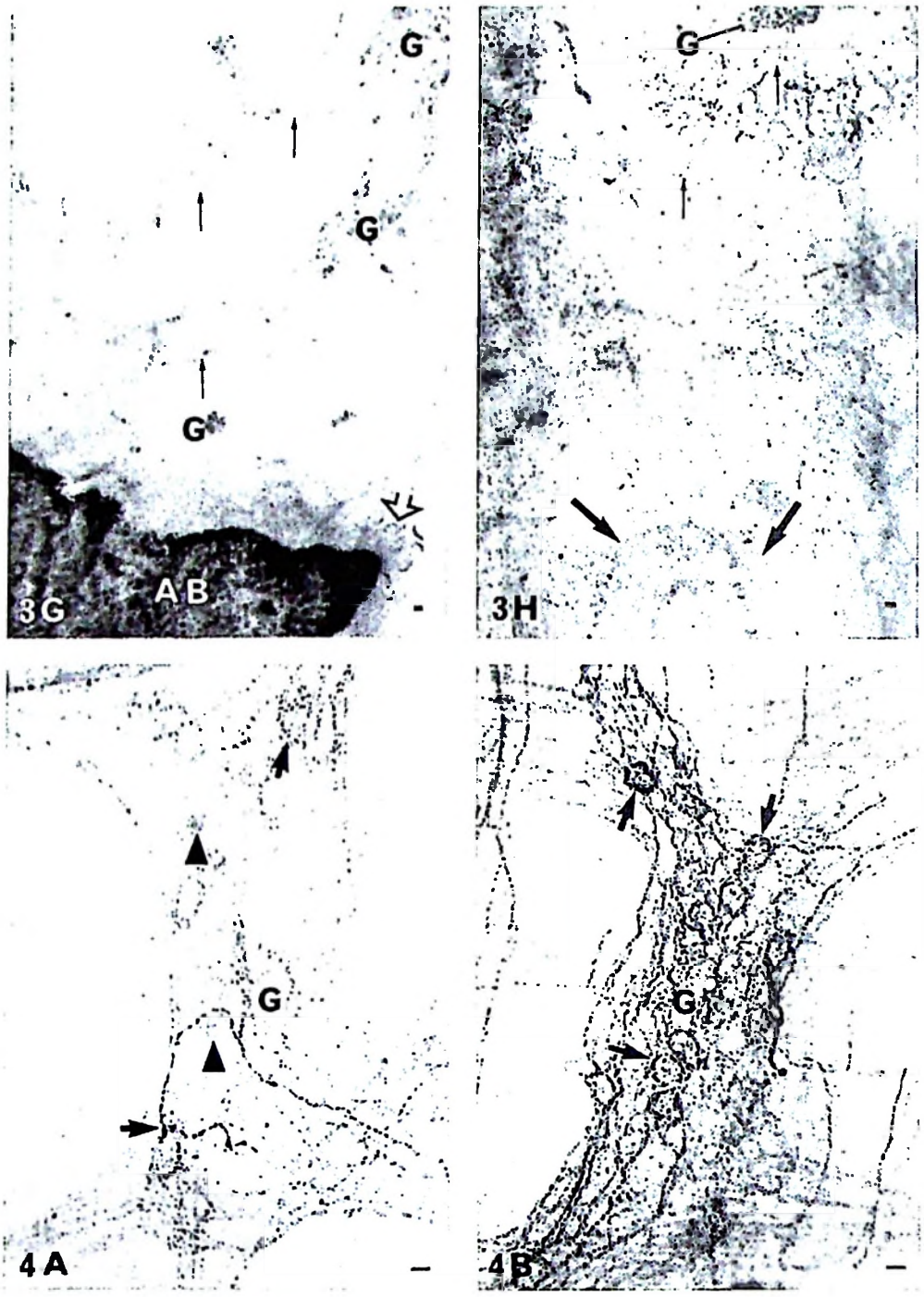

Fig. 4. (A,B) Colon, myenteric plexus. (A) Control pig, ganglion (G). Notice scarcity of substance P-like immunoreactivity varicosities in the ganglion and nerve strands. Large varicosities (arrows) are surrounding a few non reactive neurons and nerve fibres. A few, weak substance P-like immunoreactivity neurons are shown (arrow heads). × 300. (B) Severely inflamed tissue. otice increased number and staining intensity of substance P-like immunoreactivity varicosities in a ganglion (G) mostly around non reactive neurons (arrows). Compare with control (B). × 300.

staining intensity and density of immunoreactivity varicosities in the tertiary plexus, inner circular muscle, the outer longitudinal smooth muscle layers including taenia coli were also more intense and increased compared with immunoreactivity seen in control tissues. In moderately and severely inflamed tissues, the staining intensity of immunoreactivity varicosities and neurons was approximately twice as much as that of control tissues (Figs. 3C,D and 4A,B).

In the very severely inflamed tissues the number and staining intensity of substance P-like immunoreactivity neurons as well as the intensity and density of immunoreactivity varicosities in the mucous plexus, inner submucous

plexus and outer submucous plexus were highly reduced compared with control tissues (Fig. 3B,E–H). Small nerve strands were seen as pieces of interrupted varicosities. There was no immunoreactivity in eosinophil cell abscesses and composite granulomas (Fig. 3E,G). In the periphery of lesions, the number and intensity of substance P-like immunoreactivity neurons and varicosities were highly reduced with some ganglia having absolutely no immunoreactivity neurons. However, ganglia and nerve strands which were situated more peripherally showed increased staining (Fig. 3F,G). Clusters of *S. japonicum* eggs (5–30 eggs each) were seen regularly in severely inflamed areas and eosinophil cell abscesses. Some eggs were dead, others appeared to have been intact (Figs. 2C and 3B,E). Vasoactive intestinal peptide- and substance P-like immunoreactivity nerve fibres and ganglia in areas surrounding schistosome eggs and submucosal veins containing mature worms were highly reduced, even when there was no obvious macroscopic inflammation (Fig. 3H). Occasionally, inflammation was extensive affecting the muscle tunic. In such cases, focal areas showing depletion of substance P-like immunoreactivity corresponding to the size and severity of lesions were observed in the muscle tunic as well as in the myenteric plexus.

Tissues from both prenatally infected and prenatally infected and postnatally challenged pigs showed an increase in the number and staining intensity of immunoreactivity varicosities in all plexuses and a slight increase in the staining intensity of and the number of immunoreactivity neurons in ganglionated plexuses (Fig. 3H), when compared with tissues from pigs that had postnatal primary infection at 10 weeks. However, the nature and course of the reaction to schistosome eggs and worms in prenatally infected and or infected/challenged pigs, showed a similar pattern with respect to their vasoactive intestinal peptide- and substance P-like immunoreactivity changes which were correlated to the severity of histopathological lesions as seen in the primary postnatal infections described here (Table 1).

Substance P-like immunoreactivity was localised simultaneously in the enteric nervous system and a few 'open' and 'closed' types of enterochromaffin cells (Fig. 3A). Many cells were usually observed in light and moderately inflamed tissues compared to controls whereas, in severe lesions enterochromaffin cells stained weakly, and were fewer or absent. Many non specific staining mast cells were seen in inflamed areas in wholemounts which were stained for vasoactive intestinal peptide- and substance P-like immunoreactivity. They were diffusely distributed within and around granulomas and eggs. Occasionally, we observed focal, heavy mast cell infiltration around granulomas with intact eggs or egg tracts. Non-specific mast cells infiltrated into the ganglia, mainly in the inner submucous plexus, and were also in close proximity to nerve fibres especially in the inner submucous plexus and mucosal subplexuses (Fig. 3E).

4. Discussion

The nature, course and severity of the observed gross lesions caused by *S. japonicum* eggs in the pig are similar to those in rabbits (Cheever et al., 1980) and humans (Ying et al., 1990; Chen, 1991) in that the granulomas are focal, isolated and proliferative, affecting mainly the large intestine. Our observations on lesion histopathology are in agreement with other reports in pigs (Yason and Novilla, 1984; Hurst et al., 2000) in humans (Chen et al., 1978), in *S. bovis* infected calves (Balemba et al., 2000) and in the proximal colon (Varilek et al., 1991) and ileum (Bogers et al., 2000) of *S. mansoni* infected mice. The observation of enlargement of neurons, cytoplasm and nuclear changes are similar to those of Varilek et al. (1991) in the myenteric and submucous plexuses in the distal ileum and proximal colon of mice infected with *S. mansoni*. These observations are in agreement with observation of significant damage of enteric neurons in both the submucous and myenteric plexuses in

Table 1
Summary of the correlation of severity of inflammation and VIP- and SP-like immunoreactivities

	Vasoactive intestinal peptide				Substance P			
Level of pathology	MUC	ISP	OSP	MP	MUC	ISP	OSP	MP
Control	+++++[a]	+++++	+++ +	+++	++	+++ +	+++	++
Microscopically normal	+++++	+++++	+++ +	+++	++	+++ +	+++	++
Lightly inflamed	+++ +[b]	+++	+++	+++	+++	+++ +	+++ +	+++
Moderately inflamed	+++[c]	++	+++	+++	+++	+++++	+++ +	+++
Severely inflamed	++[d]	+[e]	++	++	+++	+++	+++	++
Very severe inflamation	+/−[f]	+/−	+/−	+/−	+/−	+/−	+/−	+/−

[a] +++++, Very intense and abundant IR.
[b] +++ +, Intense abundant IR.
[c] +++, Moderate IR.
[d] ++, Weak IR.
[e] +, Sparse IR
[f] +/−, very scarce/absent IR.

the ileum of mice infected with *S. mansoni*by Van Nassauw et al. (2001). The difference between our observations and those of rare neuronal cell death in the schistosome-infected mouse ileum by Bogers et al. (2000) and Van Nassauw et al. (2001) is probably due to differences in the severity of infections/lesions.

The features of increased inflammatory cells in tissues and their infiltration into ganglia is similar to those in calves infected with *S. bovis* (Balemba et al., 2000), in mice infected with *S. mansoni* (Bogers et al., 2000), in Crohn's disease (Szabo and Feher, 1991), in rats infected with *Nippostrongylus brasiliensis* (Arizono et al., 1994), and in mice infected with *Trichinella spiralis* (Galeazzi et al., 2000). Our findings support the hypotheses that increased immunological effector cells and their products are responsible for the changes in the neuronal elements (Szabo and Feher, 1991; Belai et al., 1997; Bogers et al., 2000; Galeazzi et al., 2000). The consequences of increased inflammatory cellular infiltration into ganglia in the enteric nervous system during schistosomosis are not yet fully understood.

Observations of changes in the staining intensity, density and number of vasoactive intestinal peptide- and substance P-like immunoreactivity varicosities and neurons correlating with severity of inflammation (Table 1) and increasing with distance away from the lesions are generally in accordance with those for mice (Varilek et al., 1991) and calves (Balemba et al., 2000). But, in contrast to the observations of increased vasoactive intestinal peptide-like immunoreactivity in granulomas (Varilek et al., 1991; Balemba et al., 2000), the present study showed a reduced immunoreactivity (depletion) of vasoactive intestinal peptide-like immunoreactivity in all plexuses of moderate to severely inflamed tissues; the reasons for this difference are not apparent. Our findings are, however, similar to findings in mice infected with *T. cruzi* (Maifrino et al., 1999), ulcerative colitis (Renzi et al., 1998), neonatal necrotising enterocolitis (Sigge et al., 1998) and horses with grass sickness (Bishop et al., 1984).

The finding of increased substance P-like immunoreactivity in all except severely inflamed tissues is in agreement with the observations in the ileum and colon of *S. mansoni* infected mice (Varilek et al., 1991), rats infected with *T. spiralis* (Swain et al., 1992) and in inflammatory bowel diseases (Shanahan, 1998, review). However, in the present study, we observed an increase in the density and staining intensity of substance P-like immunoreactivity varicosities in nerve strands and smaller fine nerve fibres in the submucosal layer of inflamed tissues compared with control. It is not yet clear whether increased substance P-like immunoreactivity varicosities was due to proliferation of nerve fibres or re-innervation of inflamed areas, as suggested by Miampamba and Sharkey (1998) during experimental colitis in rats.

Further, the observation of reduced substance P-like immunoreactivity in the most severely inflamed tissues and the absence of vasoactive intestinal peptide- and substance P-like immunoreactivity in eosinophil cell abscesses and composite granulomas is consistent with other reports in inflammatory bowel diseases such as *T. spiralis* infection in guinea pigs (Palmer and Koch, 1995) and rats (Hurst and Collins, 1994), colitis in rabbits (Eysselein et al., 1991), experimental ileitis in guinea-pigs (Miller et al., 1993) and human ulcerative colitis (Renzi et al., 1998). Decreased substance P levels have also been reported in horses with grass sickness where vasoactive intestinal peptide and substance P were virtually absent in the ileum (Bishop et al., 1984) and in *T. cruzi* infected mice (Maifrino et al., 1999). The finding of a significant reduction of vasoactive intestinal peptide- and substance P-like immunoreactivity in very severe lesions may be due to the observed degeneration and necrosis of neurons and nerve fibres such that production and transport of these peptides was impaired or because of an enhanced release from neurons and their nerve terminals. Neuronal damage and concomitant impairment of transmitter metabolism and or release could also have occurred as a result of cytotoxic substances and reactive oxygen metabolites released by activated eosinophils, lymphocytes, neutrophils, macrophages and mast cells (Dvorak, 1980; Sunoraha et al., 1989; Galeazzi et al., 2000; Van Nassauw et al., 2001), as eosinophils in schistosome granulomas produce neurotoxins (Durack et al., 1979). These inflammatory mediators may be part of the cause of the observed changes in vasoactive intestinal peptide- and substance P- like immunoreactivity, however the exact nature and effect remains to be elucidated.

In the present study, the inner submucous plexus and the mucous plexus were the most damaged, the outer submucous plexus was less affected and myenteric plexus was least affected which is consistent to the observations of Balemba et al. (2000) in calves infected with *S. bovis* but, different from those of Varilek et al. (1991) in mice. It has been shown that mucosal inflammation alters enteric neuromuscular function which may persist after recovery from infection and mucosal restitution (Collins, 1996; Barbara et al., 1997). Whether this phenomenon occurs after recovery in schistosomosis and what would be the consequences are uncertain.

The observation of reduced or absence of vasoactive intestinal peptide- and substance P-like immunoreactivity in nerve fibres and ganglia in areas around submucosal veins containing adult schistosome worms, and *S. japonicum* eggs even where there was no obvious inflammation, provided histologic evidence for a local, immediate proinflammatory response of neuronal vasoactive intestinal peptide and substance P in the defence mechanisms against these parasites. The finding of a higher number and intensity of vasoactive intestinal peptide- and substance P-like immunoreactivity varicosities in nerve fibres and neurons in biopsies from prenatally infected/challenged pigs compared to pigs that had primary infection signifies the role of neuronal substance P and vasoactive intestinal peptide in immune mechanisms.

Neurogenic plasticity and cellular reactions revealed by the present investigation support the proposition that damage to the mucosa and injury to enteric nervous system plexuses

could alter the regulatory functions of the enteric nervous system and enteroendocrine cells and play an important role in the pathogenesis of granulomas and diarrhoea seen in schistosomosis (Varilek et al., 1991; Balemba et al., 2000; Bogers et al., 2000; Van Nassauw et al., 2001)) and in causing the severe changes outlined in the introduction.

In the present study, substance P-like immunoreactivity was localised simultaneously in the enteric nervous system and a few 'open' and 'closed' types of enterochromaffin cells supporting the report that substance P is localised in enterochromaffin cells (Heitz et al., 1976). Continuous endoluminal secretion of 5-hydroxytryptamine from enterochromaffin cells occurs both in normal and pathological states (Schworer and Racke, 1991). Whether the observation of substance P-like immunoreactivity in bipolar enterochromaffin cells reflects endoluminal release of substance P is not known. The observation of increased substance P-like immunoreactivity enterochromaffin cells in light and moderately inflamed biopsies is similar to those seen in diabetic mice (Elsalhy and Spangeus, 1998) whereas, that of a reduced number or absence of enterochromaffin cells in severe lesions is apparently new information. The precise role of neuroendocrine cells in intestinal schistosomosis needs to be established.

The observation of many non-specific staining mast cells in granulomas and inflamed tissues compared with control tissues is in accordance to our earlier findings and interpretations based on results from calves infected with *S. bovis* (Balemba et al., 2000). The complex interactions between schistosome egg excretions, endothelial cells, fibroblasts, immune system cells, the enteric nervous system and epithelial cells may provide new information on the host-parasite relationship and an insight into the mechanisms of schistosome egg trapping, migration and egress through the intestinal wall, alterations in bowel motility and diarrhoea.

Acknowledgements

The authors wish to thank the Danish International Development Agency and Centre for Experimental Parasitology for funding the study. The kind donation of the monoclonal rabbit anti-swine vasoactive intestinal peptide by Dr J. Fahrenkrug and monoclonal rabbit anti-substance P by Dr P.J. Larsen, is warmly acknowledged. The technical assistance by Mrs G. Holden, H. Holm, A.M. Thomsen, B. Makatta and Mr M. Mukama and Mr M. Mwangalimi is highly appreciated.

References

Arizono, N., Yamada, M., Tegoshi, T., Okada, M., Uchikawa, R., Matsuda, S., 1994. Mucosal mast cell proliferation following normal and heterotopic infections of the nematode *Nippostrongylus brasiliensis* in rats. Acta Pathol. Microbiol. Et Immunol. Scand. 102 (8), 589–96.

Balemba, O.B., Grøndhal, M.-L., Mbassa, G.K., Semuguruka, W.D., Hay-Schmidt, A., Skadhauge, E., Dantzer, V., 1998. The organization of the enteric nervous system in the submucosal and mucosal layers of the small intestine of the pig studied by vasoactive intestinal peptide and neurofilament protein immunohistochemistry. J. Anat. 192, 257–67.

Balemba, O.B., Mbassa, G.K., Assey, R.J., Kahwa, C.K.B., Makundi, A.E., Hay-Schmidt, A., Dantzer, V., Semuguruka, W.D., 2000. Lesions of the enteric nervous system and the possible role of mast cells in the pathogenetic mechanisms of migration and egress of schistosome eggs in the small intestine of cattle during *Schistosoma bovis* infection. Vet. Parasitol. 90, 57–71.

Barbara, G., Vallance, B.A., Collins, S.M., 1997. Persistent intestinal neuromuscular dysfunction after acute nematode infection in mice. Gastroenterology 113, 1224–32.

Belai, A., Boulos, P.B., Robson, T., Burnstock, G., 1997. Neurochemical coding in the small intestine of patients with Crohn's disease. Gu 40 (6), 764–7.

Bishop, A.E., Hodson, N.P., Major, J.H., Probert, L., Yeats, J., Edwards, G.B., Wright, J.A., Bloom, S.R., Polak, J.M., 1984. The regulatory peptide system of the large bowel in equine grass sickness. Experientia 40, 801–6.

Bogers, J., Moreels, T., De Man, J., Vrolix, G., Jacobs, W., Pelckmans, P., van Marck, E., 2000. *Schistosoma mansoni* infection causing diffuse enteric inflammation and damage of the enteric nervous system in the mouse small intestine. Neuro Gastroenterology Motil. 12, 431–40.

Bøgh, H.O., Lee Willingham III, A., Johanson, M.V., Eriksen, L., Christensen, N.Ø., 1997. Recovery of *Schistosoma japonicum* from experimentally infected pigs by perfusion of liver and mesenteric veins. Acta Vet. Scand. 38 (2), 147–56.

Ch'ing-Fan, C., 1957. Schistosomiasis japonica of the colon complicated with carcinoma. Chin. Med. J. 75, 500–8.

Cheever, A.W., 1981. Schistosomiasis and colon cancer. Lancet 1 (8234), 1369–70.

Cheever, A.W., Duvall, R.H., Minker, R.G., 1980. Extrahepatic pathology in rabbits infected with Japanese and Philippine strains of *Schistosoma japonicum*, and the relation of intestinal lesions to passage of eggs in the feces. Am. J. Trop. Med. Hyg. 29 (6), 1316–26.

Chen, M.C., Wang, S.C., Chang, P.Y., Chuang, C.Y., Chen, Y.J., Tang, Y.C., Chou, S.C., 1978. Granulomatous disease of the large intestine secondary to schistosome infection. A study of 229 cases. Chin. Med. J. 91, 371–8.

Collins, S.M., 1996. The immunomodulation of the enteric neuromuscular function: implications for motility and inflammatory disorders. Gastroenterology 111 (6), 1683–99.

Durack, D.T., Sumi, S.M., Klebanoff, S.J., 1979. Neurotoxicity of human eosinophils. Proc. Natl. Acad. Sci. U.S.A. 76, 14431447.

Dvorak, A., 1980. Ultrastructural evidence for release of major basic protein-containing crystalline cores of eosinophil granules in vivo: cytotoxic potential in Crohn's disease. J. Immunol. 125, 460–2.

Elsalhy, M., Spangeus, A., 1998. Substance P in the gastrointestinal tract of non obese mice. Scand. J. Gastroenterology 33 (4), 394–400.

Eysselein, V.E., Reingen, M., Cominelli, F., Et, A.L., 1991. Calcitonin gene related peptide and substance P decrease in the rabbit colon during colitis. A time study . Gastroenterology 101, 1211–9.

Galeazzi, F., Haapala, E.M., Van Rooijen, N., Bruce, A., Vallance, B.A., Collins, S.M., 2000. Inflammation-induced impairment of enteric nerve function in nematode-infected mice is macrophage dependent. Am. J. Gastrointest. Liver Physiol. 278 (2), G259–65.

Giaroni, C., De ponti, F., Cosentino, M., Lecchini, S., Frigo, G., 1999. Plasticity in the enteric nervous system. Gastroenterology 117, 1438–58.

Hansen, M.B., Skadhauge, E., 1995. New aspects of the pathophysiology and treatment of secretory diarrhoea. J. Physiol. Res. 44, 61–78.

Heitz, P., Polak, J.M., Timson, C.M., Pearse, A.G.E., 1976. Enterochromaffin cells as the endocrine source of gastrointestinal substance P. Histochemistry 49, 343–7.

Holzer, P., 1998. Implications of tachykinins and calcitonin gene-related peptide in inflammatory bowel disease. Digestion 59 (4), 269–83.

Hurst, S.M., Collins, S.M., 1994. Mechanisms underlying tumor necrosis

factoralpha suppression of norepinephrine release from rat myenteric plexus. Am. J. Physiol. 266, G1123–9.

Hurst, M.H., Lee Willingham III, A., Lindberg, R., 2000. Tissues responses in experimental schistosomiasis japonica in the pig: a histopathologic study of different stages of low- or high-dose infections. Am. J. Trop. Med. Hyg. 62 (1), 45–56.

Johansen, M.V., Bøgh, H.O., Giver, H., Eriksen, L., Nansen, P., Stephenson, L., Knudsen, K.E.B., 1997. *Schistosoma japonicum* and *Trichuris suis* infections in pigs fed diets with high and low protein. Parasitology 115, 257–64.

Johansen, M.V., Iburg, T., Bøgh, H.O., Christensen, N.Ø., 2001. Postnatal challenge infections of congenitally *Schistosoma japonicum* infected piglets. J. Parasitol. In press.

Maifrino, L.B., Liberti, E.A., de Souza, R.R., 1999. Vasoactive intestinal peptide- and substance P-immunoreactive nerve fibres in the myenteric plexus of the mouse colon during the chronic phase of *Trypanosoma cruzi* infection. Ann. Trop. Med. Parasitol. 93 (1), 49–56.

Miampamba, M., Sharkey, K.A., 1998. Distribution of calcitonin gene-related peptide, somatostatin, substance P, and vasoactive intestinal polypeptide in experimental colitis in rats. Neuro Gastroenterology Motil. 10 (4), 315–29.

Miller, M.J.S., Sadowska-Krowicka, H., Jeng, A.Y., Et, A.L., 1993. Substance P levels in experimental ileitis in guinea pigs: effects of misoprostil. Am. J. Physiol. 265, G321–30.

Ming-Chai, C., Shan-Chi, C.W., 1957. Acute colonic obstruction in schistosomiasis japonica. A clinical study of 40 cases-14 associated with carcinoma . Chin. Med. J. 75 (7), 517–32.

Ming-Hsin, H., Shao-Chi, C., Cheng-Wei, L., Kuo-Juei, Y., Juei-P'eng, P., Ju-Sun, P., Pnag-Fu, K., 1957. Schistosomiasis dwarfism. Chin. Med. J. 75, 448–61.

Nai-Kuang, C., Pen-Chung, C., 1957. Pyloric obstruction and sigmoidal fistula due to schistosomiasis. Chin. Med. J. 75, 324–7.

Palmer, J.M., Koch, T.R., 1995. Altered neuropeptide content and cholinergic enzymatic activity in the inflamed guinea pig jejunum during parasitism. Neuropeptides 28, 287–97.

Renzi, D., Mantellini, P., Calabro, A., Panerai, C., Amorosi, A., Paladini, I.C.M., Salvadori, G., Garcea, M.R., Surrenti, C., 1998. Substance P and vasoactive intestinal polypeptide but not calcitonin gene-related peptide concentrations are reduced in patients with moderate and severe ulcerative colitis. Italian J. Gastroenterology Hepatol. 30 (1), 62–70.

Schworer, H., Racke, K., 1991. Regulation of serotonin release from intestinal mucosa. Pharmacol. Res. 23 (1), 23–25.

Shanahan, F., 1998. Enteric neuropathophysiology and inflammatory bowel disease. Neuro. Gastroenterology Motil. 10, 185–7.

Sharkey, K.A., Kroese, A.B.A., 2001. Consequences of intestinal inflammation on the enteric nervous system: Neuronal activation induced by inflammatory mediators. Anat. Rec. 262, 79–90.

Sigge, W., Wedel, T., Kühnel, W., Krammer, H.J., 1998. Morphologic alterations of the enteric nervous system and deficiency of non-adrenergic non-cholinergic inhibitory innervation in neonatal necrotizing enterocolitis. Eur. J. Pediatr. Surg. 8 (2), 87–94.

Sunoraha, N., Furukawa, S., Nishio, T., Mukoyama, M., Satayoshi, E., 1989. Neurotoxicity of eosinophils towards peripheral nerves. J. Neurol. Sci. 92 (1), 17.

Swain, M.G., Argo, A., Blennerhassett, P., Stanisz, A., Collins, S.M., 1992. Increased levels of Substance P in the myenteric plexus of Trichnella-infected rats. Gastroenterology 102, 1913–9.

Szabo, V., Feher, E., 1991. Ultrastructural changes in nerve elements in Chrohn's disease. Acta Chir. Hung. 32 (1), 25–32.

Tomita, R., Tanjoh, K., Fujisaki, S., Fukuzawa, M., 2000. Peptidergic nerves in the colon of patients with ulcerative colitis. Hepato. Gastroenterology 47 (32), 4000–4.

Van Nassauw, L., Bogers, J., Van Marck, E., Timmermans, J.-P., 2001. Role of reactive nitrogen species in neuronal cell damage during intestinal schistosomiasis. Cell Tissue Res. 303 (3), 329–36.

Varilek, G.W., Weinstock, J.V., Williams, H., Jew, J., 1991. Alterations of the intestinal innervation in mice infected with *Schistosoma mansoni*. J. Parasitol. 77, 472–8.

Warren, K.S., 1969. Intestinal obstruction in murine schistosomiasis japonica. Gastroenterology 57 (6), 697–702.

Yason, C.V., Novilla, M., 1984. Clinical and pathological features of experimental *Schistosoma japonicum* infection in pigs. Vet. Parasitol. 17, 47–64.

Ying, Y.Y., Lei, X.X., Yang, Y.Q., 1990. Pathology. In: Mao, S.P. (Ed.). Schistosome Biology and Control of Schistosomiasis, 1st Ed. People's Health Publishing House, Beijing, pp. 331–69.

MS Edelle Neylon
Elsevier Science Ireland Ltd.
Login Department,
Elsevier House
Brookvale Plaza
East park
Co. Clare
Ireland

Dear Madam,

RE: MANUSCRIPT PARA 1646: REPLY TO QUERIES AND/OR REMARKS

Thank you very much for your email, the proof (PARA 1646) and the query form. I am pleased to have the proof really fast as well as with good quality for illustrations.
Please, find out reply to the two queries, and a list of corrections/requests in the table below.
This document has been sent as attached file (word format) to ensure you get the correct table.
I shall be grateful, if possible, to have the legends to Figs. 2A-H, and 3A-F each, appearing in opposite pages ie. facing each other so that it easier for readers to follow the illustrations.

Queries and/or remarks Manuscript page/line	Details required	Authors Response
Page 14, line 13	Chen, 1991- missing reference	Please, delete Chen, 1991 at page 9, line 977 in the proof.
	Page numbers for Belai et al., 1997	Please, change page numbers in the proof at page 11, line1189 to 767-74.
Please, make these changes in the proof		
Page 2, line 222		Delete the words 'was carried out as' described by...
Page 3, line277 in legend		Please, put a space before the word 'Compare'..
Page 5, line 450		Delete 'were' before the word characterized....
Page5 line 453		Insert a word 'which' after ... areas
Page 5 line 491		Replace the term intergalndular with 'outer' and the letters IG in the abbreviation with O to read (OPP)
Page 5, lines 498- 504		Change all words reading immunoreactivity to immunoreactive
Page 6 lines 567, 570, 618, 622 and 623		Change the word immunoreactivity to immunoreactive
Page 7, line 675		Change the word immunoreactivity to immunoreactive, delete 's' in the word fibres.
Page 7, lines, 677, 682, 683, 693, 696, 698, 705-706		Change the word immunoreactivity to immunoreactive.
Page 7, line706		Insert a word 'fibre' after a word nerve
Page 7, line 715		Change the abbreviation IGPP to OPP
Page 7, lines 721-722		Change the word immunoreactivity to immunoreactive.
Page 7, lines 723-724		Change the word immunoreactivity to immunoreactive.
Page 7, lines 725-726		Change the word immunoreactivity to immunoreactive.
Page 7, lines 725-728		Move the legends to Figs. 3G-H to page 8 before that for Figs. 4A-B.
Page 7, lines 736, 739, 755, 760, 765		Change the words immunoreactivity to immunoreactive.

Page 8, lines 829-832		Change the word immunoreactivity to immunoreactive. Insert a letter 'N' after the word otice to read: Notice
Page 8, lines 890-896		Change the words immunoreactivity to immunoreactive.
Page 9, lines 903, 904, 911, 923, 925		Change the words immunoreactivity to immunoreactive.
Page10, line 1009		Replace the word by with 'with'.
Page10, lines 1031, 1053, 1113.		Change the words immunoreactivity to immunoreactive.
Page 11, line 1138		Change the word immunoreactivity to immunoreactive.
Page 11, lines 1187-1188	In the reference for Belai et al.	Replace the name for the Journal Gu with Gut

I do really hope that the information given here is enough for making corrections in the proof. Please, let me know just in case any addition information is required.

Yours sincerely,

Dr. Vibeke Dantzer

Paper VI

Neuronal nitric oxide synthase activity is increased during granulomatous inflammation in the colon and caecum of pigs infected with *Schistosoma japonicum*

O.B. Balemba[1], K. Mortensen[3], W.D. Semuguruka[2], A. Hay-Schmidt[4], M.V. Johansen[5], V. Dantzer[3]

Departments of Veterinary [1]Anatomy and [2]Pathology, Sokoine University of Agriculture, Morogoro, Tanzania. [3]Department of Anatomy and Physiology, The Royal Veterinary and Agricultural University, [4]Institute of Medical Anatomy, Copenhagen University, [5]Danish Bilharziasis Laboratory, Charlottenlund, Copenhagen, Denmark.

Address for correspondence:

Dr. Vet. Sci. Vibeke Dantzer, Department of Anatomy and Physiology, RVAU, Grønnegärdsvej 7, 1870 Frederiksberg C, Copenhagen, Denmark.

Telephone: 45+35282543, Telefax: 45+35282547

E-mail: *Vibeke.Dantzer@iaf.kvl.dk*

Abstract

Neuronal nitric oxide is a non-adrenergic non-cholinergic (NANC) neurotransmitter in the enteric nervous system (ENS) and plays a role in a variety of enteropathies including Crohn's and Chagga diseases, ulcerative colitis, diabetes, atrophy and hypertrophy. The content of neuronal nitric oxide synthase (nNOS) in the colon and caecum from pigs infected with *Schistosoma japonicum* was studied using immunohistochemical and histochemical staining for nNOS and nicotinamide adenine dinucleotide phosphate diaphorase (NADPH-d) respectively. In the infected pigs, lightly, moderately and less severely inflamed tissues showed increased nNOS and NADPH-d activities in neurons and nerve fibres in the enteric plexuses compared to control pigs. There was a significant increase in the numerical density of nNOS-like immunoreactive neurons in the inner submucous plexus, outer submucous plexus and in the myenteric plexus. More intensely stained neurons and varicosities were observed in tissue from prenatally infected and prenatally infected, postnatally re-infected pigs compared to postnatally infected pigs. However, the latter showed the highest numerical density of nNOS immunoreactive neurons. Marked increases were seen in the inner submucous plexus followed by the myenteric plexus, inner circular muscle, outer submucous plexus and the mucous plexus. However, in very severe inflamed tissues, the number and staining intensity of neurons and nerve fibre varicosities were reduced in plexuses located in the lesions with the inner submucous and mucous plexuses being the most affected. There was no staining in the nervous tissue within the eosinophilic cell abscesses and productive granulomas. The apparent plasticity of the activities of enzymes responsible for the generation of nitric oxide (NO) show possible alterations in the NO mediated NANC reflexes in the enteric nervous tissue. These alterations might contribute to impaired intestinal motility and absorption, and other pathophysiological conditions seen during *S. japonicum* infections.
Key words: Porcine, large intestine, *S. japonicum*, neuroplasticity, NOS, NADPH-d.

Introduction

Nitric oxide (NO) is involved in neuronal communication, regulation of blood flow and pressure, smooth muscle activity and intestinal motility, and modulation of immunity and inflammatory reactions, neuronal defence mechanism and regeneration of axons during injury (Grozdanovic et al., 1994; Schmidt and Walter, 1994; Robbins and Grisham, 1997; Belai et al., 1997; Sigge et al., 1998; Bredt, 1999). NO is generated intracellularly by an enzyme called nitric oxide synthase (NOS). The NOS catalysed reaction requires several co-factors including flavones, tetrahydrobiopterin and nicotinamide adenine dinucleotide phosphate (NADPH) for oxidation of L-arginine to NO and L-citrulline (Grozdanovic et al., 1994; Schmidt and Walter, 1994; Robbins and Grisham, 1997; Bredt, 1999).

Neuronal nitric oxide synthase (nNOS) has been detected at all levels in the intestine of the pig in a subpopulation of neurons and nerves using immunohistochemical and histochemical staining for NOS and NADPH diaphorase (NADPH-d) respectively (Krammer et al., 1992; Barbiers et al., 1993, 1994, 1995; Timmermans et al., 1994; Bogers et al., 1994). A direct correlation and co-localisation between immunohistochemical staining for bNOS immunoreactivitiy (IR) and NADPH-d histochemical staining was observed in the brain and peripheral nervous tissue in rats (Dawson et al., 1991) and in the nerve plexuses in the small intestine (Timmermans et al., 1994) and the large intestine (Barbiers et al., 1994) in the pig implying that both methods can be used to visualise bNOS-expression. Staining for NADPH-d activity has been suggested to be more useful than determination of NOS activity since there exists multiple isoforms of NOS in the gut (Koch et al., 1996).

In animals infected with *S. japonicum* the intestinal tract may be highly damaged by granulomatous inflammation causing diarrhoea, proliferation and disruption of the epithelium, bleeding, fibrosis and thickening of the submucosa and alteration of bowel motility which can lead to intestinal fistula, distortion, stricture and obstruction (Nai-Kuang et al., 1957; Chen et al., 1978; Yason and Novilla, 1984; Cheever, 1985; Wu, et al., 1999; Hurst et al., 2000). In addition, granulomas can displace and damage enteric nerves, neurons and ganglia (Varilek et al., 1991; Balemba et al., 2000). In mice infected with *S. mansoni*, enteric nerves and neurons showed increased staining intensity for NADH and vasoactive intestinal peptide (VIP) and cell death. The extent of injury was related directly to the number of granulomas (Varilek et al., 1991). In similar studies in the ileum of mice, Bogers et al. (2000) recorded ganglionitis with few apototic cells in the boundaries of ganglia in the myenteric plexus in the ileum. Van Nassauw et al., (2001) observed significant increase in the number of 3-nitrotyrosine-immunoreactive neurons (a biomarker of reactive nitrogen species) and of active caspase-3 (a key executioner of apotosis) in both the submucous and myenteric plexuses causing damage in a significant number of enteric neurons. However, neuronal cell death was rarely seen. In the colon and caecum from pigs infected with *S. japonicum*, the content of VIP in the ENS in the inflamed tissues was reduced. That of substance P (SP) was increased at lower levels of inflammation and decreased in severe lesions. The alterations of the levels of VIP, SP, correlated with severity of inflammation (Balemba et al., 2001). It has been suggested that injury to the enteric nervous system (ENS) may partly account for clinical and pathological features seen in schistosomosis (Varilek et al, 1991; Balemba et al., 2000; 2001; Bogers et al, 2000; Van Nassauw et al., 2001). However, studies of neuronal plasticity in the ENS in terms of release and expression of neurotransmitters, structural changes and cell death during schistosomosis are not adequate.

The highest levels of NO in the body are found in neurons (Bredt, 1999). Probably, plasticity of neuronal NOS plays a role in the inflammatory processes, immune mechanisms and enteropathy

seen in schistosomosis. The time of infection, duration and re-infection might also influence the NOS activity. In the present study, immunohistochemical and histochemical staining for NOS and NADPH-d activity respectively was used to study changes of neuronal NOS activity in the colon and caecum of the pig infected postnatally with *S. japonicum* as well as prenatally infected pigs with or without a postnatal challenge infection (Johansen et al., 2001).

Materials and methods

Samples were obtained from 13 Danish Landrace-Yorkshire crossbred pigs which were allocated into three groups. The first group included five,18 week (w) old pigs infected i.m. with 1000 *S. japonicum* cercariae each at 10 w of age. The second, prenatally infected group, comprised of six, 19 - 20 w old pigs, the offspring of sows which were infected with 10,000 *S. japonicum* cercariae each at the 10th w of gestation. In this group, four pigs were challenged (re-infected) with 1000 *S. japonicum* cercariae at 10 w of age and two were left unchallenged. Two, 18 w old pigs raised in the same environment were used in the third group, the control group.

Pigs were sedated by i.m. injection of 3.0 mg/kg Zoletil (even mixtures of zolazepam/tiletamin) and 2.0 mg/kg Narcoxyl (Xylasinum, NFN) and given heparin (500 IU/kg) intravenously. Thirty minutes later, they were euthanised by an overdose of intravenous pentobabitone (30 mg/kg) and subsequently perfused to isolate *S. japonicum* worms as described by Bøgh et al. (1997). Immediately after perfusion, the caecum and colon were cut open and examined for pathological lesions. Inflamed tissues were macroscopically classified as either, a) macroscopically normal showing no obvious gross pathologic reaction, (b) lightly inflamed tissues characterised by small, localised, multifocal haemorrhagic foci within the otherwise grossly normal intestinal mucosa, (c) moderately inflamed tissues characterised by small, patchy, reddened, swollen, thickened and haemorrhagic mucosa, (d) severely inflamed tissues characterised by larger patches of reddened, swollen, thickened and haemorrhagic mucosa with or without necrotized areas and (e) very severely inflamed tissues which were reddened, swollen, thickened with haemorrhagic patches covering fairly large areas which occasionally were up to two third of mucosal surface of the caecum. They had also isolated blackish, necrotized areas that often exhibited fibrinous exudate and occasionally calcified, sandy-like materials at the centre. Sometimes, lesions affected the entire thickness of the intestinal wall.

Two pieces of tissue segments of ~ 3cm^2 each were cut from macroscopically normal and inflamed areas (a - e above) from caecum and the proximal ascending colon. They were immersed in cold (4 °C) 0.01M phosphate buffered saline (PBS) (pH 7.3). Each tissue was rinsed briefly in cold PBS, trimmed to ~ 2cm^2, placed on a polystyrene serosal surface down and pinned while being

maximally stretched. Tissues were fixed by immersion in 4.5% buffered formaldehyde for 1 hr, freed from the polystyrene and split into two pieces. They were fixed in fresh fixative at 4°C for 47 hrs, processed for microdissection to obtain the mucous, submucous and myenteric plexuses as described elsewhere (Balemba et al., 1998). When the submucosal layer was highly thickened, it was meticulously dissected into two, the outer and inner submucosal layers. Freshly dissected wholemounts were stored in 0.1% sodium azide in 0.01M PBS (pH 7.3) containing 0.5% triton X-100, at 4 °C. Prior to staining, tissues were washed 3 x 20 minutes each in 0.01M PBS containing 0.5% triton X-100 and thereafter overnight in PBS at 4 °C. For each sample, tissues from one piece were stained for NOS-like immunoreactivity (IR) using polyclonal rabbit anti-rat cerebellar NOS (B220-1, Eurodiagnostica, Sweden) by the two step indirect streptavidin-ABComplex/HRP immunohistochemical method described by Balemba et al. (1998) and wholemounts evaluated and photographed by light microscopy.

Wholemounts from the second piece of tissues were stained for NADPH-d- activity by incubation in 0.1M TRIS/HCL (pH 7.2) containing 1mM β-NADPH (Sigma, St. Louise, MO, USA) and 0.2 mM nitro blue tetrazolium (Sigma), 0.2% triton x-100, 0.01% NaN_3 for 1 hour at 37 °C (Scherer-Singler et al., 1983). Reaction product of NADPH-d appeared as a dark blue granular deposit. After staining the tissues were washed in PBS and mounted in glycerol gelatine and examined directly by light microscopy. The evaluation of reactivity was not really blindfolded because tissues from infected and from control pigs were in both methods stained simultaneously and with an overlap of new pieces of tissue from animals whose tissues had been stained in the previous incubations. The degree of pathological reaction was both evaluated at the time of sampling, microdissection and during microscopical evaluation after staining. Findings were combined to classify tissues as being lightly, moderately, severely or very severely inflamed. The semi-quantification was done based on the staining intensity and occurrence of IR varicosities and neurons as detailed in the footnotes.

Controls: The specificity and sources of background staining were checked by substituting the primary and secondary antibodies with 5% nonimmune swine serum, for NADPH-d it was performed without adding NADPH.

Quantification of NOS IR neurons was done using wholemounts from three pigs for each group of animals studied. A set of fields of vision were examined under projection onto a table using a Leica DMLB microscope fitted with a projection arm at 20x objective (x333 total magnification). The counting was done using the unbiased counting frame (optical dissector) (Gundersen, 1978). With a random start, the projected image was systematically randomly sampled using a predetermined fraction of the sampling frame which was used as an unbiased sampling frame. Neurons completely

inside and those only intersecting the "inclusion" edges were counted, provided they in no way intersected the "exclusion" edges. By focussing though the tissue all neurons that fitted the counting rule were counted. Numerical densities were calculated based on the sampling fractions, the results were analysed for variance using Statistical Analysis Systems (edition 6, 1987) and significance was assumed at $P<0.05$.

Results

Lesions due to granulomatous inflammation against *S. japonicum* eggs and worms varied amongst infected pigs. Results of NOS IR and NADPH-d staining are summarised in table 1 and illustrated by Figs. 1a-d; 2a-h; 3a-d; 4a-d; 5a-c; 6a-f; 7a-d. Immunohistochemistry for NOS IR correlated well with histochemical staining for NADPH-d activity. However, neurons and nerve fibre strands were revealed better by staining for NADPH-d activity compared to NOS IR. In the tissues from control pigs (Figs. 1c; 2a-b; 3a; 4a; 5a; 6a; 7a) the staining revealed extremely scarce NOS IR and NADPH-d positive nerve fibres and weakly stained NOS and NADPH-d stained neurons in the outer proprial subplexus (OPP) and the interglandular proprial subplexus (IGPP) in the basal parts of the mucosa (Figs. 1c; 5a). Many moderately stained nerve fibres and extremely scarce IR neurons were seen in the lamina muscularis mucosae subplexus (LMMP). The inner submucous plexus (ISP) (Figs. 2a-b; 6a) showed variations in the staining pattern, intensity and number of both NOS IR and NADPH-d stained nerves and neurons. Moderate staining and more neurons were observed in the inner smaller ganglia and primary nerve strands located close to lamina muscularis mucosae (LMM) (Fig. 2d). The staining intensity was weak and stained neurons were sparse in the more externally located large ganglia and nerve strands (Fig. 2c). In the outer submucous plexus (OSP) there were many intensely stained NOS IR and NADPH-d positive neurons and varicosities giving a clear overview of ganglia, primary and secondary nerve strands (Figs. 3a; 6d). NOS IR nerve fascicles were many and intense in the inner circular muscle (ICM) but, few and sparse in the outer longitudinal smooth muscle (OLM) layers (Fig. 3c). In the myenteric plexus (Fig. 4a; 7a), there were many intensely and a few moderate stained NOS and NADPH-d positive neurons. Some of the neurons stained by NADPH-d showed intensely stained "spots or plaques" in the cytoplasm (not shown). In all plexuses NOS IR and NADPH-d positive neurons varied in sizes (small, medium and large) and staining intensity, with the majority of the small neurons being moderately stained.

In inflamed tissues the number and staining intensity of NOS IR and NADPH-d positive neurons and nerve fibres varicosities were increased in all plexuses in tissues which showed light, moderate and severe inflammation (Table 1). In the mucosa, NOS IR and NADPH-d revealed fairly more neurons and nerve fibres in the OPP and IGPP and many, intensely stained nerve fibres in the

LMMP (Figs.1d; 5b-c). The staining pattern and intensity of both NOS IR and NADPH-d in the ISP in tissues from infected pigs which appeared normal were similar to that of tissues from control pigs. However, an increased number and staining intensity of neurons and more intensely stained nerve fibre strands were seen in the ISP within the light, moderate and severe inflamed tissues (Table 1; Figs.2-f; 5b-c). The number and intensity of stained neurons varied depending on the size of the ganglion and its location in relation to the granulomas. Increased staining intensity was commonly encountered in the innermost, small to medium sized ISP ganglia situated close to lamina muscularis mucosae (LMM). Increased number and intensity of neurons and varicosities was also seen in the large ISP ganglia situated close to granulomas. Usually, large and medium sized neurons were intensely stained whereas, most small neurons stained moderately. Primary and secondary nerve strands were moderately stained. More ISP ganglia, neurons and nerve strands were visualised within the inflamed tissues compared to controls and apparently normal tissues from infected animals. Ganglia located close to granulomas had many and more intensely stained neurons and varicosities than those situated in the granulomas which had few and weakly stained neurons and varicosities (Figs. 2c-f; 6c). In severely inflamed areas, ISP ganglia showed reduced staining intensity and number of neurons and nerve fibres varicosities such that neurons and varicosities became very few and weak.

The pattern and course of staining to NOS IR and NADPH-d in the OSP and the myenteric plexus were similar to that in the mucous plexus and ISP. In moderate and less severe inflamed tissues there were increased number and staining intensity of neurons and varicosities in the ganglia, primary, secondary and tertiary nerve strands. However, NOS IR and NADPH-d positive neurons and varicosities in the myenteric plexus were even more abundant compared to OSP which showed more intensely stained neurons (Figs. 3a-b; 6e- f; 7b- c). In very severely inflamed tissues more and intense stained neurons and varicosities and isolated neurons in nerve strands were recorded in the myenteric plexus. Occasionally, in the myenteric plexus and ISP some of the neurons were enlarged showing foamy or vacuolated cytoplasm instead of "plaques" as seen in control tissues (Fig. 7d). The inner circular (ICM) and outer longitudinal (OLM) smooth muscle layers also exhibited an increased number and staining intensity of varicosities (Fig. 4d). Larger nerve fascicles in the ICM were more intense compared to small nerve strands. Often, eosinophil cell abscesses and composite granulomas were encountered in very severe inflamed tissues during acute inflammation. In these lesions, the ISP and OSP ganglia and associated nerves and the ICM situated close to the lesions showed marked reduction of staining intensity and number of stained neurons and nerve fibres varicosities. Where the entire intestinal wall was inflamed, NOS and NADPH-d staining intensity and number of positive neurons in the myenteric plexus within the lesion were reduced. There was no staining within the eosinophil cell abscesses and composite granulomas (productive stages) (Fig. not shown).

As the lesions became chronic, NOS IR and NADPH-d positive neurons and nerve fibres often stained more intensely in areas where multiple involutional granulomas were present. NOS IR varicosities were seen in the perivascular nerve fibres around proliferating blood vessels within the involuting granulomas.

In the present study, there was variation in the pattern and course of intestinal reaction to migrating schistosome eggs between individual pigs and between groups of experimental animals. The numerical densities of NOS IR neurons in the enteric plexuses of postnatally infected pigs were greater than those of prenatally infected/challenged pigs. However, comparing tissues of about the same level of inflammation, tissues from prenatally infected/challenged pigs showed more intensely stained NOS IR and NADPH-d positive neurons and varicosities in all plexuses compared to pigs which were infected postnatally. In all plexuses, usually, large neurons were very intensely stained while others were either intensely or moderately or weakly stained and small sized neurons were encountered more often in inflamed tissues compared to those from control pigs. Comparing the extent of damage of ganglia and nerve fibres, the ISP was the most damaged followed by the mucous plexus and OSP while the myenteric plexus was least affected. However, increased NOS and NADPH-d activities were most marked in the ISP followed by the myenteric plexus, OSP, muscular plexus in the ICM, OLM, lamina muscularis mucosae and lastly the OPP and IGPP in the mucous plexus.

In both the control and infected pigs, the highest numerical density (N_d) of NOS IR neurons was observed in the ISP followed by the myenteric plexus. The lowest N_d was seen in the OSP (Figs: 1, b). Compared to control pigs, highly significantly increases of the N_d were observed in all plexuses studied. The increase was most marked in the ISP, followed by the myenteric plexus and OSP. In both caecum and colon the highest Nd was observed in tissues from postnatally infected pigs compared to prenatally/challenge infected pigs (Figs. 8a- b).

Discussion

In the present study, we have shown an apparent plasticity of NOS/NADPH-d in the ENS during *S. japonicum* infection in the pig model and highlighted the differences among intestinal plexuses in responding to trauma caused by migrating schistosome eggs or their toxic excretions and subsequent inflammation. The description of the organisation and nomenclature of the ENS is according to earlier reports (Balemba et al., 1998; Timmermans et al., 1997, 2001). Our observations of the occurrence, variation in the size and distribution and arrangement of NOS IR and NADPH-d stained neurons and nerve fibres in the mucous plexus, ISP, OSP, myenteric and the muscular plexuses in tissues from control pigs are basically similar to earlier observations in the pig (Krammer

et al., 1992; Barbiers et al., 1993, 1994, 1995; Timmermans et al, 1994; Bogers et al., 1994). The detection of sparse, weakly stained NOS IR and NADPH-d positive neurons in the mucosa is new information. Our findings differ from those in human ileum which show complete absence of NOS IR neurons within the submucous plexuses and abundant NOS IR nerve fibres in the ICM and OLM (Dhatt and Buchan, 1994). The differences may be due variation between species as well as methodology and/or fixation time and antibodies used.

In the present study, there was an apparent increase in NOS/NADPH-d activities in the ENS in all plexuses in lightly, moderate and severely inflamed tissues and a significant increase of the numerical density of NOS IR neurons in the ISP, OSP and myenteric plexus. These findings support earlier observations of increased staining intensity for the NADH in the myenteric plexus in the ileum and colon of mice infected with *S. mansoni* (Varilek et al., 1991). However, we have provided a detailed account of variations in the plasticity of activities of NOS and NADPH-d among different enteric plexuses and shown that the activities were reduced in the nervous tissue located close to granulomas or completely absent in ganglia and nerves that became entangled by composite granulomas and eosinophil cell abscesses during acute inflammation. The extent of injury to the ENS varied between animals and was related directly to the location, number, size and confluence of granulomas in a particular region of the intestine. The ISP was the most damaged followed by the mucous plexus and OSP while the myenteric plexus was least affected. These findings are similar to the observations in the small intestine of calves (Balemba et al., 2000), colon and caecum of pigs (Balemba et al., 2001) and in the colon (Varilek et al., 1991) but not the ileum of mice where the myenteric plexus was the most damaged (Varilek et al., 1991; Bogers et al., 2000; Van Nassau et al., 2001). Marked increased activity was observed in the ISP followed by the myenteric plexus, OSP, muscular plexuses in the ICM, OLM and LMM, and lastly the OPP and IGPP in the mucosa. The reasons for such a variation pattern are not known. The observation of marked changes in the myenteric plexus although the lesions were mainly located in the mucous and submucous layers shows plasticity of NOS in the NANC pathways in the ENS plexuses distant from areas with active inflammation. The observations of higher number and more intensely stained neurons in small ISP ganglia located close to LMM compared to more externally located larger ISP ganglia supports the observations of two ISP subplexuses in the small intestine of the pig (Balemba et al., 1998).

Our findings of increased NOS and NADPH-d activities are congruous to observations in the myenteric plexus and nerve fibres of the ICM during Crohn's disease (Belai et al., 1997; Belai and Burnstock, 1999) and to observations in the ICM in the colon of rats during experimental *Trypanosoma cruzi* infection (Garcia et al., 1999). The present finding of reduced NOS/NADPH-d activities in neurons and nerve fibres located very close to very severe productive granulomas and

absence of IR within these lesions probably represent focal degeneration. These findings are similar to the observation of decreased NADPH-d activity in the myenteric and submucosal neurons and nerve fibres in the muscle layers seen in humans infected with *T. cruzi* (Ribeiro, 1998) and that of reduced NOS IR myenteric plexus and its absence in the submucous plexus and ICM in humans with neonatal necrotizing enterocolitis (Sigge et al., 1998). The findings of significantly increased numerical density of NOS IR neurons in the ISP, OSP and myenteric plexus are similar to those of Ekelund and Ekblad, (1999) in the myenteric ganglia in a model of intestinal atrophy using bypassed ileum in rats, and that of increased NADPH-d positive neurons in hypertrophic ileum in rats (Ekblad et al., 1998) and duodenum of rats with acute diabetes (Furlan et al., 1999). The numerical densities observed in control pigs (Figs. 8a-b), are greater than those obtained by Van Ginneken et al. (1998) in the duodenum of weaner pigs. Reasons for the differences are not clearly evident. It could be due to segmental variations in the size and density of ganglia. For instance, in the guinea pig the total number of neurons in the colon was observed to greater than the total number of neurons in the whole small intestine (Karaosmanoglu et al., 1996). The difference is in agreement with the opinion that numerical density from different laboratories are hard to compare and therefore, biological conclusions were drawn by combining both qualitative findings with numerical density and with greater precautions because initial sampling was 'intuitive' and the influences of stretch and shrinkage were not corrected for.

In the present study, there was an increase in the number of NOS IR and NADPH-d positive neurons in the mucous, submucous and myenteric plexuses with smaller sized neurons being visualised more frequently than in controls. An intriguing possibility is that probably in healthy conditions some of the neurons have the ability to synthesise NO but, do not produce it or they produce it at extremely low levels. *De Novo* synthesis of NOS and NADPH-d in a subpopulation of these neurons occurred in response to injury caused by inflammation so that NOS and NADPH-d activities were manifested in more neurons and nerve fibres as suggested by Klimaschewski et. (1996). Filogamo and Cracco (1995), and Shahanan, (1998) suggested the possibility of presence of reserve pool of potential stem cells capable of proliferating within the ganglia and nerve strands in the ENS. It is not clear whether the observed increase in the number of NOS IR neurons indicated activation and differentiation of the stem cells or not.

An increased production of NO convert this local messenger into a very toxic peroxynitrite and excess NO inhibits deoxyribonucleic acid synthesis, mitochondrial electron transport, and citric acid cycle (Moncada et al, 1991). Thus, the observed increase in NOS and NADPH-d may partly account for the observed increased 3-nitrotyrosine-immunoreactive neurons in mice (Van Nassauw et al., 2001) and degeneration and death of neurons seen in schistosomosis (Varilek et al., 1991;

Balemba et al., 2000; Van Nassauw et al., 2001). The observed variation of intestinal reaction between individual pigs and between groups of experimental animals indicate variation of immunity to schistosome infection between individuals and between postnatally and prenatally/challenge infected pigs. Incubation of guinea pig ileum and colon with prostaglandin E_2 (PGE_2) interleukin-1β caused a concentration-dependent increase in Fos immunoreactivity (IR). The proportion of in neurons expressing Fos-like IR varied between segments and between submucosal and myenteric plexuses suggesting a similar pattern for the variability of receptors for these mediators (Sharkey and Kroese, 2001). Our findings of significant differences in the densities of NOS IR neurons between different plexuses and between segments are similar findings in the guinea pig and support the contention that during inflammation, there is selective activation of the ENS neurons in distinct neuronal pathways (Sharkey and Kroese, 2001). The observation of a highly significant difference in the numerical densities of NOS IR neurons in the myenteric plexus between caecum and colon is probably due to segmental differences and variations in the severity of lesions as in the present study the caecum was the most affected. The observation of NOS IR and NADPH-d positive neurons and nerve fibres and NOS IR varicosities in nerve fibres in the perivascular areas of proliferating blood vessels within the involuting granulomas probably show involvement of NO in re-innervation and tissue repair during remodelling of granulomatous lesions.

Although, the injury to the ENS was mostly focal showing no evidence of generalised changes in the innervation, occasionally, the caecum exhibited extensive damage. The implications of these changes in the gut are probably related with the relative distribution of schistosome eggs and severity of lesions which vary markedly among intestinal segments and infected animals (Cheever, 1985). Moreover, the occurrence of multiple areas of focal injury to the ENS could have influence as extensive ones and may lead to serious intestinal dysfunction.

The new information provided by this study indicated hyperactivity of NO mediated NANC inhibitory innervation in the intestine in areas with moderate to severe inflammation and deficiency of NANC inhibitory innervation in very severely inflamed areas. This neurochemical plasticity may contribute to the development of functional dysmotility as an excessive production of nitric oxide may cause the persistent inhibition of contractions in the smooth muscle layers. Neuronal NO has been proposed to play a part in the mechanism of secretory diarrhoeas and in maintaining proabsorptive activity (Tamai et al., 1993; Hansen and Skadhauge, 1995; Izzo et al., 1998; Schirgi-Degen and Beubler, 1998). Therefore, our observations also show possible alteration of the neuronal NO mediated regulation of intestinal absorption. The observed changes may play a role in the mechanism of diarrhoea and loose faeces (Varilek et al., 1991; Balemba et al., 2000) and retarded growth

(Johansen et al., 2001) which are seen in schistosomosis.

Conclusions

The present findings of altered NOS and NADPH-d activities in the ENS plexuses show an apparent plasticity in the NO mediated NANC neuronal reflex pathways and therefore possible alterations in intestinal motility and absorption. Neuronal NO may have a significant role in neuro-immune interactions and intestinal pathology as well as in clinical manifestations during acute inflammation induced by schistosome eggs and later on tissue repair during dissolution of granulomas.

Acknowledgments

We thank the Danish International Development Agency and the Danish National Research Foundation for financial support. The kind donation of reagents for NADPH-d staining by Prof. L.-I. Larsson and technical assistance by H. Holm, G. Holden, A-M Thomsen, O. Mwangalimi, B. Makata and M. Mukama is highly appreciated. We thank Prof. B. Pakkenberg, and Dr. T. Bock for use of the Leica DMLB microscope and Prof. H.J.G. Gundersen for consultations. We are grateful to the late Prof. Peter Nansen for his noble support during this study.

References

Balemba, O.B., Grøndahl, M.-L., Mbassa, G.K., Semuguruka, W.D., Hay-Schmidt, A., Skadhauge, E., Dantzer, V., 1998. The organisation of the enteric nervous system in the submucous and mucous layers of the small intestine of the pig studied by VIP and neurofilament proteins immunohistochemistry. *J. Anat.* (192), 257-267.

Balemba, O.B., Mbassa, G.K., Assey, R.J., Kahwa, C.K.B., Makundi, A.E., Hay-Schmidt, A., Dantzer, V., Semuguruka, W.D., 2000. Lesions of the enteric nervous system and the possible role of mast cells in the pathogenetic mechanisms of migration and egress of schistosome eggs in the small intestine of cattle during *Schistosoma bovis* infection. *Vet. Parasitol.* 90, 57-71.

Balemba, O.B., Semuguruka, W.D., Hay-Schmidt, A., Johansen, M.V., Dantzer, V., 2000. The VIP- and SP-like immunoreactivities in the enteric nervous system of the pig correlate to the severity of pathological changes induced by *Schistosoma japonicum*. *International J. Parasitol.* (In press).

Barbiers, M., Timmermans, J-P., Adriaensen, D., De Groodt-Lasseel, M.H.A., Scheuermann D.W., 1995. Projections of neurochemically specified neurons in the porcine colon. *Histochem. Cell Biol.* 103, 115-120.

Barbiers, M., Timmermans, J-P., Scheuermann, D.W., Adriaensen, D., Mayer, B., De Groodt-Lasseel, M.H.A., 1993.Distribution and morphological features of nitrigenic neurons in the porcine large intestine. *Histochem.* 100, 27-34.

Barbiers M., Timmermans, J-P, Scheuermann, D.W., Adriaensen, D., Mayer, B., De Groodt-Lasseel, M.H.A., 1994. Nitric oxide synthase-containing neurons in the pig large intestine: topography, morphology, and visceralfugal projections. *Microsc. Res. Tech.* 29, 72-78.

Belai, A., Boulos, P.B., Robson, T., Burnstock, G., 1997. Neurochemical coding in the small intestine

of patients with Crohn's disease. *Gut* 40(6), 767-774.

Belai, A., Burnstock, G., 1999. Distribution and colocalization of nitric oxide synthase and calretinin in myenteric neurons of developing, ageing, and Crohn's disease human small intestine. *Dig. Dis. Sci.* 44(8),1579-1587.

Bogers, J.J., Timmermans J-P., Scheuermann, D.W., Pelckmans, P.A., Mayer, B., van Marck, E.A., 1994. Localisation of nitric oxide synthase in enteric neurons of the porcine and human ileocaecal junction. *Anat. Anz.* 176(2), 131-135.

Bogers, J., Moreels, T., De Man, J., Vrolix, G., Jacobs, W., Pelckmans, P., van Marck, E., 2000. *Schistosoma mansoni* infection causing diffuse enteric inflammation and damage of the enteric nervous system in the mouse small intestine. *Neurogastroenterol. Motil.* 12, 431- 440.

Bredt, D.S., 1999. Endogenous nitric oxide synthesis: biological functions and pathophysiology. *Free Rad. Res.* 31, 577-596.

Bøgh, H.O., Willingham, III A.L., Johansen, M.V., Eriksen, L., Christensen, N.Ø., 1997. Recovery of *Schistosoma japonicum* from experimentally infected pigs by perfusion of liver and mesenteric veins. *Acta Vet. Scand.* 38, 147-156.

Chen, M.C., Wang, S.C., Chang, P.Y., Chuang, C.Y., Chen, Y.J., Tang, Y.C, Chou, S.C., 1978. Granulomatous disease of the large intestine secondary to schistosome infection. A study of 229 cases. *Chin. Med. J.* 4(5), 371-378.

Cheever, A.W., 1985. Schistosoma japonicum: The pathology of experimental infection. *Exp. Parasitolol.* 59, 1-11.

Dawson, T.M., Bredt, D.S., Fotuhi, M., Hwang, P.M., Snyder, S.H., 1991. Nitric oxide synthase and neuronal NADPH diaphorase are identical in brain and peripheral tissues. *Proc. Natl. Acad. Sci.* USA. 88(17), 7797-7801.

Dhatt, N., Buchan A.M.J., 1994. Colocalisation of neuropeptides with calbidin D28k and NADPH diaphorase in the enteric nerve plexuses of normal human ileum. *Gastroenterol.* 107, 680-690.

Ekblad, E., Sjuve, R., Arner, A., Sundler, F., 1998. Enteric neuronal plasticity and a reduced number of interstitial cells of Cajal in hypertrophic rat ileum. *Gut* 42(6), 836-844.

Ekelund, K.M., Ekblad, E., 1999. Structural, neuronal, and functional adaptive changes in atrophic rat ileum. *Gut* 45(2), 236-245.

Filogamo, G., Cracco, C., 1995. Models of neuronal plasticity and repair in the enteric nervous system: a review. *Ital. J. Anat. Embryol.* 100 Suppl. 1,185-195.

Furlan, M.M., de Miranda Neto, M.H., Sant'ana, D.d., Molinari, S.L., 1999. Number and size of myenteric neurons of the duodenum of adult rats with acute diabetes. *Arq. Neuropsiquiatr.* 57(3B), 740-745.

Garcia, S.B., Paula, J.S., Giovannetti, G.S., Zenha, F., Ramalho, E.M., Zucoloto, S., Silva, J.S., Cunha, F.Q., 1999. Nitric oxide is involved in the lesions of the peripheral autonomic neurons observed in the acute phase of experimental *Trypanosoma cruzi* infection. *Exp. Parasitol.* 93(4), 191-197.

Gundersen, H.J.G., 1978. Estimators of the number of objects per area unbiased by edge effects. *Microsc. Acta* 81(2), 107-117.

Grozdanovic, Z., Brüning, G., Baumgarten, H.G., 1994. Nitric oxide-a novel autonomic neurotransmitter. *Acta anat.* 150, 16-24.

Hansen, M.B., Skadhauge, E., 1995. New aspects of the pathophysiology and treatment of secretory diarrhoea. *J. Physiol. Res.* 44, 61-78.

Hurst, M.H., Lee Willingham III A., Lindberg, R., 2000. Tissues responses in experimental schistosomiasis japonica in the pig: a histopathologic study of different stages of low- or high-dose infections. *Am. J. Trop. Med. Hyg.* 62(1), 45-56.

Izzo, A.A. Mascolo, N., Capasso, F., 1998. Nitric oxide as a modulator of intestinal water and

electrolyte transport. *Dig. Dis. Sci.* 43(8), 1605-1620.

Johansen, M.V., Iburg, T., Bøgh, H.O., Christensen, N.Ø., 2001. Postnatal challenge infections of congenitally *Schistosoma japonicum* infected piglets. *J. Parasitol. 2001* (In press).

Karaosmanoglu, T., Aygun, B., Wade, P.R., Gershon, M.D., 1996. Regional differences in the number of neurons in the myenteric plexus of the guinea pig small intestine and colon: an evaluation of markers used to count neurons. *Anat. Rec.* 244, 470-480.

Klimaschewski, L., Obermuller, N., Majewski, M., Bachmann, S., Heym, C., 1996. Increased expression of nitric oxide synthase in a subpopulation of rat sympathetic neurons after axotomy-correlation with vasoactive intestinal peptide. *Cell Tissue Res.* 285, 419-425.

Koch, T.R., Schulte-Bockholt, A., Otterson, M.F., Telford, G.L., Stryker, S.J., Ballard, T., Opara, E.C., 1996. Decreased vasoactive intestinal peptide levels and glutathione depletion in acquired mega colon. *Dig. Dis. Sci.* 41(7),1409-1416.

Krammer, H., Stach, W., Kühnel, W., Meyer, B., 1992. Occurrence and distribution of nitric oxide synthase-immunoreactive neurons in the submucosal plexus of the porcine small intestine. *Brain Res.* 577, 337-342.

Moncada, S., Palmer, R.J.M., Higgs, E.A., 1991. Nitric oxide: Physiology, Pathology and Pharmacology. *Pharmacol. Rev.* 43, 109-142.

Nai-Kuang, C., Pen-Chung, C., 1957. Pyloric obstruction and sigmoidal fistula due to schistosomiasis. *Chin. Med. J.* 75, 324-327.

Ribeiro, U. J.r., Safatle-Ribeiro, A.V., Habr-Gama, A., Gama-Rodrigues, J.J., Sohn, J., Reynolds, J.C., 1998. Effect of Chagas' disease on nitric oxide-containing neurons in severely affected and unaffected intestine. *Dis. Colon Rectum* 41(11), 1411-1417.

Robbins, R.A., Grisham, M.B., 1997. Molecules in focus: nitric oxide. *Int. J. Biochem. Cell Biol.* 29, 857-860.

Scherer-Singler, U., Vincent, S.R., Kimura, H., McGeer, E.G., 1983. Demonstration of a unique population of neurons with NADPH-diaphorase histochemistry. *J. Neurosci. Methods* 9(3), 229-234.

Schirgi-Degen, A., Beubler, E., 1998. Proabsorptive properties of nitric oxide. *Digestion* 59(4), 400-403.

Schmidt, H.H.H.W., Walter, U., 1994. NO at work. *Cell* 78, 919-925.

Shahanan, F., 1998. Enteric neuropathology and inflammatory bowel disease. *Neurogastroenterol.* 10, 185-187.

Sharkey, K.A., Kroese, A.B.A., 2001. Consequences of intestinal inflammation on the enteric nervous system: Neuronal activation induced by inflammatory mediators. *Anat. Rec.* 262, 79-90.

Sigge, W., Wedel, T., Kühnel, W., Krammer, H.J., 1998. Morphologic alterations of the enteric nervous system and deficiency of non-adrenergic non-cholinergic inhibitory innervation in neonatal necrotizing enterocolitis. *Eur. J. Pediatr. Surg.* 8(2), 87-94.

Tamai H., Gaginella, T.S., 1993. Direct evidence for nitric oxide stimulation of electrolyte secretion in the rat colon. *Free Rad. Res. Comms.* 19 (4), 229-239.

Timmermans, J.-P., Barbiers, M., Scheuermann, D.W., Bogers, J.J., Adriaensen, D., Mayer, B., De Groodt-Lasseel, M.H.A., 1994. Distribution pattern, neurochemical features and projections of nitrigenic neurons in the pig small intestine. *Ann. Anat.* 176, 515-525.

Timmermans, J.-P., Adriaensen, D., Cornelissen, W., Scheuermann, D.W., 1997. Structural organisation and neuropeptide distribution in the mammalian enteric nervous system, with special attention to those components involved in mucosal reflexes. *Comp. Biochem. Physiol.* 118A(2), 331-340.

Timmermans, J.-P., Hens, J., Adriaensen, D., 2001. Outer submucous plexus: An intrinsic nerve network involved in both secretory and motility processes in the intestine of large

mammals and human. *Anat. Rec.* 262, 71-78.

Van Ginneken, C., Van Meir, F., Sommereyns, G., Sys, S., Weyns, A., 1998. Nitric oxide synthase expression in enteric neurons during development in the pig duodenum. *Anat. Embryol.* 198, 399-408.

Van Nassauw, L., Bogers, J., Van Marck, E., Timmermans, J.-P., 2001. Role of reactive nitrogen species in neuronal cell damage during intestinal schistosomiasis. *Cell Tissue Res.* 303(3), 329-36.

Varilek, G.W., Weinstock, J.V., Williams, T.H., Jew, J., 1991. Alterations of the intestinal innervation in mice infected with *Schistosoma mansoni*. *J. Parasitol.* 77, 472-478.

Wu, T.S., Chen, T.C., Chen, R.J., Chiang, P.C., Leu, H.S., 1999. *Schistosoma japonicum* infection presenting with colon perforation: case report. *Changgeng Yi Xue Za Zhi* 22(4), 676-681.

Yason, C.V., Novilla, M., 1984. Clinical and pathological features of experimental *Schistosoma japonicum* infection in pigs. *Vet. Parasitol.* 17, 47-64.

Table 1.

Table 1. Summary of the correlation of severity of inflammation with NOS IR and NADPH-d positive staining

Level of pathology	NOS IR						NADPH-d staining					
	OPP	LMMP	ISP	OSP	ICM	MP	OPP	LMPP	ISP	OSP	ICM	MP
Control	+/-	+(+)	+(+)	++(+)	++	++(+)	+/-	+(+)	+(+)	++(+)	++	++(+)
Microscopically normal	+/-[1]	+(+)	+(+)	++(+)	++	++(+)	+/-	+(+)	+(+)	++(+)	++	++(+)
Lightly inflamed	+[2]	+(+)[3]	++[4]	++(+)	++(+)	+++	+	+(+)	++	++(+)	++(+)	+++
Moderately inflamed	+	++	++(+)[5]	+++[6]	+++	+++(+)[7]	+	++	++(+)	+++	+++	+++(+)
Severely inflamed	+	++(+)	+++	+++(+)	+++	++++[8]	+	++(+)	+++	+++(+)	+++	++++
Very severely inflamed	+/-	+/-	+/-	+/-	+/-	++	+/-	+/-	+/-	+/-	+/-	++

[1] Very scarce/absent positive staining

[2] Sparse and weak staining

[3] Moderate staining

[4] Moderate to intense staining

[5] Intense staining

[6] Intense staining with many varicosities

[7] Very intense staining

[8] Very intense staining with abundant varicosities

Figures and legends

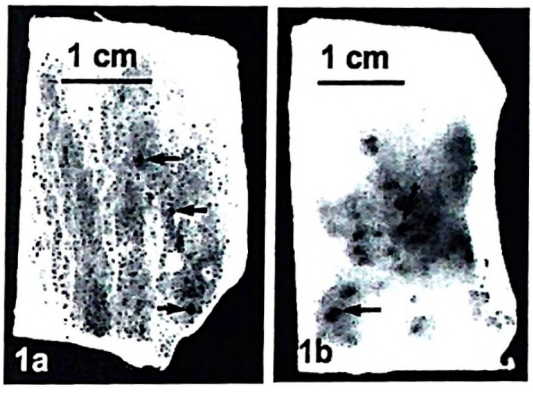

Figs. 1a - b. Gross lesions in the tissues studied. 1a. Caecum, showing diffuse multifocal haemorrhagic foci (arrows) in a less severely inflamed piece of tissue. x 1.2. 1b. Colon, showing a fairly large, less severely inflamed, focal haemorrhagic lesion (arrows) and macroscopically normal area around it. x 1.2.

Figs.1c - d. NOS IR in the mucous layer. 1a. Mucosal wholemount, caecum, control pig, showing the outer proprial subplexus (OPP) in the subglandular region. Notice moderate NOS IR in neurons (arrows) in a ganglion (G) and scarce varicosities in a nerve strand (arrow heads). (C) shows intestinal crypts. x 240. 1b. Mucosal wholemount, less severely inflamed caecum, postnatal infection, showing increased staining intensity of NOS IR in the nerve (arrow head) and a ganglion (G) with moderate to intense IR neuron in the OPP. (C) shows intestinal crypts. x 240.

Figs.2a - g. NOS IR in the ISP of control and infected pigs. 2a-b. Show IR in control pigs. Most of the neurons stained weaker and IR varicosities are weaker and sparse. 2a. Caecum, small (g) and large (G) ganglia in the ISP. NOS IR neurons (arrow) and nerve strands (arrow heads). x 96. 2b. NOS IR in a ganglion (G) with a few intense IR neuron (arrows) and varicosities. x 240. 2c. Severely inflamed caecum, postnatally infected pig. Notice, increased staining intensity and number of in NOS IR neurons (arrow) as well as IR varicosities in the ganglion (G). x 240. 2d. Moderate inflamed colon, prenatally infected, postnatally challenged pig. Notice, increased staining intensity of NOS IR neurons (arrow) and increased staining intensity and density of IR varicosities in two small ISP ganglia (g). x 240. 2e. Severely inflamed caecum, prenatally infected, postnatally challenged pig. A small ISP ganglion (g) located close to a granuloma (GR) has intense NOS IR neurons, nerve strands could not be visualised. x 240. 2f. The ISP ganglion (in a square) in the margin of an involuting granuloma (GR), severely inflamed colon, postnatally infected pig. Notice, moderate staining intensity of NOS IR neurons. Nerve strands could not be visualised. x 96. 2g. An insert showing the close up of the IR neurons in the ganglion in a square in Fig. 2e. x 240. (Compare 2a-b with 2c-g). 2h. A close up of an area shown by arrow within the involuting granuloma (Fig. 3f) showing NOS IR in the perivascular nerves (arrows). x 384.

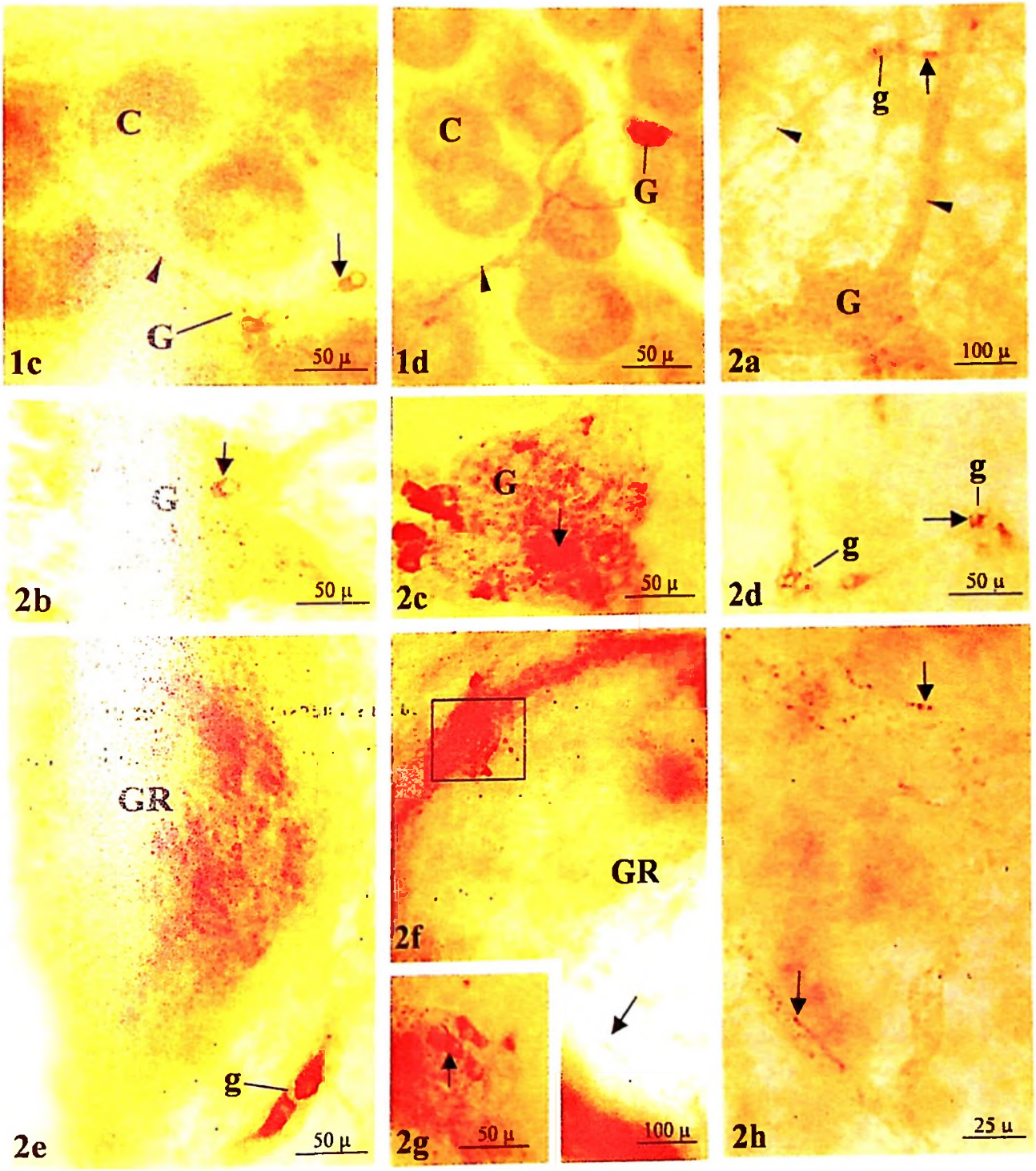
C
G
50 µ
1c
C
G
50 µ
1d
g
G
100 µ
2a
G
50 µ
2b
G
50 µ
2c
g
g
50 µ
2d
GR
g
50 µ
2e
GR
2f
50 µ
2g
100 µ
25 µ
2h

Figs. 3a - b. NOS IR in the OSP. 3a. Caecum, control pig, a small OSP ganglion (G) with fairly many intense IR neurons (arrow). Arrow head shows a primary nerve strand. x 300. 3b. Caecum, prenatally infected, postnatally challenged pig. A small OSP ganglion (G) has many, intensely stained NOS IR neurons (arrows). x 96. Figs. 3c - d. NOS IR in the ICM, colon, control and prenatal infected, postnatally challenge infected pig. x 240. 3c. ICM, control pig showing moderate to intense stained nerve fascicles (arrows) compared to Fig. 3d, which shows increased staining intensity of IR varicosities in similar fascicles (arrows). Figs. 4a - b. NOS IR, myenteric plexus. 4a. Colon, control pig, showing many intense and a few moderate IR neurons in the ganglion (G). x 96. Fig. 4b. Colon of postnatally infected pig showing increased staining intensity of IR neurons in a similar ganglion (G). Arrow heads show primary nerve strands. x 96.

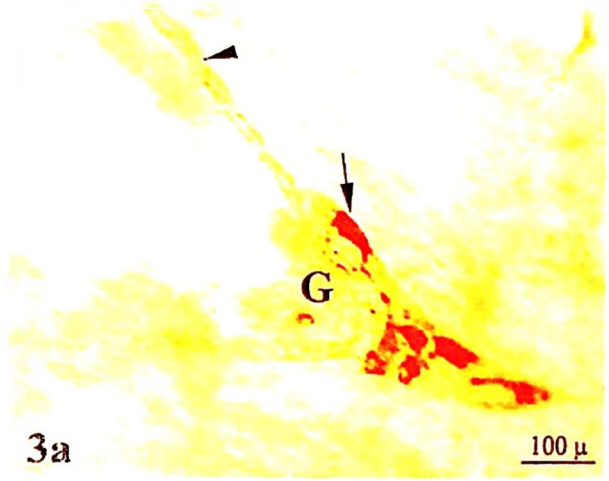
G
3a
100 µ

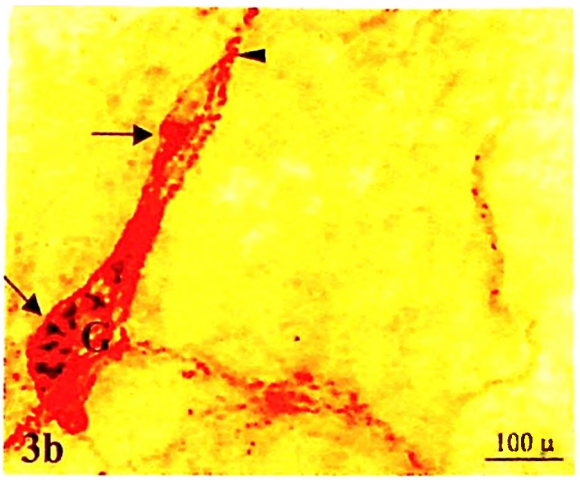
G
3b
100 µ

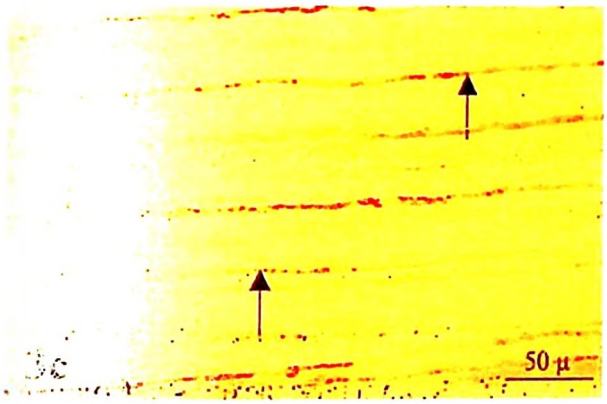
50 µ

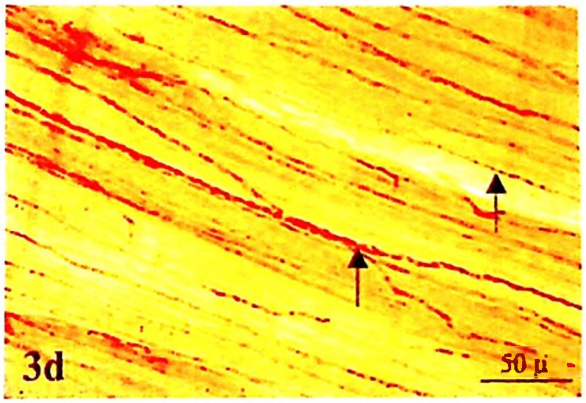
3d
50 µ

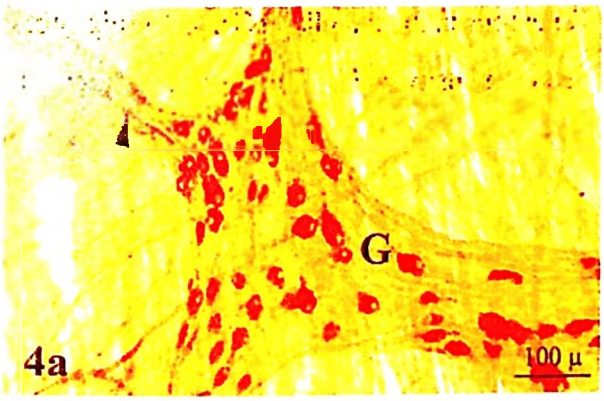
G
4a
100 µ

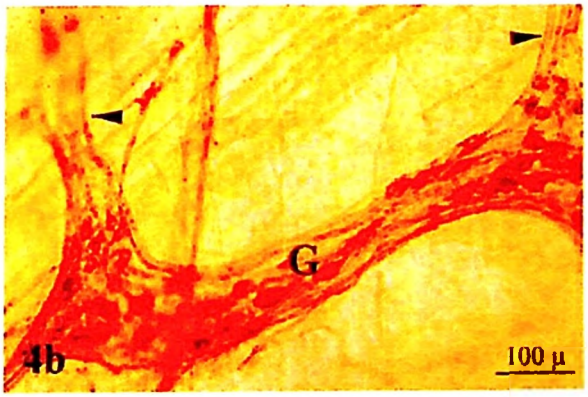
G
4b
100 µ

Figs. 5a - c. NADPH-d staining in the mucosa of control and infected pigs. 5a. Caecum, control pig showing localised weak stained neurons (arrows) in the OPP. Nerve fibres are not revealed. Intestinal crypts are labelled (C). x 240. 5b. Caecum, postnatally infected pig showing more intensely stained neurons (arrows) in the OPP in moderately inflamed tissue. Intestinal crypts are labelled (C). x 96. 5c. Colon, postnatally infected pig showing an isolated intensely stained neuron (arrow) in a nerve strand in the IGPP close to a granuloma (arrow head) in severely inflamed tissue. C, shows intestinal crypts. x 240. (Compare 5a with 5b-c).

Figs. 6a-f. NADPH-d, submucous plexuses. 6a. Caecum, control pig showing weak stained neurons (arrows) in two small ISP ganglia (g) after incubation for 2½ hrs. Nerve strands were not revealed. x 240. 6b. Colon, postnatally infected pig showing more and intensely stained neurons (arrows) in the ISP ganglion (G) in a moderately inflamed tissue after incubation for 1½ hrs. x 240. 6c. Colon, postnatally infected pig showing more and intensely stained neurons (arrows) in the ISP ganglion (G) in a severely inflamed tissues after incubation for 1½ hrs. Arrow head show adipocytes. x 240. (Compare 6a with 6b-c). 6d. Colon, control pig showing many but moderately stained neurons (arrows) in the OSP ganglion (G) after incubation for 1½ hrs. Arrow heads show adipocytes. x 96. 6e. Colon, prenatally infected, postnatally challenge infected pig. Severely inflamed tissue showing more intensely stained neurons (arrow) in the OSP ganglion (G) after incubation for 1 hr. Arrows heads show adipocytes. x 96. 6f. Caecum, prenatally infected, postnatally challenged infected pig. Severely inflamed tissue showing dark intensely stained neurons (arrow) in the OSP ganglion (G) after incubation for 1 hrs. x 96. (Compare 6d with 6e-f).

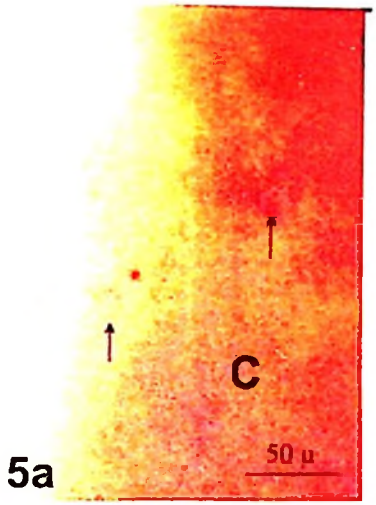

5a

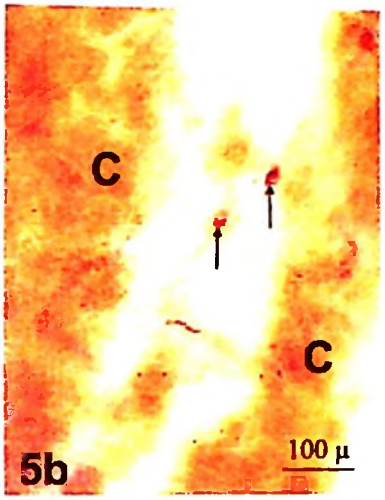

5b

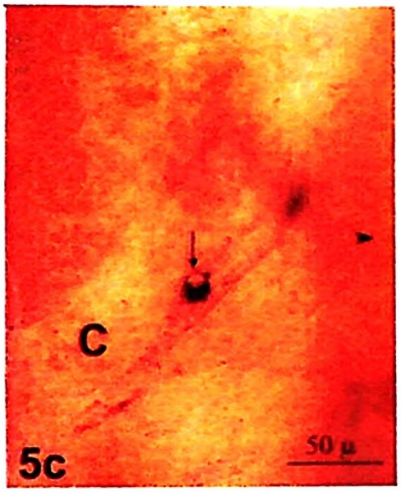

5c

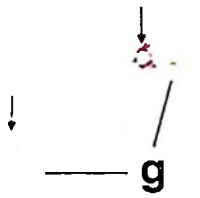

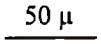

6a

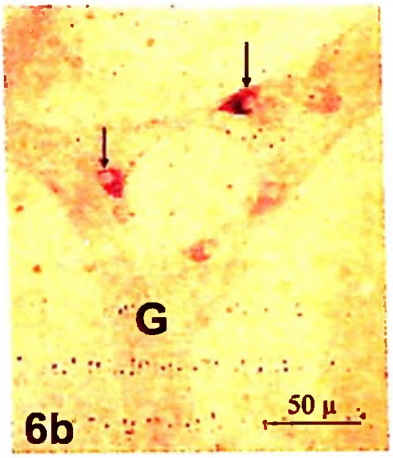

6b

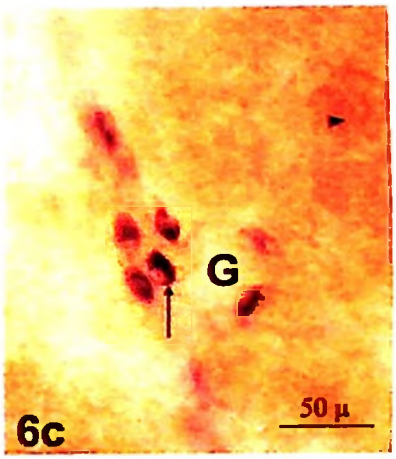

6c

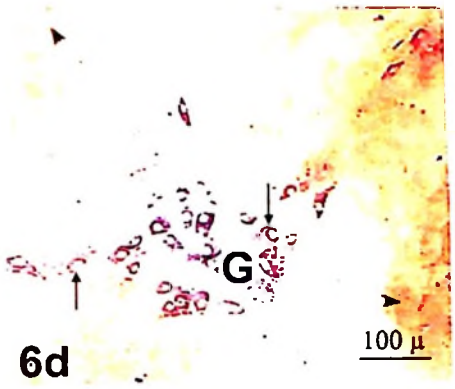

6d

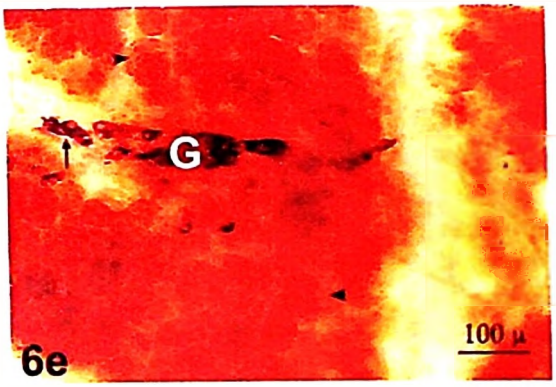

6e

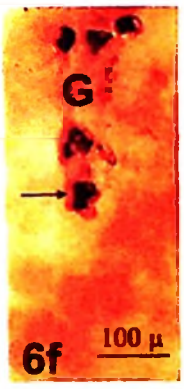

6f

Figs. 7a-d. NADPH-d , myenteric plexus. 7a. Colon, control pig showing a ganglion (G) with many but moderately stained neurons (arrows) after incubation for 1 hr. x 96. 7b. Colon, postnatal infection, severely inflamed tissue after incubation for 1 hr. Notice increased staining intensity and number of stained neurons (arrows) in the ganglion (G). x 96. 7c. Caecum, prenatally infected pig, moderately inflamed tissue showing increased staining intensity in some of the neurons (arrows) in the ganglion (G). x 96. 7d. Colon, severely inflamed tissue. Notice increased NADPH-d activities in neurons in the ganglion (G) and vacuolation of the cytoplasm in these neurons (arrows). x 384. (Compared 7a with 7b-d).

7a

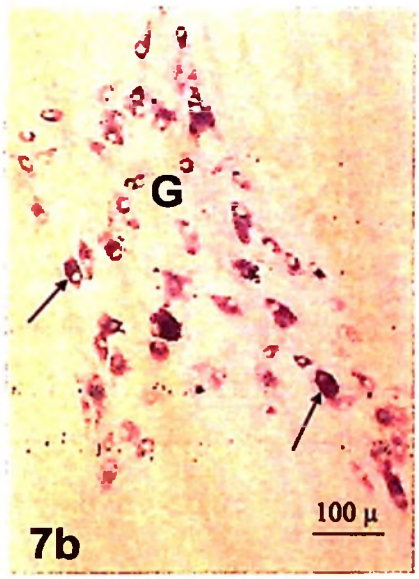

7b

7c

7d

Fig. 8a. Numerical density (N_d) of NOS IR neurons, caecum, control and *S. japonicum* infected pigs. Notice, increased N_d in postnatally (Postnat.) and prenatally/challenge (Prechall.) infected pigs compared to control (Contr.) pigs. Analysis of variance (Least squares mean, LSD) showed the following values: Myenteric plexus, contr. vs postnat., P < 0,0414* ; contr. vs prechall., P < 0,3375 not significant (n.s); postnat. vs prechall., P < 0,3002 (ns). OSP; contr. vs postnat., P < 0,0142*; contr. vs prechall., P < 0,0843 (n.s); postnat. vs prechall., P < 0,3276 (n.s). ISP; contr. vs post., P < 0,0295*; contr. vs prechall, P < 0,3021 (n.s); postnat. vs prechall. < 0,2352 (n.s). The difference between plexuses was highly significant (P < 0,0001***).

Fig. 8b. Numerical density of NOS IR neurons, colon, control and *S. japonicum* infected pigs. Notice, increased N_d in postnatally (P) and prenatally/challenge (PC) infected pigs. Myenteric plexus; contr. vs postnat., P < 0,0001***; contr. vs prechall., P < 0,0246* ; postnat. vs prechall., P < 0,0003***. OSP, contr. vs postnat., P < 0,0063**; contr. vs prechall., P < 0,0950 (n.s.); postnat. vs prechall., P < 0,4412 (n.s). ISP; contr. vs postnat., P < 0,0117*; contr. vs prechall., P < 0,1250 (n.s); postnat. vs prechall., P < 0,3989 (n.s). The difference between plexuses was highly significant (P < 0,0001***).

Comparing numerical densities in the three plexuses between caecum and colon, the overall results showed no significant difference (P < 0,3697). However the difference between N_d of caecum and colon in the myenteric plexus was highly significant with P < 0,0001***. The differences between OSP (P < 0,8820) and between ISP (P < 0,2227) were not significant.

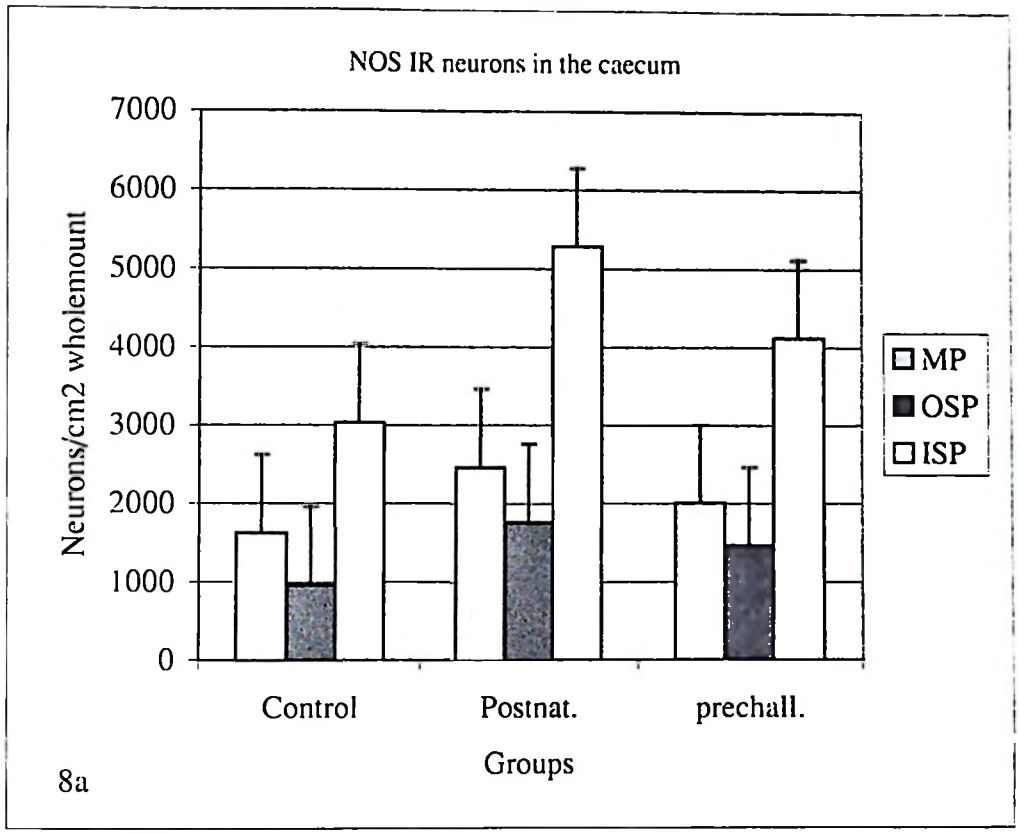

8a

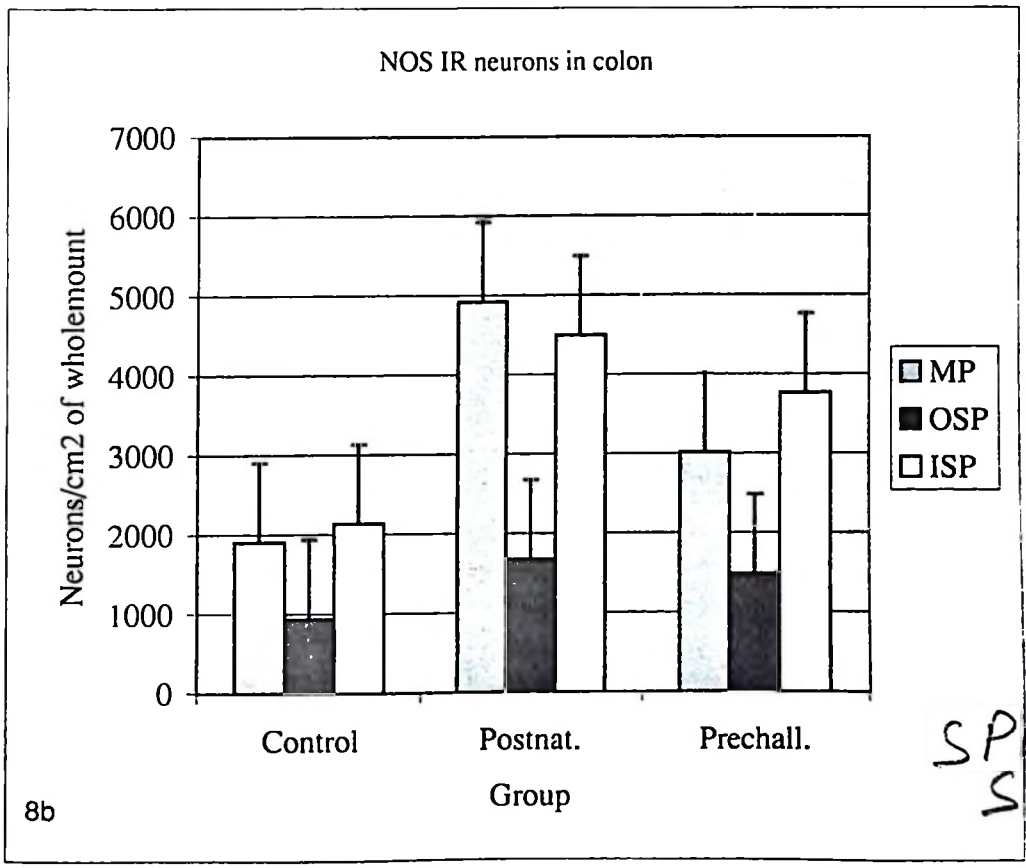

8b

SPE
SF

7/2/2012